DEVELOPMENT OF A DESIGN PROCEDURE FOR RESIDENTIAL AND LIGHT COMMERCIAL SLABS-ON-GROUND CONSTRUCTED OVER EXPANSIVE SOILS

VOLUME I

A Dissertation

by

WARREN KENT WRAY

Submitted to the Graduate College of
Texas A&M University
in partial fulfillment of the requirement for the degree of

DOCTOR OF PHILOSOPHY

December 1978

Major Subject: Civil Engineering

DEVELOPMENT OF A DESIGN PROCEDURE FOR RESIDENTIAL AND LIGHT COMMERCIAL SLABS-ON-GROUND CONSTRUCTED OVER EXPANSIVE SOILS

VOLUME I

A Dissertation

by

WARREN KENT WRAY

Approved as to style and content by:

(Chairman of Committee)

(Head of Department)

(Member)

(Member)

(Member)

December 1978

ABSTRACT

Development of a Design Procedure for Residential and Light Commercial Slabs-On-Ground Constructed Over Expansive Soils (December 1978)

Warren Kent Wray, B.S., Washburn University; B.S., Kansas State University; M.S., Air Force Institute of Technology

Chairman of Advisory Committee: Dr. Robert L. Lytton

A computer analysis of the soil-structure interaction occurring between stiffened slabs-on-ground and expansive and compressible soils was used to determine design equations for predicting the magnitude of bending moment, shear and differential deflection expected to occur under service conditions. The investigation was conducted using a finite element analysis of a plate resting on an elastic foundation. Analysis showed the maximum design moment and shear values in either bending mode to occur near the slab edge, within a distance, β, determined by the relative stiffnesses of the slab and the soil. The moment in the short dimension was typically found to be greater than the moment in the long dimension. Analysis also showed the magnitude of the maximum moment depended on the slab length with moment reduction occurring at mid-length of the slab, the amount of which depended upon the depth of the stiffening beams. The greatest amount of differential deflection was found to occur within a distance of 6β for slabs longer than this length. An additional computer analysis was conducted to analyze the

the effect of post-tensioning reinforcement on differential deflection, and cracking and ultimate strength. This analysis showed positive placement of the prestressing force offered a deflection advantage to post-tensioned slabs over those without prestressing. The investigation also showed that although moment capacity is lost after exceeding the concrete tensile strength, moment capacity is recovered with increased loading due to increased soil support.

Using the results of the computer analysis, a design procedure is developed that is applicable to either post-tensioned or conventionally reinforced slabs. A method of estimating the edge moisture variation distance is presented. The new procedure is compared to design methods presently available and is found to produce, in general, smaller design values of moment and differential deflection, particularly in long slabs.

Dedicated To

Wanda,

My Wife and Best Friend

ACKNOWLEDGMENTS

The writer takes sincere pleasure in acknowledging his appreciation to Dr. Robert L. Lytton for his guidance and patient supervision throughout this entire study. Working with Dr. Lytton in developing and reporting this research has been a unique and most rewarding experience. Appreciation is also extended to Dr. Wayne A. Dunlap, Dr. Teddy J. Hirsch, Dr. Kirk W. Brown, and Dr. Leon B. Treybig for their encouragement as well as their careful and prompt reading of the completed manuscript.

Financial support for the entire study was provided by the Post-Tensioning Institute (PTI). This support was deeply appreciated as well as the timely suggestions made by Mr. Clifford Freyermuth, Executive Director of the PTI, and members of the ad hoc committee who reviewed the progress of the research. Hopefully, the efforts of this study will assist not only designers of post-tensioned slabs-on-ground, but designers of slabs with other types of reinforcement as well, by providing a better analytical understanding of the interaction occurring between a slab-on-ground and the soil on which it is resting.

The writer also extends appreciation to Mrs. Kahne Haynes, Mrs. Bea Cullen, and Mrs. Joy Taylor for typing various parts of the manuscript.

The full and complete cooperation, encouragement, and understanding of the writer's parents as well as his wife's father is gratefully acknowledged and deeply appreciated.

Finally, to his wife, Wanda, he extends his deepest and most heartfelt appreciation for her constant assistance, encouragement, and

support displayed throughout this period of graduate study, as well as for typing most of the final manuscript. For these reasons, it is with great pleasure that this work is dedicated to her.

Warren Kent Wray

Texas A&M University
College Station, Texas
August 1978

TABLE OF CONTENTS

TABLE OF CONTENTS (CONT'D)

TABLE OF CONTENTS (CONT'D)

TABLE OF CONTENTS (CONT'D)

LIST OF TABLES

LIST OF TABLES (CONT'D)

LIST OF FIGURES

LIST OF FIGURES (CONT'D)

LIST OF FIGURES (CONT'D)

LIST OF FIGURES (CONT'D)

LIST OF FIGURES (CONT'D)

LIST OF FIGURES (CONT'D)

CHAPTER I

INTRODUCTION

The Expansive Soil Problem

Clay soils with the potential to shrink or swell are found throughout the United States (Figure 1) and in almost all parts of the world (Figure 2). Soils with this shrink-swell potential create design problems, particularly for slabs-on-ground, because as the soil moisture content changes so does the soil volume, i.e., as the soil moisture content increases, the ground surface moves upward and as the moisture content decreases, the ground surface recedes.

Structural damage caused by expansive clay soils in the United States annually exceeds that caused by earthquakes, hurricanes, and floods combined, according to Jones and Holtz (40). Their conservative estimate of damage to various types of structures caused by soil movement is given in Table 1 in terms of 1970 dollars. It is obvious from this list that single family homes and commercial buildings account for almost one-third of the total monetary damage received by all structures as a result of soil movement. Wiggins (104) found that on a state-by-state basis, California and Texas account for 35% of all expansive soil losses. When it is realized that most residences and light commercial buildings in these two states are con-

---

The format of this page and the following pages follow the style of the Journal of the Geotechnical Engineering Division, Proceedings of the American Society of Civil Engineers.

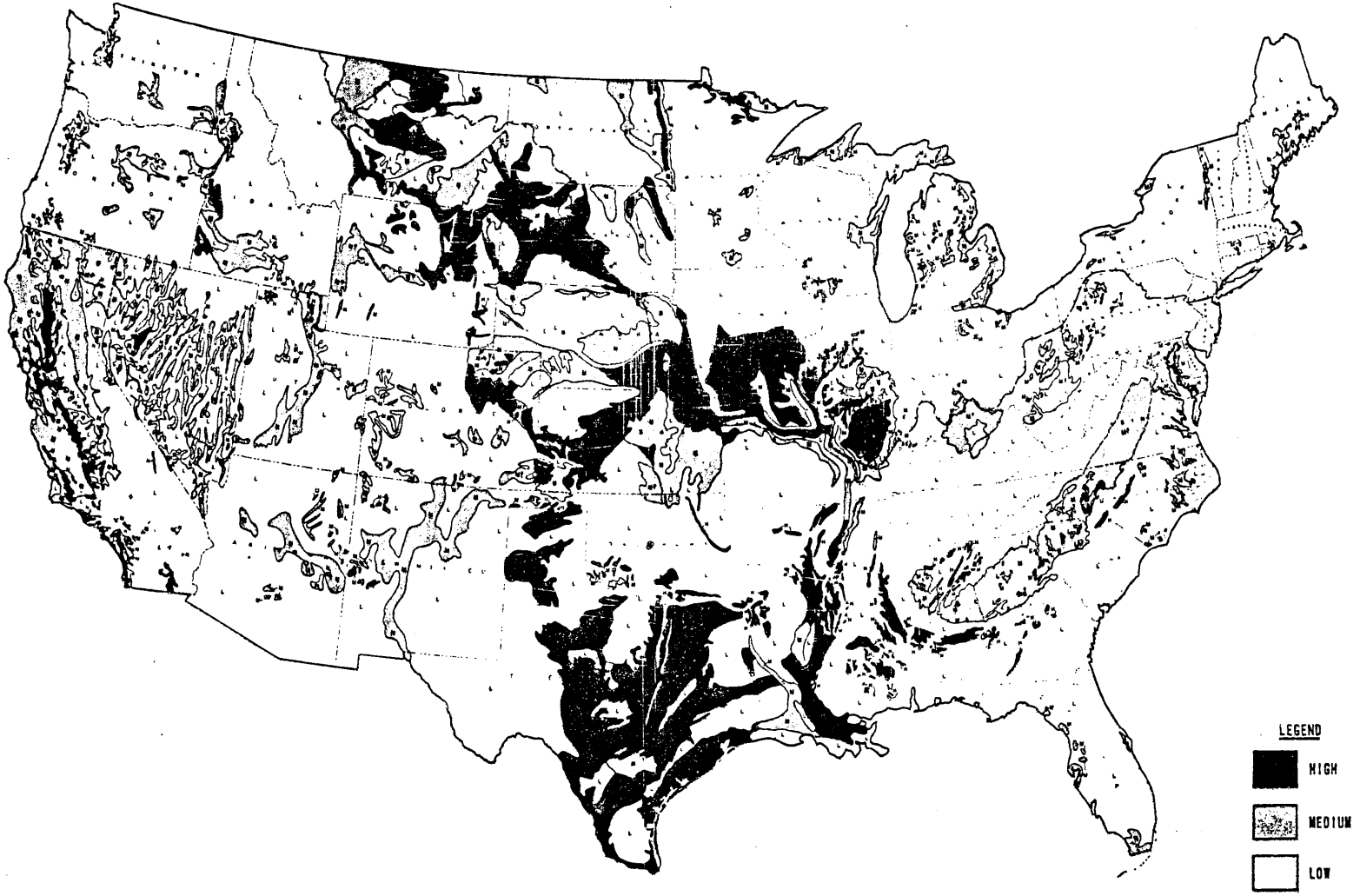

Figure 1. Distribution of expansive soils in the United States and their relative activity [After Wiggins (104)].

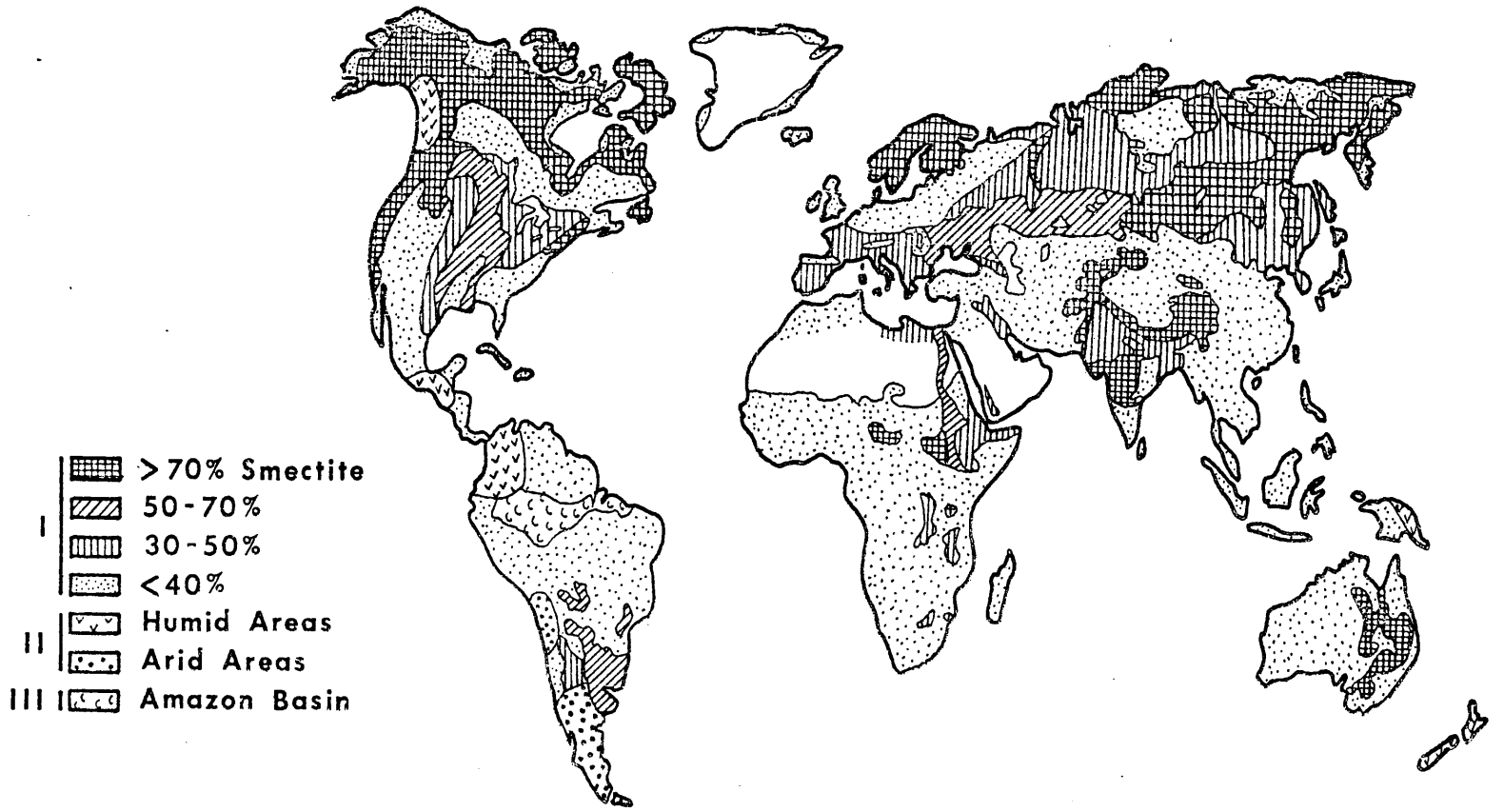

Figure 2. Areas of the world showing different proportions of smectite in clay fractions of A1 and/or A2 horizons. [(I) Soils with smectite; (II) Soils formed in ashfalls; (III) Soils of the Amazon basin.] (After Borchardt(19))

TABLE 1. Structural Damage From Soil Movements (40)

Single Family Homes	$300,000,000
Commercial Buildings	360,000,000
Multi-Story Buildings	80,000,000
Walks, Drives, and Parking Areas	110,000,000
Highways and Streets	1,140,000,000
Buried Utilities and Services	100,000,000
Airport Installations	40,000,000
Involved in Urban Landslides	25,000,000
Other	100,000,000
	$2,255,000,000

structed with slab-on-ground foundations, the real importance of slab-on-ground design in expansive soil areas becomes evident.

The time required for structural distress and damage to occur, as well as the degree of severity of this distress, depends very much upon the local climate. In wet climates, such as in east Texas, Louisiana, Mississippi, Alabama, Georgia, and the Carolinas, where the rainfall usually exceeds the potential evapotranspiration (the amount of moisture the soil would give up to the atmosphere if it were available), the greatest incidence of damage occurs during periods of drought. Consequently, it is possible in these areas for slab-on-ground foundations which have performed in an excellent manner for a period of several years to suddenly be subjected to severe distress.

Design of slab-on-ground foundations in these wetter areas will necessarily be different from those located in areas such as central and west Texas, Oklahoma, Kansas, Colorado, New Mexico, Arizona, and

California where the movement of the supporting soil is more cyclic and seasonal in nature. In these semi-arid climates, potential evapotranspiration usually exceeds rainfall and the probability of having a substantial amount of movement around the edges of a slab becomes greater. This consideration affects the design of the stiffening beams and the amount of reinforcing steel that is placed in them. Thus, a design procedure must be able to provide a uniform guide for design by engineers in each climate without unfairly penalizing engineers in the wetter climates for the greater uncertainties in design that occur in drier climates. Similarly, engineers in drier climates should be allowed the greater reliability that will be provided by more substantial sections and reinforcing than is adequate in wet climates. Because of this, it should be recognized that any proposed design procedure cannot simply consist of a series of standard sections, each for a given size of building in a given geographical location, but that it will involve calculations of structural design quantities such as bending moment, shear force, and differential deflection, each of which will have to be calculated from appropriate soil and climatic conditions as well as the size of the building and its expected loads.

Early Application of Slabs-On-Ground

Concrete slabs-on-ground have been used as the primary floor surface for residences and light commercial buildings for many years, gaining particular favor with builders in the southern regions of the United States following World War II. Many of these slab foundations

were developed as a result of invention and trial-and-error rather than design based on analyses. Although many of these slabs performed successfully over the years, a significant number of the slabs were considered to be failures. In many cases, the failures caused alteration and revision to the design until subsequent versions performed successfully. As the use of the slab as the principal floor surface and foundation spread, many foundation sections that were performing well in one area were used in other geographical locations. Frequently, the result of this geographical relocation was an unsuccessful performance. It was eventually realized that these poor slab performances were frequently due to either a failure to recognize, or an inability to cope with, the wide differences in soil properties, climate, construction abilities and experience, as well as other variables.

In recognition of this, the Federal Housing Administration (FHA) in 1957 requested the Building Research Advisory Board (BRAB), an agency of the National Research Council, to determine "criteria for proper design and construction of heated and unheated slabs-on-ground to ensure structural soundness" including "standards of construction for heated and unheated slabs-on-ground that will ensure structural soundness in areas of expansive soils" (9).

Post-Tensioned Slabs-On-Ground

Although the general concepts of prestressed concrete were first formulated in Europe in the period 1885-1890, practical application of this construction method was not widespread in the United States until

the late 1920's (99). Even then, little serious linear prestressing was practiced until about 1950, when the Walnut Lane Bridge in Philadelphia was constructed as the first major linear prestress project in this country. During the mid-1960's, the process of post-tensioning ground-supported slabs was developed and in 1968 the U. S. Department of Housing and Urban Development (HUD) issued the first general approval for the use of these prestressed slabs-on-ground (69).

During the next few years, competition between the mild steel reinforcing and the post-tensioned slab-on-ground industries became very intense. In many instances this competition resulted in inferior foundation slabs. In an effort to protect both its slab-on-ground industry and the public interest, the Prestressed Concrete Institute (PCI), a technical advisory group of the prestressed concrete trade, authored a rather stringent set of design criteria and specifications in late 1975. (In early 1976 the Post-Tensioning Division of the PCI separated from the PCI and established itself as the Post-Tensioning Institute (PTI).) One of the objectives of this publication was stated in the commentary as "It is hoped that the publication of these tentative recommendations for post-tensioned slabs will result in a requirement that comparable standards be required [by governmental agencies] for conventionally reinforced slabs" (69).

Unfortunately for the post-tensioned slab industry, its mild steel slab competitors did not follow its lead and develop a similar set of design specifications. To compound the problem, most of the government agencies began to rigidly enforce post-tensioned slab construction and design in accordance with the published PTI design

recommendations but did not hold the mild steel designers to the same standards. The result was a definite economical advantage to the mild steel slab trade and the need for a general design procedure that could be rationally applied to either type of slab-on-ground reinforcement became obvious.

Current Design Procedures

The final form of the BRAB design criteria was published in 1968 and was quickly termed conservative by both engineers and builders because it was said to require "overdesigned" sections. This conclusion was based on the commonly observed fact that many foundations with much lighter stiffening beams than those required by the BRAB criteria were found to perform "well". Although it was subjective, this observation was, and still is, so widely held that builders and engineers alike feel they will not be acting in the best financial interests of the eventual owner of the building if they design and build in strict accordance with the BRAB criteria (35).

Until the BRAB criteria, the only published design procedures were empirical. It is not known how widely these procedures were used but apparently they either were not used often or were not successful when they were used, otherwise, the BRAB procedure would not have been necessary. In a series of papers between 1966 and 1973, Lytton (49,50,52, 53,54,55) and Lytton and Meyer (51,58) presented the first rational design procedure which resulted from analysis of the soil-structure interaction problem using models of a beam resting on a curved coupled spring foundation (edge heave) and a Winkler foundation (center heave)

as well as an interacting plate to develop the moment relations in the long and short directions.

In 1974, Walsh (97) proposed a design procedure that combined parts of the BRAB criteria with Lytton's procedure. Fraser and Wardle (23) presented the most recent approach to the problem by using an elastic soil model instead of a coupled spring. Their work was based on an interacting plate rather than the beams used by Lytton and Walsh.

Shortcomings of Current Design Procedures

Each of the currently available design procedures has some shortcomings on which a new procedure could improve. The support and bending patterns in long and intermediate length slabs are not considered by the BRAB procedure. Consequently, this procedure will usually produce very conservative beam depths and steel requirements, particularly in the longer slab lengths. In addition, this procedure assumes a relationship between a weighted plasticity index (PI) and a "climatic rating" to determine the degree of support the soil is expected to provide to the slab. The weighting procedure used to obtain the design PI can produce an artificially low or high value, depending upon where the most reactive soil layer is located. Additionally, the relation between PI and the "climatic rating" has never been verified with field data.

Lytton's method was developed from the analysis of a beam on Winkler and coupled spring foundations. Although the coupled spring model fairly represents a soil if there is no lateral displacement,

the Winkler model cannot represent shear stiffness, whereas, a real soil will display resistance to shear. Additionally, because a beam was used in the basic analysis, the two dimensional interaction present in a slab is not as well accounted for as it would be if a plate analysis were performed. Lytton's method does, however, consider the fact that moment increases at a reduced rate as length increases.

The Walsh and Fraser and Wardle efforts, despite using finite element plate analysis, have been directed towards producing sets of standard sections, beam depths, and reinforcement for slabs constructed in specific geographical locations, particularly in the Melbourne, Australia, area. Although their work has been thorough, they have not developed a general design procedure that can be used in any geographical area.

Present Need

From the preceding discussion, it can be seen that a design procedure is needed which will not contain the inadequacies of the procedures presently in use but at the same time will be rational, easy to use, and can be used in any geographical location by practicing engineers. To adequately develop such a procedure, the interaction between the soil and the foundation must be considered. In subsequent chapters the factors affecting the magnitude of soil expansion are identified and the models used to investigate the soil-structure interaction are defined. The results of this analysis are used to develop a set of easily solved design equations and a proper design procedure is introduced. Finally, through design examples, the

proposed procedure is compared to the principal design methods presently being used.

CHAPTER II

FACTORS AFFECTING THE EXPANSIVE SOIL PROBLEM

Many of the factors that determine if expansive soil movement will occur have been identified by Donaldson (20), Gromko (26), Holland, et al. (32), Jennings (38), Meyer and Lytton (58), and Mathewson, et al. (57). For the most part, these factors may be divided into two broad categories: (1) soil or climatic properties that normally cannot be altered by the engineer or owner, and (2) site conditions and other factors that may be influenced or altered by the engineer or owner.

Conditions That Normally Cannot be Altered

Type and Amount of Clay Mineral. - The magnitude of the change in volume of soils as water content changes is controlled by the type and amount of clay present (59). For most engineering purposes, clay minerals are generally classified into three main groups, i.e. kaolinite, illite, and montmorillonite (41). As Mitchell (59) points out: "Montmorillonites and vermiculites undergo greater volume changes on wetting and drying than do kaolinites and hydrous micas (illites). Experience clearly indicates this to be the case."

That type and amount of clay influences swelling was clearly shown by Skempton (59), whose test results are reproduced in Figure 3. The term "clay activity", A, in Figure 3 is defined as:

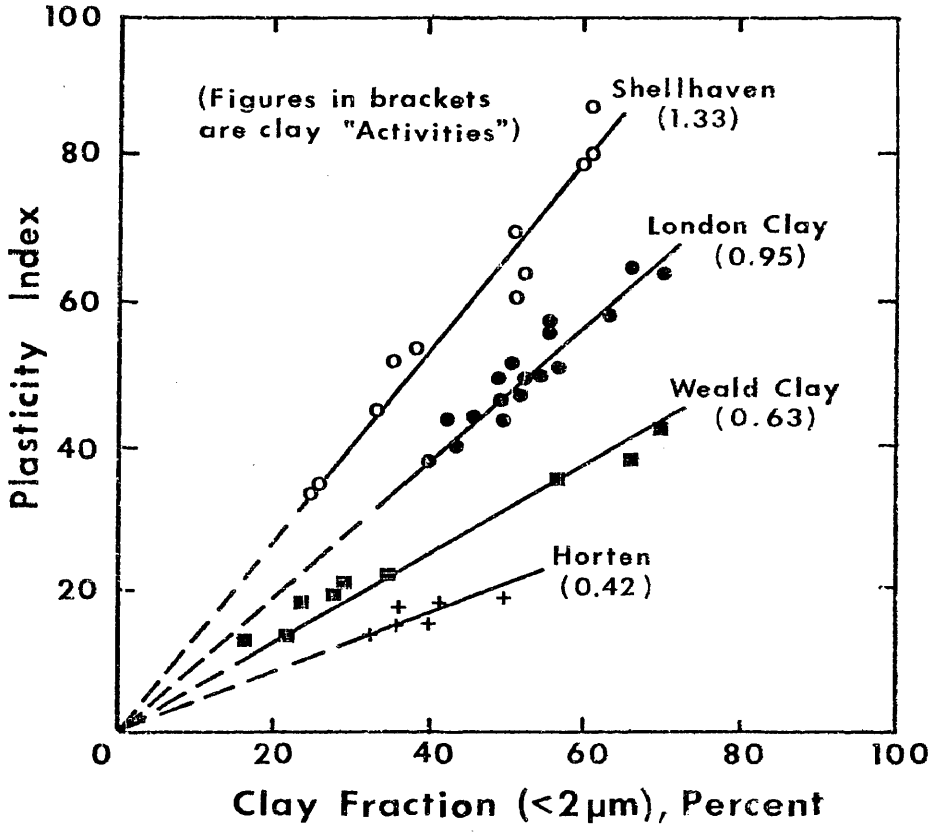

Figure 3. Relationship between plasticity index and clay fraction (From Mitchell (59) After Skempton).

$$A = \frac{\text{Plasticity Index}}{\text{\% By Weight Finer Than } 2\mu \text{ Size}} \quad \ldots\ldots\ldots\ldots\ldots\ldots \quad (2\text{-}1)$$

and the larger the activity ratio, the greater is the shrink-swell potential.

Pearring (65) and Holt (34) modified Skempton's definition to account for the contribution to the overall soil plasticity by the silt-sized particles. Pearring continued to call this modified ratio the "Activity Ratio" but defined it as "the ratio of the plasticity index of a soil to the percentage of the minus U.S. No. 200 sieve material which is smaller than 2μ" and represented it with the symbol "Ac". For finer grained soils that contain no material coarser than the No. 200 sieve, the activity ratios of Skempton and Pearring are the same.

Pearring (65) also devised a term he called "cation exchange activity", CEAc. This term is defined as the ratio of the cation exchange capacity (C.E.C.) to the percentage of clay content of the soil. Using these two parameters, CEAc and Ac, he found that a soil could be classified according to its dominant clay mineral (Figure 4). Holt (34) extended Pearring's work and showed that Figure 4 was also applicable to montmorillonitic and interstratified soils.

Thus, one could reasonably expect a soil with a high percentage of particles passing the No. 200 sieve and which consists predominantly of montmorillonite to experience a greater amount of shrink-swell than a soil with a low percentage of clay sized comprised of kaolinite.

Climate. - Change in volume of expansive soils is directly

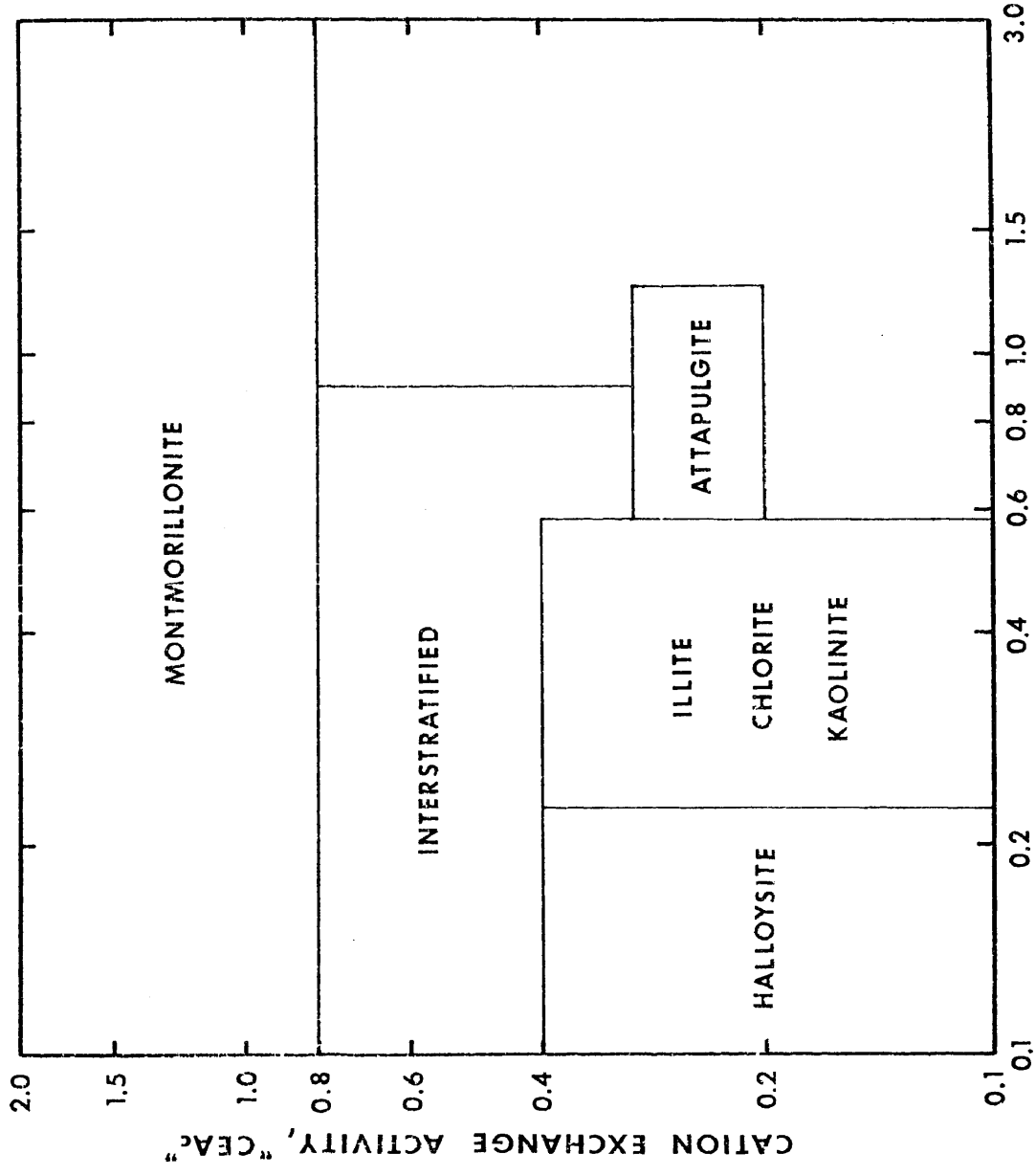

Figure 4. Clay Type Classification According to Cation Exchange and Clay Activity Ratio [After Pearring (65) and Holt (34)].

related to a change in moisture content; if the moisture content of a soil remains constant then no volume change or swelling will occur (105). The greatest amounts of shrink-swell are normally experienced by expansive soils found in climates that are termed semi-arid, i.e., a climate that has periods of rainfall followed by extended periods without rainfall. These necessary semi-arid conditions exist in Texas, as well as much of the Great Plains and many of the western states of the United States.

Soil Profile. - The location and depth of the expansive soil layer has a great influence on the actual amount of change in elevation the ground surface will experience. If the reactive layer is located at a depth below the active zone or the depth of seasonal moisture change, then no shrink-swell will occur. If the expansive layer is found to be in the active zone but a layer of non-expansive soil of low permeability lies above the expansive soil, a lesser amount of moisture change will occur in the expansive layer and, consequently, little change in volume; if the conditions causing the change in soil moisture content persist so that the reactive layer has an opportunity to experience the changing moisture content, swelling will still occur but at a slower rate than if the low permeability layer were absent. Finally, if the expansive layer underlies several feet of material, the weight of this overburden material will resist or inhibit the swelling of the reactive layer even if it should experience a change in moisture content. Lytton and Woodburn (55) have shown this effect of overburden to be true, as shown in Figure 5.

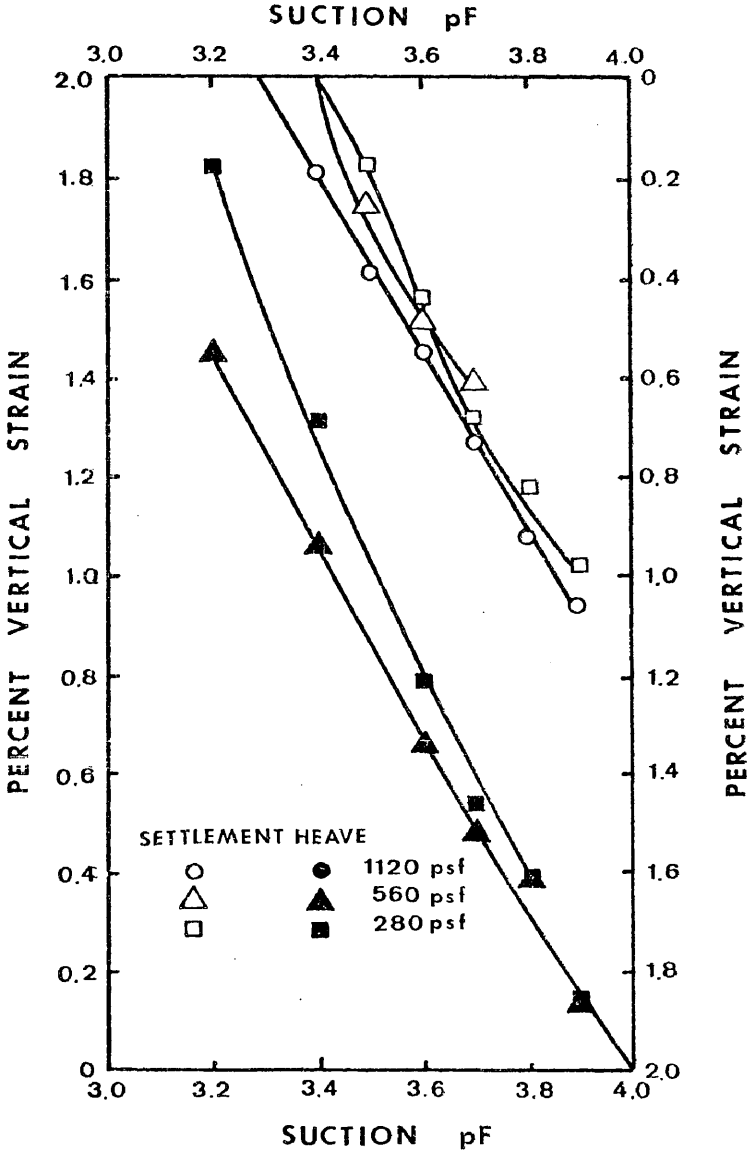

FIGURE 5. RELATIONSHIP BETWEEN LOADING, CHANGE IN SOIL SUCTION, AND VERTICAL STRAIN [FROM LYTTON (55)]

Soil Permeability. - Cracks which form in expansive soils have been found to influence the field permeability of soil to a great degree. Adams, et al. (1) and Hartman, et al. (28), found the infiltration rate of expansive soil to be influenced by the size and depth of the cracks. They also found the infiltration rate is affected by the rate at which the cracks close with respect to the precipitation rate. When the soil is dry and cracked, rainfall from an intense rain may enter the cracks before they close but the same amount of rain received over several hours or days may result in considerably more runoff since the cracks have had an opportunity to swell shut. Additionally, the deeper the crack extends, the drier is the soil and the deeper the infiltrating water is transmitted. The result of this combination is a greater amount of total heave experienced (105).

Depth of Seasonal Movement. - The depth of seasonal movement, also termed active zone, is the depth to which the soil experiences a change or variation in soil moisture content. This depth is influenced by the climate, the groundwater table (GWT), and the soil cracking pattern, as well as the type and amount of clay mineral and the soil profile.

The depth of the active zone is important because the greater the depth of the active zone, the greater the amount of material that experiences a moisture change and, consequently, the greater the volume change. If the GWT is close to the surface (less than 20 feet according to Aitchison, et al. (2)), the depth of the active zone is likely to be very shallow. If the climate is predom-

inately wet, and particularly if the GWT is close to the surface the active zone may be almost negligible. Similarly, if the climate is dry, and the GWT deep, the active zone may be very limited. It is the intermediate conditions such as periods of rainfall followed by extended periods of no rainfall or a fluctuating GWT that can create active zones that extend to considerable depth. The influence of the cracking pattern, the type and amount of clay mineral, and the soil profile have been discussed above.

A number of investigators have observed active zone depths. A summary of these reported depths is reflected in Table 2.

Soil Suction. - Soil suction theory is explained very well by a number of investigators, particularly Aitchison (2) and Lytton (47), and it will not be repeated here. However, in very general terms, soil suction can be described as the affinity of a soil for water and is usually expressed in either negative centimeters of water or as the common logarithm (base 10) of the absolute value of this pressure, written as pF; the larger the number, the drier the soil. An upper bound to soil suction is generally considered to be pF 4.8 (47). At a pF greater than 4.8, a vacuum dessicator or a drying oven is necessary to remove the adsorbed water; a pF of 7 corresponds to an oven dry condition (47). The basic defining equation for suction, h, is as a free energy in the form of the ideal gas law:

$$h = \frac{RT}{mg} \ln \frac{H}{100} \quad \ldots\ldots\ldots\ldots\ldots\ldots\ldots\ldots \quad (2\text{-}2)$$

TABLE 2. Reported Active Zone Depths

Investigator	Active Zone	Location	Reference
Crichton	0.6-2 m	Australia	14
Holland, et al.	0.6-2 m	Australia	32, 30, 31
Lytton and Woodburn	9-12 ft	Australia	55
Mohan, Jayne and Sharma	3 m	India	60
Zeitlan and Komornik	2-4.5 m	Israel	106
Shagra, et at.	6 m	Israel	80
Donaldson	3 m	South Africa	20
de Bruijn	3 m	South Africa	17
Lee and Kockerhans	10 ft	California	44
Glenn	5 ft	Texas	57
Ritchie	1.75 m	Texas	73
Tucker and Poor	5-7 ft	Texas	93, 94

where R = universal gas constant, 8.314×10^7 ergs/mole^{o}C

T = absolute temperature

g = gravitational constant

m = mass of 1 mole of water

H = relative humidity, %

Suction becomes zero when the relative humidity reaches 100% and becomes a larger negative number as the humidity decreases (the natural logarithm of a fraction is a negative number).

Conditions That Can be Altered

There are a number of additional factors that can influence whether a soil might shrink or swell and the magnitude of this movement. For the most part, either the owner or the designer has some control over whether the factor will be avoided altogether or if not avoided, the degree to which the factor will be allowed to influence the shrink-swell process. Castleberry (10) made a study of what many of these factors might be and their relative influence on the overall shrink-swell problem.

Antecedent Rainfall Ratio. - This is a measure of the local climate and is defined as the total monthly rainfall for the month of and the month prior to laying the slab divided by twice the average monthly rate measured for the period. The intent of this ratio is to give a relative measure of ground moisture conditions at the time the

slab is placed. Thus, if a slab is placed at the end of a wet period, the slab should be expected to experience some loss of support around the perimeter as the wet soil begins to dry out and shrink. The opposite effect could be anticipated if the slab is placed at the end of an extended dry period; as the wet season occurs, uplift around the perimeter may occur as the soil at the edge of the slab gains in moisture content.

Age of Slab. - The length of time since the slab was cast provides an indication of the type of swelling soil profile that can be expected to be found beneath the slab.

Lot Drainage. - This provides a measure of the slope of the ground surface with respect to available free surface water that may accumulate around the slab. Most builders are aware of the importance of sloping the final grade of the soil away from the structure so that rain water is not allowed to collect and pond against or adjacent to the foundations. If water were allowed to accumulate next to the foundation, it would provide an available source of free water to the expansive soil underlying the foundation. Similarly, surface water drainage patterns or swales must not be altered so that runoff is allowed to collect next to the foundation.

Topography. - This provides a measure of the downhill movement that is associated with light foundations built on slopes in expansive soil areas. The designer should be aware that as the soil swells, it

heaves perpendicularly to the ground surface or slope, but when it shrinks, it recedes in the direction of gravity and gradually moves downslope in a sawtooth fashion over a number of shrink-swell cycles. In addition to the shrink-swell influence, the soil will exhibit viscoelastic properties and creep downhill under the steady influence of the weight of the soil. Therefore, if the building constructed on this slope is not to move downhill with the soil, it must be designed to compensate for this lateral soil influence.

Pre-Construction Vegetation. - Large amounts of vegetation existing on a site before construction may have dessicated the site to some degree, especially where large trees grew before clearing. Constructing over a dessicated soil can produce some dramatic instances of heave and associated structural distress and damage as it wets up.

Post-Construction Vegetation. - The type, amount, and location of vegetation that has been allowed to grow since construction can cause localized dessication. Planting trees or large shrubs near a building can result in loss of foundation support as the tree or shrub removes water from the soil and dries it out. Conversely, the opposite effect can occur if flower beds or shrubs are planted next to the foundation and these beds are kept well watered or flooded. This practice can result in swelling of the soil around the perimeter where the soil is kept wet.

Loading. - This factor was not addressed by Castleberry but it is common knowledge among engineers that swell can be reduced if a large load is applied opposite to the swelling direction; in fact, if

a sufficiently large load is applied, no swell may occur at all. With this knowledge, most engineers attempt to transfer as much structural load as possible to the supporting soil through a system of piers and grade beams; however, when the foundation used is a slab-on-ground rather than a pier and beam system, concentration of load cannot be obtained since the slab distributes the superstructure load to the soil in an essentially uniform manner.

Summation

It is beyond the scope of this investigation to do more than point out that the above factors have a definite influence on the amount and type of swell to which a slab-on-ground is subjected during its useful life. The design engineer must be aware of these factors as he develops his design and make adjustments as necessary according to the results of special measurements or from his engineering experience and judgement.

CHAPTER III

DESIGN PROCEDURES PRESENTLY AVAILABLE

Washusen (101) acknowledges the existence of eight design methods. The methods of Dawson (15) and Rigby and Dekena (72) can also be added to Washusen's list to give the ten available design procedures listed in Table 3.

TABLE 3. Known Design Methods for Slabs-On-Ground Over Expansive Soils

DESIGN METHOD	DATE INTRODUCED	REFERENCE
Rigby & Dekena	1951	72
Salas & Serratosa	1957	77
Dawson	1959	15
Building Research Advisory Board	1968	9
City of Knox	1968	102
Lytton	1966-1973	49,50,52,53,54,55
City of Oakleigh	1971	102
Fargher	1973	102
Walsh	1974-1975	97
Fraser & Wardle	1975	23

Of the ten procedures listed in Table 3, only the methods of the Building Research Advisory Board (BRAB), Lytton, Walsh, and Fraser and Wardle appear to be based on rational procedures and have the potential

to be applied to general use. Each of the ten design methods will be discussed below, particularly the four more rational methods, in order that a comparison can be made between the results of each of the methods and, ultimately, compared to the results of the design procedure presented in Chapter VII.

Building Research Advisory Board Procedure (9)

The BRAB method was developed from experience and underwent several revisions between 1957, when the study was initiated, and 1968, when the final report was published.

The first step in the procedure is to determine the slab type necessary to accomodate the prevailing soil and climatic conditions. These conditions are shown in Table 4. BRAB separated all slabs into four types:

Type I	Unreinforced
Type II	Lightly reinforced against shrinkage and temperature cracking
Type III	Reinforced and stiffened
Type IV	Structural (not directly supported on the ground).

After a soil investigation is completed, one of the four slab types is selected as being appropriate.

Type I slabs are used only on soils which will develop no change in volume with time. These slabs are typically 4-inch thick separating

TABLE 4. Slab Type Recommendations on Soil and Climatic Conditions (From Brab (9))

Soil Type[1]	Minimum Density or PI or q_u[2]	Climatic Rating[3]	Recommended Slab Type[4]
GW, GP	All Densities	All	I
GM, GC, SW, SP SM, SC, ML, MH	Dense or Medium Dense	All	I
GM, GC, SW, SP SM, SC, ML, MH	Loose	All	II[5]
CL, OL, CH, OH	PI < 15 and	All	II
	$q_u/w \geq 7.5$		
	PI > 15 and	c_w 45	II
	$q_u/w \geq 7.5$	c_w 45	III
	$7.5 > q_u/w > 2.5$	All	III
	$q_u/w < 2.5$	All	IV
Pt	All	All	IV

1 As classified under the Unified Soil Classification System.

2 Unconfined compression strength of undisturbed sample.

3 From Figure 6, page 28.

4 Minimum requirement believed adequate for particular condition.

5 Type I slab may be used if soil is densified by compaction to its entire depth before placement of concrete slab.

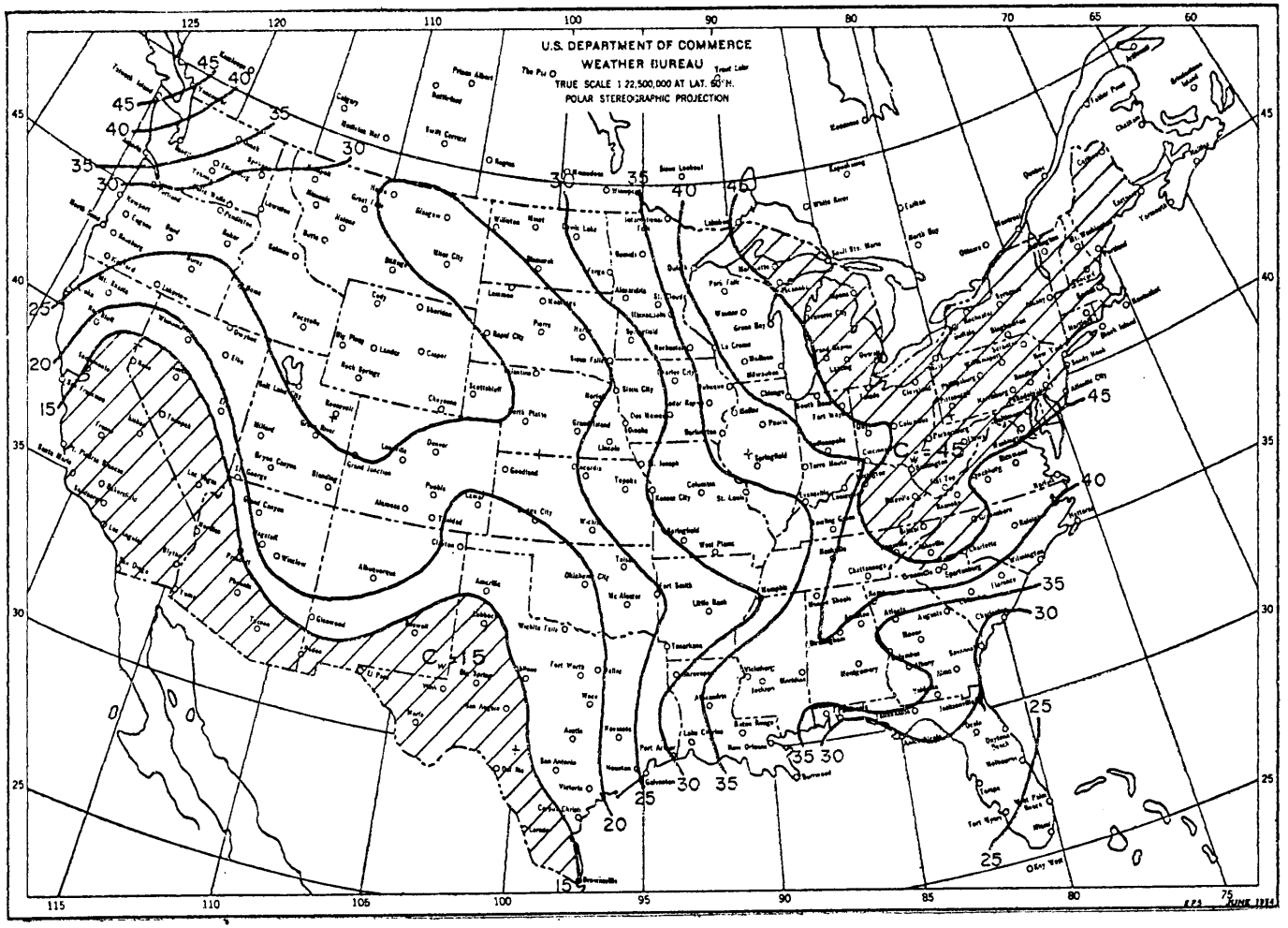

FIGURE 6. Climatic Ratings, C_w, for Continental United States (9).

elements (separating the living space from the underlying soil) with all load being carried through this slab-on-ground to conventional strip footings. The slab is generally not reinforced unless it is irregularly shaped or has heating coils through it. The shrinkage of the concrete is controlled by jointing regularly under walls.

The Type II slab is also 4 inches thick and is used where very slight movements may occur. It is essentially the same as a Type I slab except that nominal shrinkage and temperature reinforcement is placed at mid-depth of the slab and the slab may be placed monolithically with the footings. The amount of reinforcement used depends on the maximum slab dimension.

The Type III slab is an interacting structural element, used mainly on clays with movement potential. An extensive design procedure is presented which is used as the basic design philosophy of most of the later methods. The principal assumptions of Type III slab analysis are:

1. The design loads of the superstructure are uniformly distributed over the entire area of the slab;
2. After the supporting soil swells, the support pressure is distributed evenly to the center or ends of the slab, depending on the swelling mode;
3. The support index, C, is constant for all slab sizes.

The Type IV slab is structurally supported or suspended wherever the soil has insufficient bearing capacity to support the slab. BRAB recommends that the slab be supported by piers founded in soil of suit-

able bearing capacity and that design be carried out by following normal structural and soil engineering practice.

Once the slab type is known, the "support index", C, which is dependent upon the climatic rating, C_w, and either the soil PI or some measurement of the soil swelling potential, is determined. The BRAB figure for selecting C is reproduced as Figure 7. The support index is a measure of the expected fraction of the slab being supported by the soil underlying the slab.

Separating the slab into overlapping rectangular elements of length L and width L', and having determined the superstructure load as a uniformly distributed load, the design parameters of moment, shear, and deflection are calculated from the following equations:

$$\text{Maximum Moment } (M_{max}) = \frac{w\ L^2\ L'\ (1-C)}{8} \quad \ldots\ldots\ldots (3\text{-}1)$$

$$\text{Maximum Shear } (V_{max}) = \frac{w\ L\ L'\ (1-C)}{2} \quad \ldots\ldots\ldots (3\text{-}2)$$

$$\text{Maximum Deflection } (\Delta_{max}) = \frac{w\ L^4\ L'\ (1-C)}{48\ EI} \quad \ldots\ldots\ldots (3\text{-}3)$$

where L = slab length

L' = slab width

I = moment of inertia of the slab cross-section

E = modulus of elasticity of the concrete

C = support index, which varies from 0.6 to 1.0

w = uniformly distributed load

When determining parameters in the opposite dimension, the terms L and L' are transposed.

The climatic rating term is important in determining the amount of

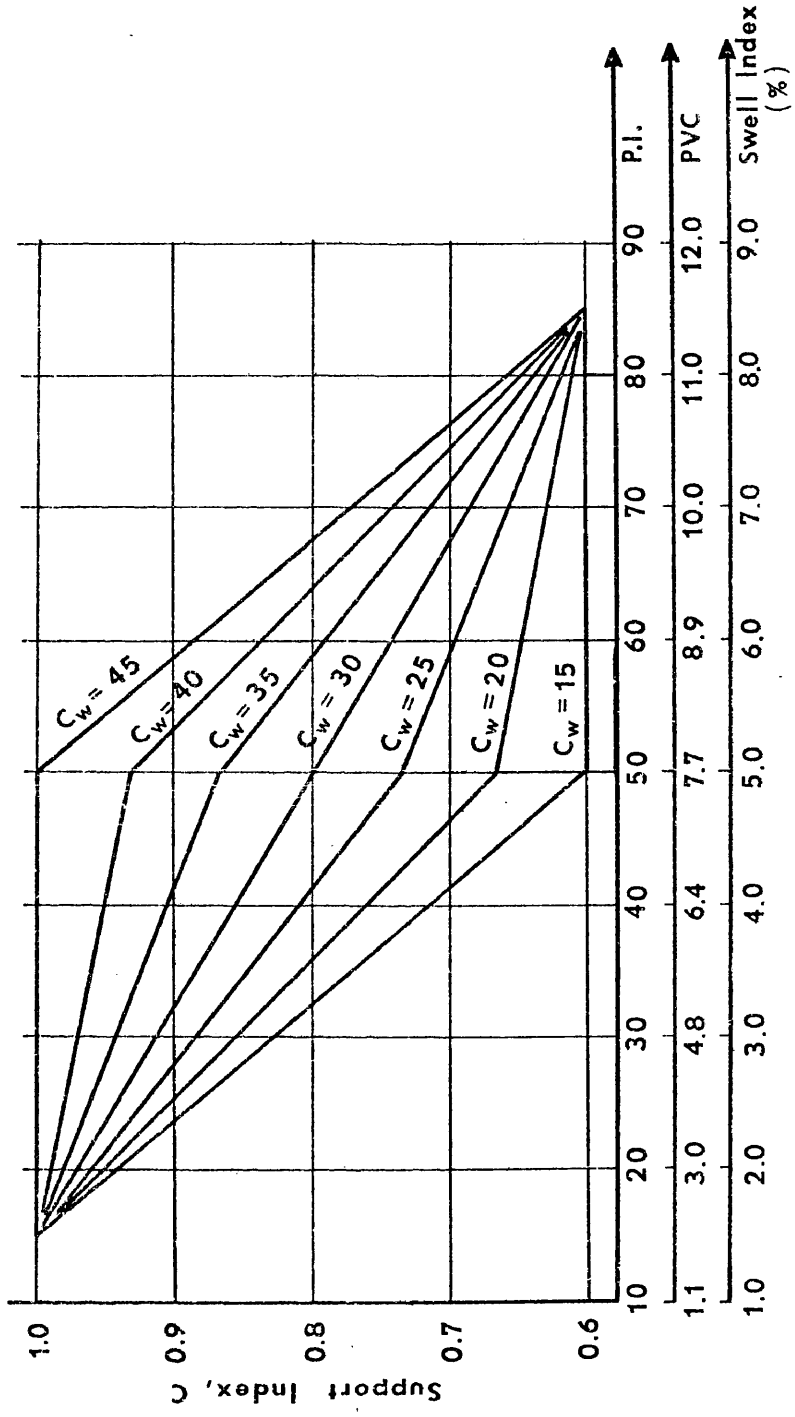

Figure 7. Support Index, C, based on criterion for soil sensitivity and Climatic Rating, C_w [After B.R.A.B. (9)]

support a slab can be expected to receive from a swelling or shrinking soil. However, the method of determining the set of curves reproduced in Figure 7 is not rational and is based entirely upon engineering judgment and U.S. Weather Service studies of five variables affecting climate:

a. Yearly annual precipitation;

b. Degree of uniformity through the year in distribution of precipitation;

c. Number of times precipitation occurs;

d. Duration of each occurrence; and

e. Amount of precipitation at each occurrence.

The set of curves of Figure 7 cannot be adjusted for known local climatic conditions.

The other major disadvantage of the BRAB method is that the percentage of support, C, remains constant regardless of the slab dimensions. This assumption is not in accordance with observed measurements (Chapter IV).

Lytton Procedure (49, 50, 52, 53, 54, 55)

Lytton developed his design method by using a finite difference analysis for a beam on a curved mound. He used a Winkler foundation for center lift (See Figure 11, p. 42) analysis, and a coupled spring foundation for edge lift analysis. The derivation of these models is discussed fully in his series of papers and their presentation is not necessary here.

For slabs with a maximum dimension of less than about 70 feet (52),

Lytton's design procedure can be summarized as follows:

1. Separate the foundation into overlapping rectangles,
2. Separate all loads in each direction into three categories:
   a. Line loads acting along the perimeter (wall loads), q_e;
   b. Line loads acting through the center of the building, q_c;
   c. Uniformly distributed loads resulting from slab weight, interior dead and live loads, w_ℓ
3. Calculate the maximum possible moments resulting from these load categories. In doing so, it is assumed that both the soil and the slab are rigid and the soil provides only line support.

Using symbols defined in the BRAB procedure (above), the maximum moment in the direction being considered, L, is:

Center Lift

$$M_{max} = \frac{q_e L'L}{2} + \frac{L^2}{8}(2q_e + q_c + w_\ell L') \quad \ldots\ldots\ldots \quad (3\text{-}4)$$

Edge Lift

$$M_{max} = \frac{q_c L'L}{4} + \frac{L^2}{8}(2q_e + w_\ell L') \quad \ldots\ldots\ldots \quad (3\text{-}5)$$

The center lift condition produces a negative moment and the edge lift condition produces a positive moment.

4. To account for the compressibility of the soil, a moment correction term is introduced. This correction term is used to reduce the magnitude of the maximum moment (either positive or negative) to give a "one-dimensional" design moment:

$$M_1 = M_{max} - \Delta M \quad \ldots\ldots\ldots\ldots\ldots\ldots\ldots\ldots \quad (3\text{-}6)$$

where $$\Delta M = c \frac{TL}{8} \quad \ldots\ldots\ldots\ldots\ldots\ldots\ldots\ldots \quad (3\text{-}7)$$

and T = total load on the rectangle

L = length in the direction being considered

c = support index

5. The "one-dimensional" design moment obtained from Equation (3-6) is adjusted to account for plate action:

Long Dimension

$$M_L = M_1 \left(1.4 - 0.4 \frac{L}{L'}\right) \quad \ldots\ldots\ldots\ldots\ldots\ldots\ldots\ldots \quad (3\text{-}8)$$

where $$M_L \geq M_1 (1.5 - c) \quad \ldots\ldots\ldots\ldots\ldots\ldots\ldots\ldots \quad (3\text{-}9)$$

Short Dimension

$$M_S = M_1 \left[1 + 0.9(1.2 - c)\left(\frac{L}{L'} - c\right) \right] \quad \ldots\ldots\ldots\ldots\ldots\ldots \quad (3\text{-}10)$$

6. Values of the design shear and deflection are determined using equations similar to Equations (3-2) and (3-3), respectively:

Shear: $$V = \frac{4M}{L} \quad \ldots\ldots\ldots\ldots\ldots\ldots\ldots\ldots \quad (3\text{-}11)$$

Deflection: $$\Delta = \frac{M L^2}{12 EI} \quad \ldots\ldots\ldots\ldots\ldots\ldots\ldots\ldots \quad (3\text{-}12)$$

Where BRAB requires design using the cracked concrete section, Lytton assumes an uncracked beam section. He reasons (50):

> . . . because of the economics and inconvenience of the labor involved, grillage raft and slab practice has tended to use very light quantities of reinforcing steel, usually no more than the minimum required flexural steel required by the SAA Code, (Standard Association of Australia) which is .003 of the total area of concrete. It is obvious from this practice that in general, foundation sections have not been designed as flexural elements. It would be unreasonable in view of this economical and many times successful practice, to devise a design procedure which requires reinforcing steel based on a cracked concrete section. Rather it would be more reasonable to view steel placed in the foundation only as a safety factor which increases the ductility of the beams, slabs, and rafts, and to design the foundation sections based on a full, uncracked concrete section with tensile cracking stress as the design stress. Once this stress is exceeded, the structural element so designed loses much of its flexural stiffness and deflects much more easily. After cracking occurs, differential movements in the house will increase at nearly the same rate as the differential movements in the soil itself.

Whereas BRAB presents a support index originating from engineering experience and empirical consideration of expected site conditions, Lytton derives a support index, c, by using the rational analysis of the interaction between the expected heave profile and the slab (assumed to be rigid). The solution for c can be obtained directly from Equation (3-13) below, or from the nomograph (53) reproduced in Figure 8.

$$c = \frac{m+1}{m+2}\left[\frac{m+1}{m}\cdot\frac{T}{A}\cdot\frac{1}{ky_m}\right]^{1/(m+1)} \qquad \ldots\ldots (3\text{-}13)$$

where T = total load acting on rectangle, in lbs

A = total slab (rectangle) area, in inches^2

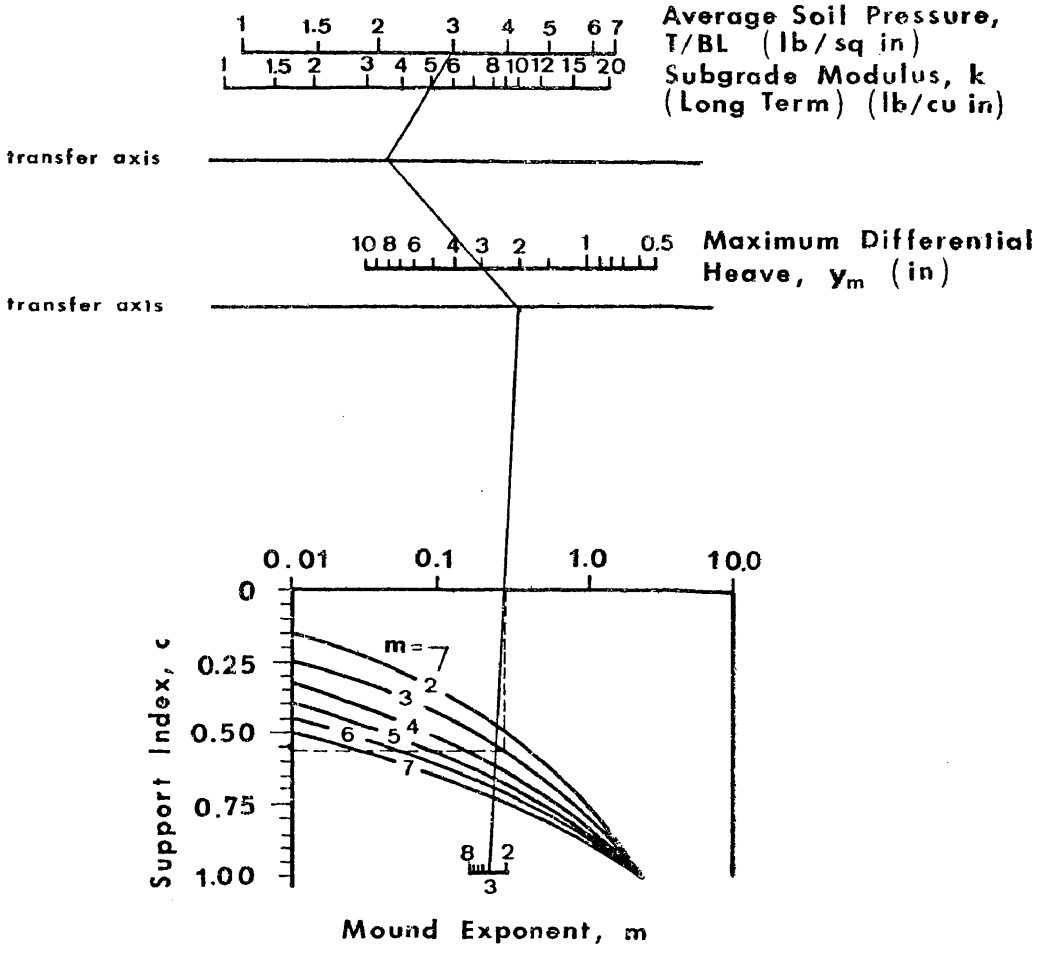

Figure 8. Nomograph for determining Support Index, c, for Lytton design method [After Lytton (53)].

k = Winkler foundation modulus, in lbs/in^3

y_m = maximum differential movement of the supporting soil, in inches

m = mound exponent

To assist in estimating k and y_m, the design aids in Figures 9 and 10 were presented by Lytton in 1972. He also suggested the mound exponent, m, could be estimated from:

$$m = \frac{L}{Z} \quad \ldots\ldots\ldots\ldots\ldots\ldots\ldots\ldots\ldots\ldots \quad (3\text{-}14)$$

where L = length in the direction of bending

Z = depth of the active zone

The shape of the mound is discussed in Chapter IV.

Walsh Procedure (97)

The design procedure proposed by Walsh is essentially a combination of the BRAB and Lytton methods. Similar to BRAB, Walsh proposes four types of slabs:

1. Thin Slab - 100mm slab with light edge beam.
2. Light Stiffened Raft - 100mm slab with stiffening beams at 3-4m spacing and a beam depth of 0.4m ($\sim$ 16 inches).
3. Heavy Stiffened Raft - similar to (2) but with deeper, more strongly reinforced beams.
4. Suspended Slab On Deep Foundation - slab is supported clear of the ground on walls and deep strip footings or on edge beams supported on deep piers.

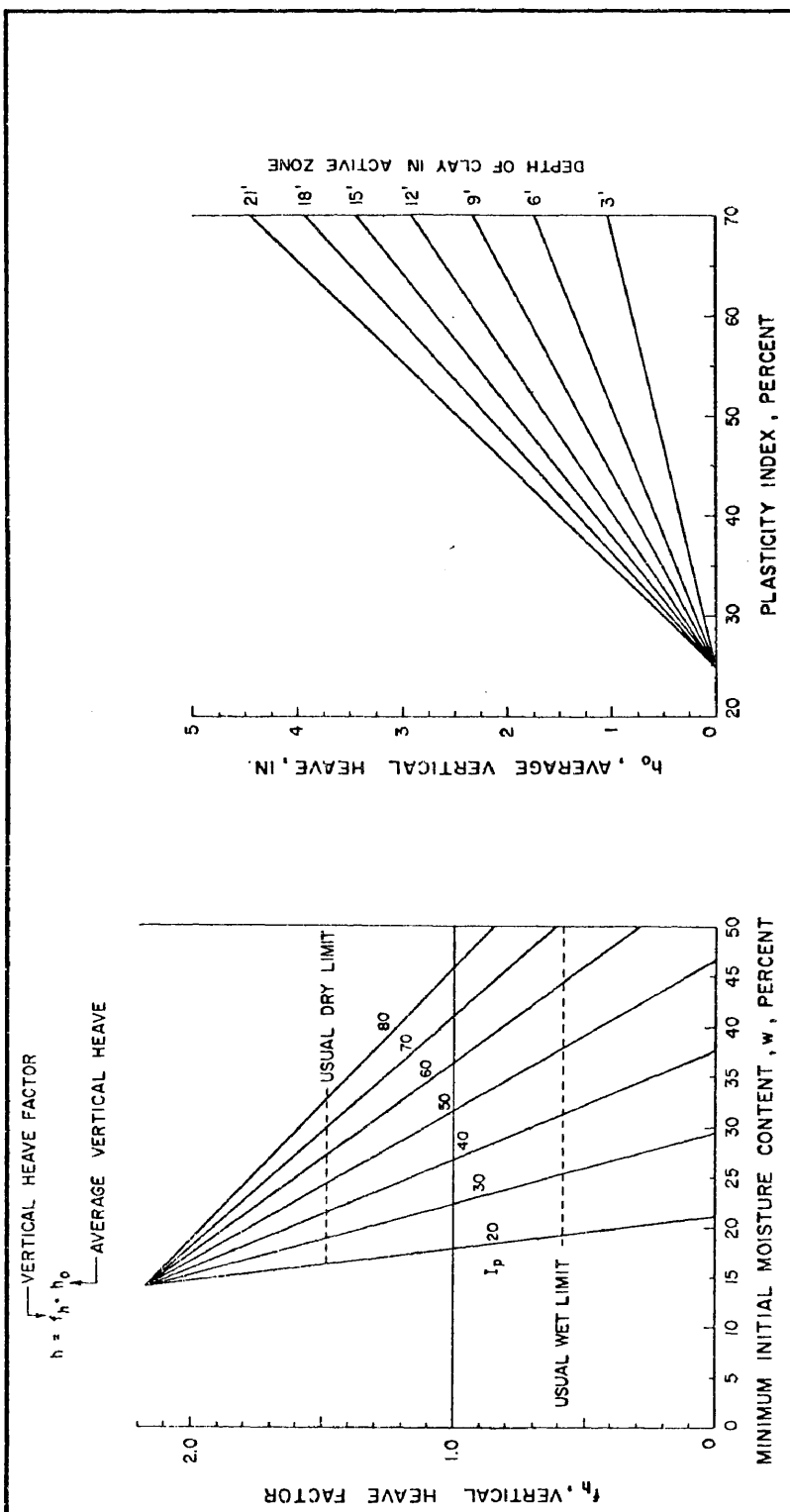

Figure 9. Design Aid For Estimating Differential Swell, [After Lytton (53)].

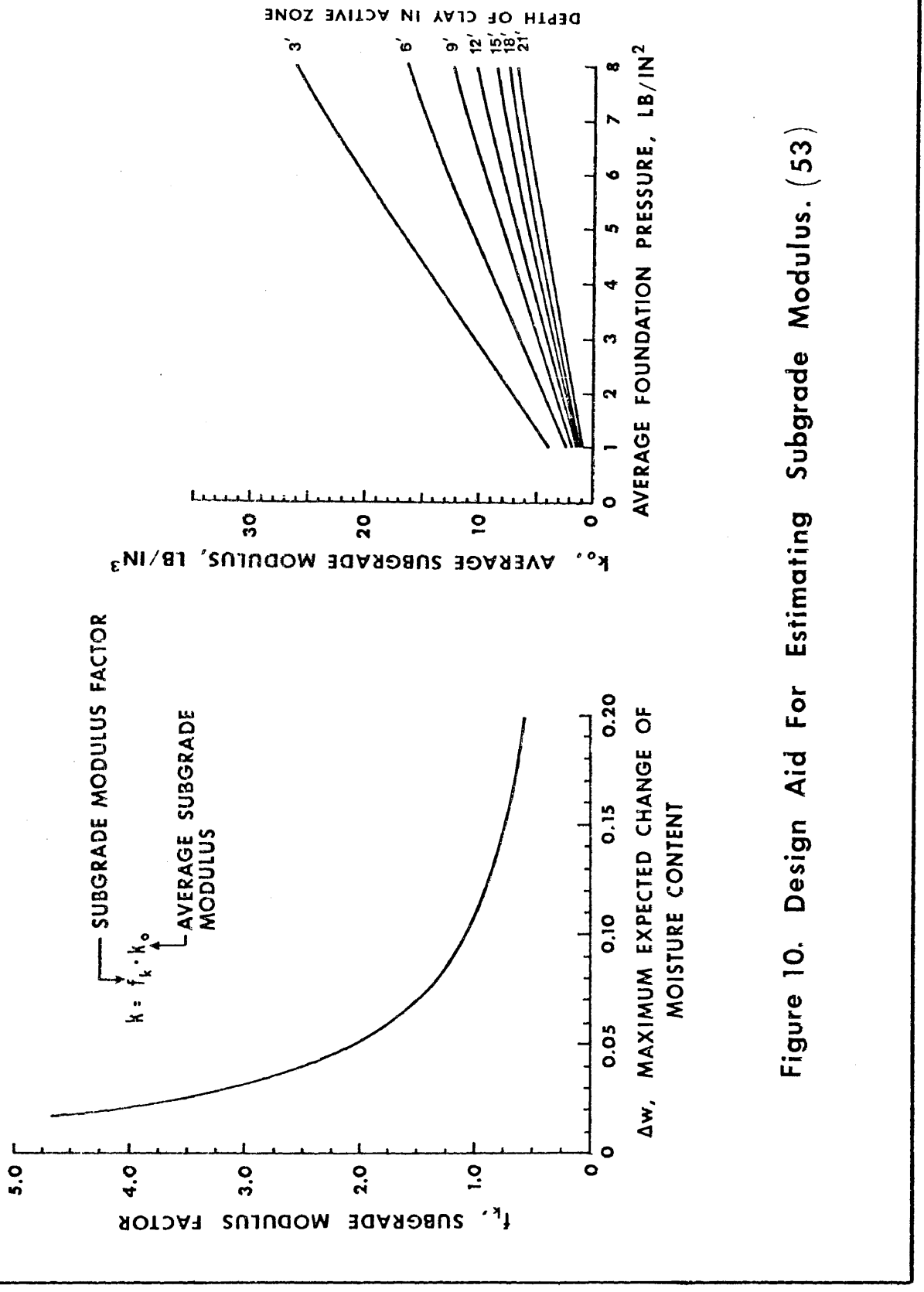

Figure 10. Design Aid For Estimating Subgrade Modulus. (53)

From the soil profile and the expected y_m value, the required slab can be selected from Table 5.

Walsh's method is based on the simplified center and edge lift soil profiles shown in Figure 11. The parabolic mound shape adopted by Lytton is modified to a flat topped mound with parabolic ends. This simplifies the interaction analysis and overcomes problems associated with large values of y_m that is experienced with Lytton's method (101). Walsh assumes the slab to be non-rigid and that it interacts with the soil mound. The loading, w, is assumed to be uniformly distributed over the whole slab area as in the BRAB procedure and the postulated soil-structure interaction is depicted in Figure 12.

As in the other two procedures, Walsh's model requires the difficult-to-quantify edge penetration or distance of non-support, e, around the slab perimeter. Additionally, a value of the modulus of subgrade reaction, k, is required as in the Lytton method.

Walsh uses the same type of spring foundation model used by Lytton but with the previously described modified mound shape and solves the same differential equation used by Lytton (51, 53). He obtains his support index, C, by finite element methods.

The design procedure proposed by Walsh is stated concisely in 6 steps:

1. Estimate k, y_m, and e.

2. Calculate the total long duration load, w, averaged over the entire slab area.

3. Subdivide the slab into overlapping rectangular components.

TABLE 5. Selection of Slab Type From Foundation Conditions (From Walsh (97))

SOIL TYPE	EXPECTED DIFFERENTIAL MOVEMENT y_m	RECOMMENDED SLAB TYPE	
Gravel and sands[A]	Stable < 10mm	1	(Thin Slab)
Silts[B]	Stable < 10mm	1	(Thin Slab)
Clays and silty clays	Stable < 10mm	1	(Thin Slab)
	Intermediate < 25mm	2	(Light Stiffened Raft)
	Unstable > 25mm	3	(Heavy Stiffened Raft)
Peats and low strength soils	---	4	(Suspended slab on deep foundation)

[A] Loose sands should be compacted or a type 3 or 4 slab may be required.

[B] For moderately low strength soils for which the unconfined compressive strength is less than 7½ times the average loading on the slab, a type 3 slab is required. For very low strength soils a type 4 slab should be used.

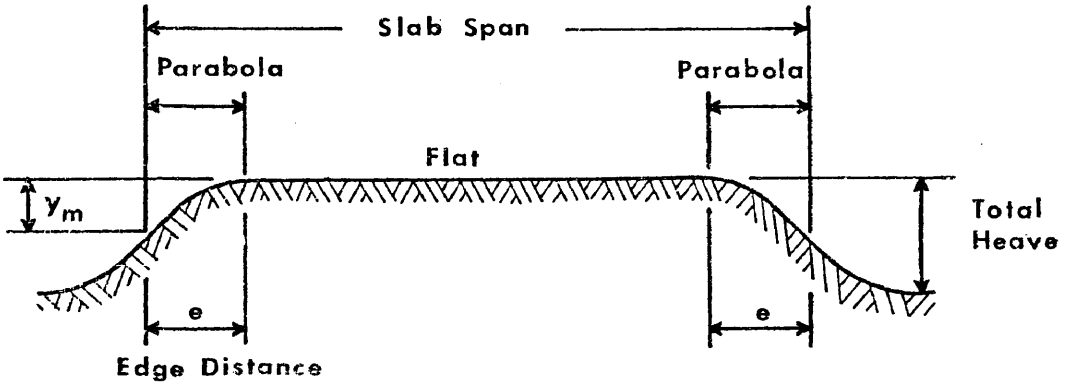

CENTER LIFT

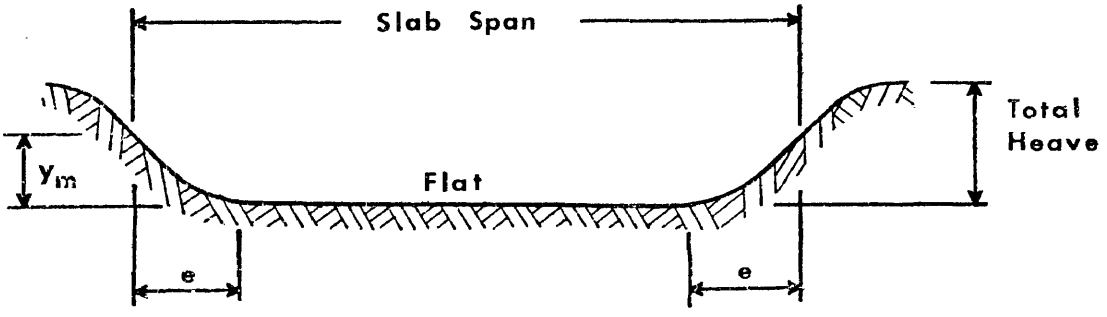

EDGE LIFT

Figure 11. Mound Shapes Assumed by Walsh (97).

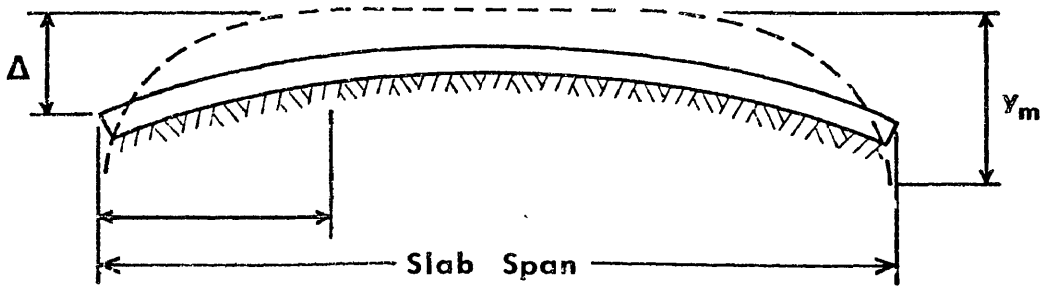

CENTER LIFT

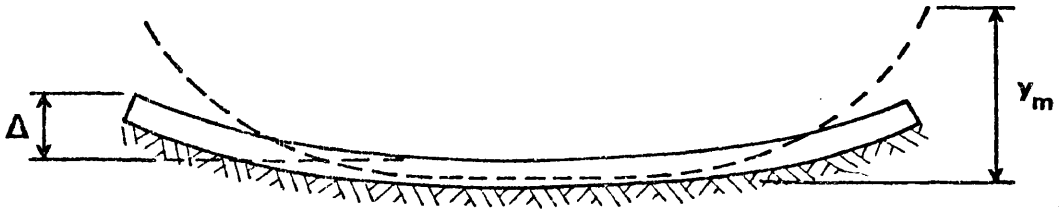

EDGE LIFT

Figure 12. Soil-Structure Interaction With Initial Mound As Assumed by Walsh (97).

4. Determine the allowable differential movement, Δ, from a recommended value of Δ/L for various types of superstructure construction (See Table 12, p.86).

5. From the values of $\frac{w}{k\, y_m}$, $\frac{e}{L}$, $\frac{\Delta}{y_m}$, and the anticipated swelling profile, determine the support index from Table 6. (This is a product of his finite element interaction analysis).

6. Using the simplified support conditions described above and Equations (3-1), (3-11), and (3-12) for moment, shear, and deflection, respectively, determine the perimeter and interior beam depths, beam spacings, and steel reinforcement from Table 7. Beam spacing is limited to a maximum of 4 meters (13.12 feet).

Fraser and Wardle Method (23)

Fraser and Wardle modified the Lytton and Walsh approaches by using a three-dimensional semi-infinite elastic soil foundation model instead of a Winkler or coupled spring model (101). Their model was analyzed using the Commonwealth Scientific and Industrial Research Organization (SCIRO) FOCALS computer program as an interacting plate rather than the two-dimensional beams used by Lytton and Walsh. Their approach produced smaller sections than any of the previously described methods, however, they apparently had the same problem as the other methods, i.e., defining the mound shape and edge penetration distance (101).

The finite element plate resting on a semi-infinite elastic soil is a sophisticated approach to the problem. However, these investigators stopped short of producing a general design procedure

TABLE 6. Computed Support Coefficients From Beam on Mound Analysis, for Different Values of Δ/y_m (After Walsh (97))

$\frac{e}{\text{span}}$	$\frac{w}{ky_m}$	Support Index C						
		Centre heave					Edge heave	
		0.1	0.2	0.4	0.6	0.8	0.1	0.2
0.100	0.1	0.81	0.84	0.89	0.92	0.92	0.96	+[A]
	0.2	0.80	0.83	0.87	0.91	0.95	+	+
	0.3	0.80	0.83	0.87	0.90	0.97	+	+
	0.4	0.81	0.83	0.86	0.94	+	+	+
	0.5	0.81	0.83	0.87	+	+	0.96	+
0.125	0.1	0.78	0.81	0.86	0.89	0.92	0.97	+
	0.2	0.77	0.80	0.85	0.89	0.95	+	+
	0.3	0.78	0.80	0.84	0.88	0.97	+	+
	0.4	0.79	0.81	0.84	0.88	+	+	+
	0.5	0.80	0.81	0.85	+	+	0.96	+
0.167	0.1	0.72	0.76	0.81	0.85	0.90	0.96	0.97
	0.2	0.73	0.76	0.81	0.85	0.92	0.96	+
	0.3	0.74	0.76	0.81	0.85	+	0.97	+
	0.4	0.75	0.78	0.81	0.85	+	+	+
	0.5	0.77	0.79	0.82	0.96	+	+	+
0.200	0.1	0.67	0.71	0.77	0.82	0.87	0.95	0.97
	0.2	0.69	0.72	0.77	0.82	0.87	0.96	+
	0.3	0.71	0.74	0.78	0.83	0.95	0.96	+
	0.4	0.73	0.75	0.79	0.83	+	0.96	+
	0.5	0.75	0.76	0.81	0.91	+	+	+
0.250	0.1	0.61	0.65	0.71	0.77	0.83	0.94	0.96
	0.2	0.64	0.67	0.73	0.78	0.84	0.95	+
	0.3	0.67	0.70	0.74	0.79	0.89	0.95	+
	0.4	0.70	0.72	0.76	0.81	+	0.96	+
	0.5	0.72	0.74	0.78	0.89	+	0.95	+
0.333	0.1	0.51	0.54	0.61	0.68	0.76	0.92	0.96
	0.2	0.57	0.59	0.65	0.71	0.79	0.93	0.96
	0.3	0.61	0.64	0.69	0.75	0.89	0.93	+
	0.4	0.65	0.67	0.72	0.79	+	0.94	+
	0.5	0.67	0.70	0.76	0.90	+	0.78	+
0.50	0.1	0.38	0.40	0.45	0.53	0.68	0.90	0.93
	0.2	0.48	0.50	0.56	0.64	0.84	0.90	0.94
	0.3	0.55	0.57	0.63	0.73	+	0.90	0.95
	0.4	0.59	0.62	0.69	0.88	+	0.90	0.95
	0.5	0.56	0.60	0.81	+	+	0.87	0.93

[A] A_C = 0.98-1.00. (Use minimum section beams, as per light stiffened raft.)

TABLE 7. Allowable Section Capacities - Per Meter of Beam (After Walsh (97))

Allowable section capacities - per metre width of beam							
		f_{sy} = 230 MPa			f_{sy} = 450 MPa		
p (%)	H (m)	M (MN.m)	EI_2 (MN.m^2)	V (kN)	M (MN.m)	EI_2 (MN.m^2)	V (kN)
0.5	0.4	0.070	75	164	0.082	75	164
		-			0.099	50	164
		-			0.115	37	164
	0.5	0.119	150	211	0.131	150	211
		-			0.164	93	211
		-			0.196	68	211
	0.6	0.182	262	258	0.191	263	258
		-			0.245	158	258
		-			0.299	115	258
	0.7	0.258	421	305	0.263	421	305
		-			0.344	248	305
		-			0.424	182	305
	0.8	0.347	634	352	0.347	634	352
		0.347	633	352	0.459	368	352
		0.347	632	352	0.571	271	352
	0.9	0.442	909	399	0.442	909	399
		0.446	981	399	0.591	661	399
		0.450	875	399	0.739	523	399
	1.0	0.549	1253	446	0.549	1253	446
		0.557	1212	446	0.739	716	446
		0.556	1174	446	0.929	531	446
(Tables for p = 0.75% and 1.00% not included.)							

and the cost of this sophisticated analytical procedure places it out of the reach of most engineers attempting to arrive at a designed slab-on-ground section.

Other Design Methods

Rigby and Dekena (72). These investigators suggest the bending moment produced by a center heave condition can be calculated from:

$$M = \frac{K W \ell^2}{2} \quad \ldots\ldots\ldots\ldots\ldots\ldots\ldots\ldots\ldots\ldots \quad (3\text{-}15)$$

where W = weight of the wall plus all the loads which rest on it, expressed as per unit length

ℓ = half the length of the wall

K = empirical coefficient

The empirical coefficient K has an apparent maximum of 1.0 for the case of a point load acting beneath the center of the house (77) but Rigby and Dekena state the values normally applied in South Africa range from 0.5 to 0.8 "according to site conditions." The actual selection of the value to be used for K appears to be a purely subjective selection and is probably based completely on engineering experience.

Dawson (15). Dawson did not present any design equations but presented an approach to design that was apparently a forerunner to 1968 BRAB procedure. He suggests that "A stiff, reinforced concrete slab acts like a boat on expansive clay and 'rides out' the movement of the soil. The slab must be properly reinforced to support

the structure under all conditions that will occur." He presents a table of "Climatic Ratings" which, in association with the Unified Soil Classification System of identifying the soil type, allows the designer to enter a second table and determine the slab type recommended for those particular soil and climatic conditions. Dawson's tables are reproduced as Tables 8 and 9; Dawson's second table (Table 9) is very similar to the final BRAB recommendation table (Table 4, p.27) and the slab types (I, II, III, IV) are the same in both.

Dawson's final contributions to a design approach are to present a correlation between climatic conditions and the plasticity index to obtain a "C factor" which is defined as the "minimum effective support area of the slab" (Figure 13), and a correlation between *PI* and Climatic Rating to obtain recommended site compaction requirements (Figure 14).

Salas and Serratosa. Building on the empirical formula of Rigby and Dekena, Salas and Serratosa propose two equations for calculating the bending moment resulting from a center lift condition. The first equation assumes no reduction of swelling pressure before the swelling mound begins to distort the overlying foundation. In this case the bending moment is given by:

$$M = \frac{w\ell^2}{2}\left(1 - \frac{w}{q_f}\right) \quad \text{(3-16)}$$

where w = total weight transmitted by the slab to the soil divided by the total slab area

TABLE 8. Climatic Ratings (From Dawson (15))

RATING	SYMBOL	NORMAL PRECIPITATION VARIATION	MAXIMUM PERIOD OF DROUGHT*
Favorable	F	Small Variation	4 weeks
Intermediate	I	Moderate Variation	6 weeks
Unfavorable	U	Considerable Variation	6 to 12 weeks
Extremely unfavorable	EU	Large Variation	Over 12 weeks

* This is the probable maximum during the life of the structure, not the annual expected maximum.

TABLE 9. Slab Type Recommendations Based on Soil and Climatic Conditions (From Dawson (15))

SOIL TYPE[1]	MINIMUM DENSITY OR CONSISTENCY	CLIMATIC RATING[2]	RECOMMENDED SLAB TYPE
GW, GP	All Densities	All	I
GM, GC, SW, SP, SM	Medium	All	I
SC, ML	Dense	All	I
GM, GC, SW, SP, SM	Loose	All	II[4]
SC, ML, MH	Loose[3]	All	II[4]
CL, OL	Stiff	F and I	II
CL, OL	Stiff	U and EU	III[5]
CL, OL	Soft	All	III[3]
CH, OH	Stiff	F	II
CH, OH	Soft	F	III[3]
CH, OH	All	I, U, and EU	III[3]
PT	All	All	IV

[1] Unified Soil Classification.

[2] See Table 8

[3] Where very soft or very loose materials are encountered, Type IV is recommended, because of probably large settlements.

[4] Type I slabs can be used if these soils are densified by compaction before placing concrete.

[5] For CL soils with a Plasticity Index of less than 45, a Type II slab may be used.

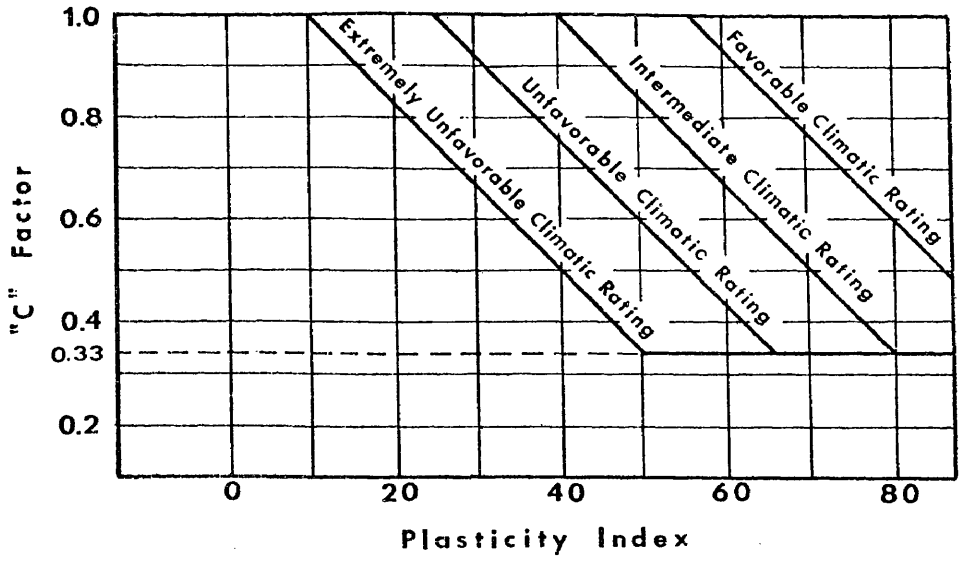

Figure 13. Minimum effective support area of slab as a function of soil plasticity index and climatic ratings [After Dawson (15)].

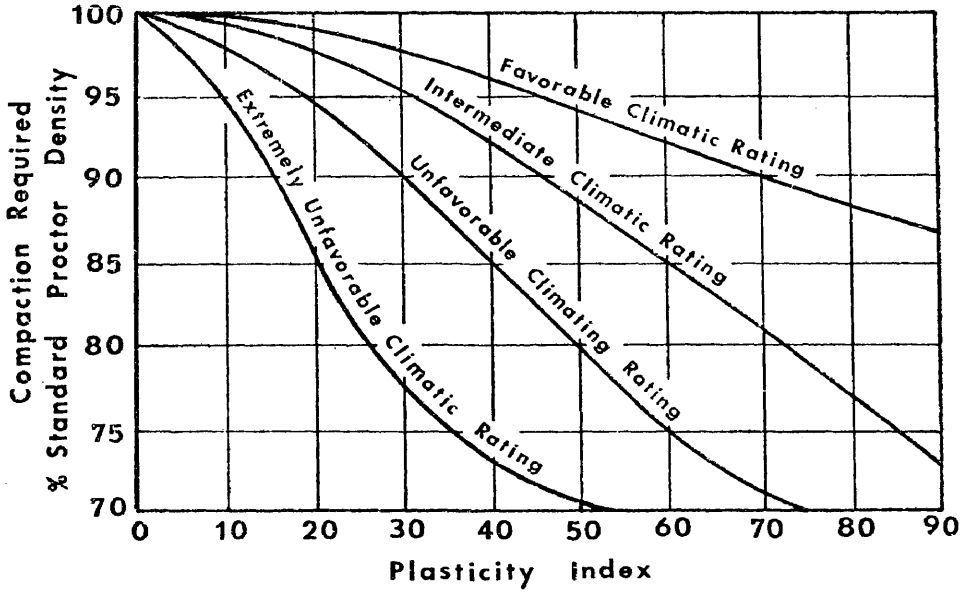

Figure 14. Site compaction requirements based on soil plasticity index and climatic ratings [After Dawson (15)].

ℓ = one-half the slab length in the direction being considered

q_f = ultimate load of the foundation soil

They obtain the value of $\frac{w}{q_f}$ by using the constant K from Rigby and Dekena, which, according to those investigators, ranges practically between 0.5 and 0.8:

$$K = 1 - \frac{w}{q_f} \quad \ldots\ldots\ldots\ldots\ldots\ldots\ldots\ldots \quad (3\text{-}17)$$

If some measures are taken, however, to allow some dissipation of the swelling pressure through deformable layers between the soil and the foundation (cinders, rubber, cork, and asphalt were suggested), Salas and Serratosa recommend the bending moment to be calculated from

$$M = \frac{(p_1 - w)\,\ell^2}{6} \quad \ldots\ldots\ldots\ldots\ldots\ldots\ldots\ldots \quad (3\text{-}18)$$

where w and ℓ are as previously defined and:

p_1 = swelling pressure on the foundation.

Since p_1 must be measured, they suggest that K can now be directly calculated from

$$K = \frac{p_1 - w}{3w} \quad \ldots\ldots\ldots\ldots\ldots\ldots\ldots\ldots \quad (3\text{-}19)$$

In one test of this proposal, they determined the value of K to be 0.063 rather than the 0.5 - 0.8 used with Equation (3-15).

City of Knox (101). This suburb of Melbourne, Australia, proposed the following equation for calculating the bending moment:

$$M = 0.125w\,(E_{\ell s})^2 \left[\frac{1.22 - D}{0.905}\right]^2 \quad \ldots\ldots\ldots\ldots \quad (3\text{-}20)$$

where M = bending moment, in kNM

w = total live load in direction being considered

$E_{\ell s}$ = effective linear shrinkage

D = depth of beam below the soil surface, in meters

This equation is based on three assumptions (101).

1. Two mounds form beneath the footing,
2. The slab is perfectly flexible, and
3. The seasonal movement occurs to a depth of 1.2 meters.

City of Oakleigh (101). Oakleigh is also a suburb of Melbourne, Australia, and uses equations developed by Lytton (53) but specifies the support index, c, to range between 0.7 and 0.9, depending on the site conditions, and allows no correction for plate action.

Fargher (101). This method is a modification of Lytton's method in which it is assumed that only the end portions of rafts are subject to reduced support. Design proceeds by assuming a slab only 6 meters long and the mound shape, m, to have a value of 4. There is no opportunity for deviation by using actual slab dimensions or a different mound shape exponent (101).

Summation

The four design procedures that are considered to be the most rational have several things in common. All of the methods require either a support index, c, or an edge "lift-off" distance; both parameters are difficult to measure or predict. They all require some estimate of the differential swell of the supporting soil. Additionally, they each require some estimate of either the subgrade modulus or the modulus of elasticity of the soil in order to describe the interaction occurring between the slab and the underlying soil. If a new design procedure is to be developed, it must incorporate design parameters that are familiar to the design engineer and can be easily obtained and used by him in his design efforts. To this end, the best features of each of the four present principal design procedures are used as guides in developing the investigative model used in this study.

CHAPTER IV

MODELING THE PROBLEM

There are eight principal variables involved in designing a slab-on-ground that is to be constructed over expansive soil. Of these, one is climate; three are soil parameters: (1) the swelling soil profile beneath the slab, (2) the differential soil movement, and (3) the edge moisture variation distance; and four are structural parameters; (1) slab length, (2) beam spacing, (3) depth of stiffening beams, and (4) magnitude of the superstructure loading.

Climate

When designing foundations for use on expansive soils, the engineer must realize that damaging soil movement is not a necessary consequence of construction. If the structure is to be located at a site which has a high swelling potential but the climate is such that little change in the soil moisture content occurs, then there is little opportunity for detrimental swelling or shrinking to occur. If the site is in an area that has high rainfall or the climate remains relatively wet throughout the year, then the soil has probably already experienced considerable expansion; application of additional soil moisture will produce only a very small amount of additional swell. The danger of a potentially high swelling soil in a region of wet climate derives less from swelling and more from soil shrinkage during periods of little or no rainfall. Conversely, if the site is in an area that has low rainfall and the climate remains relatively

dry throughout the year, then there is less opportunity for large differential swelling to occur. Thus, to arrive at a proper design, the engineer needs some environmental indicator or knowledge of the climate at the project site in order to estimate the severity of the shrink-swell activity of the soil on which his foundation will reside.

One such environmental indicator is the index of potential evapotranspiration which was introduced by Thornthwaite (88). This quantity is defined as the amount of water which would be returned to the atmosphere by evaporation from the ground surface and transpiration by plants if there was an unlimited supply of water to the plants and soil. A positive Thornthwaite Moisture Index measurement, I_m, indicates a net surplus of soil moisture while a negative number indicates a net soil moisture deficit. The determination of this measurement index is entirely rational and can be applied to any location throughout the world. A map of this quantity as it is distributed across the United States is shown in Figure 15 ; a more detailed map of the distribution in Texas is shown in Figure 16 .

Soil Parameters

Swelling Soil Profile. - Designers face a degree of uncertainty as to the pattern of deformation or heave that the soil will develop beneath the slab because of the number of unpredictable or uncontrollable causes of moisture change which may occur. In a study of 69 residential slabs in Arlington, Texas, by Tucker and Poor (93) none of the slabs showed exactly the same distortion pattern , but most

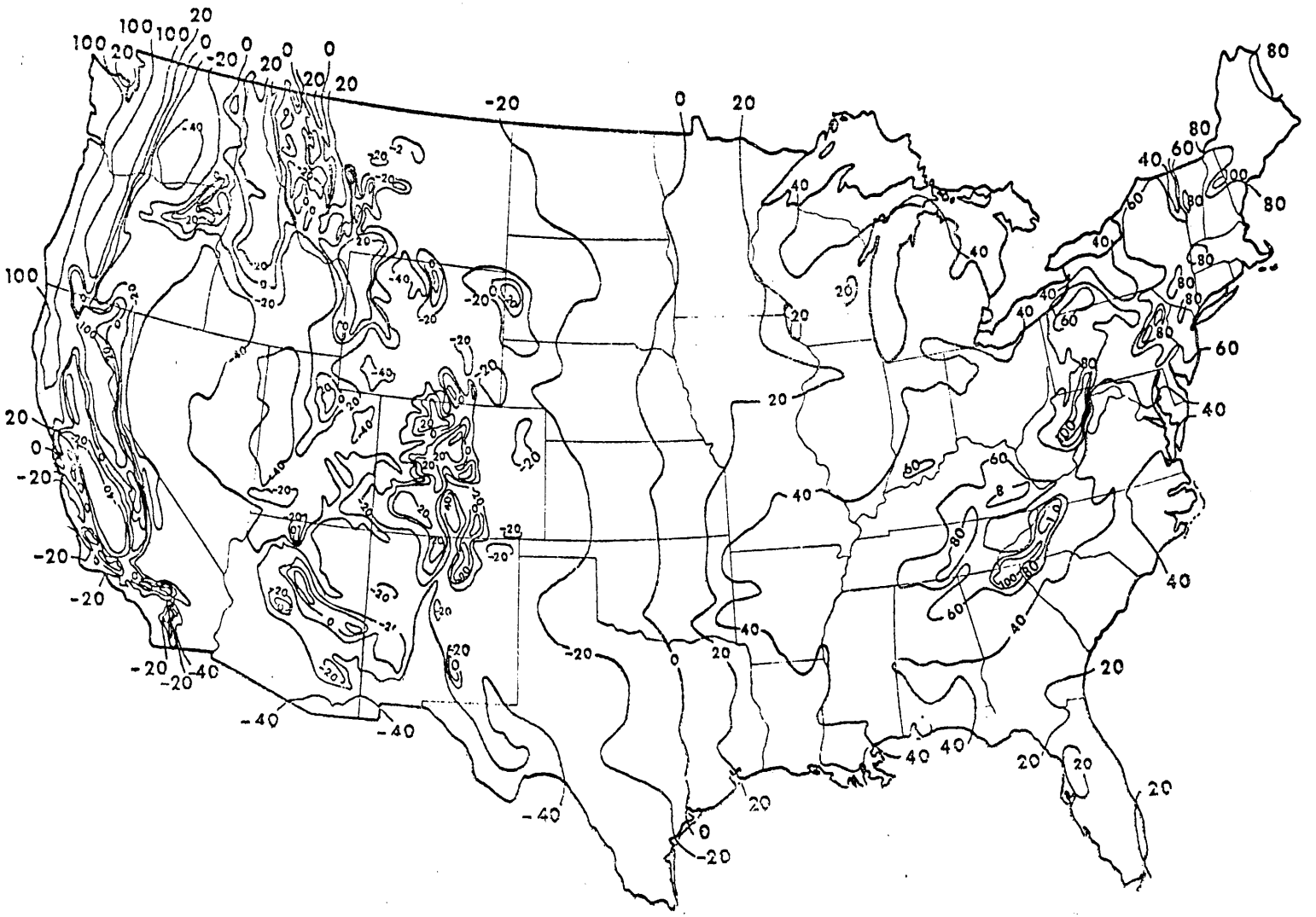

FIGURE 15. THORNTHWAITE MOISTURE INDEX DISTRIBUTION IN THE UNITED STATES (88).

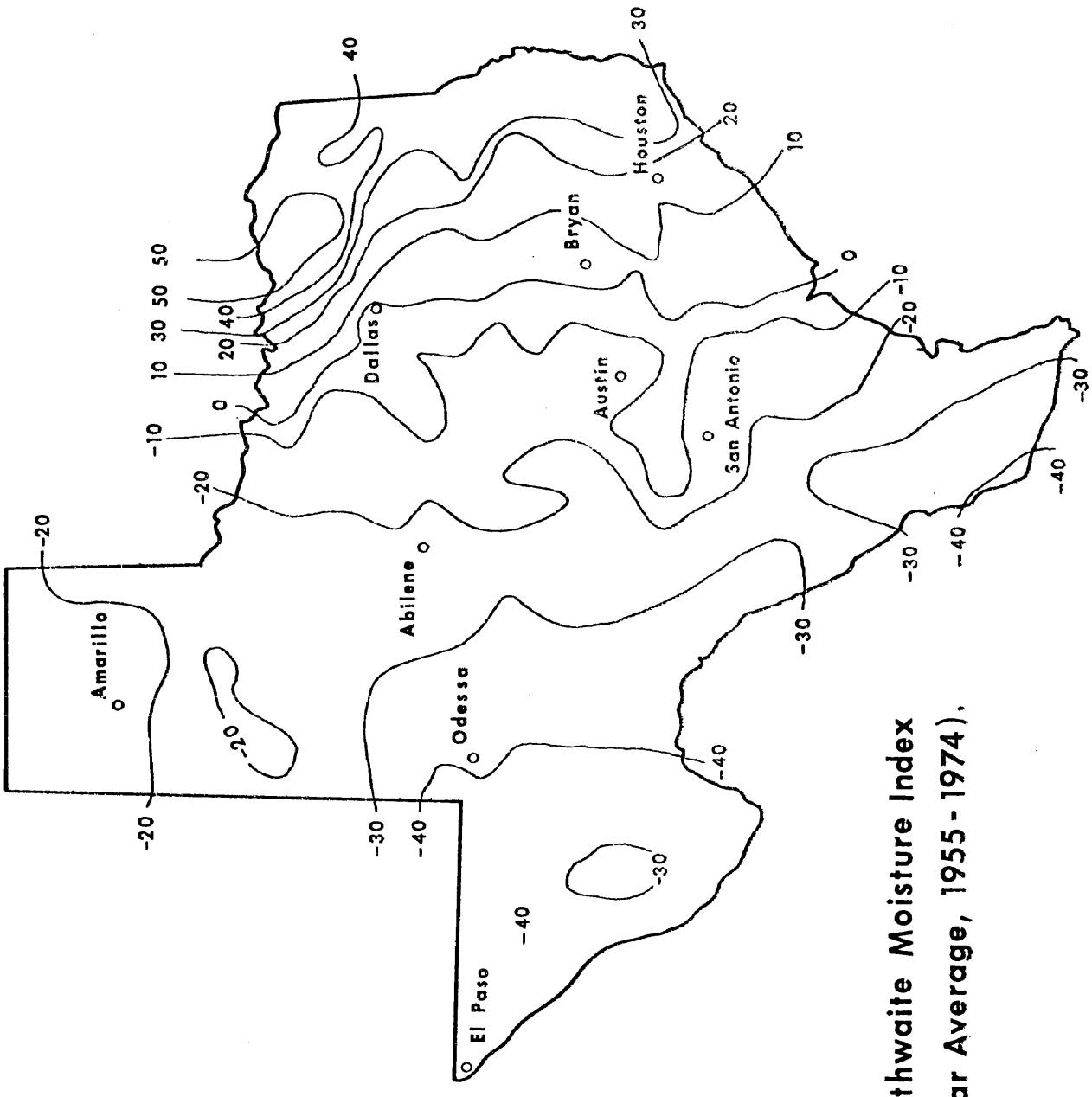

Figure 16. Thornthwaite Moisture Index for Texas (20 Year Average, 1955-1974).

showed a tendency to have a higher elevation near the center of the slab than around the perimeter. These houses were 9 to 17 years old when investigated and this distortion pattern is in accordance with observations by other investigators (16,32,51,100). This particular distortion mode has been given several descriptive terms, including center lift, doming, and center heave. An exaggerated sketch of this distortion mode is shown in Figure 11.p. 42.

The opposite swelling mode most often mentioned in the literature is termed edge lift, dishing, or edge heave (32,51,57,97). Although the center lift mode is generally a long term effect, the edge lift mode is typically a short term or a seasonal effect (57). Castleberry (10) could not find any statistically significant correlation between edge lift and age of slab, implying that the edge lift condition was not a long term condition.

Several theories have been proposed to explain the development of these two principal swelling shapes (31,32,39,57,100) but most of these explanations can be summarized in two statements.

1. The center lift condition occurs either due to an increase in moisture content beneath the interior of the slab (also termed "wetting up"), a decrease in moisture content around the perimeter of the slab ("edge drying"), or a combination of these two conditions.

2. The edge lift condition occurs when the moisture content increases around the perimeter of the slab.

Regardless of which soil distortion mode occurs, the slab will also be bent or distorted according to the movement of the soil beneath the slab. Lytton (50) made a careful study of plate bending

and distortion. The types of distortion considered in his study were the four principal modes of:

1. Center Lift - Cylindrical
2. Edge Lift - Cylindrical
3. Center Heave (or Perimeter Drying)
4. Corner Heave (or Diagonal Drying)

These distortion patterns are shown in Figure 17. Figures 17a and 17c exhibit unimodal bending while Figures 17b and 17d are higher order bending modes producing both positive and negative bending moment values. Lytton found that the higher the order of bending mode, the lower the values of moment, shear, and deflection. He also found the center doming condition to be both the simplest and most severe case, inducing the greatest bending moments in both directions in a rectangular plate. Thus, using the distortion pattern of Figure 17c for either the center lift or edge lift condition will produce the largest values for the design parameters of moment, shear, and differential deflection, i.e., the most conservative design values.

Differential Swell.

Determining Differential Swell. - The amount of swell expected beneath a slab is important to the design problem. However, if the soil beneath the slab were to swell uniformly, then no distortion would be caused in the slab and the superstructure it supports. Distortion occurs when the supporting soil swells non-uniformly or differentially. Thus, the differential swell is more important than the total expected swell.

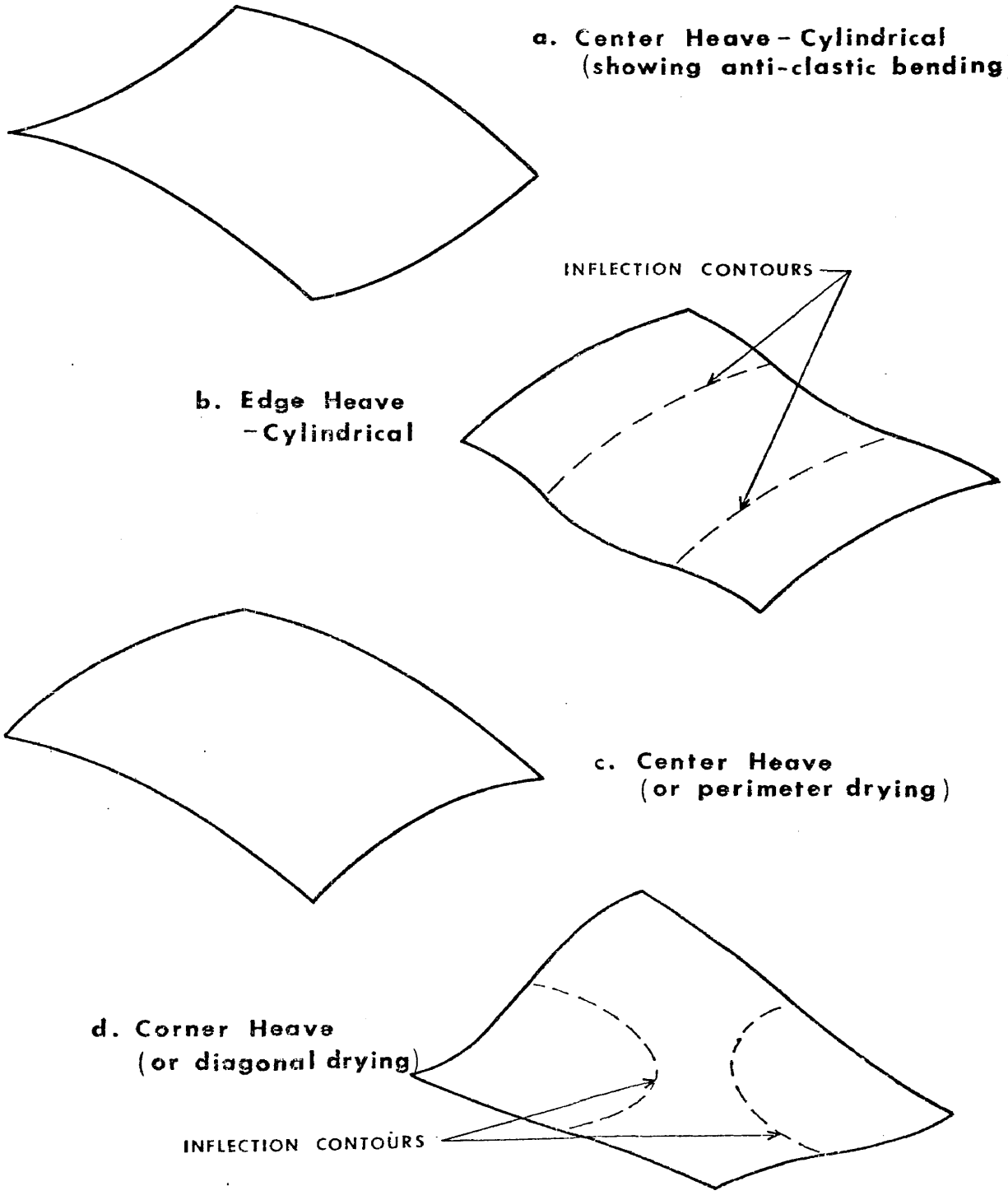

Figure 17. Principal distortion modes for rectangular plates [After Lytton (50)].

There are a number of procedures for testing soils to determine the amount or percent of volume change to be expected. Most of these can be classified into four general types: (1) oedometer or consolidometer tests, (2) linear shrinkage tests, (3) Cofficient of Linear Extensibility (C.O.L.E.), and (4) empirical methods

1. Consolidometer Methods. Despite the fact that the consolidometer test is used extensively for evaluating swelling clays, the procedures used by investigators are quite varied. For some detailed procedures see references 12 , 24 , and 78 . However, almost all test procedures can be divided into two general groups: The free swell (FS) test and the constant volume (CV) test.

In either test, the sample is placed in the consolidometer and subjected to some pre-determined pressure. The samples are then allowed access to water. In the FS test, the sample is allowed to change volume until equilibrium is reached. The sample is then loaded and unloaded in the conventional manner of the consolidation test. The pressure required to reduce the volume of the sample to its original volume is termed the swelling pressure. In the constant volume test, the total pressure on the sample is increased as necessary in order to maintain the sample at a constant volume. The pressure at which there is neither a tendency for volume increase nor decrease is termed the swelling pressure of the soil. However, according to Fredlund (24), who has extensively studied the procedural aspects of the consolidation method of testing swelling soils, the procedural factors inherent in both the FS and CV tests produce results that underestimate the field swelling pressures.

2. Linear Shrinkage Tests. The swell potential is assumed to be inversely related to the supposedly opposite property of shrinkage. The theory of this very simple test is that the shrinkage characteristics of a soil should be a reliable and consistent index to the swelling potential. Thus, by drying samples whose water content and length are known, an estimate of the percentage of expected swell can be determined.

3. C.O.L.E. Test. Developed by the Soil Conservation Service (22), this test is similar in concept to the linear shrinkage test except it uses irregularly shaped clods of 2-3 inches in diameter and the volume is measured rather than the length.

4. Empirical Methods. A number of methods have been developed from either experience or laboratory testing that will quickly give an estimate of swelling by performing simpler, quicker tests. A few methods are briefly described.

a. Chen (12). For any clay type, Chen proposes a relationship between the swelling potential and percentage of clay size:

$$S = KC^X \quad \ldots\ldots\ldots\ldots\ldots\ldots\ldots\ldots \quad (4\text{-}1)$$

where S = swelling potential expressed as a percentage of swell under 1-psi surcharge for a sample compacted at optimum moisture content to maximum density in the Standard AASHTO compaction test

C = percentage of clay sizes finer than 0.002mm

x = an exponent depending on the type of clay

K = coefficient depending on the type of clay.

b. Plasticity Index. A number of investigators have developed *PI* vs swell or percent swell curves from test results. Some of these are shown in Figures 18, 19, and 20.

c. Seed, Woodward, and Lundgren (59) found a correlation between expansion and the clay activity and the percent of clay sizes less than 2 μm:

$$S = 3.6 \times 10^{-4} A^{2.44} C^{3.44} \quad \ldots\ldots\ldots\ldots\ldots\ldots \quad (4\text{-}2)$$

where S = percent of swell

A = activity of PI/(C - n)

n = 5 (natural soils) or 10 (artificial soils)

C = percent of clay (<0.002mm)

Further analysis produced a similar relation between swell, *S* and the *PI*:

$$S = 2.16 \times 10^{-3} (PI)^{2.44} \quad \ldots\ldots\ldots\ldots\ldots\ldots \quad (4\text{-}3)$$

d. Ranganathon and Satyanarayana (59) developed a similar relation using the shrinkage index (SI)

$$S = 41.13 \times 10^{-5} (SI)^{2.67} \quad \ldots\ldots\ldots\ldots\ldots\ldots \quad (4\text{-}4)$$

Center Lift Swelling Profile. - The amount of differential

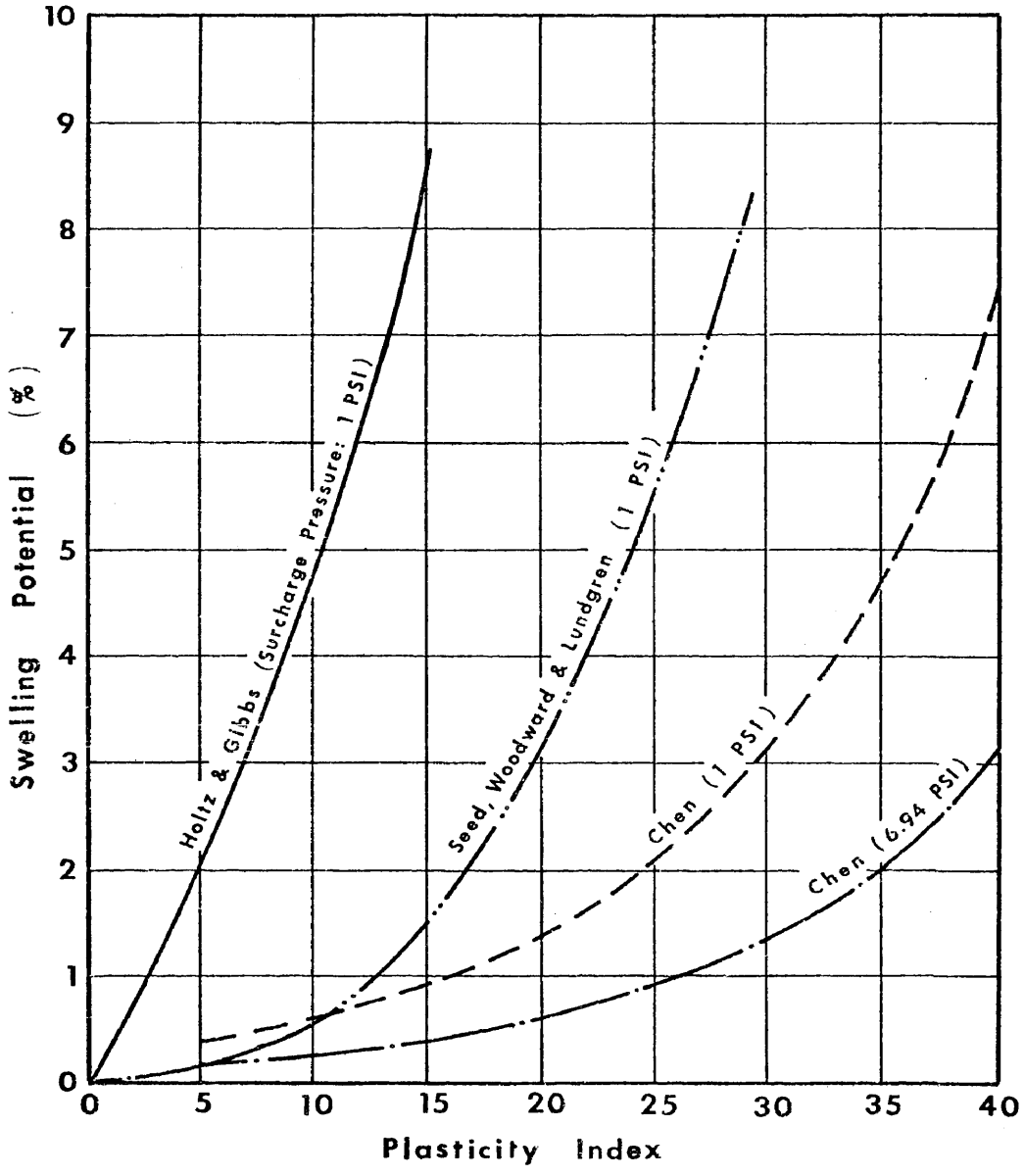

Figure 18. Relationship of volume change to plasticity index as predicted by Holtz, Seed, and Chen [After Chen (12)].

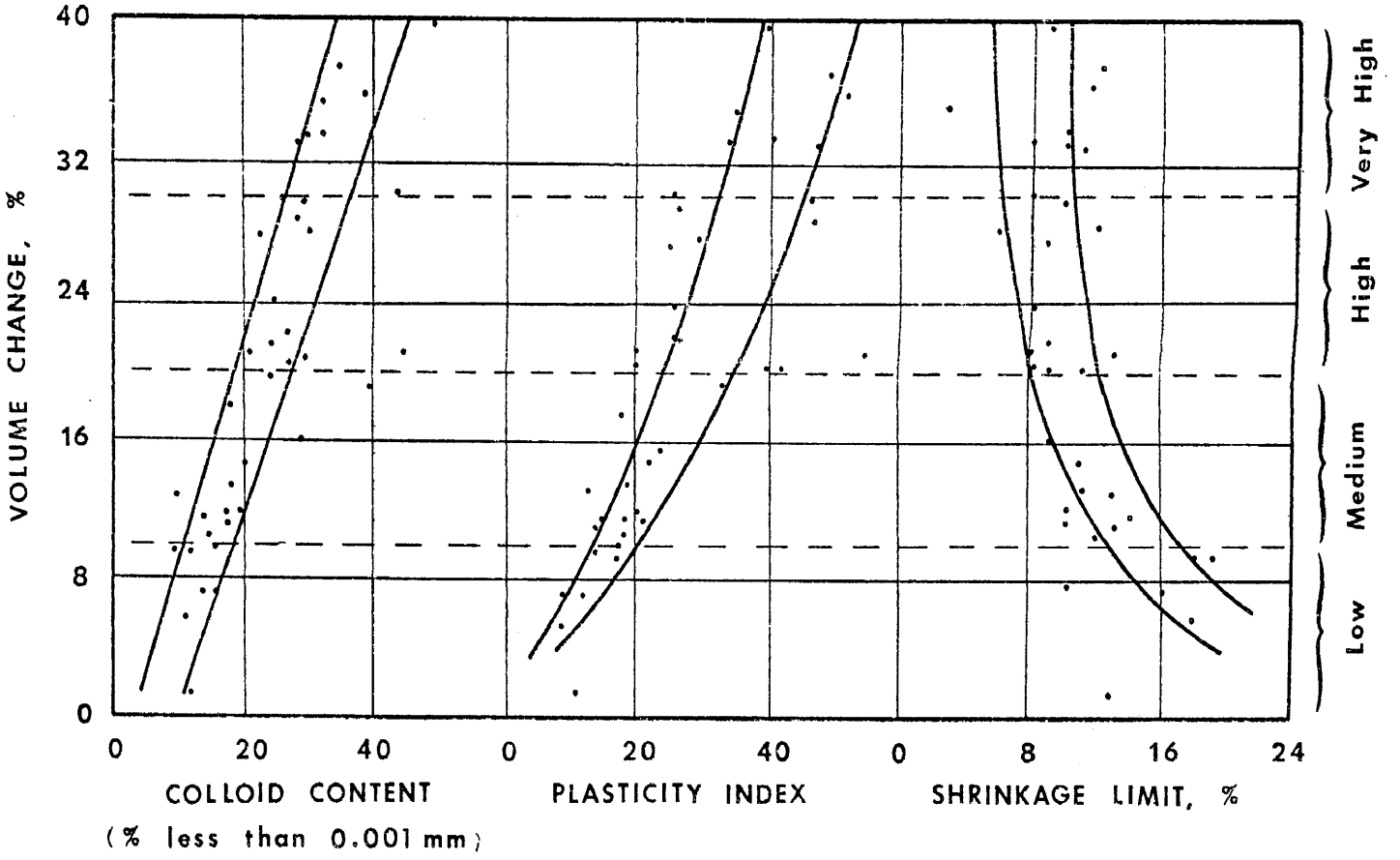

Figure 19. Relation of Volume Change to Colloid Content, Plasticity Index, and Shrinkage Limit [From Chen (12) After Holtz and Gibbs].

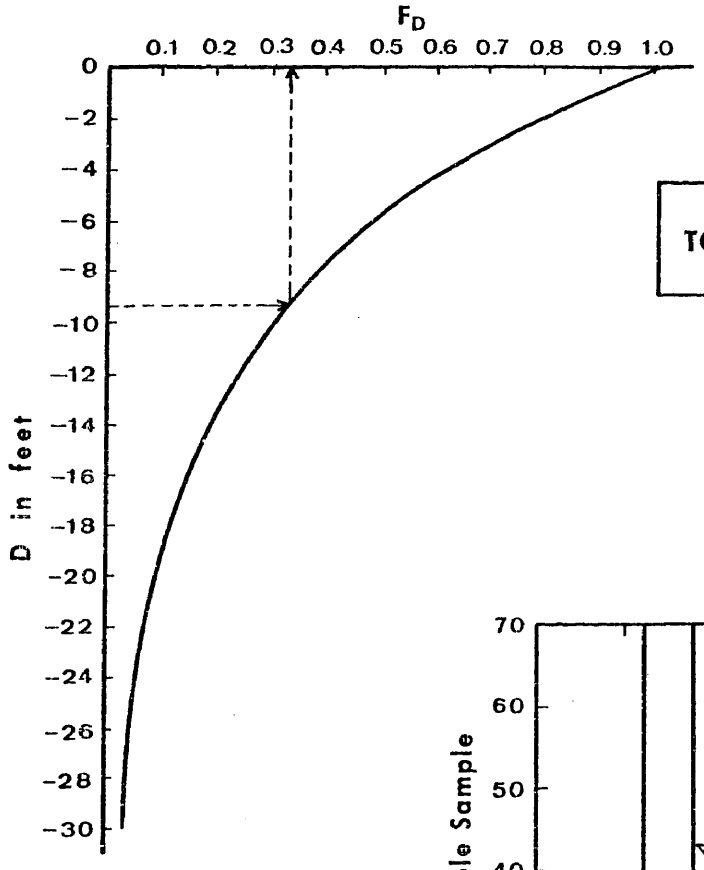

$$\text{TOTAL HEAVE} = \sum_{D=1}^{n} F_D \cdot (\text{P.E.})_D$$

P.E., POTENTIAL EXPANSIVENESS	HEAVE (in/ft)
Very High	1.0
High	0.5
Medium	0.25
Low	0

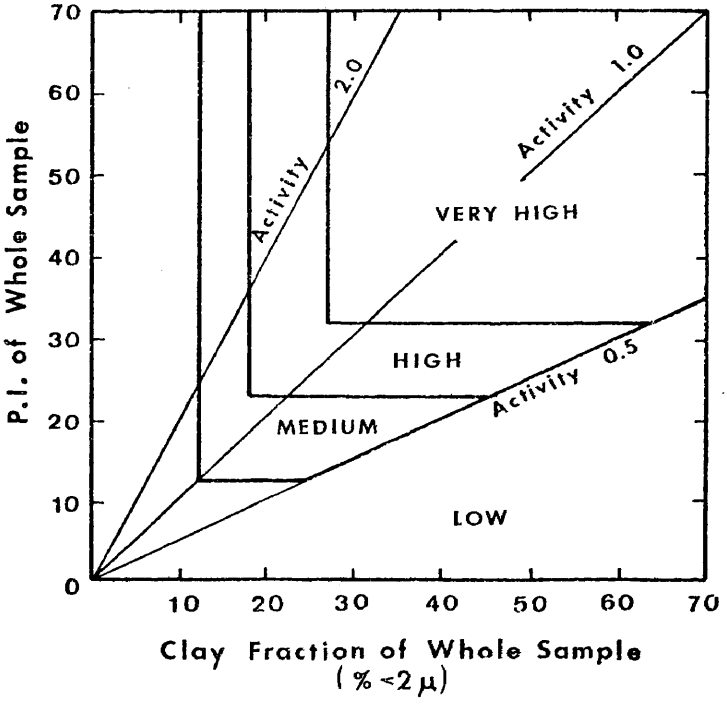

Figure 20. Prediction of heave from the Plasticity Index and percentage of clay fraction of soils [After Van der Merwe (95)].

swell or heave expected to occur beneath a slab over expansive clay can range from zero to several inches. Lytton (51) found a 1-inch differential would produce a Δ/L ratio of no more than 1/360, which is usually acceptable for houses with plastered walls. Although Chen (12) reported an extreme case of a 12-inch heave beneath a basement slab, most design engineers will select a different type of foundation if a differential heave greater than approximately 4 inches is expected (62). Thus, by analyzing conditions of differential deflection ranging between 0 and 4 inches, and particularly between 1 and 4 inches, most cases of slab-on-ground design will be included.

The shape of the swelling soil profile or swelling mound was a matter of uncertainty as well as being somewhat controversial until Lytton published photographs of an in situ swollen mound (51). He proposed that the shape of this swollen mound could be represented mathematically by a simple exponential relation:

$$y = cx^m \quad \ldots\ldots\ldots\ldots\ldots\ldots\ldots\ldots \quad (4\text{-}5)$$

where y = an offset below the high point of the mound

x = the horizontal distance from the high point

c = a constant

m = an exponent

De Bruijn (16) reported the measured shape of the swelling mound occurring beneath a covered surface in South Africa. Applying Equation (4-5) to de Bruijn's data, Figure 21, shows the validity of Lytton's equation.

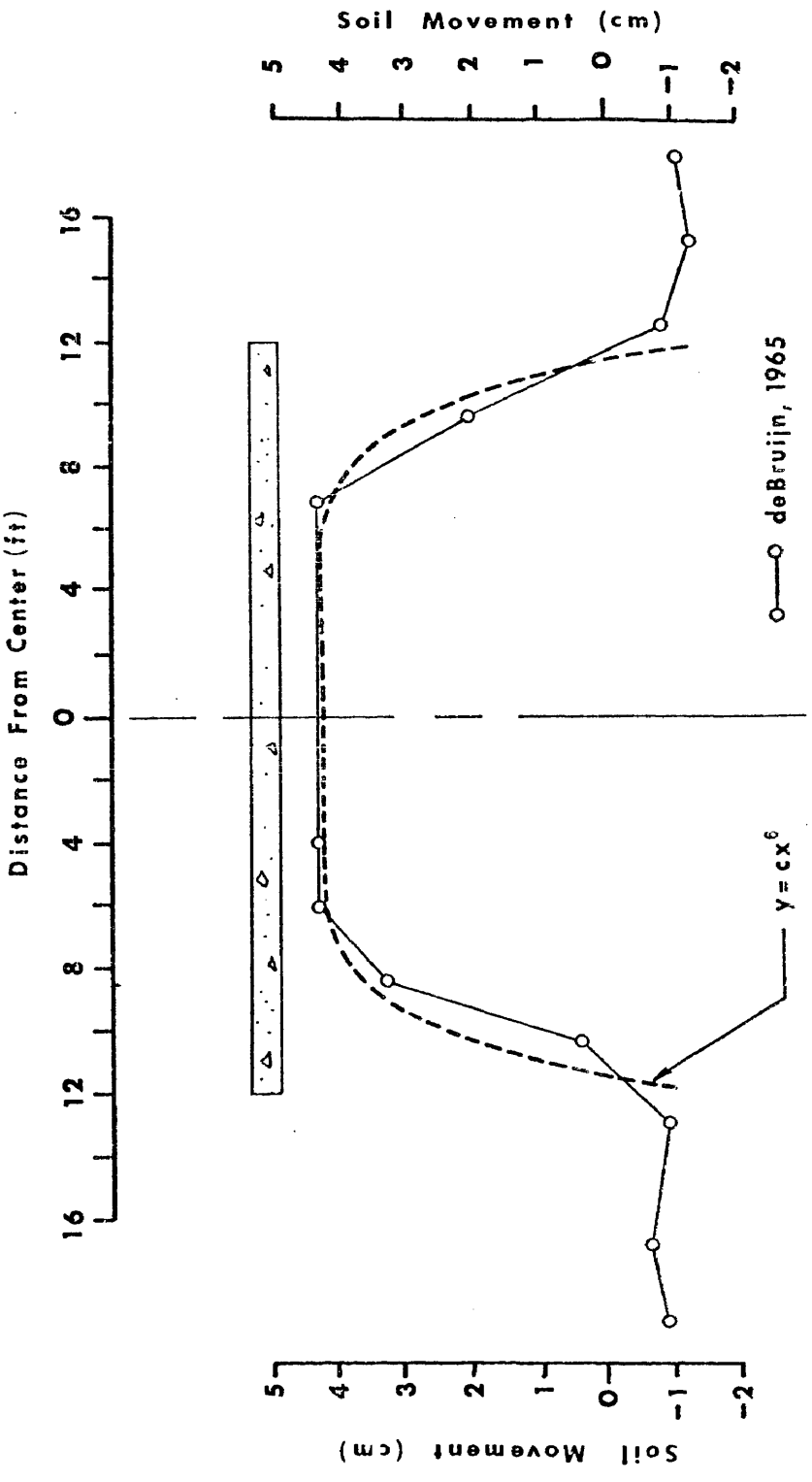

Figure 21. Comparison of deBruijn's Measured Swell Profile Beneath a Covered Surface to the Profile Predicted by Lytton's Exponential Equation.(16)

Using Equation (4-5) for longer slabs requires a very large value of m; see Table 10. Walsh modified the application of Equation (4-5) so that the shape of the swollen mound was flat beneath the interior of the slab and parabolic near the edge of the slab (Figure 11, p. 42). By doing this, the mound exponent, m, will seldom be required to exceed 7 or 8, which Lytton (53) implied was the maximum value of m to be expected, and the shape of the parabolic part of the swollen profile will be more rounded and the sharp change in slope caused by the large values of m will be avoided (Figure 22).

From Figure 22 it can be seen that a mound exponent of 2 produces the least support beneath the slab; an increasing value of m provides increasing slab support. Using a mound exponent value of 3 is not the most conservative value but is probably still sufficiently small enough to produce conservative values of moment, shear and differential deflection when compared to the exponent fitting de Bruijn's data (Figure 21).

Edge lift Profile. To this writer's knowledge, there have been no reported observations of the shape of the swollen soil in the edge lift condition, such as have been observed and reported for the center lift condition by de Bruijn and Lytton. There have been some measurements of slabs distorted by edge lift swelling reported (21, 39), but no measurements of only the swelling soil mound. Either reversing or inverting the parabolic shape of the center lift profile produces a swelling surface that is difficult to imagine occurring in nature, particularly with large values of mound exponent. These unlikely profiles are shown in Figures 23a and

TABLE 10. Variation of Mound Exponent, m, with Slab Length

SLAB LENGTH (ft)	EDGE PENETRATION (ft)	DIFFERENTIAL DEFLECTION (in)	MOUND EXPONENT
10	5	1	2
10	5	4	2
20	5	1	11
20	5	4	13
30	5	1	19
30	5	4	22
40	5	1	26
40	5	4	31
50	5	1	33
50	5	4	41

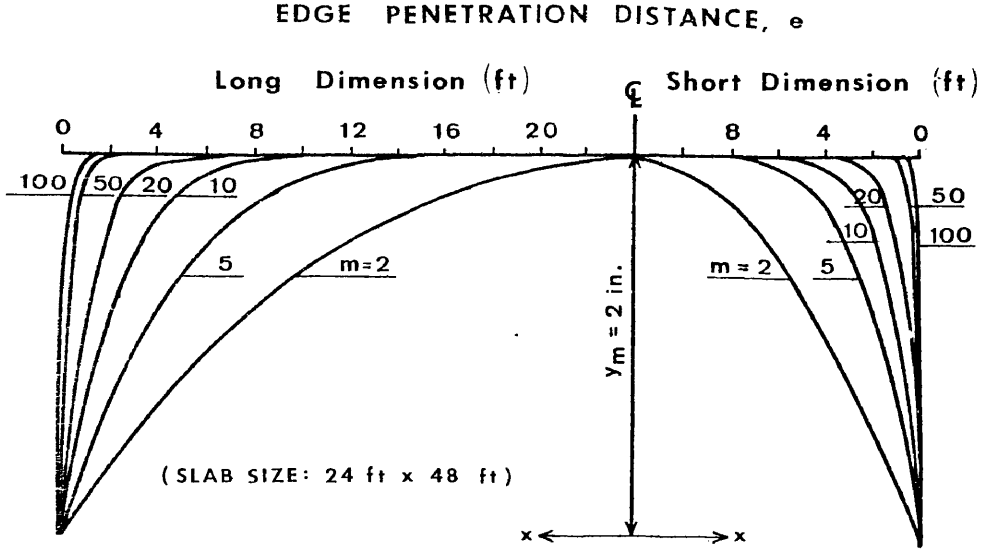

$$y = c x^m$$

Figure 22. Effect of Mound Exponent, m, and Edge Penetration Distance, e, on the Shape of the Swelling Soil Profile. [After Washusen (101)]

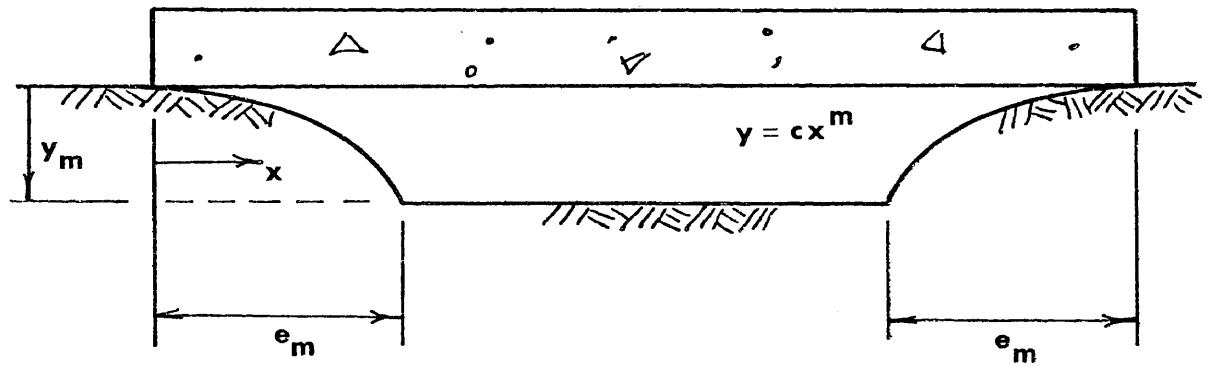

a. Reversed Exponential Profile, where $2 \leq m \leq 7$ (Exaggerated)

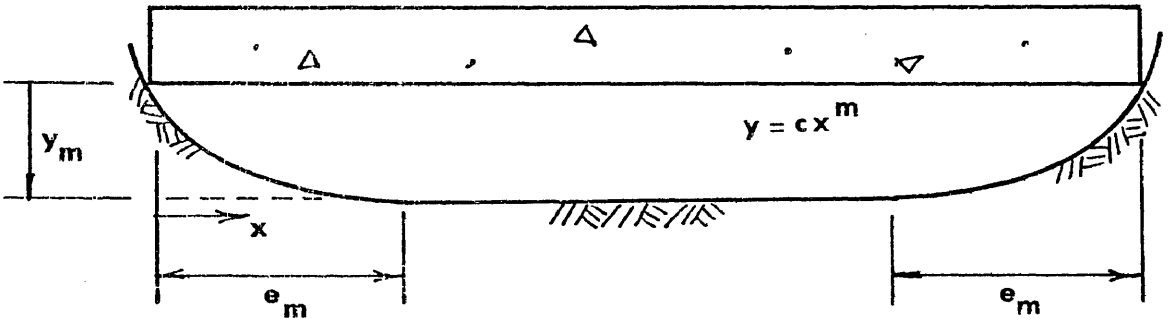

b. Inverted Exponential Profile, where $0.15 \leq m \leq 0.5$ (Exaggerated)

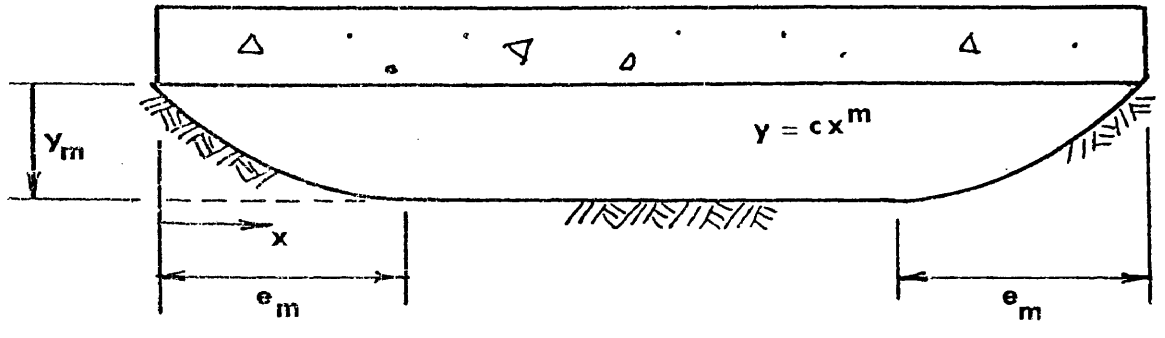

c. Inverted Exponential Profile, where $0.85 \leq m \leq 1.0$ (Exaggerated)

FIGURE 23. POSSIBLE SWELLING PROFILES FOR EDGE LIFT CONDITION.

23b.

Gardner (18) related the permeability of clays to the suction causing water movement:

$$K = \frac{a}{|\tau|^{n}+b} \quad \ldots\ldots\ldots\ldots\ldots\ldots\ldots\ldots \quad (4\text{-}6)$$

where K = permeability

$\frac{a}{b}$ = saturated permeability

$|\tau|$ = absolute value of the suction causing water movement

n = an exponent which varies with grain size (larger for courser grains)

Using a form of Gardner's relation and a second relation expressing the total potential of the soil water, Lytton (18 , 47 , 48) developed an iterative procedure that can estimate not only the expected amount of differential swell but the shape of the swollen soil surface as well.

The total potential of the soil water is defined as the sum of the gravitational potential and soil water potential (64). The soil water potential is comprised of matric, osmotic, and pneumatic potentials; however, the air pressure differences are usually very small and are usually neglected. Adding the overburden potential, Ω, to the total potential of the soil water (18) produces:

$$\psi = -h + x_3 \pm \Omega \quad \ldots\ldots\ldots\ldots\ldots\ldots\ldots\ldots \quad (4\text{-}7)$$

where ψ = flow potential

h = suction (sum of matric and osmotic potentials)

x_3 = gravitational potential

Although moisture flow in a partly saturated soil occurs in both vapor and fluid form, for most practical purposes the mass velocity of flow can be expressed as a form of Darcy's equation:

$$v = -k \frac{\partial \psi}{\partial x} \quad \ldots\ldots\ldots\ldots\ldots\ldots\ldots\ldots \quad (4\text{-}8)$$

where v = velocity of flow

k = coefficient of permeability

if Ω is not immediately considered, then substituting Equation (4-7) into Equation (4-8) results in:

$$v = -k \frac{\partial}{\partial x} (-h + x_3) \quad \ldots\ldots\ldots\ldots\ldots\ldots \quad (4\text{-}9)$$

Then, if there is a steady flux, v, and a known value of suction, h, somewhere in the vertical profile, Equation (4-9) can be numerically integrated:

1. At a nodal point i, where the suction, h_i is known

$$k_i = \frac{k_o}{1 + a\,|h_i|^n} \quad \ldots\ldots\ldots\ldots\ldots\ldots\ldots\ldots \quad (4\text{-}10)$$

where k_o = saturated permeability

a = a constant

2. The change of suction in the vertical direction (subscript 3 indicating vertical direction (18) is:

$$\Delta h_i = \Delta x_3 + \Delta x_3 \frac{v_3}{k_i} \quad \ldots\ldots\ldots\ldots\ldots\ldots \quad (4\text{-}11)$$

3. The suction at nodal point $(i + 1)$ is

$$h_{i+1} = \Delta h_i + h_i \quad \ldots\ldots\ldots\ldots\ldots\ldots \quad (4\text{-}12)$$

Substituting $h_i + 1$ into Equation (4-10) as the new value for h_i the calculations are repeated until a complete vertical profile is known.

Equation (4-10) is a form of Gardner's relation, Equation (4-6). The values of a, k_o, and n can be taken from Table 11 if not determined experimentally.

Once the soil surface is covered with an impervious cover, such as a foundation slab, the loss of soil moisture by evapotranspiration is eliminated. Thus, a gradual increase in soil moisture content occurs beneath the slab until an equilibrium condition is reached.

Lytton and Woodburn (55) showed that a vertical strain of approximately 2% could be expected to occur in a swelling soil experiencing a decade change in suction value, i.e., a change in pF from 4.0 to 3.0. This strain was dependent upon the overburden pressure; a heavier pressure from overburden and/or surcharge reduced the amount of measured strain. McKeen (63) carried this work a step further by determining equations for the rate of strain as a

TABLE 11. Field Values of Expansive Clay Permeability (18)

SOIL	k_o (cm/sec)	a	n
Yazoo	4.5×10^{-7}	. . .	1.0
Lackland	2.7×10^{-6}	. . .	. . .
Horsham	2.0×10^{-6}	. . .	. . .
West Laramie Clay Shale	2.7×10^{-6}	10^{-9}	3.0
Flagstaff Gully Dam	2.0×10^{-6}	. . .	. . .

function of the predominant type of clay mineral and the amount of clay present in the soil:

$$\text{Kaolinite:} \quad \gamma_h = 0.00018\ (\%\ \text{Clay}) - 0.000098 \qquad (4\text{-}13)$$

$$\text{Illite:} \quad \gamma_h = 0.00047\ (\%\ \text{Clay}) - 0.00351 \qquad (4\text{-}14)$$

$$\text{Montmorillonite:} \quad \gamma_h = 0.00056\ (\%\ \text{Clay}) - 0.00433 \qquad (4\text{-}15)$$

where γ_h is termed the coefficient of suction change compressibility (56).

The steady state swelling surface profile can be determined by altering Equation (4-11) and performing the same series of calculations as before except in the horizontal direction (designated by a subscript 1):

$$\Delta h_i = \Delta x_1 \frac{v_1}{k_i} \qquad (4\text{-}16)$$

The difference between Equations (4-11) and (4-16) is that there is no change in gravitational potential in the horizontal direction.

Thus, knowing the suction before covering the surface and the equilibrium suction after covering, the amount of heave per increment of depth, ΔH, can be predicted:

$$\frac{\Delta H}{H} = \gamma_h \left(pF_{final} - pF_{initial}\right) = \gamma_h \left(\Delta pF\right) \qquad (4\text{-}17)$$

However, any volume change resulting from a change in suction is either inhibited by the weight of the soil overburden when swelling or reinforced if the soil is shrinking. If the common logarithm of the

overburden pressure is pP, then the actual predicted heave per vertical increment is:

$$\frac{\Delta H}{H} = \gamma_h (\Delta pF) - \gamma_h (\Delta pP) \quad \ldots\ldots\ldots\ldots\ldots\ldots \quad (4\text{-}18)$$

The compressibility coefficient, γ_h is assumed to apply equally well to the overburden as to the suction term. Thus, the swelling profile can be determined by plotting the predicted heave of each successive "soil column," as in Figure 24. The procedure is fully illustrated in Appendix B. A computer program, *SOILSUK*, was written to perform this procedure easily and a listing, typical output, and user instructions are included in Appendices B, D, and C.

A review of the literature (16, 73 , 94 , 105) shows soil suctions at depths equal to observed active zone depths (see Table 2, p.20) to typically range from pF 3.2 - 3.7. Assuming an active zone of 7 feet and a soil suction of pF 3.4 at that depth to be typical of Texas, a swelling edge lift profile was calculated for use in this investigation. This is the profile shown in Figure 24, and is similar to Walsh's assumed edge lift profile (shown exaggerated) in Figure 12, p. 43.

Edge Moisture Variation Distance. - The term "edge moisture variation distance", "edge effect", or "edge distance" is used to describe the distance beneath the slab measured inward from the edge over which the soil moisture content varies enough to cause soil movement. Of all the design parameters, this is the one that is most difficult to estimate. Very few measurements of this value have been reported.

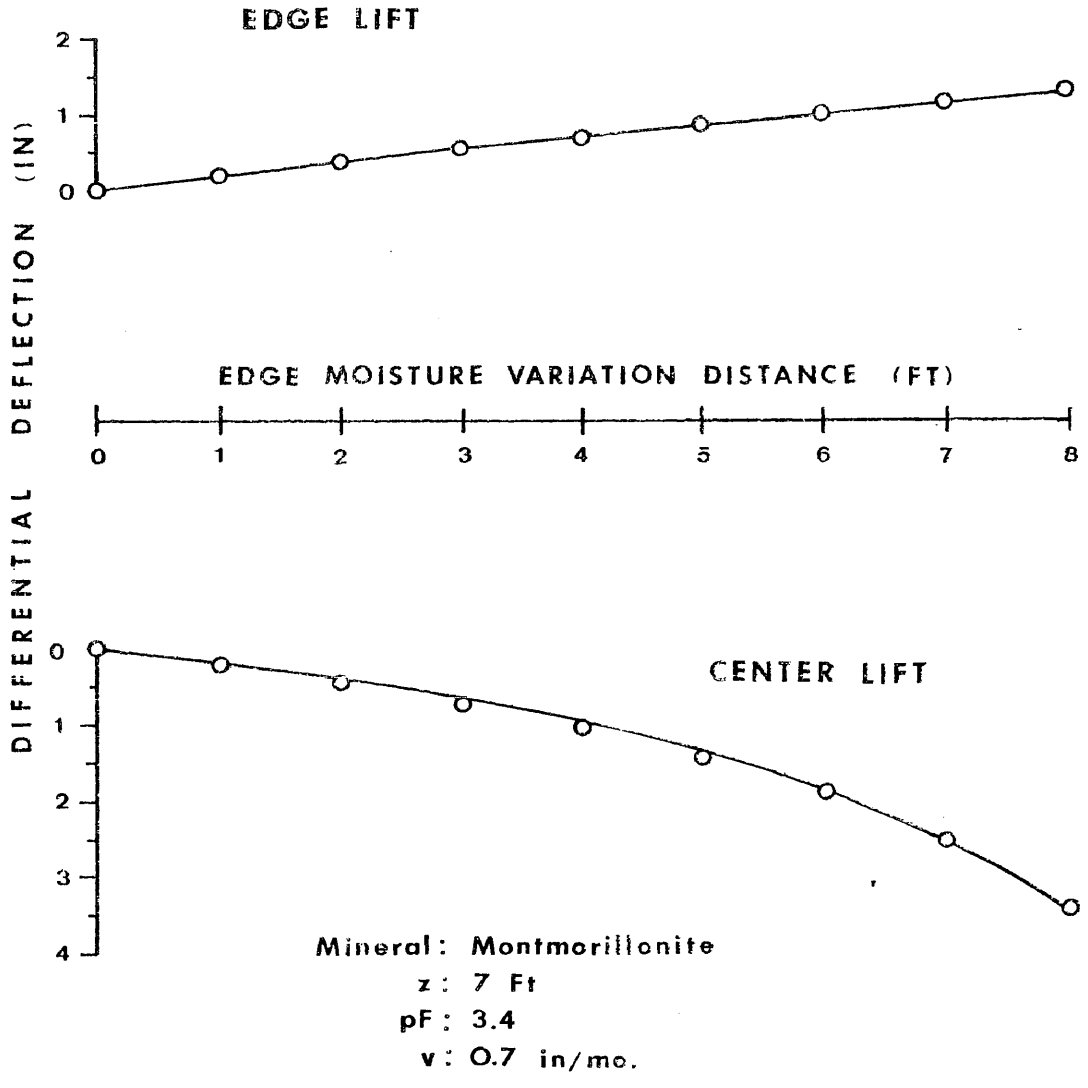

FIGURE 24. SWELLING SOIL PROFILES CALCULATED BY COMPUTER PROGRAM SOILSUK

Aitchison (2) states: "For most engineering purposes, involving relatively impermeable pavement covers, the lateral extent of the zone of edge effects can be considered to be limited and to be less than the depth of seasonal moisture changes. In many cases the zone will be less than 3 feet in width. The soil beneath the cover and beyond the zone of edge effects in such cases can be therefore considered to be isolated from rapid moisture changes and tend to a stable moisture distribution."

Review of de Bruijn's plotted data (16) implies the maximum edge effect distance to be approximately 6 feet. Holland (33) indicated to this writer that the greatest edge distance that he had observed was "about 1½ meters" (4.92 feet). Washusen (101) concluded "the lateral extent of seasonal moisture variations under the edges of a seal, do not generally exceed 1 meter" (3.28 feet). Russam (76) observed a seasonal movement of 0.6 to 1 meter (1.97 to 3.28 feet) beneath the outer edges of a pavement. Inspection of Ward's data (100) suggests an edge effect distance of approximately 3 feet.

From the 6 observations noted above, it appears that the magnitude of the edge moisture variation distance could most often be expected to range between 0.6 to 1½ meters or between 2 to 5 feet. These measurements or observations were obtained in such widely separated locations as Australia (Aitchison, Holland, Washusen), South Africa (de Bruijn), Great Britian (Russam), and the United States (Ward). Unfortunately, no method or procedure is known to this writer to predict the magnitude of this important design variable.

Although there are apparently no procedures available to

predict the edge penetration distance, experience has shown grade beam depths in the eastern part of Texas, e.g., Houston, are not required to be as deep as beam depths typically used in cities to the west, e.g., Dallas-Ft. Worth. Similarly, beam depths in Dallas-Ft. Worth are typically less than those commonly used in San Antonio, which is west of the Dallas-Ft. Worth location. From Figure 16, p. 58, it can be seen that I_m decreases from east to west, indicating a progressively drier climate, i.e., I_m for Houston, Dallas, and San Antonio is approximately +18, -1, and -16, respectively.

Thus, a method is suggested whereby the edge moisture variation distance may be estimated: If slab designs that have a history of successful performance in various cities can be analyzed using the design equations developed in Chapter V, then the edge moisture variation distance can be related to the Thornthwaite moisture index.

However, some estimate of what values of edge penetration should be used in this investigation must be made in order to ensure that most design situations are included in this study. Since all of the reported observations of edge effect distance were 6 feet or less, it would appear that if this investigation analyzed situations where e_m ranged from 2 to 8 feet, most design situations would be included.

Structural Parameters

Beam Depth. - The typical loading placed on a slab-on-ground is one of relative lightness and, consequently, the slab does not require much thickness to be structurally adequate. Due to construction

limitations and building code specifications, 4 inches is usually the minimum thickness of a constructed slab and this is usually more than adequate structurally for typical slab-on-ground loadings.

The bending stiffness of a slab is determined from the familiar moment of inertia equation (82):

$$I = \frac{bh^3}{12} \quad \text{. . . . . (4-19)}$$

where I = moment of inertia

b = width of the rectangular section

h = height of the rectangle

Thus, a deeper section will have a greater stiffness or resistance to bending than a lesser section.

If the slab is subjected to differential movement by its supporting soil, it will be forced to bend or distort to conform with this differential soil movement unless it is stiff enough to resist the bending or distorting tendency. In one extreme, a perfectly rigid slab will not bend at all; in the other extreme a thin membrane, such as a sheet of plastic, will move almost exactly with the underlying soil and assume the same distorted shape of the soil.

A 4-inch deep slab as described above is a relatively flexible structural section and will tend to deform as dictated by the movement of the supporting soil. If this deformation is sufficiently large, the tensile strength of the concrete slab is exceeded and the material cracks. Once cracked, the slab more easily conforms with

the shape of the supporting soil. In doing so, this distortion is transmitted to the superstructure being supported by the soil. Depending upon the type of structure and the materials used in the construction, the foundation distortion may cause only a slight amount of damage or it may effectively result in the total destruction of the facility.

If a structure must be constructed on a site of expansive soil, then there are two solutions to the problem of superstructure damage; (1) make the foundation and the structure being supported so strong and rigid that no amount of differential movement by the soil will cause distress and damage, or (2) make the structure so flexible that no matter how much the foundation slab distorts, no damage to the superstructure will occur.

It should be evident that even if such a strong, rigid structure could be constructed, the cost of doing so would probably be prohibitive with respect to its ultimate use. Thus, the strong and rigid approach is not the solution. In the other extreme, even if such a flexible structure that could withstand large soil movements could be constructed, it would probably not be satisfactory for use as a residence or light commercial building, the eventual use of most slabs-on-ground.

The solution adopted by most designers is to allow the slab to move up and down with the shrink-swell cycle of the soil but to construct the slab with enough stiffness to limit its differential deflection to some acceptable magnitude commensurate with the type of construction it is supporting. It is assumed that wood-frame

construction can tolerate deformations about twice as great as concrete block construction before warping and cracking cause mechanical problems or objectionable appearances (9). Thus, for various types of superstructure construction, a limit on the maximum differential vertical displacement of any two points on the slab is generally imposed on the design. This limit is usually of such a value that a particular wall or wall-finishing material will not crack or distort if differential movements of less than this amount occur. Table 12 lists some of the deflection ratios commonly used.

One method of decreasing the deflection that constant thickness slabs will experience is to increase its depth. However, to do so will make the slab unnecessarily strong; the slab does not need more strength, only more stiffness. This needed stiffness can be obtained by adding stiffening beams to the underside of the slab. By adding only the stiffening beams instead of making the entire slab an equal depth, a large amount of concrete is saved as well. Thus, increasing the beam depth will increase the stiffness of a given slab section and reduce the amount of differential deflection the slab will experience under a given set of conditions. The relative increase in stiffness as beam depth increases for a 4-inch slab, 30 feet wide with 3 stiffening beams is shown in Table 13.

Beam Spacing. - The distance from one stiffening beam to another affects the stiffness of the entire section. Thus, a section with widely spaced stiffening beams will not have as great a stiffness as a section with closer spaced beams. This is demonstrated in Table 14.

Several maximum beam spacings have been recommended and are

TABLE 12. Permissible Differential Deflections for Slabs-On-Ground to Limit Damage to Superstructure

TYPE OF CONSTRUCTION	MAXIMUM PERMISSABLE DEFLECTION RATIO (Δ/L)	REFERENCE
Wood Frame	1/200	9
Non-Masonry, Timber or Pre-Fabricated	1/200	98
Unplastered Masonry or Gypsum Wallboard	1/300	9
Non-Masonry, Frame & Panel	1/300	98
Stucco or Plaster	1/360	9
Brick Veneer (Articulated)	1/300	98
Brick Veneer	1/480	69
Brick Veneer (Standard)	1/500	98
Masonry (completely Articulated)	1/500	98
Masonry (partially Articulated)	1/800	98
Masonry, solid or cavity wall	1/1500 - 1/2000	98

TABLE 13. Relative Increase in Stiffness as Beam Depth Increases for a 4-Inch Slab, 30 Feet Wide with Three 10-Inch Stiffening Beams

SLAB DEPTH (in)	BEAM DEPTH (in)	MOMENT OF INERTIA OF TOTAL CROSS-SECTION (in^4)	RATIO OF STIFFNESS OF STIFFENED SECTION TO UNSTIFFENED SECTION
4	0	1,920	1.0
4	10	16,586	8.6
4	20	82,908	43.2
4	30	221,802	115.5

TABLE 14. Relative Increase in Stiffness as Beam Spacing Decreases for a 4-Inch Slab of 30 Feet Width

NUMBER OF BEAMS[a]	BEAM SPACING (ft)	MOMENT OF INERTIA OF TOTAL CROSS-SECTION (in^4)	RATIO OF STIFFNESS OF STIFFENED SECTION TO UNSTIFFENED SECTION
0	----	1,920	1.0
2	30.0	60,331	31.4
3	15.0	82,908	43.2
4	7.5	102,644	53.5
6	5.0	136,175	70.9

[a] Beam Depth = 20 inches; Beam Width = 10 inches

shown in Table 15. Regardless of the maximum recommended spacing, in each instance the reference emphasizes that the beams should be evenly spaced across the slab cross-section. The exception to this is the case where a beam is needed under an exceptionally heavy load, such as a fireplace, or where geometry dictates a slight variation in spacing.

TABLE 15. Recommended Maximum Spacings of Stiffening Beams

BEAM SPACING (ft)	REFERENCE
8 - 15	9
20	69
9.8 - 13.1	97

As seen from Table 14, the stiffness of the section increases as the number of beams increase. However, it has been the observation of this writer from observing current construction projects and from questioning engineers engaged in designing stiffened slabs-on-ground to be used for light commercial or residential construction, that most slab dimensions are such that beam spacings are in the 10 to 15 feet range, or more, up to a maximum of 20 feet. Thus, by using beam spacings from 12 feet to 20 feet, this investigation will analyze the cross-sections most typically encountered in the field. In those instances where beam spacings are less than 12 feet, the analysis would prove to be conservative.

Beam Width. - It is difficult to excavate a beam with a width less than 8 inches, particularly if the excavation is deep. Most excavation equipment used in this type of construction will result in beam widths of 8 to 12 inches. As pointed out in the BRAB Criteria (9), "...it must be recognized that selection of wider beams does not lead to savings in beam depth or in the amount of reinforcement..." Consequently, unless a wider beam is necessary due to high shear stresses, most designers will specify beam widths between 8 and 12 inches. Using the more narrow beam width, i.e., 8 inches, in this investigation will provide slightly more conservative results.

Slab Lengths. - The length of the slab is usually a fairly inflexible design parameter, generally being fixed either by the owner for utility purposes or by architectural considerations.

Loading. - Construction practices presently being followed, in general, do not rely on load bearing interior partitions, but instead transfer all roof loads to the exterior or perimeter walls. Additionally, many homes being built today have a brick or rock veneer finish on at least part of the exterior wall. Thus, the perimeter of the slab experiences the greatest portion of the loading that the superstructure transmits to the slab. Perimeter wall loads for a very light frame structure and a heavy, 2-story masonry structure might typically be found to be 600 lb/ft and 1500 lb/ft, respectively. Loading conditions representative of these two values are used in this investigation.

Every building, whether it is a residence or a light commercial building, has some loading besides the perimeter wall loads transmitted

to the slab. This loading is typically comprised of non-load bearing interior partitions, plumbing and mechanical systems, appliances, and furnishings. It is difficult to know the magnitude and location of these loadings except on a case by case basis. However, if the weight of all these items were to be totalled and distributed uniformly over the entire area of the slab, the loading would only be a few pounds per square foot. A more conventional, as well as a more conservative method of accounting for these loadings is to turn to building code design loads. The American National Standard Building Code Requirements for Minimum Design Loads in Buildings and Other Structures, National Bureau of Standards, specifies a minimum design load of 40 pounds per square foot for both private apartments and for the first floor of private dwellings (101).

Having accounted for interior loadings, the only loading left is the weight of the slab itself. This is found by calculating the volume of concrete required by the slab and multiplying by the weight of the concrete being used, usually 145 pounds per cubic foot.

The Model Used to Analyze the Problem

Since the objective of this investigation is to produce a general design procedure that can be used to estimate the magnitude of the design parameters of bending moment, shear force, and differential deflection to be expected to occur under a given set of soil and structural conditions, the analysis leading to this procedure should cover as completely as possible the range of design conditions that might typically be encountered. From the discussion of the various

design parameters in the preceding section of this chapter, the following limits or boundaries appear to best represent the extreme conditions encountered in design:

1. Differential Soil Swell, y_m:

   0, 1, 4 inches (center lift)

   0, 1.12 inches (edge lift)

2. Edge Moisture Variation Distance, e_m:

   0, 2, 5, 8 feet

3. Beam Depth, d:

   18, 30 inches

4. Beam Spacing, S:

   12, 20 feet

5. Perimeter Loading, P:

   613, 1477 pounds per linear foot

6. Slab Length, L:

   24, 48, 96, 144 feet.

The beam widths remain a constant 8 inches and a uniform loading of 40 psf plus the slab weight is applied in all cases. The models used in both the center lift and the edge list swelling situations are shown in Figure 25.

Computer Program *SLAB 2*

A FORTRAN IV computer program developed by Y.H. Huang (36, 37) was modified and used in the investigation. The program used the finite element method to analyze slabs resting on an elastic continuum.

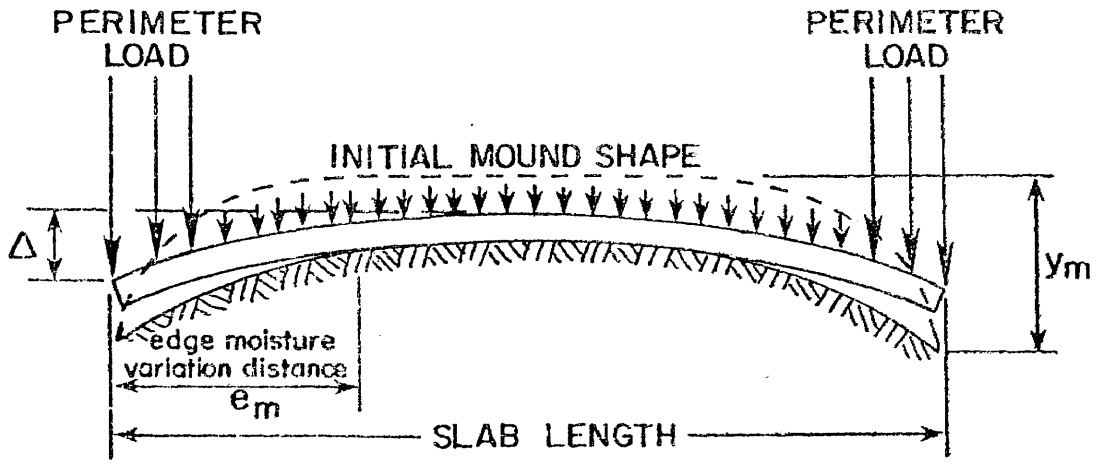

CENTER LIFT

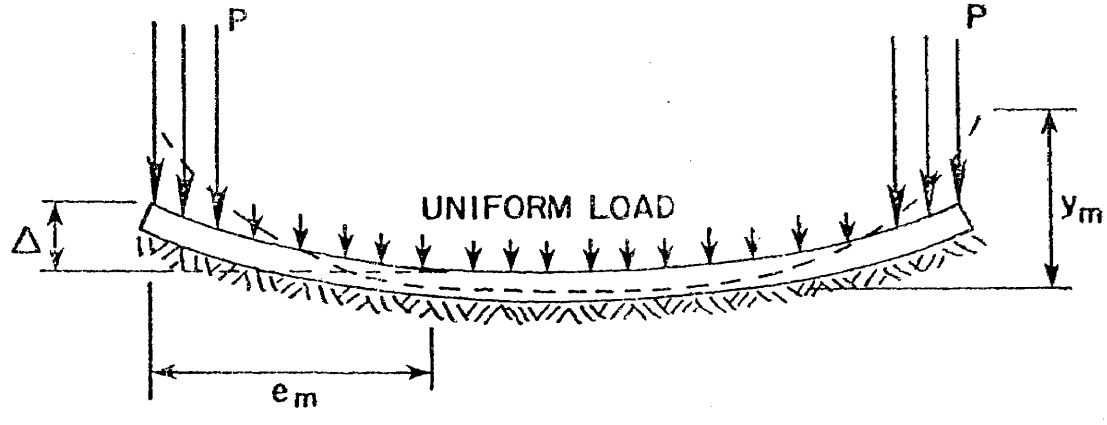

EDGE LIFT

FIGURE 25. SOIL-STRUCTURE INTERACTION MODEL.

The original unnamed program was designated as SLAB1; a modified version was designated SLAB2. A listing for the modified program, a user's guide, and typical output are included as Appendices E, F, and G.

Although the program and its iterative procedure are described elsewhere (36 , 37), it would be well to briefly describe some of the input parameters and how they were obtained or determined for this investigation.

Material Properties. - Values of several properties are required in order for the program to correctly analyze the stresses and strains occurring in the materials.

Poisson's Ratio of the soil. - Poisson's ratio, v_s, is defined as the ratio of the strain normal to the applied stress to the strain parallel to the applied stress. The ratio varies between zero for an inelastic material to 0.5 for a material that exhibits no volume change during deformation. Poisson's ratio for soil is not as well defined as it is for steel or concrete. Values usually reported for clay range from 0.4 to 0.5 for weak, stiff, or semi-solid clay (45). The value of 0.4 was adopted for this investigation as being representative of swelling clays.

Poisson's Ratio of the Concrete. - Values for Poisson's ratio of concrete, v, are reported to range between 0.15 (68) and 0.20 (82). In this investigation, the more conservative 0.15 value is used.

Modulus of Elasticity (Young's Modulus) of the Soil. - Values of the modulus of elasticity for soil, E_s, are reported in the literature as either a subjective soil description or a specific soil, e.g. Boston Blue Clay. Some reported values for the more general

descriptive terms are shown in Table 16.

TABLE 16. Reported Values of Modulus of Elasticity, E_s, for Clay Soils

SOIL DESCRIPTIONS	MODULUS OF ELASTICITY (psi)	REFERENCES
Clay Semi-solid	1,000 - 2,000	45
Clay, Stiff Plastic	600 - 1,200	45
Clay, Weak Plastic	200 - 600	45
Soft Clay	250 - 600	7
Medium Clay	600 - 1,200	7
Hard Clay	1,000 - 1,500	7

Since there is an apparently wide variation in the reported values for E_s, the same slab problem was run with three different values of E_s to determine the sensitivity of the program to this parameter. The results are shown in Table 17.

The value of E_s = 100 psi is a very low value. This weak soil provided little resistance to the slab loading and, consequently, the slab was deflected more and higher bending stresses were the result. The E_s = 10,000 psi modulus is much higher than any of the reported values in Table 16. This very stiff soil offered more resistance to compression under the slab loading, particularly in the interior nodal locations, with the result being less differential deflection and lower bending stresses. Since the average of the reported values

TABLE 17. Stresses Induced in a Slab-On-Ground Due to Varying the Soil Modulus of Elasticity, E_s

E_s (psi)	MAXIMUM STRESS (ksi)	PERCENT CHANGE IN STRESS (%)	MAXIMUM DIFFERENTIAL DEFLECTION OF SLABS (IN)
100	0.504		2.381
		-3.42	
1,000	0.487		0.837
		-12.48	
10,000	0.426		0.285

of Table 16 is 979 *psi*, a value of 1,000 *psi* was used in this investigation.

Modulus of Elasticity for Concrete. - The value of E_c is a function of the compressive strength of the concrete, f'_c as shown by Hognestad (68, 99). The ACI Building Code (3) allows the use of the empirical formula:

$$E_c = 57{,}000\sqrt{f'_c} \quad \ldots\ldots\ldots\ldots\ldots\ldots \quad (4\text{-}20)$$

to estimate the modulus of normal weight concrete. For general construction grade concrete, usually exhibiting a 28-day compressive

strength of 2,500 psi, E_c is taken to be 2,850,000 psi.

Concrete is subject to creep and shrinkage, which are time dependent deformations. Shrinkage is broadly defined as volume change that is unrelated to load application. Most of the shrinkage deformation changes occur in the early part of the life of the slab, e.g., 91% by the end of the first year (46). Creep, on the other hand, continues with time under sustained loads at unit stresses within the elastic range. Although creep occurs at a decreasing rate with time, the total magnitude may be several times as large as the short-time elastic deformation. Wang and Salmon (99) note that even after 5 years only 90% of the total creep deformation had occurred (also Appendix H). The average long-term (creep) modulus of elasticity for concrete is taken as $E_c/2$ (References 9 , 50 , and Appendix H) and this value is applicable to this investigation since heave beneath a slab is a long term event and the loading applied to the slab remains essentially constant throughout this life of the slab. Therefore, for this investigation, a creep modulus of elasticity of 1.5×10^6 psi was used.

Slab Dimensions and Finite Element Grids. - SLAB2 can take advantage of symmetry and, thereby reduce the amount of core storage required, the number of calculations necessary, and the computer cost per problem. Since both the loading and the soil support conditions were assumed to be symmetrical, only one-fourth of the slab was actually modeled.

Calculated Moments, Stresses, and Deflections. - The original program was designed to calculate stresses and total deflections

occurring in concrete pavements. However, for slab-on-ground foundation design, the design parameters of moment, shear and differential deflection are the needed design parameters. Since SLAB1 provided the final total deflection at each finite element node (hereafter referred to as simply "node"), the differential deflection data was not difficult to obtain. SLAB2 converted the stresses of SLAB1 into moments, and the moments to shear forces. The modifications to SLAB1 were accomplished as follows.

Converting Bending stresses to Bending Moments. - From Timoshenko and Woinowsky-Krieger (91), the relation between bending stress and bending moment is:

$$\sigma = \frac{6M}{h^2} \quad \ldots\ldots\ldots\ldots\ldots\ldots\ldots\ldots \quad (4\text{-}21)$$

where σ = bending stress

M = bending moment per unit width

h = plate or slab thickness

Thus, stresses can be easily converted to bending moments by:

$$M = \frac{\sigma h^2}{6} \quad \ldots\ldots\ldots\ldots\ldots\ldots\ldots\ldots \quad (4\text{-}22)$$

where the symbols have the same definition as in Equation (4-21).

Converting Bending Moments to Shear Forces. - Assuming that the loads acting on the slab are normal to its surface and that the deflections of the slab at its edges are small in comparison to its

thickness, then it can probably also be assumed that the loads are still acting normally to the slab surface after deflection. If these assumptions, as well as the other plate assumptions (91), hold true, then from Timoshenko and Woinowsky-Krieger (91):

$$Q_x = \frac{\partial M_{yx}}{\partial y} + \frac{\partial M_x}{\partial x} \quad \ldots\ldots\ldots\ldots\ldots\ldots \quad (4\text{-}23)$$

and

$$Q_y = -\frac{\partial M_{xy}}{\partial x} + \frac{\partial M_y}{\partial y} \quad \ldots\ldots\ldots\ldots\ldots\ldots \quad (4\text{-}24)$$

where Q_x, Q_y = Shear force in the x direction and y direction, respectively, (per unit length)

M_x, M_y = Bending moments in the x and y direction, respectively, (per unit length).

M_{xy}, M_{yx} = Twisting Moments (per unit length).

Since

$$M_{xy} = -M_{yx} \quad \ldots\ldots\ldots\ldots\ldots\ldots \quad (4\text{-}25)$$

then

$$Q_x = \frac{\partial M_x}{\partial x} - \frac{\partial M_{xy}}{\partial y} \quad \ldots\ldots\ldots\ldots\ldots\ldots \quad (4\text{-}26)$$

and

$$Q_y = \frac{\partial M_y}{\partial y} - \frac{\partial M_{xy}}{\partial x} \quad \ldots\ldots\ldots\ldots\ldots\ldots \quad (4\text{-}27)$$

become the basic equations for determining the shear forces.

By converting Equations (4-26) and (4-27) to finite difference form, the solution for shearing forces can be obtained directly from the results of SLAB 2:

$$Q_{x_i} = \frac{M_{x_i} - M_{x_{i+b}}}{x_i - x_{i+b}} - \frac{M_{xy_i} - M_{xy_{i+1}}}{y_i - y_{i+b}} \quad \ldots\ldots\ldots \quad (4\text{-}28)$$

$$Q_{y_i} = \frac{M_{y_i} - M_{y_{i+1}}}{y_i - y_{i+1}} - \frac{M_{xy_i} - M_{xy_{i+b}}}{x_i - x_{i+b}} \quad \ldots\ldots\ldots \quad (4\text{-}29)$$

where i = node at which shearing forces are being determined

$i+1$ = an adjacent node in the y-direction

b = the total number of nodes in each column of nodes in the y-direction

$i+b$ = an adjacent node in the x-direction

Since this procedure requires an imaginary node located outside the slab edge, the iterative process can be reversed and proceed from the upper right corner of the finite element grid towards the origin and thus take advantage of the slab symmetry when "imaginary" nodes are

required, i.e., the "imaginary" nodes are actually real nodes located in a quadrant of the slab that is symmetrical to the quadrant being analyzed.

A listing of this algorithm is included in Appendix E as Subroutine SHEAR in the SLAB2 listing.

Slab Thickness and Stiffening Beams. - SLAB1 was written to analyze pavement sections of constant thickness. In doing so, the program calculates the slab stiffness on basis of unit width or length. Whereas the moment of inertia of a beam or an irregular section, if its geometry is known, can be found using Equation (4-19), the moment of inertia of a constant thickness plate or slab is expressed on a per unit length basis using the flexural rigidity, D, which also accounts for the 2-way plate action effect through Poisson's ratio (91):

$$D = \frac{E_c h^3}{12(1 - \nu^2)} \quad \text{. . . . . (4-30)}$$

Since the slabs being investigated in this study are not constant thickness slabs but are stiffened with grade beams running in both directions, neither Equation (4-19) nor Equation (4-30) are strictly applicable.

Equation (4-30) can be used if the actual "plate" stiffness of the stiffened section can be put in terms of an equivalent flexural rigidity. This equivalent rigidity can be broadly described as "spreading" the rigidity of the stiffened section across the length and width of the slab so as to create a constant thickness section of

equal or equivalent rigidity. If the stiffness of the stiffened section is calculated and found to be I_s, then the equivalent rigidity is equated to D and the constant thickness h to give an equivalent rigidity is:

$$h = \sqrt[3]{\frac{12(1-\nu^2)\, I_s}{E_c}} \qquad \text{(4-30)}$$

An alternative procedure is to account for the increased stiffness given to the slab by the grade beams. In such cases, Timoshenko and Woinowsky-Krieger maintain that transverse contraction can be neglected (91), i.e., ν goes to zero. This assumption was supported in tests by German investigators Pfluger (67) and Trenks (92).

The impact of this is shown in Figure 26, which is the stress matrix used in SLAB1 to calculate the stresses occurring in the slab. The terms in the stress matrix are defined as:

$p = \frac{a}{b}$, where a and b are elemental dimensions

M = internal moments

δ = nodal displacements

$$D_x = D_y = \frac{E_c h^3}{12(1 - \nu^2)} \qquad \text{(4-31)}$$

$$D_{xy} = \frac{1 - \nu}{2} \cdot \frac{E_c h^3}{12(1 - \nu^2)} = \frac{E_c h^3}{24(1 + \nu)} \qquad \text{(4-32)}$$

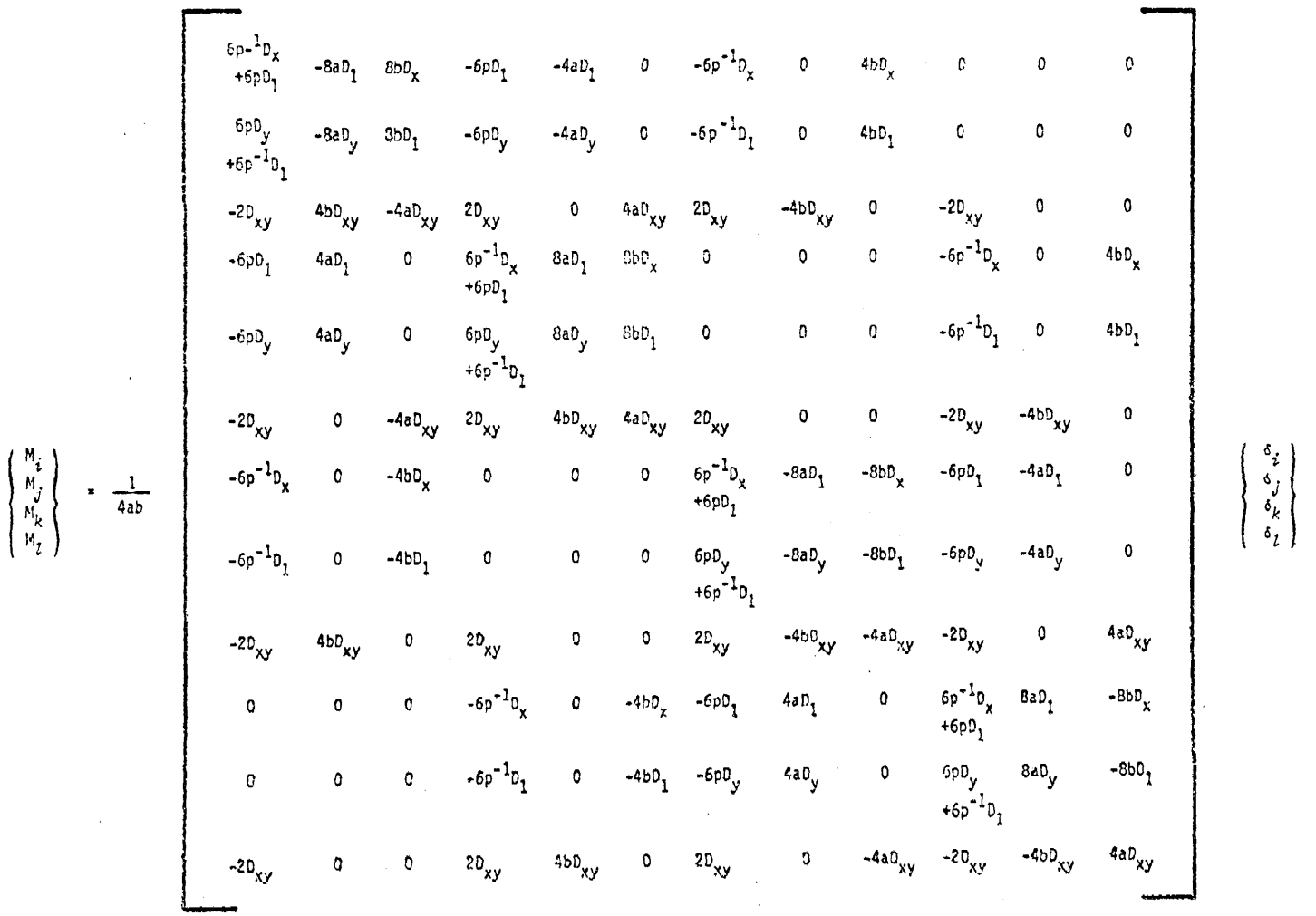

WHERE: 2a = Long Dimension of Element; 2b = Short Dimension of Element; p = a / b

FIGURE 26. STRESS MATRIX OF ZIENKIEWICZ USED IN COMPUTER PROGRAM SLAB2.(107)

$$D_1 = \nu \cdot \frac{E_c h^3}{12(1 - \nu^2)} = \frac{E_c h^3 \nu}{12(1 - \nu^2)} \quad \ldots\ldots\ldots\ldots \quad (4\text{-}33)$$

Thus, if $\nu = 0$ as assumed by Pfluger, Trenks, and Timoshenko and Woinowsky-Krieger, then

$$D_1 = 0 \quad \ldots\ldots\ldots\ldots\ldots\ldots\ldots\ldots\ldots\ldots \quad (4\text{-}34)$$

$$D_{xy} = \frac{E_c h^3}{24} \quad \ldots\ldots\ldots\ldots\ldots\ldots\ldots\ldots\ldots\ldots \quad (4\text{-}35)$$

$$D_x = D_y = \frac{E_c h^3}{12} \quad \ldots\ldots\ldots\ldots\ldots\ldots\ldots\ldots\ldots\ldots \quad (4\text{-}36)$$

and the stress matrix of Figure 26 becomes the stress matrix of Figure 27. A listing of the Subroutine *TEE* incorporating this algorithm into SLAB2 is included in Appendix E.

Computer Program *PRESS2*

A second computer program was used to analyze the effect of post-tensioning reinforcement eccentricity on differential deflection and to investigate the relationship between differential deflection, and cracking and deflection and ultimate strength. The finite difference program was written by D.M. Pierce (68) in FORTRAN II for use on the CDC 6600 computer system. The program was converted to double-

$$\begin{Bmatrix} M_i \\ M_j \\ M_k \\ M_l \end{Bmatrix} = \frac{1}{4ab} \begin{bmatrix}
6p^{-1} & 0 & 8b & 0 & 0 & 0 & -6p^{-1} & 0 & 4b & 0 & 0 & 0 \\
6p & -8a & 0 & -6p & -4a & 0 & 0 & 0 & 0 & 0 & 0 & 0 \\
-2D_{xy} & 4bD_{xy} & -4aD_{xy} & 2D_{xy} & 0 & 4aD_{xy} & 2D_{xy} & -4bD_{xy} & 0 & -2D_{xy} & 0 & 0 \\
0 & 0 & 0 & 6p^{-1} & 0 & 8b & 0 & 0 & 0 & -6p^{-1} & 0 & 4b \\
-6p & 4a & 0 & 6p & 8a & 0 & 0 & 0 & 0 & 0 & 0 & 0 \\
-2D_{xy} & 0 & -4aD_{xy} & 2D_{xy} & 4bD_{xy} & 4aD_{xy} & 2D_{xy} & 0 & 0 & -2D_{xy} & -4bD_{xy} & 0 \\
-6p^{-1} & 0 & -4b & 0 & 0 & 0 & 6p^{-1} & 0 & -8b & 0 & 0 & 0 \\
0 & 0 & 0 & 0 & 0 & 0 & 6p & -8a & -8b & -6p & -4a & 0 \\
-2D_{xy} & 4bD_{xy} & 0 & 2D_{xy} & 0 & 0 & 2D_{xy} & -4bD_{xy} & -4aD_{xy} & -2D_{xy} & 0 & 4aD_{xy} \\
0 & 0 & 0 & -6p^{-1} & 0 & -4b & 0 & 0 & 0 & 6p^{-1} & 0 & -8b \\
0 & 0 & 0 & 0 & 0 & 0 & -6p & 4a & 0 & 6p & 8a & 0 \\
-2D_{xy} & 0 & 0 & 2D_{xy} & 4bD_{xy} & 0 & 2D_{xy} & 0 & -4aD_{xy} & -2D_{xy} & -4bD_{xy} & 4aD_{xy}
\end{bmatrix} \begin{Bmatrix} \delta_i \\ \delta_j \\ \delta_k \\ \delta_l \end{Bmatrix}$$

WHERE: 2a = Long Dimension of Element; 2b = Short Dimension of Element; p = a / b

FIGURE 27. ZIENKIEWICZ STRESS MATRIX MODIFIED TO NEGLECT TRANSVERSE CONTRACTION.

precision FORTRAN IV language and adapted for use on the Texas A&M University AMDAHL system by the writer.

The program was also modified to consider a swelling soil profile when analyzing soil-structure interaction between the slab and the spring foundation. The soil pressure acting against the imposed loading of the slab and superstructure is a function of the amount of compression of the soil spring. This is explained in Figure 28. The initial position of the slab with respect to the swelling soil profile is shown in Figure 28a. When loaded, the slab will compress the swelling mound or "settle" in the soil. As seen in Figure 28b, the result of the compression or settlement is an increase in the supported slab length (or a decrease in the unsupported length). In attaining this final position, the slab travels downward through some distance y_m before it comes in contact with the soil and compresses it some amount w. Since the program calculates the soil pressure as $S\ (w + y_m)$, it calculates an incorrectly high reaction. This is compensated for by adding at each location where the beam was unsupported a load of opposite sign, given by:

$$Q_{add} = Sy_m \quad \ldots\ldots\ldots\ldots\ldots\ldots\ldots\ldots \quad (4\text{-}37)$$

where Q_{add} = added load of opposite sign to the foundation reaction

S = long-term modulus of subgrade reaction

y_m = distance from initial slab position to swelling soil profile.

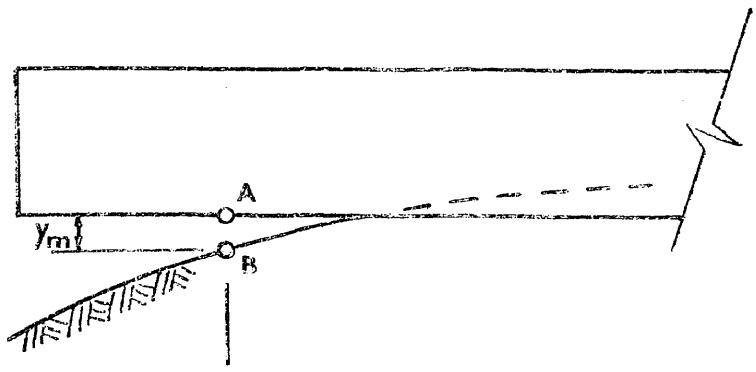

A. POSITION OF SLAB WITH RESPECT TO SWELLING SOIL PROFILE BEFORE LOADING.

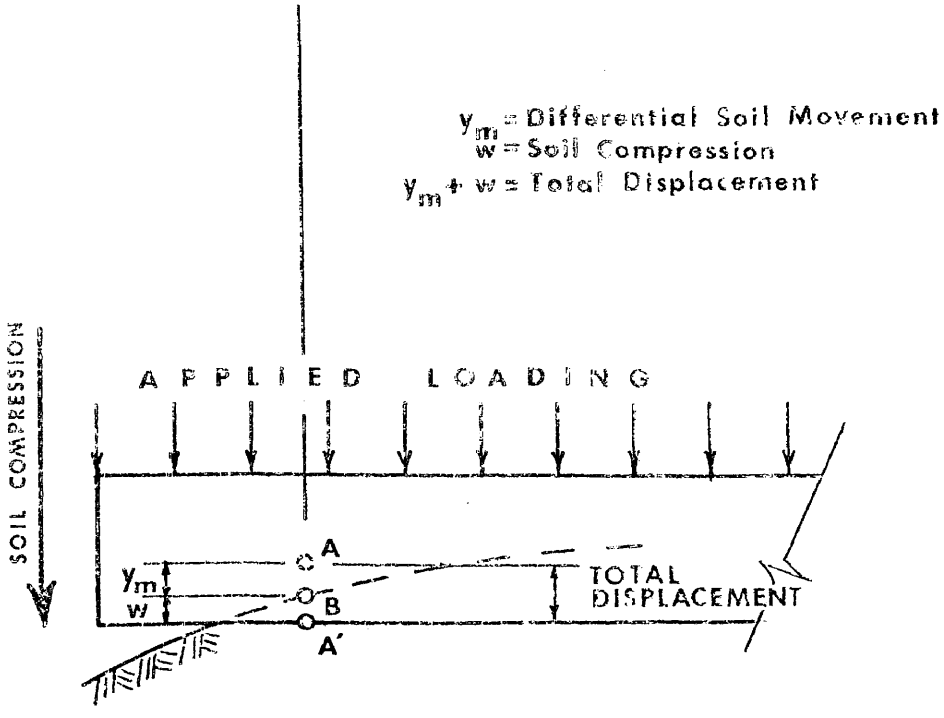

B. POSITION OF SLAB WITH RESPECT TO SWELLING SOIL PROFILE AFTER LOADING SHOWING DIFFERENCE BETWEEN SOIL COMPRESSION AND TOTAL DISPLACEMENT.

FIGURE 28. PRESS2 MODIFICATION FOR DIFFERENCE BETWEEN TOTAL DISPLACEMENT AND ACTUAL SOIL COMPRESSION.

Additionally, at each location where the slab has not come in contact with the soil, the subgrade modulus (spring constant) is set to zero to indicate non-contact.

PRESS2 can consider a combination of reinforcement, including bonded or unbonded and pre-, post-, or unstressed reinforcement. The iterative procedure of the program allows it to calculate stresses and revise them, if necessary, as the flexural stiffness of the slab is altered or loading conditions change.

Material properties input to the program were similar to those used in SLAB2 with three exceptions.

1. Modulus of Subgrade Reaction, k. Since the problem is a long-term one, the long-term modulus of subgrade reaction is used as the value for the stiffness of the spring foundation. As reported by Lytton (52), this value generally ranges between 1 and 10 pounds per cubic inch (pci) and typically this value is found to be 5 pci.

2. Stress-Strain Curve. In order to realistically determine the stress-strain changes occurring in post-tensioned cables, stress-strain data on ½" diameter, 7-wire 270K cable used by the VSL Corporation (61) was used to construct the stress-strain curve used by PRESS2.

3. Concrete Tensile Stress. Concrete exhibits a nonlinear stress-strain relationship from initial loading to failure. PRESS2 uses the compressive stress-strain curve of Hognestad (68) to calculate the stress condition existing in the extreme concrete fibers resulting from a given strain. The maximum tensile stress in the prestressed concrete is determined from the compressive cylinder strength, f'_c, as suggested

by Warwaruk, et al. (68). The maximum concrete tensile strength is assumed to be reached when the tensile strain in the extreme fiber is sufficiently large to correspond to this tensile stress on Hognestad's stress-strain curve.

A listing of PRESS2 is included as Appendix I. A user's guide and typical output are included as Appendices J and K.

CHAPTER V

ANALYSIS OF RESULTS

The principal thrust of the analysis was to develop equations relating the design parameters of moment, shear, and differential deflection to the design variables of beam depth, beam spacing, slab length, perimeter load, differential soil movement, and edge moisture variation distance. The analysis of the soil-structure interaction, which produced the data necessary to develop the design equations, was accomplished with the computer program SLAB2 (Appendix E). Once all the soil-structure interaction data had been accumulated, a numerical analysis was made using a select regression procedure. The regression analysis resulted in the equations which related the design variables to the desired design parameters of moment, shear, and differential deflection.

After developing the basic design equations, the edge moisture variation distance, e_m, applicable to different geographical locations was determined. In addition to developing the basic design equations and determining the effective values of e_m, two related problems associated with post-tensioning were also investigated. One problem was to determine if the prestressing placed in the slab portion of the stiffened section, which is normally above the neutral axis (center of gravity) of the gross section, had any influence on the amount of differential deflection the slab experienced under service conditions. The second problem was to

determine the relationship between cracking moment, ultimate moment, and differential deflection. Both studies were conducted with the computer program PRESS2 (Appendix I).

Selection of Stiffness for Model

Although the parameters to be used in the soil-structure interaction and their boundaries had been determined (Chapter IV), one decision remained prior to initiating the total parametric study.

Subroutine TEE had been developed to consider the effect of the stiffening beams as well as take advantage of the reduction of the stress matrix due to neglecting of transverse contraction (91) (Figures 26 and 27, pp. 102 and 104). To determine if this modification produced any advantage over the alternative procedure of "spreading" the slab stiffness over a constant depth section, 19 separate problems were accomplished using a 48 ft x 24 ft slab. The results of this study are tabulated in Table 28, Appendix L, and show that the average ratio of maximum moment in the long direction from Subroutine TEE to the maximum moment in the long direction from Subroutine SOLID is 1.00. The lowest ratio was 0.83 and the greatest was 1.17. Consequently, the decision was made to use the distributed stiffness method in the analysis due to its greater ease in preparing the input data for the computer.

Regression Analysis

A computerized numerical analysis of the data resulting from the soil-structure interaction was made using the Hocking-LaMotte-Leslie select regression analysis (29,42). The analysis produces the statistically optimum regressions on subsets of the independent variables of size 1 to n $\leq$ 80. The result is either a linear equation of the form:

$$y = a_0 + a_1x_1 + a_2x_2 + \ldots + a_ix_i \quad \ldots\ldots\ldots\ldots \quad (5\text{-}1)$$

or a logarithmic equation of the form:

$$y = a_0x_1^{b_1}x_2^{b_2} \ldots x_{i-1}^{b_{i-1}}x_i^{b_i} \quad \ldots\ldots\ldots\ldots \quad (5\text{-}2)$$

where y = dependent variable

x = independent variable

a = constant

b = regression coefficient or power

The logarithmic regression was used in this study to analyze the gathered data and the form of the resulting equations was that of Equation (5-2).

Results of Center Lift Analysis

Moment. - The magnitude of the negative bending moment, in general, first increased rapidly, peaked, and then decreased as the distance from the edge of the slab increased. The typical shape of the moment profile is shown in Figure 29 where the moments along the

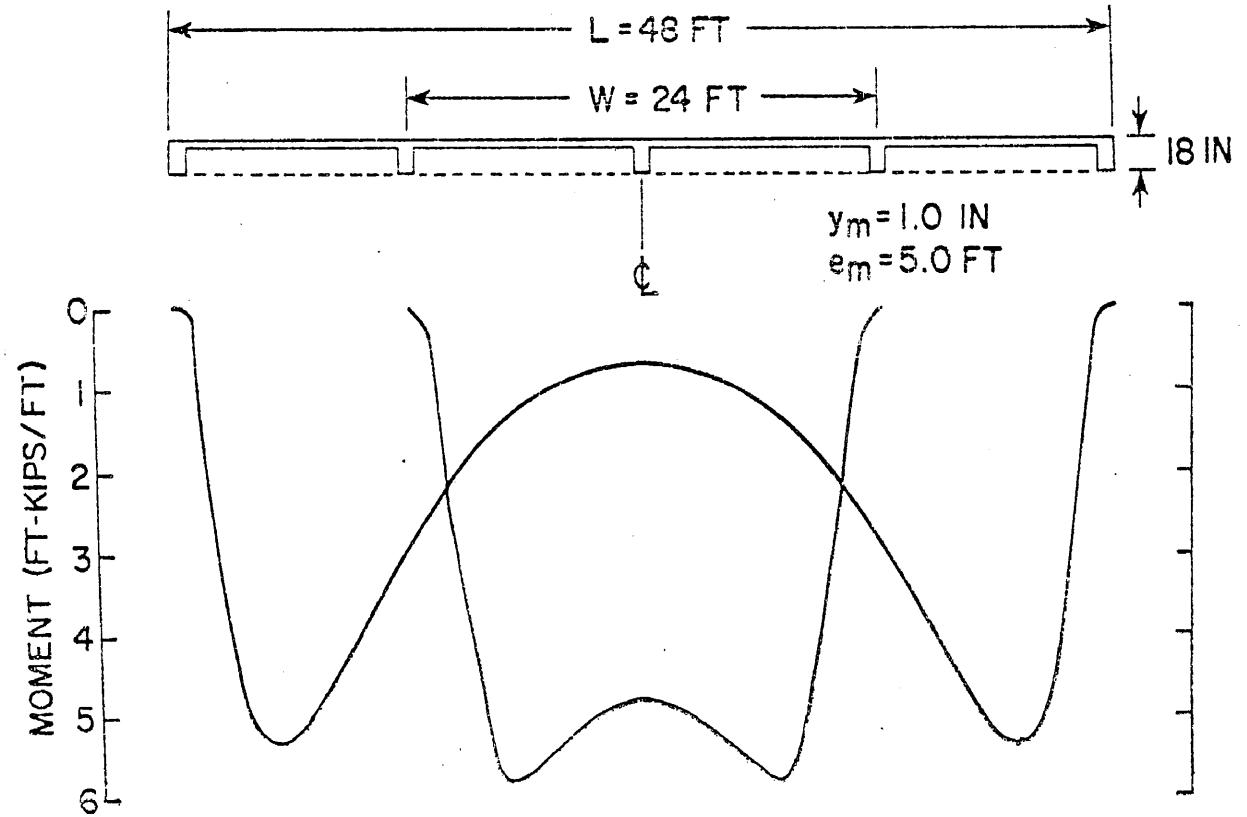

FIGURE 29. TYPICAL VARIATION OF MOMENT ALONG THE LONGITUDINAL AND TRANSVERSE AXES OF A RECTANGULAR SLAB.

longitudinal and transverse axes are plotted for a 48 ft x 24 ft slab. Three characteristics are noted from this figure.

1. The magnitude of the longitudinal moments decreases significantly as the midpoint of the slab is approached.

2. The magnitude of the transverse moments decreases only slightly as the midpoint of the slab is approached.

3. The maximum moment occurs near the perimeter of the slab in both directions, not near the center.

Not shown in the figure but discovered in the overall analysis is that the amount of moment reduction occurring near the midpoint of the slab is dependent upon the stiffening beam depth; the deeper the beam, the less is the decrease in moment.

A plan view of the distribution of the bending moment in both the long and short directions is shown in Figure 30. As in Figure 29, the moment "peak" can be identified in both directions near the slab perimeter. It is significant to note that a particular magnitude of moment extends essentially from one edge of the slab to the other (perpendicular to the direction being considered) in both the long and short directions. The importance of this observation is that there is not any significant amount of localizing or concentration of moment that could be satisfied in the slab design while providing a reduced section for the remainder of the slab.

A comparison of the moment profiles along the longitudinal axes of slabs similar in all respects except length is shown in Figure 31. Four characteristics are noted in this comparison.

1. As in Figure 29, the magnitude of the moment in all four slab

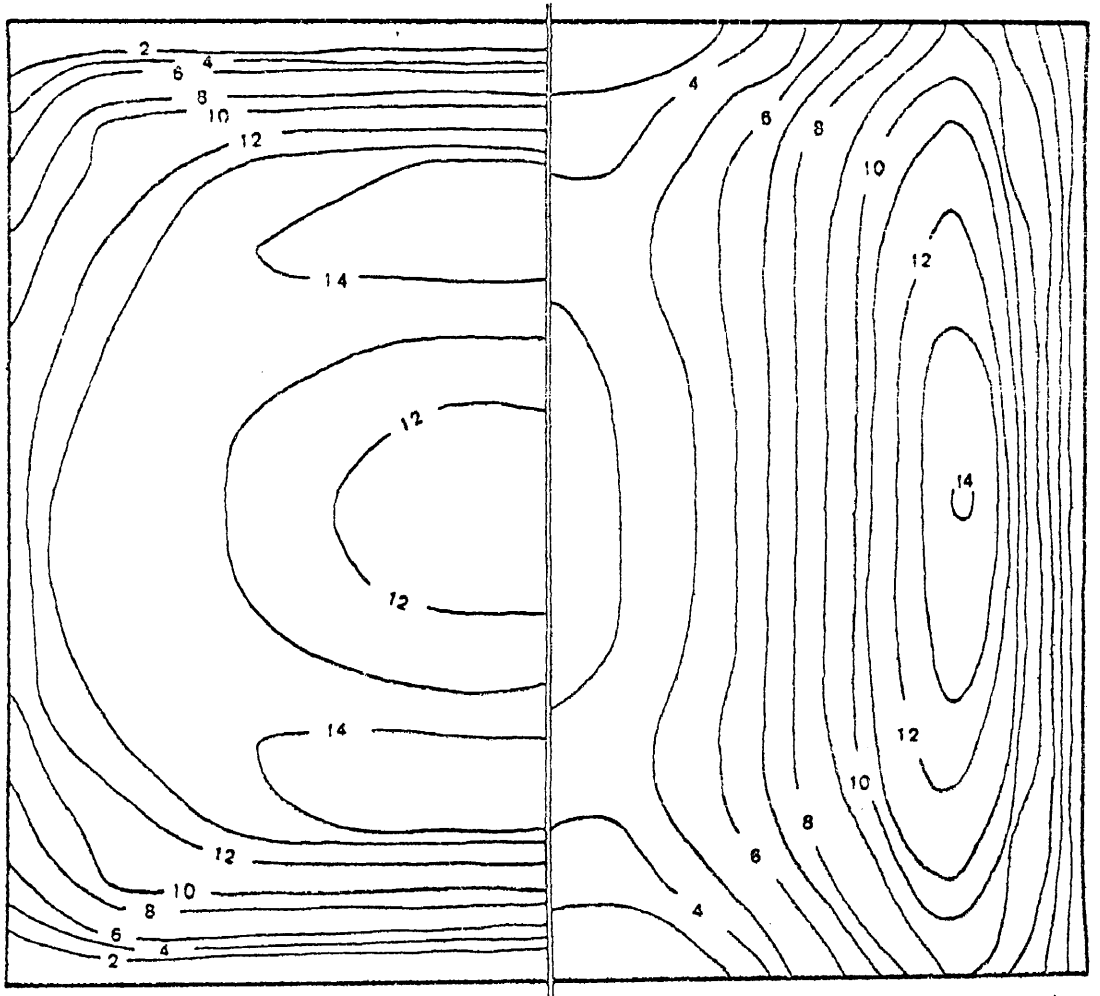

(MOMENTS IN SHORT DIRECTION) (MOMENTS IN LONG DIRECTION)

SLAB SIZE:
48 ft × 40 ft
d = 30 in
y_m = .1 in
e_m = 5 ft

(MOMENTS IN FT-KIPS/FT)

FIGURE 30. TYPICAL DISTRIBUTION OF BENDING MOMENT OVER SURFACE OF SLAB.

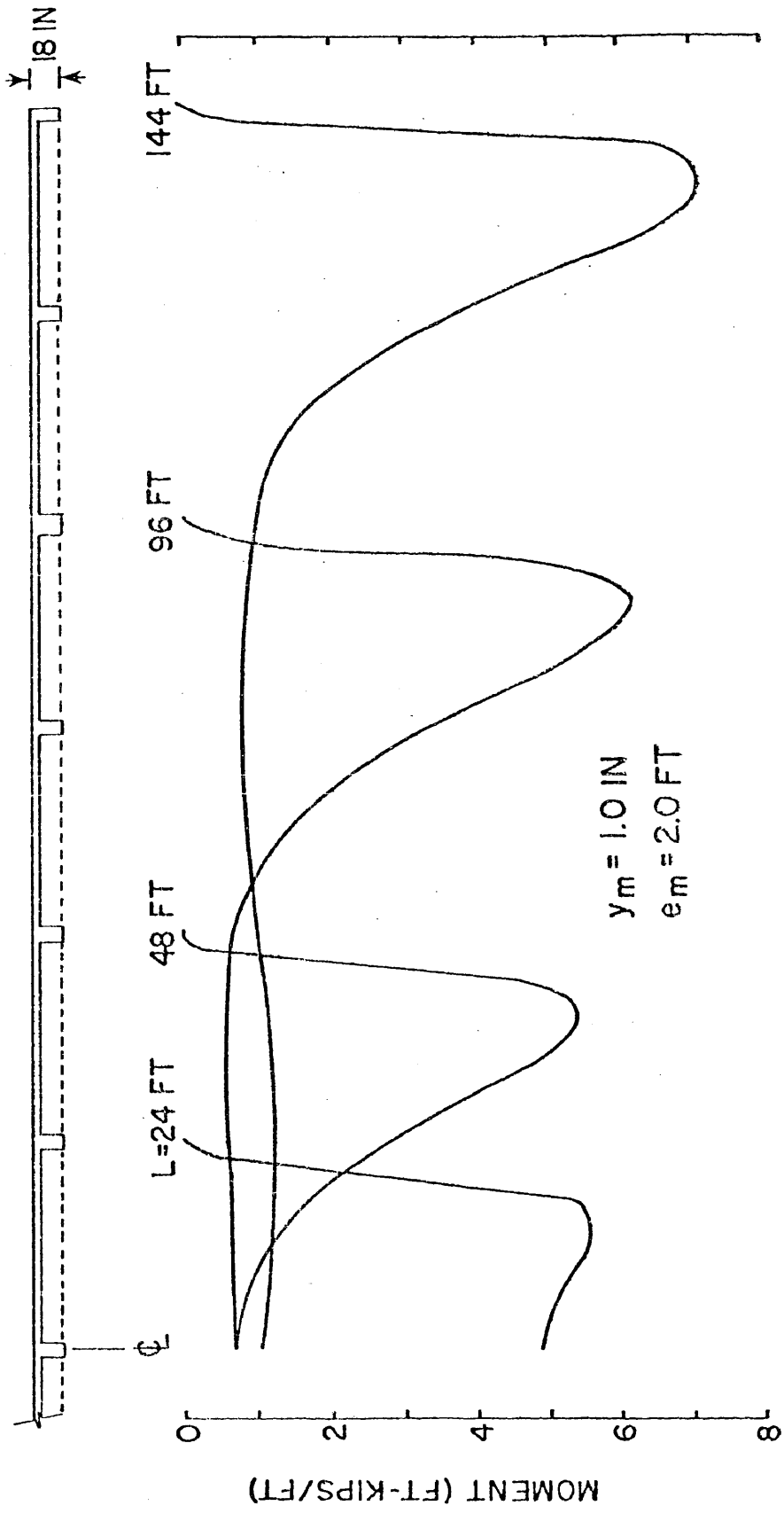

FIGURE 31. TYPICAL VARIATION OF MOMENT ALONG THE LONGITUDINAL AXIS AS SLAB LENGTH INCREASES.

lengths, increases rapidly, peaks, and then decreases as the distance from the edge of the slab increases. Also, the location of the maximum moment is relatively unchanged in each case. The distance from the edge of the slab to the location of the maximum moment can be estimated by the relative stiffness length, β:

$$\beta = \frac{l}{12} \sqrt[4]{\frac{E_c I}{E_s}} \quad \ldots\ldots\ldots\ldots\ldots\ldots\ldots\ldots \quad (5\text{-}3)$$

where β = relative stiffness length, in feet

E_c = creep modulus of concrete, in psi

E_s = modulus of elasticity of the soil, in psi

I = gross moment of inertia of the cross-section perpendicular to the direction being considered, in inches^4.

2. The moment values at the midpoint of the slab for slabs 48 feet or longer are significantly smaller than the peak or maximum moment but the moment at the midpoint for the 24 foot slab is only slightly less than the maximum moment value. Additionally, the slope of the moment profile near the midpoint of the 48 foot slab suggests that if the slab were any shorter, the moment value at the midpoint would not be as small. These observations suggest that slabs 48 feet or longer may be termed "long" slabs whose principal moment requirements occur within approximately two β-lengths from the edge of the slab (one β-length on either side of the maximum moment). Slabs 24 feet or less may be termed "short" slabs and have essentially the same magnitude of moment at any location in the slab that is one β-length or more from the slab perimeter. A slab whose length is

between 24 and 48 feet may be termed an "intermediate" slab and could be expected to have moment magnitudes at the slab midpoint transitioning from the relatively high moments of the short slab to the relatively low moments of the long slab.

3. The maximum moment is approximately the same for the 24 ft and 48 ft slabs but the maximum moment becomes increasingly larger as slab length increases beyond 48 feet. Once again, 48 feet appears to be the threshold of the "long" slab.

4. The 144-ft slab exhibits a small secondary peak occurring at approximately 9ß from the edge. The 96 ft slab also shows a tendency to exhibit a secondary peak but there does not appear to be enough length for the peak to develop properly. Thus, a slab longer than approximately 96 feet is of sufficient length to develop additional but much smaller moment peaks. Slabs of this length might be termed "extra long."

Plotting moment as a function of edge moisture variation distance (edge penetration), the moment data is shown in Figures 32, 33 and 34. It can be noted that the following trends appear:

1. Increasing moment with increasing edge penetration.
2. Increasing moment with increasing beam depth.
3. Increasing moment with increasing differential soil movement.
4. Increasing moment with increasing perimeter load.

One contradiction to the trend of increasing moment with increasing edge penetration is observed when a heavy perimeter load, edge penetration greater than 5 feet, and a differential soil movement

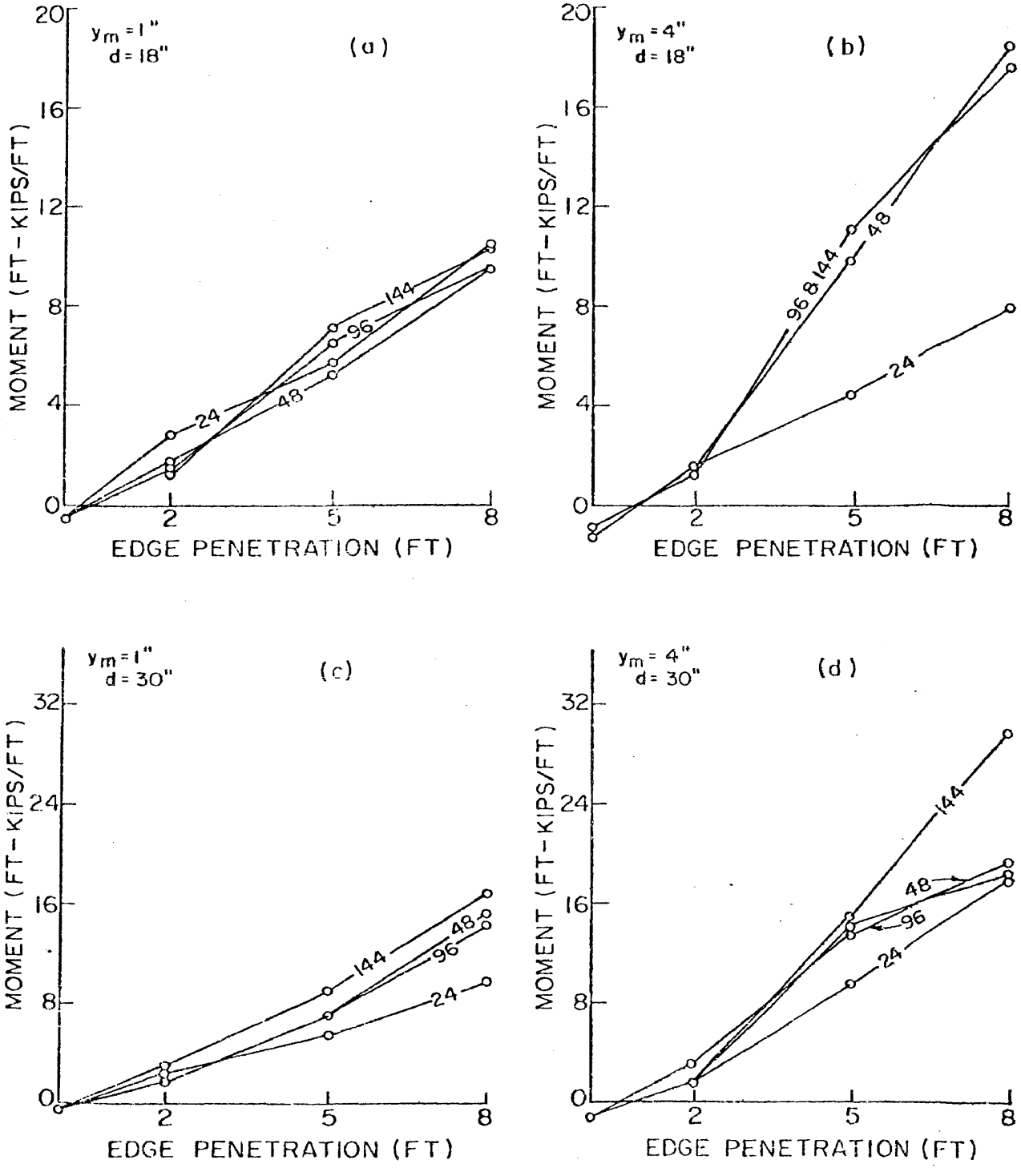

FIGURE 32. MAXIMUM NEGATIVE MOMENT OCCURRING AS A RESULT OF A PERIMETER LOAD AND CENTER LIFT CONDITION (PERIMETER LOAD = 613 LB/FT) IN 24 FT WIDE SLABS 24, 48, 96, AND 144 FT IN LENGTH.

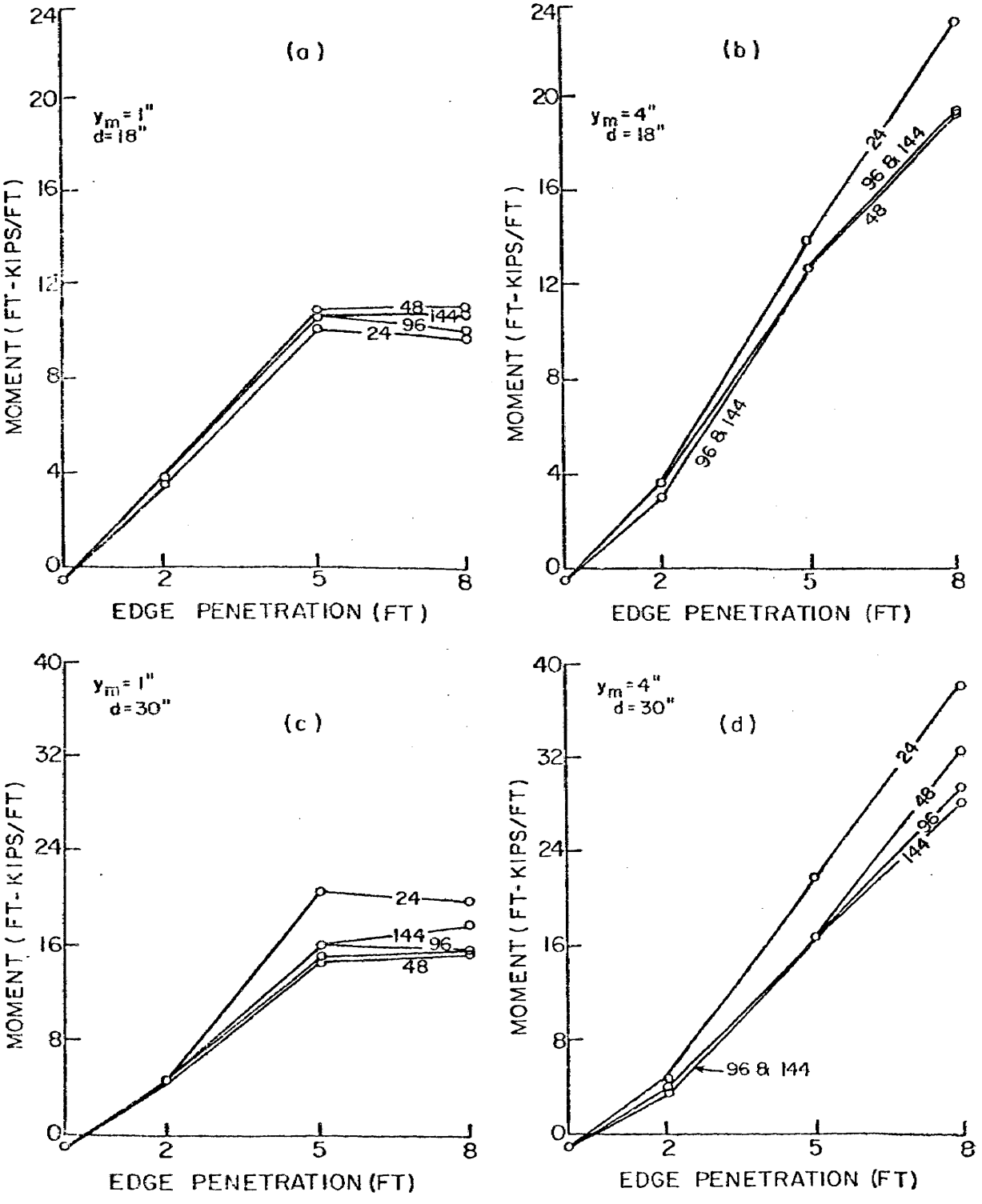

FIGURE 33. MAXIMUM NEGATIVE MOMENT OCCURRING AS A RESULT OF A PERIMETER LOAD AND CENTER LIFT CONDITION (PERIMETER LOAD = 1477 LB/FT) IN 24 FT WIDE SLABS 24, 48, 96, AND 144 FT IN LENGTH.

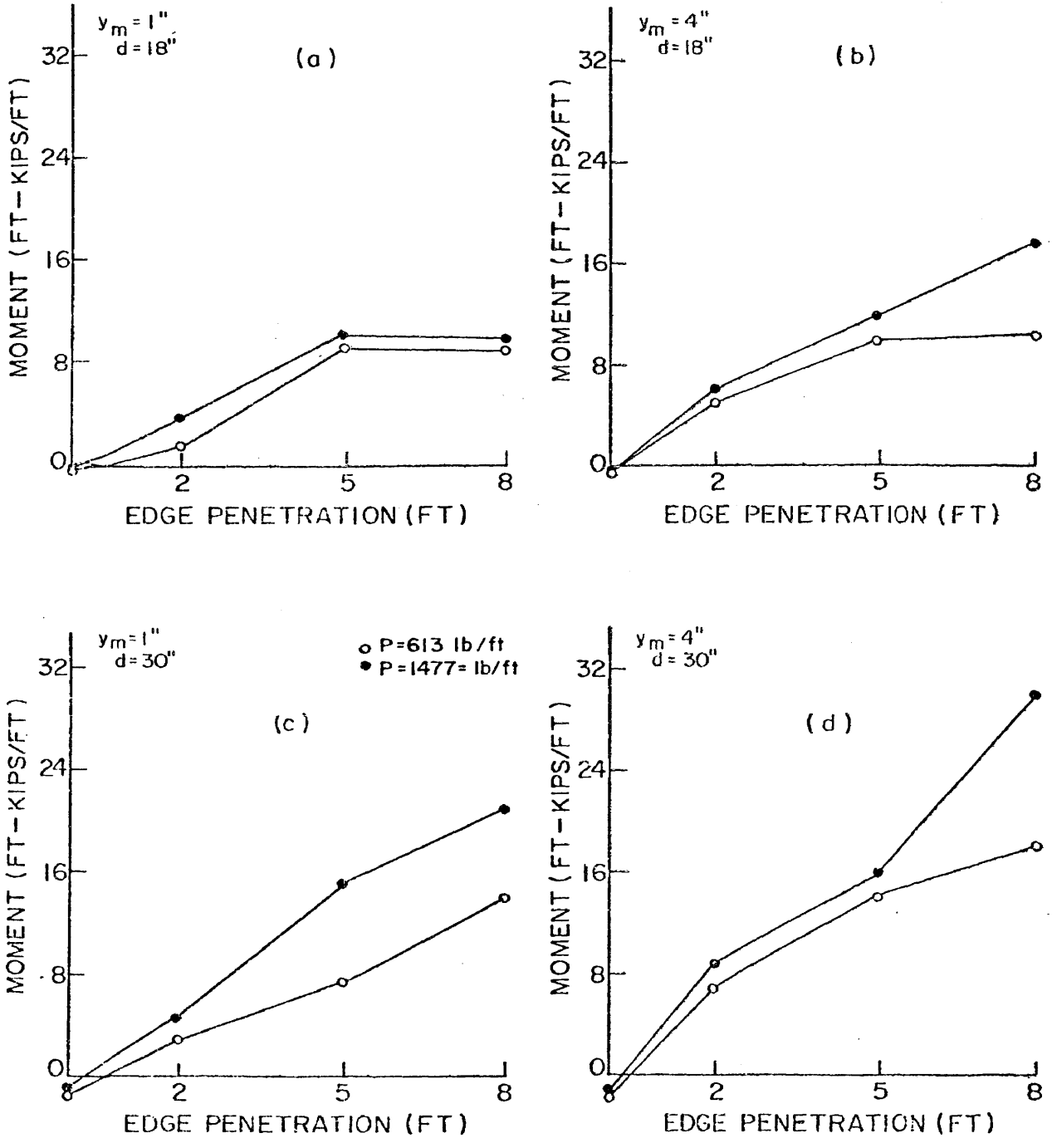

FIGURE 34. MAXIMUM NEGATIVE MOMENT OCCURRING AS A RESULT OF A PERIMETER LOAD AND CENTER LIFT CONDITIONS ACTING ON A 48 FT X 40 FT SLAB.

of 1-inch are included as variables. Close inspection of the computer results for the 5-ft edge penetration problems revealed the slab edge to either be in contact or very close to being in contact with the supporting soil. Thus, when the 8-ft edge distance problem was analyzed, there was little opportunity for an increase in the induced moment since the soil would support the slab as it was being compressed into the subgrade.

The regression analysis of the maximum moment data for the long direction produced an equation relating the design variables to the moment as follows:

$$M_{\ell} = \frac{1}{727}\left[(L)^{0.013}(S)^{0.306}(d)^{0.688}(P)^{0.534}(y_m)^{0.193}(e_m)^{1.238}\right] \quad \ldots \quad (5\text{-}4)$$

By comparing the exponents on the terms in Equation (5-4), it is seen that the edge moisture variation distance, e_m, is the most important variable in determining the magnitude of the expected moment while the slab length is the least important.

Equation (5-4) predicts well except for those conditions discussed above where heavy perimeter loads and small differential soil movements occur. Modifying the regression Equation (5-4) to permit it to account for those conditions resulted in the final design equation being of the form:

$$M_{\ell} = A_{\phi}\left[B(e_m)^{1.238} + C\right] \quad \ldots \quad (5\text{-}5)$$

where M_ℓ = design moment in the long direction, in ft-kips/ft

and

$$A_o = \frac{1}{727}\left[(L)^{0.013}(S)^{0.306}(d)^{0.688}(P)^{0.534}(y_m)^{0.193}\right] \quad \text{((5-6))}$$

where A_o = an intermediate variable

L = total slab length, in feet

S = spacing of stiffening beams, in feet

d = depth of stiffening beams, (measured from top off slab to bottom of beam), in inches

P = perimeter load, in lbs/foot

e_m = edge moisture variation distance, in feet

y_m = differential soil movement, in inches

B, C = constants, whose value is dependent upon e_m

When the edge moisture variation distance, e_m, is 5 feet or less, Equation ((5-4)) is still valid; thus:

$$\text{for } 0 \leq e_m \leq 5 \quad B = 1, \quad C = 0 \quad \text{((5-7))}$$

but when e_m is greater than 5 feet:

$$\text{for } e_m \geq 5 \quad B = \frac{y_m - 1}{3}, \quad C = \left[8 - \left(\frac{P - 613}{255}\right)\right]\left(\frac{4 - y_m}{3}\right) \quad \text{((5-8))}$$

Comparing the moment in the short direction to the moment in the long direction, it was found that, in general, the short direction moment was larger than the long direction moment. There was also a trend for the short direction moment to increase slightly as the edge moisture variation distance increased. These two trends were found to be essentially linear and the relationship between long and short direction moment was developed as:

$$M_s = \left[\frac{58 + e_m}{60}\right] M_\ell \quad \ldots\ldots\ldots\ldots\ldots\ldots \quad (5\text{-}9)$$

where M_s = moment in the short direction, ft-kips/ft

and all other symbols are as previously defined. The moment data resulting from the soil-structure interaction analysis is presented in Table 23, Appendix M.

The correlation coefficient, expressed as "R-Squared", measures how well the regression model fits the data. R-squared values near zero are expected for completely random data, whereas, an R-squared value of 1.00 would imply all data to be falling on a straight line, i.e., the best possible fit. R-squared values for the regression equations resulting from the analysis of the various SLAB2 data sets are listed in Table 18 and indicate the equations provide a relatively good fit.

Differential Deflection. - Plotting differential deflection, Δ, as a function of edge penetration, e_m, the differential deflection data obtained in the analysis is shown in Figures 35 - 37. Five

TABLE 18. R-Squared Values from Regression Analysis for Principal Design Equations

DISTORTION MODE	DESIGN PARAMETER	SYMBOL	EQUATION NUMBER	R-SQUARED VALUE
Center Lift	Moment	M_ℓ	5-5	0.88
	Differential Deflection	Δ_0	5-10	0.85
	Shear	V_ℓ	5-11	0.70
		V_s	5-12	0.69
Edge Lift	Moment	M_ℓ	5-13	0.94
	Differential Deflection	Δ	5-15	0.88
	Shear	V	5-16	0.64

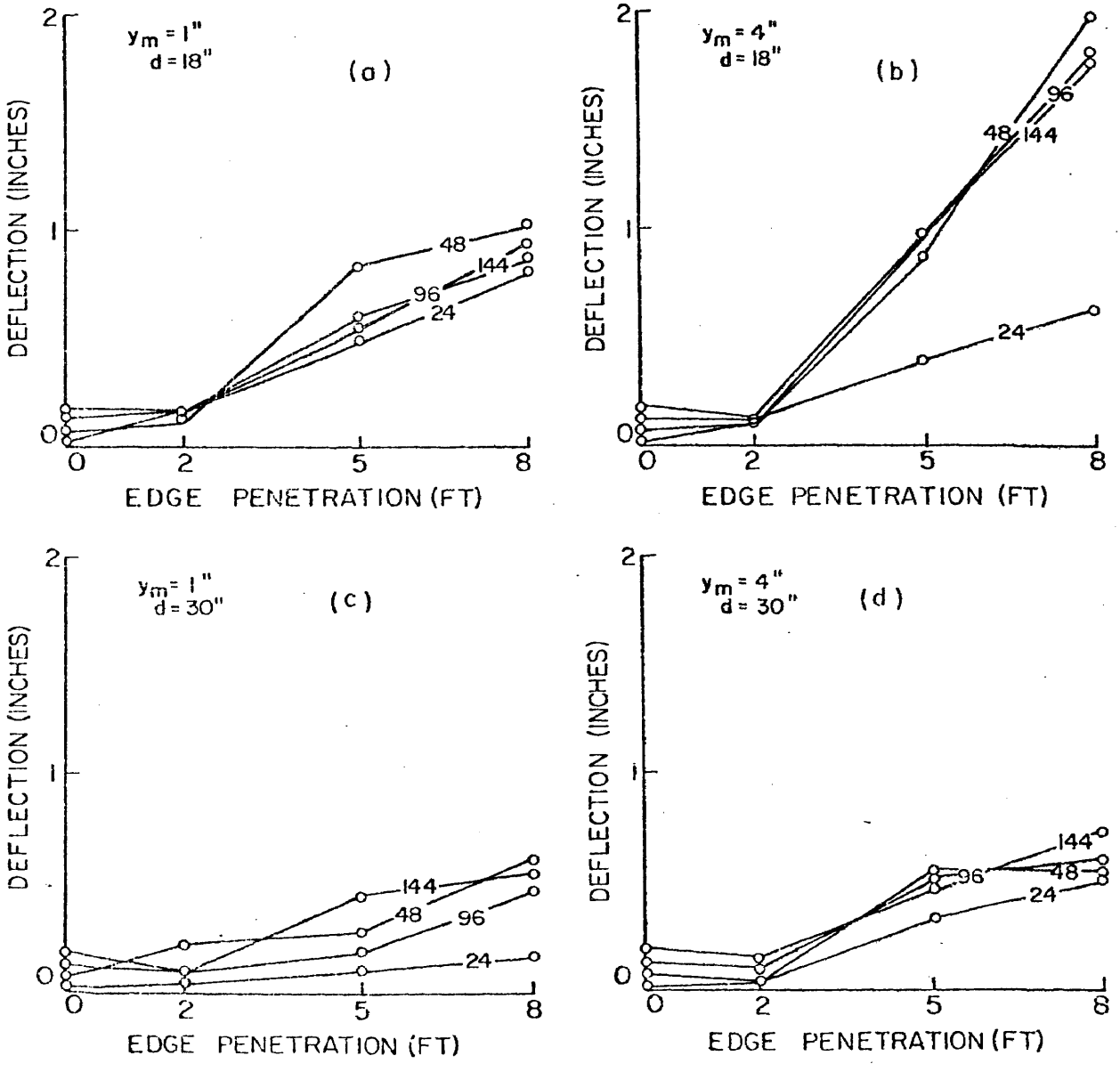

FIGURE 35. MAXIMUM DIFFERENTIAL DEFLECTION OCCURRING AS A RESULT OF A PERIMETER LOAD AND CENTER LIFT CONDITION (PERIMETER LOAD = 613 LB/FT) IN 24FT WIDE SLABS 24, 48, 96, AND 144 FT IN LENGTH.

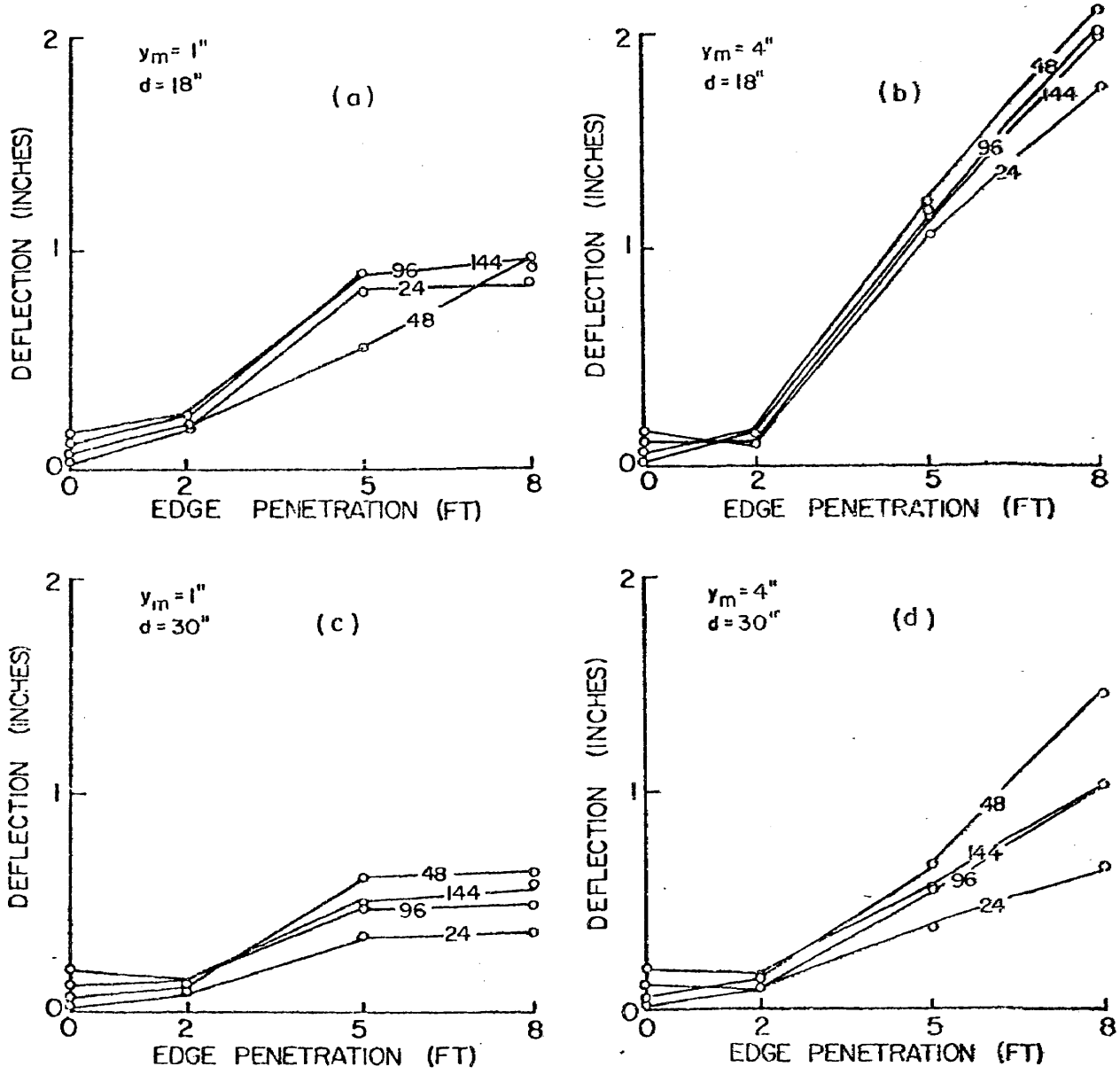

FIGURE 36. MAXIMUM DIFFERENTIAL DEFLECTION OCCURRING AS A RESULT OF A PERIMETER LOAD AND CENTER LIFT CONDITION (PERIMETER LOAD= 1477 LB/FT IN 24 FT WIDE SLABS 24, 48, 96, AND 144 FT IN LENGTH.

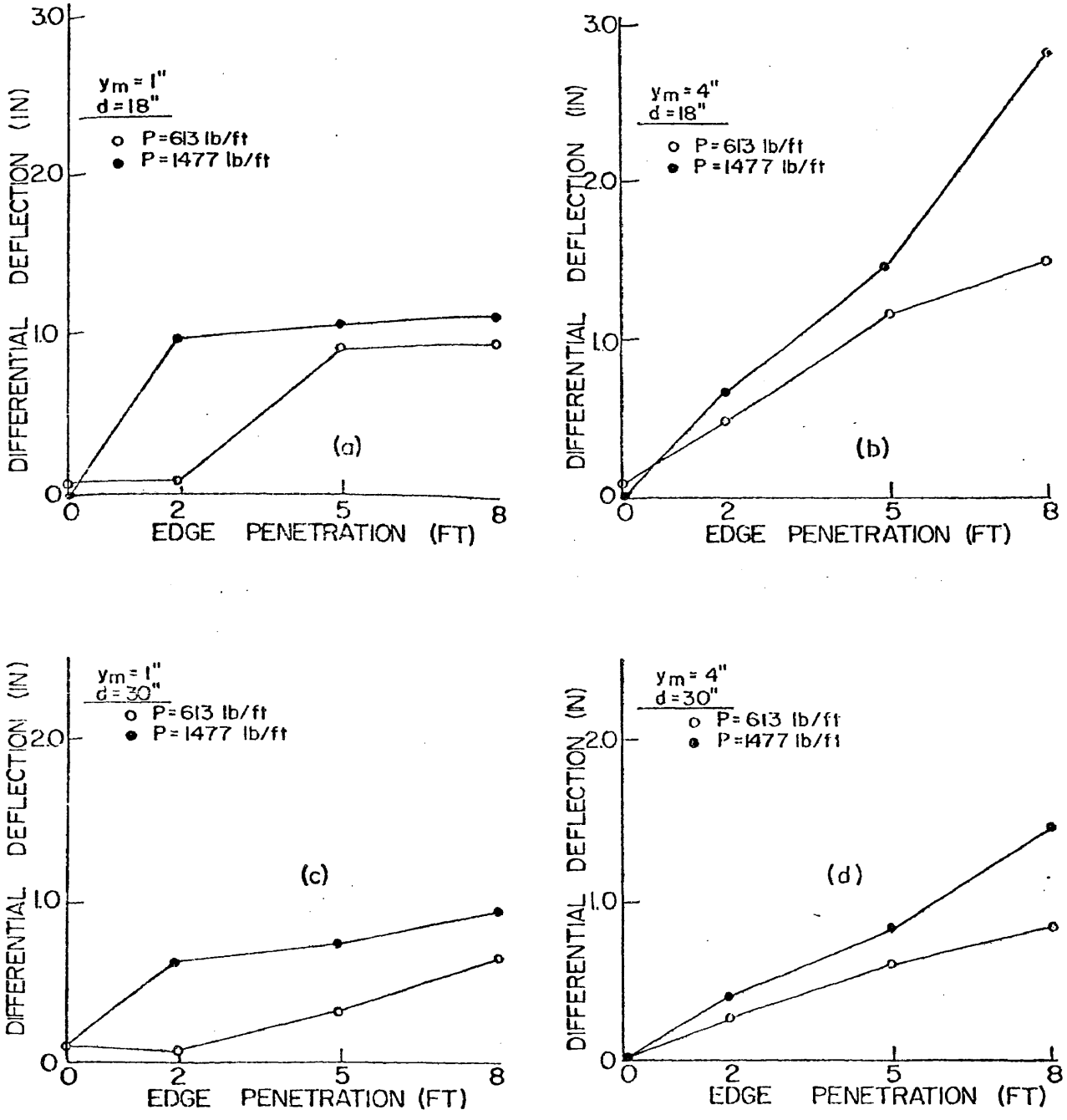

FIGURE 37. MAXIMUM DIFFERENTIAL DEFLECTION OCCURRING AS A RESULT OF A PERIMETER LOAD AND CENTER LIFT CONDITIONS ACTING ON A 48FT X 40FT SLAB.

general observations can be made from these figures:

1. In general, there is little increase in differential deflection from the "no swell" condition (e_m = 0 ft) until the edge penetration distance exceeds 2 feet.

2. The slab with 18-inch deep stiffening beams experiences greater differential deflection than the slab with 30-inch beams.

3. Slightly greater differential deflection occurs when the differential soil movement is 4 inches than when it is 1 inch.

4. Only a small amount of increase in differential deflection is noted as y_m increases from 5-feet to 8-feet when the heavy perimeter load is applied. This observation is in agreement with the bending moment observations for the same conditions noted above.

5. The two longest slabs, L = 96 ft and L = 144 ft, exhibit almost identical differential deflection values, implying that extra long slabs may exhibit similar differential deflections regardless of length. This trend was not as noticeable in the bending moment data.

Analysis of the maximum and minimum deflection locations showed that the distance between these two points was not always the total slab length. In most instances where the slab length was longer than 48 feet, it was found that the greatest differential deflections occurred within a distance of approximately 6β, not the greater distance of total slab length. Figure 38 shows how deflection typically varied along the longitudinal axis of four identical slab problems where only the length varied. It can be seen in this figure that multi-modal bending occurs in the longer slabs and that more than one differential deflection value can be determined in the long direction.

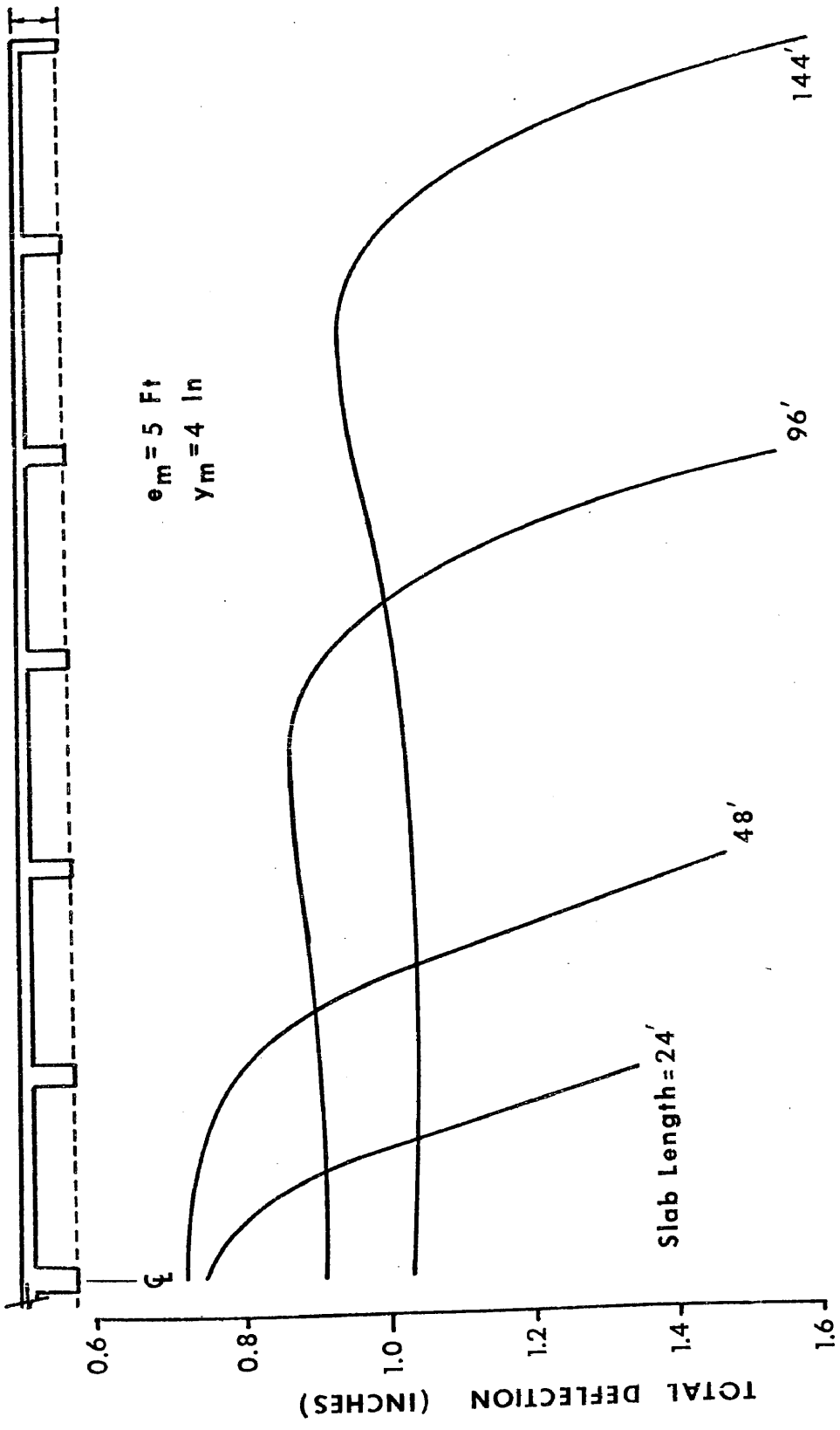

FIGURE 38. RELATIONSHIP BETWEEN SLAB LENGTH AND DEFLECTION OF SLAB SURFACE.

The regression analysis of the maximum differential deflection data (Table 25, Appendix M) resulted in the following equation:

$$\Delta_0 = \left[\frac{(y_m L)^{0.205}(S)^{1.059}(P)^{0.523}(e_m)^{1.296}}{380(d)^{1.214}} \right] \quad \ldots\ldots \quad (5\text{-}10)$$

where Δ_0 = differential deflection, in inches

L = slab length in the direction being considered, in feet.

and all other symbols are as previously defined.

Examination of Equation (5-10) shows the edge moisture variation distance e_m, the beam depth, d, and the beam spacing, S, to have the greatest influence on the magnitude of the differential deflection; differential deflection increases with either increasing beam spacing or edge penetration and Δ_0 decreases with increasing beam depth. The slab length and the differential soil movement have the least influence on the magnitude of the expected deflection.

Shear. - Shear forces resulting from the center lift analysis were found to be approximately two times larger than values obtained from check calculations using statics. The shears were also found to be approximately twice as large as the shear forces calculated by computer program PRESS2 for similar conditions of loading and soil support. The reason for the large values obtained from the SLAB2 analysis are attributed to the numerical technique used to accomplish the calculations and the relatively large elements used in the analysis. Consequently, all of the center lift shear results were multiplied by a factor of 0.5 in order to better comply with the principles of statics. The modified

values of shear force are plotted as a function of edge penetration distance in Figures 39 - 41 . From these figures, five observations are noted:

1. In general, shear force increases as edge penetration distance increases.

2. Shear force increases as beam depth increases.

3. Shear force increases slightly as perimeter load increases.

4. Shear force increases only slightly as the edge penetration distance increases from 0 to 2 feet.

5. Shear force increases slightly as the differential soil movement increases.

Analysis of the distribution as well as the location of the maximum shear force showed it to be concentrated near the perimeter edge of the slab. (Figure 42). In each case, the maximum shear force occurred within one-β distance from the slab edge.

The regression analysis of the maximum shear force data (Table 24, Appendix M) produced the following equations:

Long Direction:

$$V_{\ell} = \frac{1}{1940} \left[(L)^{0.90}(S)^{0.71}(d)^{0.43}(P)^{0.44}(y_m)^{0.16}(e_m)^{0.93} \right] \quad \ldots (5\text{-}11)$$

Short Direction:

$$V_s = \frac{1}{1350} \left[(L)^{0.19}(S)^{0.45}(d)^{0.20}(P)^{0.54}(y_m)^{0.04}(e_m)^{0.97} \right] \quad \ldots (5\text{-}12)$$

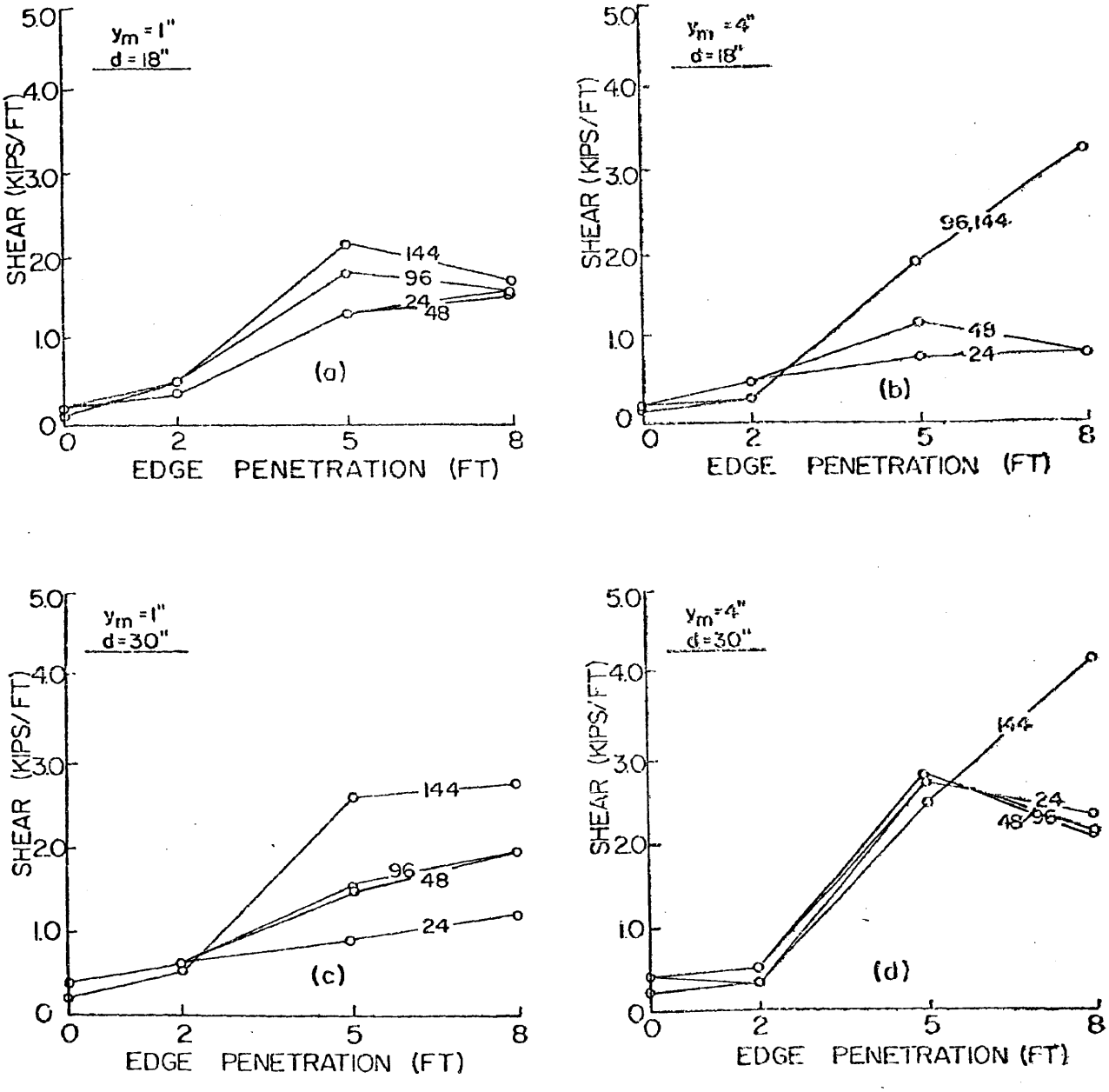

FIGURE 39. MAXIMUM SHEAR FORCE OCCURRING AS A RESULT OF A PERIMETER LOAD AND CENTER LIFT CONDITION (PERIMETER LOAD = 613/LB FT) IN 24-FT WIDE SLABS 24, 48, 96, AND 144-FT IN LENGTH.

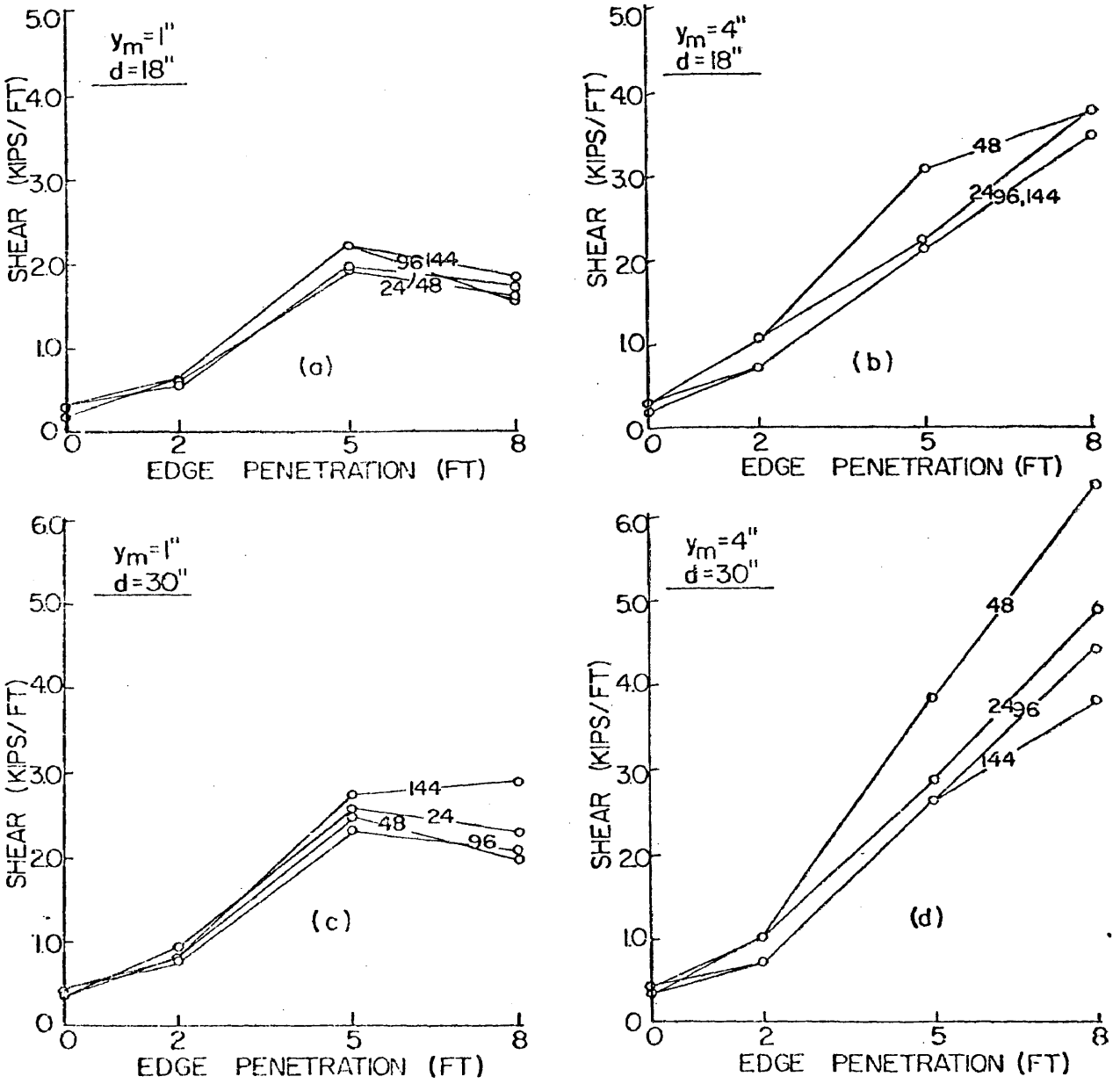

FIGURE 40. MAXIMUM SHEAR FORCE OCCURRING AS A RESULT OF A PERIMETER LOAD AND CENTER LIFT CONDITION (PERIMETER LOAD = 1477 LB/FT) IN 24 FT WIDE SLABS 24, 48, 96, AND 144 FT IN LENGTH.

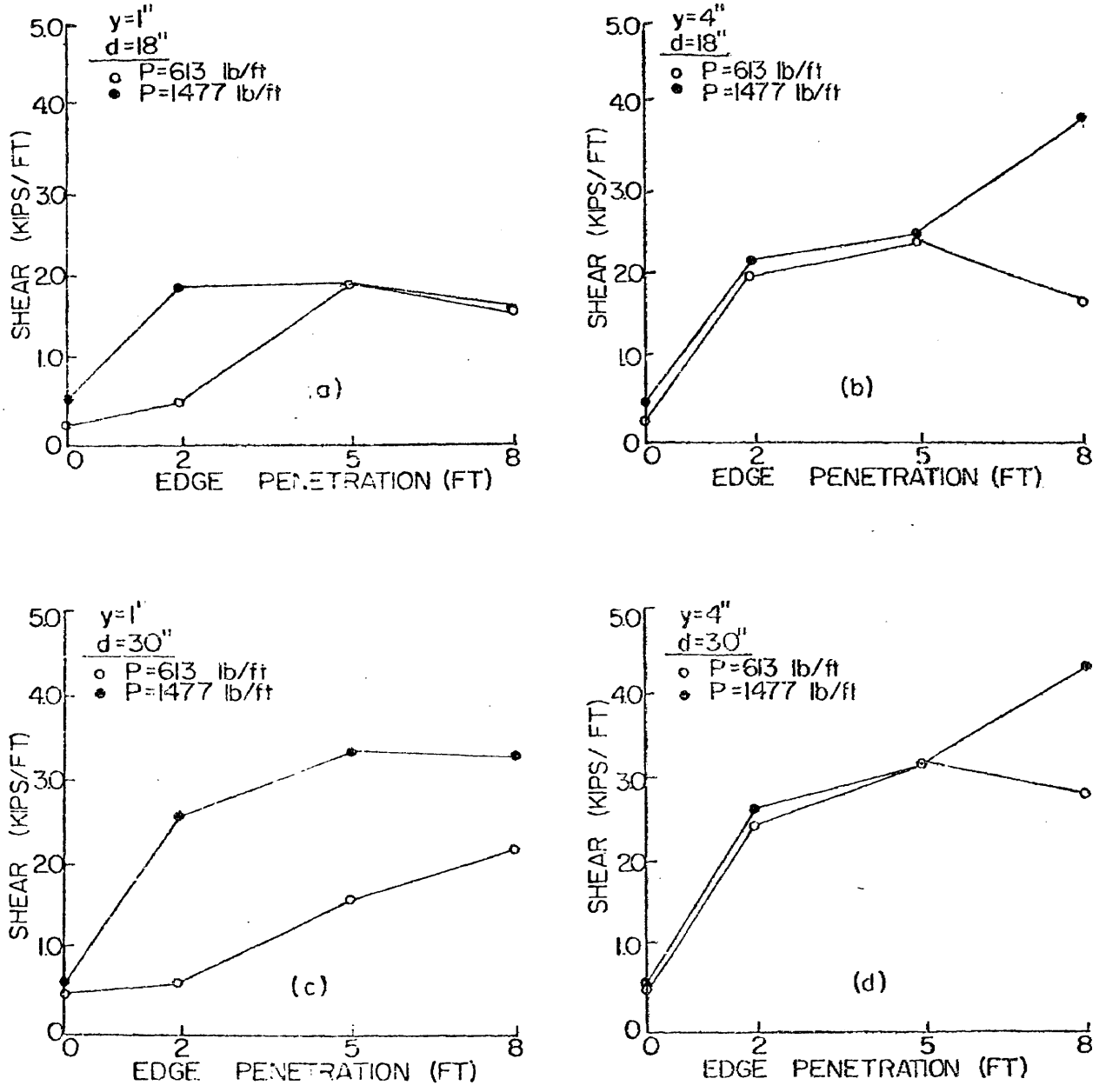

FIGURE 41. MAXIMUM SHEAR FORCE OCCURRING AS A RESULT OF A PERIMETER LOAD AND CENTER LIFT CONDITIONS ACTING ON A 48FT X 40FT SLAB.

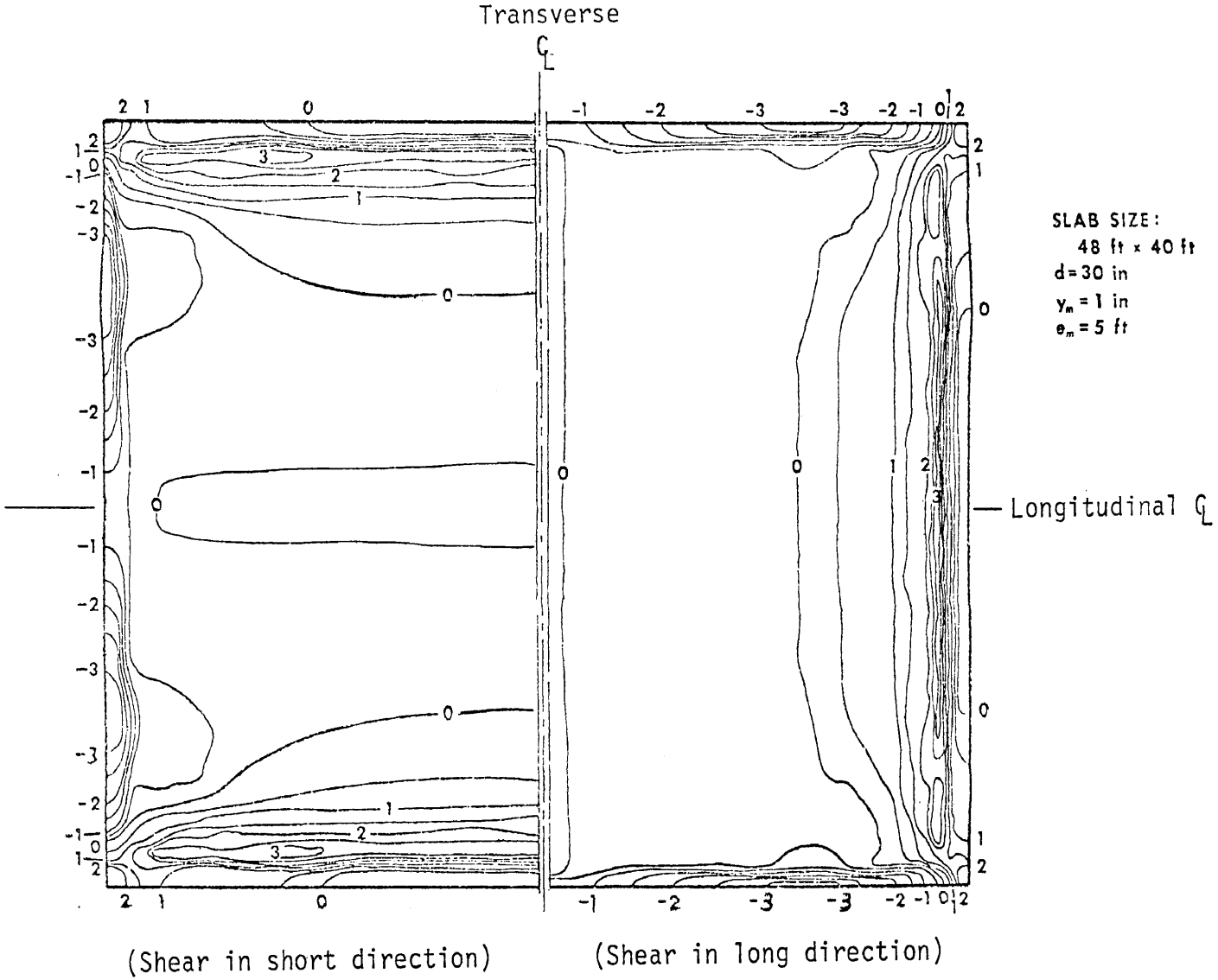

FIGURE 42. TYPICAL DISTRIBUTION OF SHEAR FORCE OVER SURFACE OF SLAB.

where V_ℓ = shear force in the long direction, in kips/ft

V_s = shear force in the short direction, in kips/ft

Examination of the two equations show the edge penetration distance to have the greatest influence on the magnitude of the expected shear while the slab length has the least influence. These two variables had similar influences in the moment equation, Equation (5-5).

Results of Edge Lift Analysis

Moment. - As with the negative bending moments, the magnitude of the positive bending moment first increased rapidly, peaked, and then decreased as the distance from the edge of the slab increased. Figure 29, p. 112, is also typical of the moments resulting from the edge lift analysis.

Whereas the center lift moments showed a tendency for the moment to increase slightly with increasing slab length, the edge lift moments showed no apparent trend of either increasing or decreasing magnitude of maximum moment with increasing length.

Figures 43 - 47 show the edge lift moment data plotted as a function of edge penetration distance. Three observations can be made from these figures.

1. As beam depth increases, the moment increases.
2. As perimeter load increases, the moment decreases.
3. In general, moment increases with increasing edge penetration distance.

The regression analysis of the maximum moment data for the long

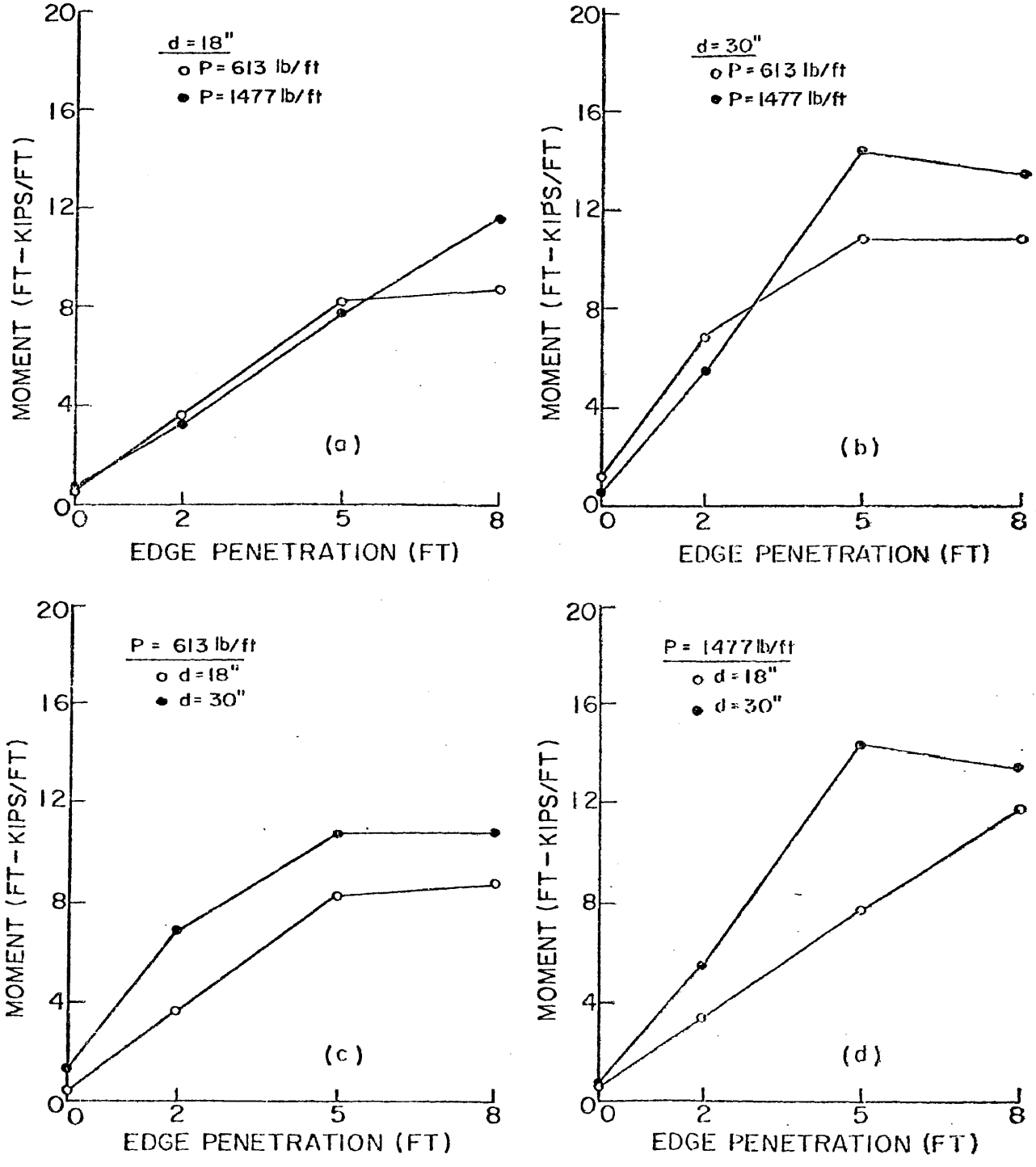

FIGURE 43. MAXIMUM POSITIVE MOMENTS OCCURRING AS A RESULT OF PERIMETER LOADING AND EDGE LIFT CONDITIONS. (SLAB SIZE: 24FT X 24FT).

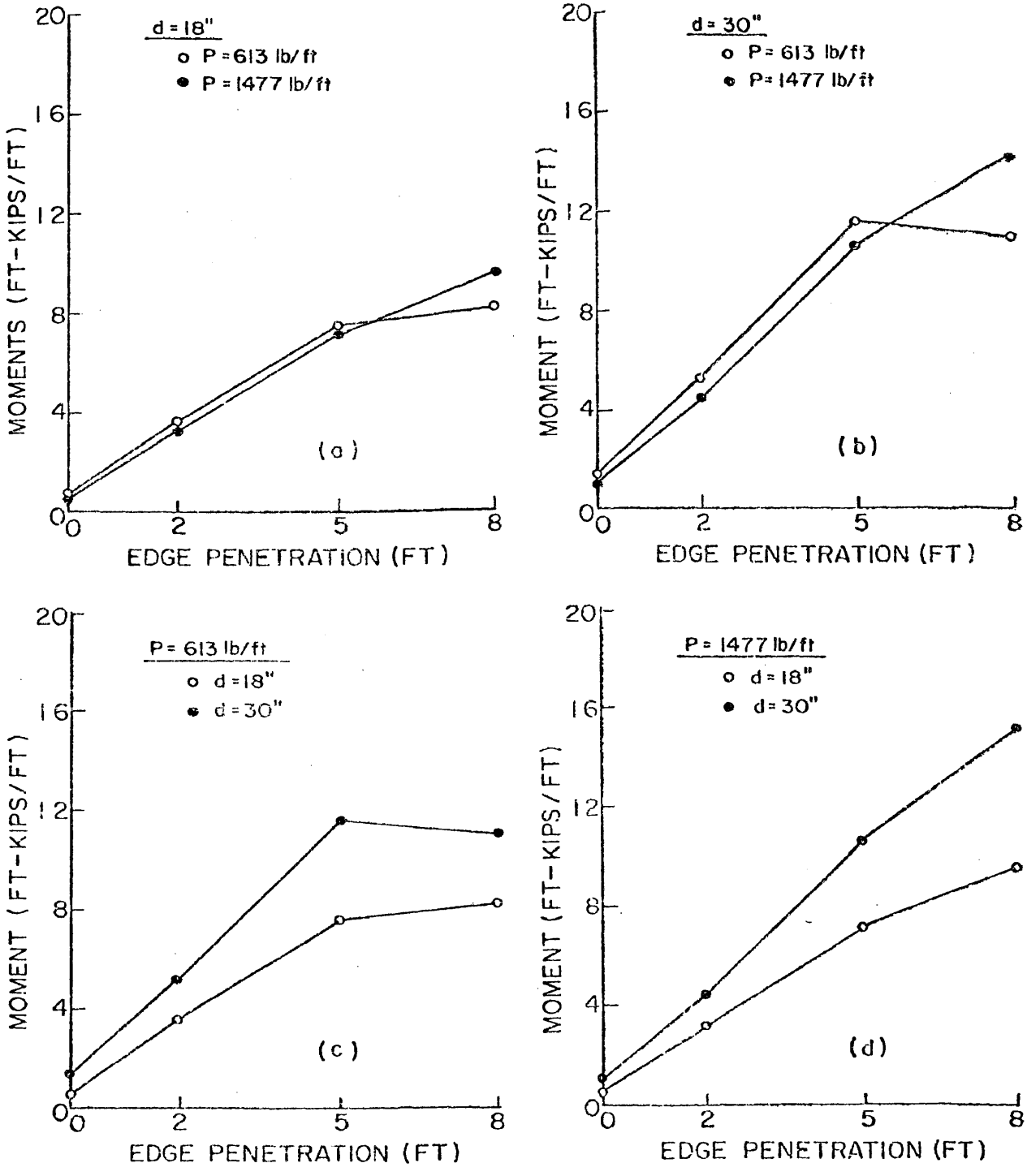

FIGURE 44. MAXIMUM POSITIVE MOMENTS OCCURRING AS A RESULT OF PERIMETER LOADING AND EDGE LIFT CONDITIONS. (SLAB SIZE: 48FT X 24FT).

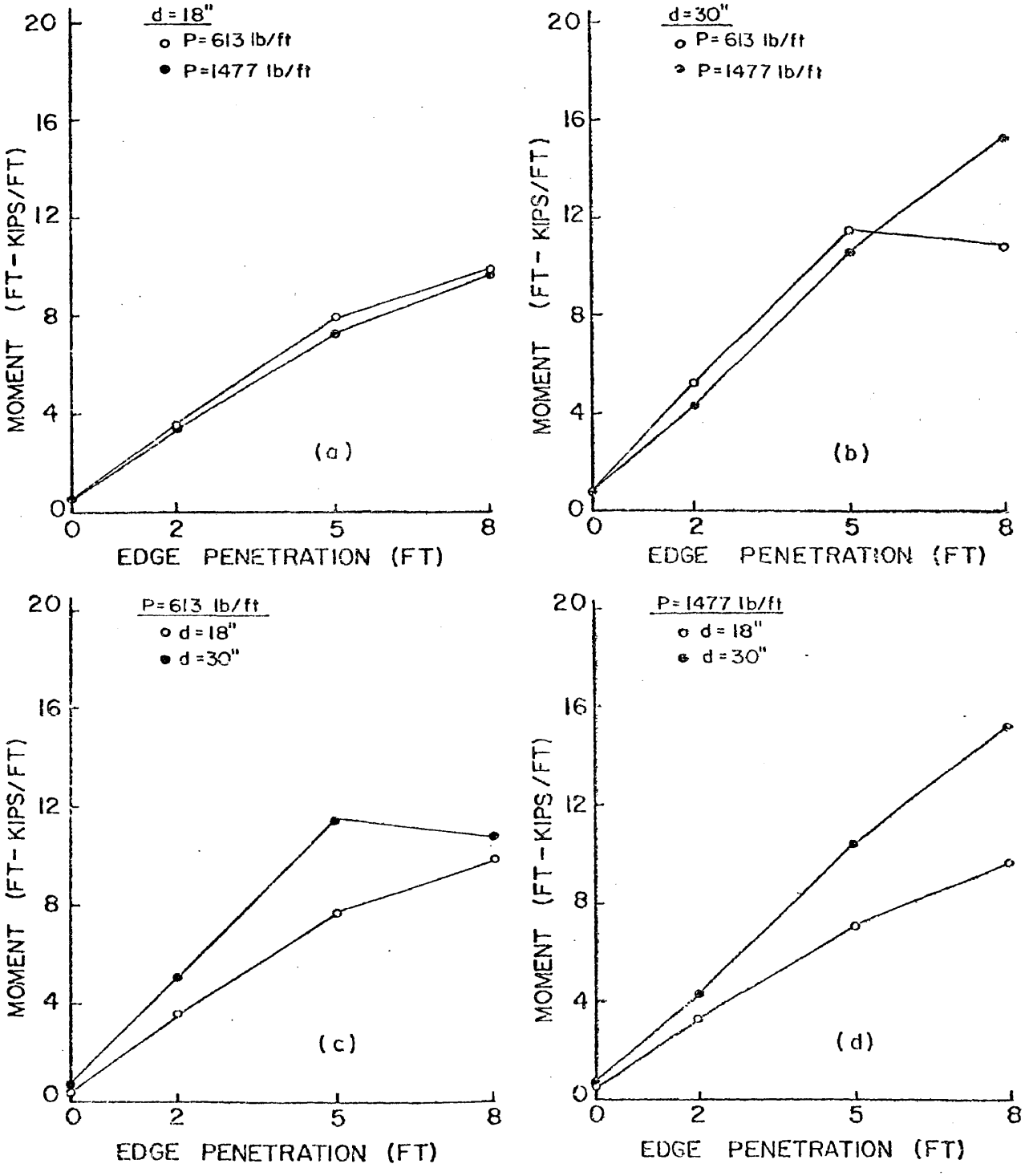

FIGURE 45. MAXIMUM POSITIVE MOMENTS OCCURRING AS A RESULT OF PERIMETER LOADING AND EDGE LIFT CONDITIONS. (SLAB SIZE: 96FT X 24FT).

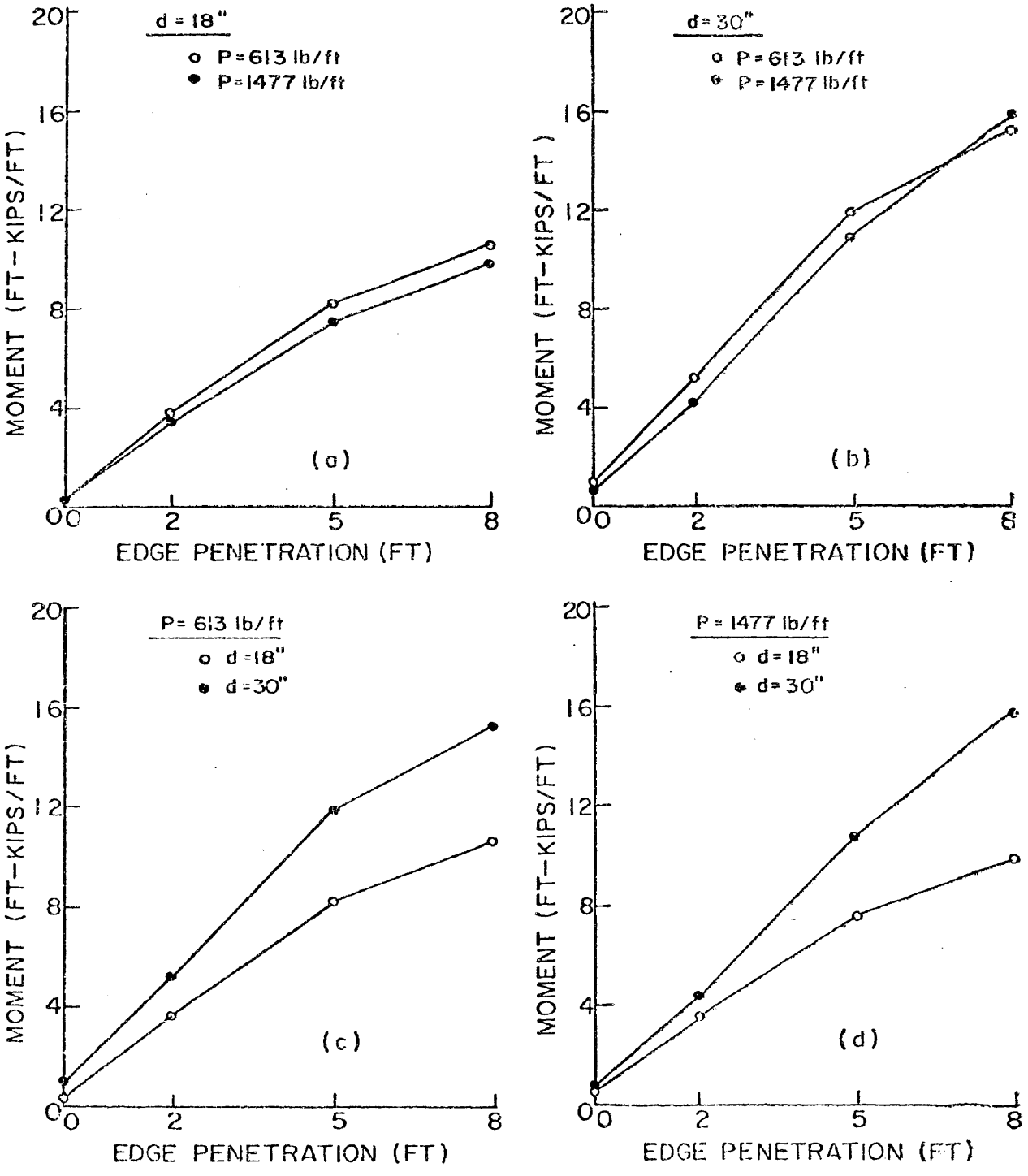

FIGURE 46. MAXIMUM POSITIVE MOMENTS OCCURRING AS A RESULT OF PERIMETER LOADING AND EDGE LIFT CONDITIONS. (SLAB SIZE: 144FT X 24FT).

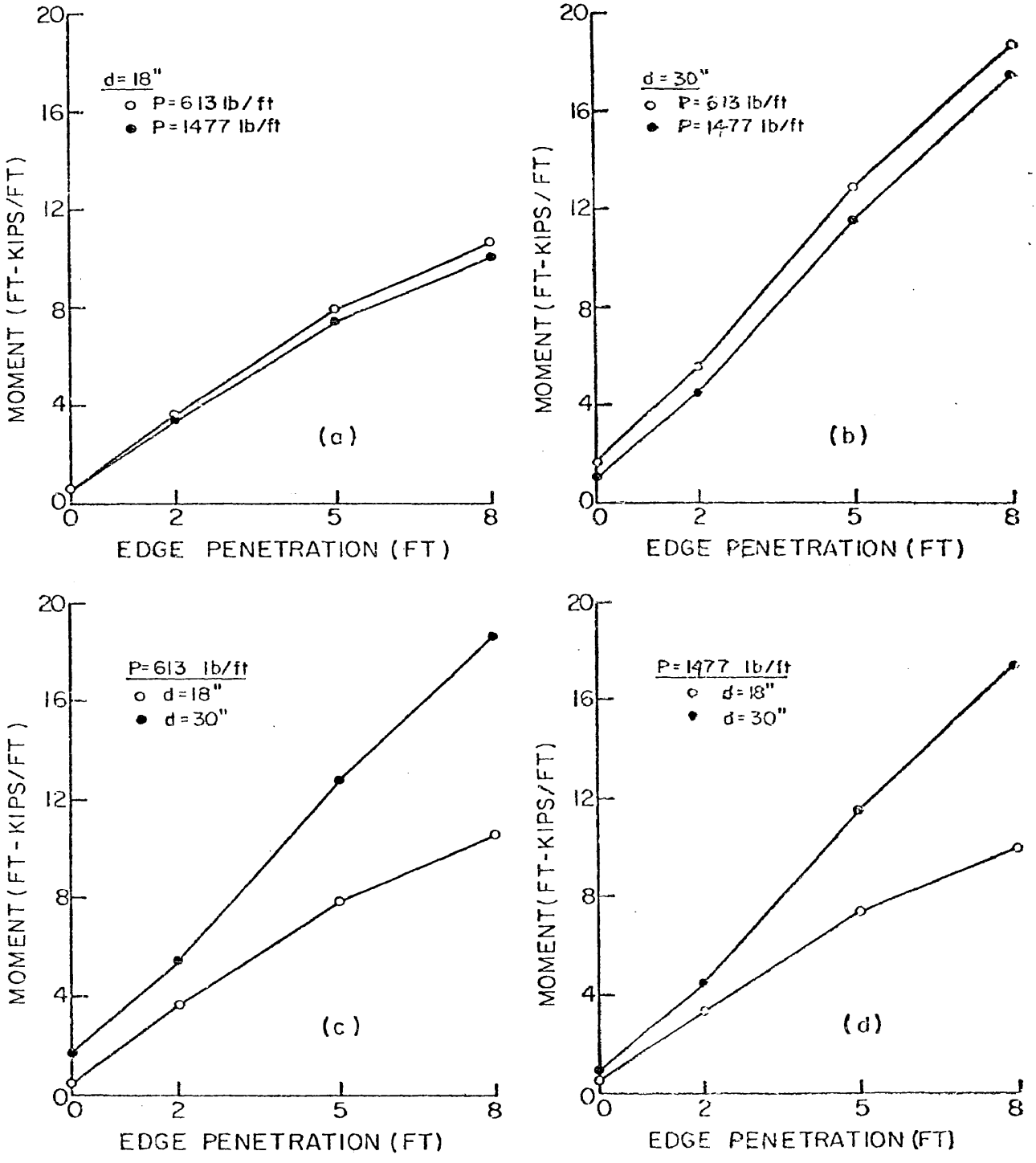

FIGURE 47. MAXIMUM POSITIVE MOMENTS OCCURRING AS A RESULT OF PERIMETER LOADING AND EDGE LIFT CONDITIONS. SLAB SIZE: (48 FT x 40FT).

direction produced a design equation of the form:

$$M_{\ell} = \left[\frac{(S)^{0.10}(e_m d)^{0.78}(y_m)^{0.66}}{7.2\ (L)^{0.0065}(P)^{0.04}} \right] \quad \ldots\ldots\ldots\ldots \quad (5\text{-}13)$$

where M_{ℓ} = moment in the long direction, in ft-kips/ft

and all other symbols are as previously defined.

Examination of Equation (5-13) shows the beam depth and edge penetration distance to equally have the greatest influence on the magnitude of the moment with the differential soil movement to have almost as much influence as d and e_m.

The observation that there was no discernible trend regarding moment increase or decrease with increasing slab length was borne out by the regression analysis. Although the regression indicated a slight tendency for moment to decrease with increasing length, the exponent on the L term is so small as to have an almost negligible effect on final value of the expected moment.

The regression analysis showed the expected value of moment would decrease slightly with increasing perimeter load. The small magnitude of the exponent was not surprising after examining curves (a) and (b) of Figures 43 - 47 , which show only a small amount of moment reduction with heavier perimeter loads.

In comparing the maximum moments in the short direction to the maximum moments in the long direction, it was found that in every case, the short direction moment was either almost equal to or

greater than the long direction moment. It was also found that the increase in the short direction moment increased faster with increasing depth of the stiffening beam. Thus, the expected value of the moment in the short direction can be found from:

$$M_s = (d)^{0.35} \left[\frac{19 + e_m}{57.75} \right] M_\ell \quad \ldots\ldots\ldots\ldots \quad (5\text{-}14)$$

The maximum moment data resulting from the soil-structure interaction analysis is reported in Table 26, Appendix M.

Differential Deflection. - The differential deflection data from the edge lift analysis is plotted as a function of edge penetration in Figures 48 - 52. Four observations are made from these figures.

1. As perimeter load increases, differential deflection decreases.
2. As stiffening beam depth increases, differential deflection decreases.
3. As edge penetration distance increases, differential deflection increases.
4. As slab length increases, differential deflection increases.

The regression analysis of the maximum differential deflection data (Table 28, Appendix M) resulted in the following equation:

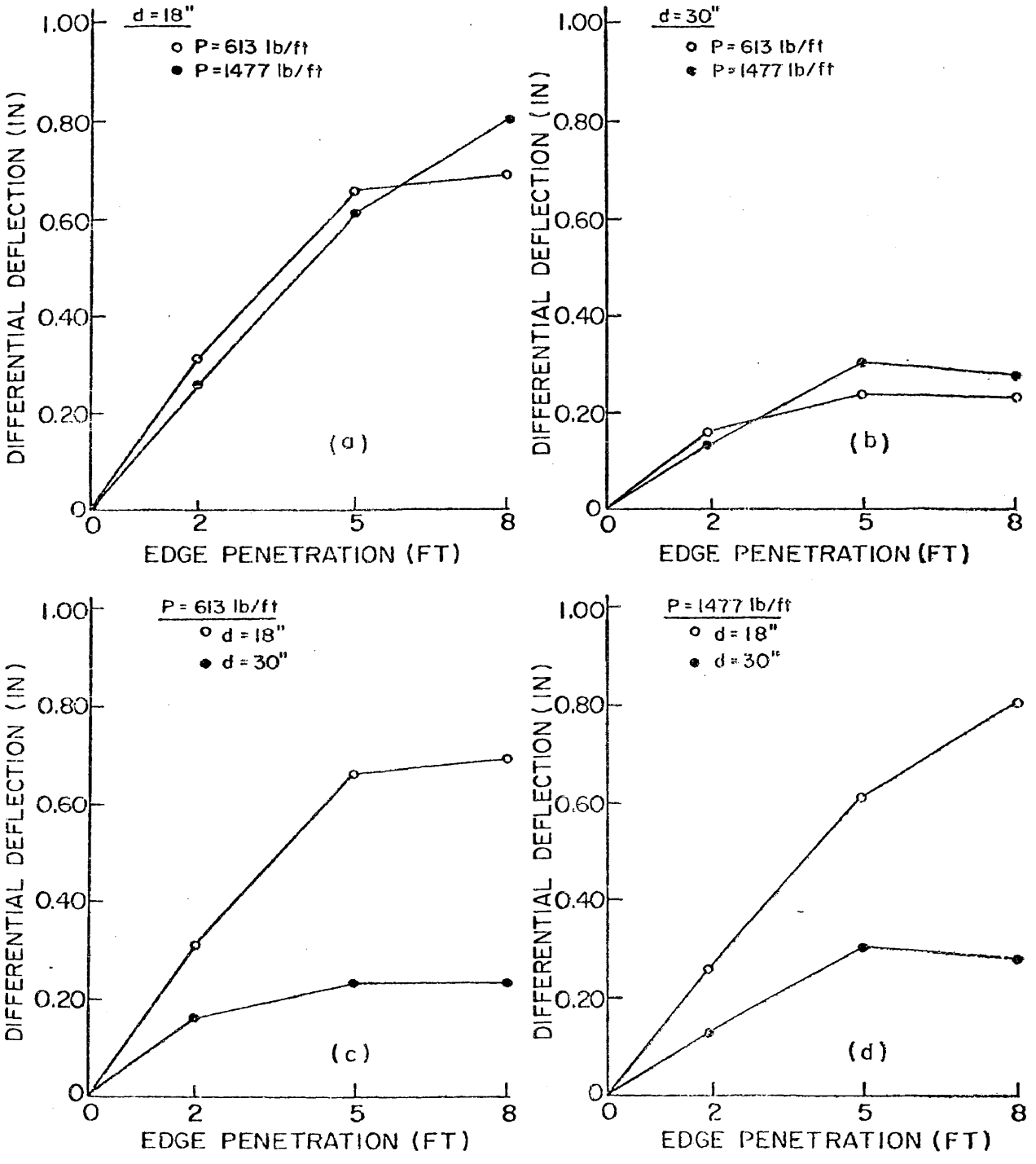

FIGURE 48. MAXIMUM DIFFERENTIAL DEFLECTION OCCURRING AS A RESULT OF PERIMETER LOAD AND EDGE LIFT CONDITIONS. (SLAB SIZE: 24 FT X 24 FT).

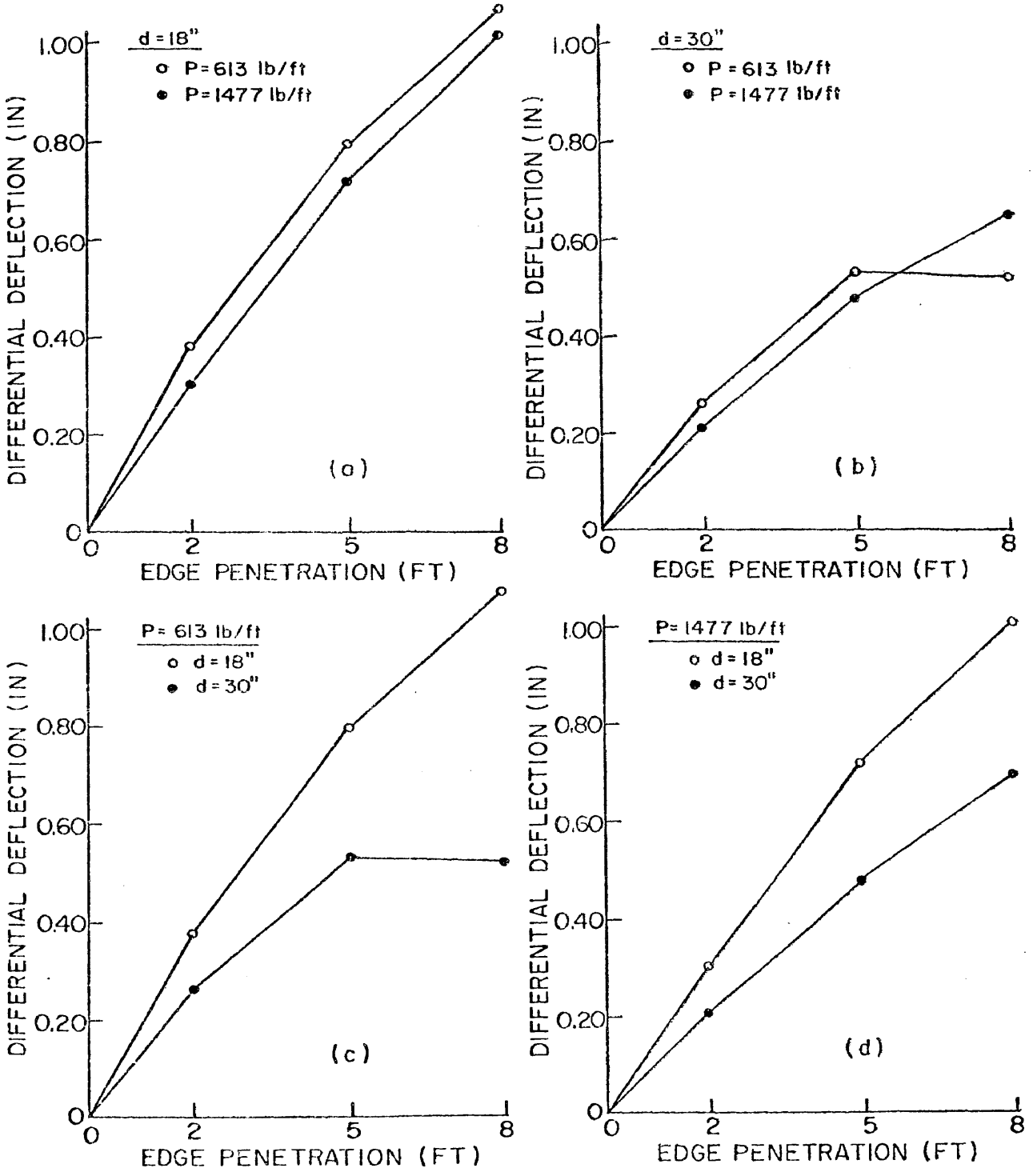

FIGURE 49. MAXIMUM DIFFERENTIAL DEFLECTION OCCURRING AS A RESULT OF PERIMETER LOADING AND EDGE LIFT CONDITIONS. (SLAB SIZE: 48FT X 24FT).

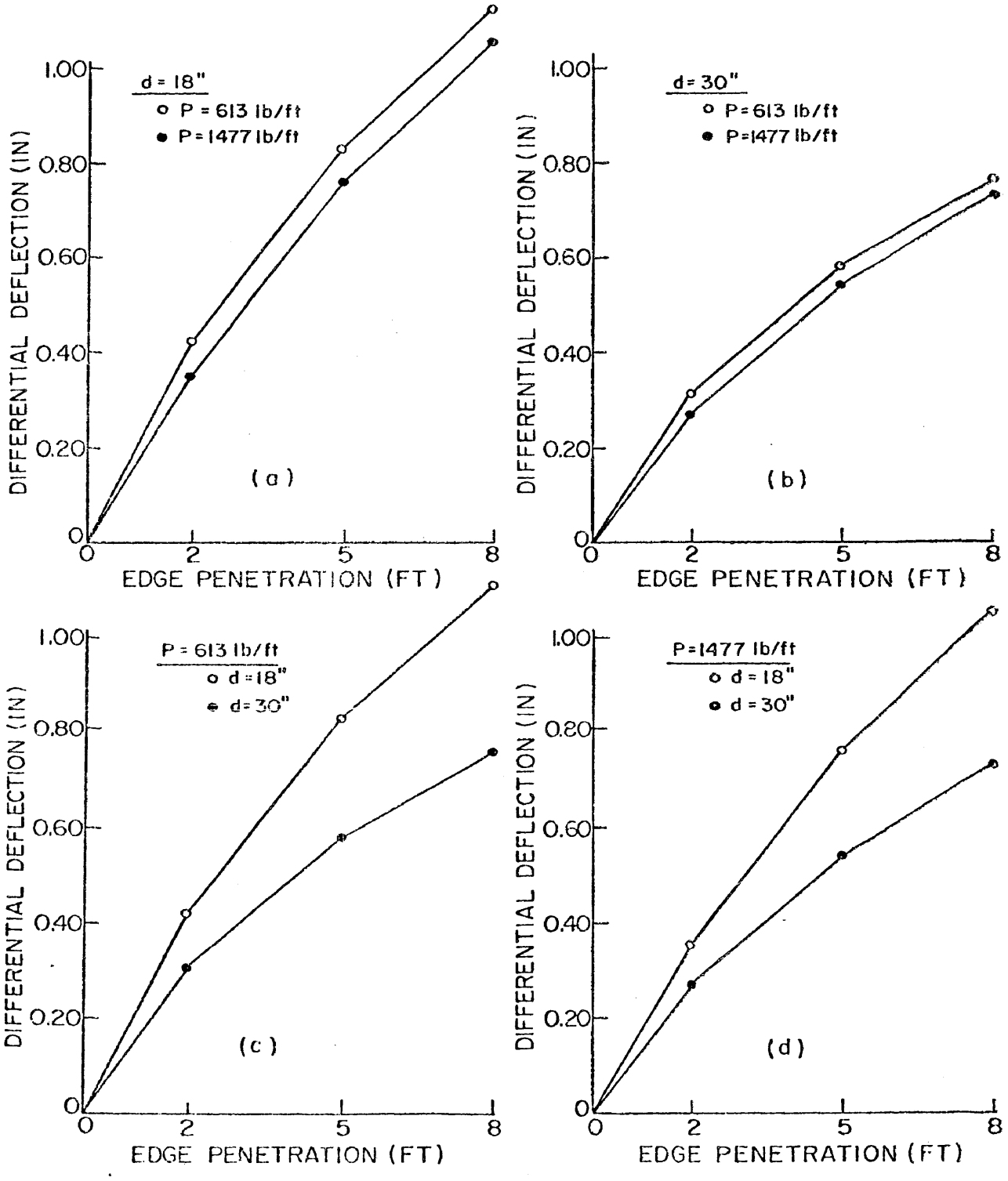

FIGURE 50. MAXIMUM DIFFERENTIAL DEFLECTION OCCURRING AS A RESULT OF PERIMETER LOADING AND EDGE LIFT CONDITIONS. (SLAB SIZE: 96FT X 24FT).

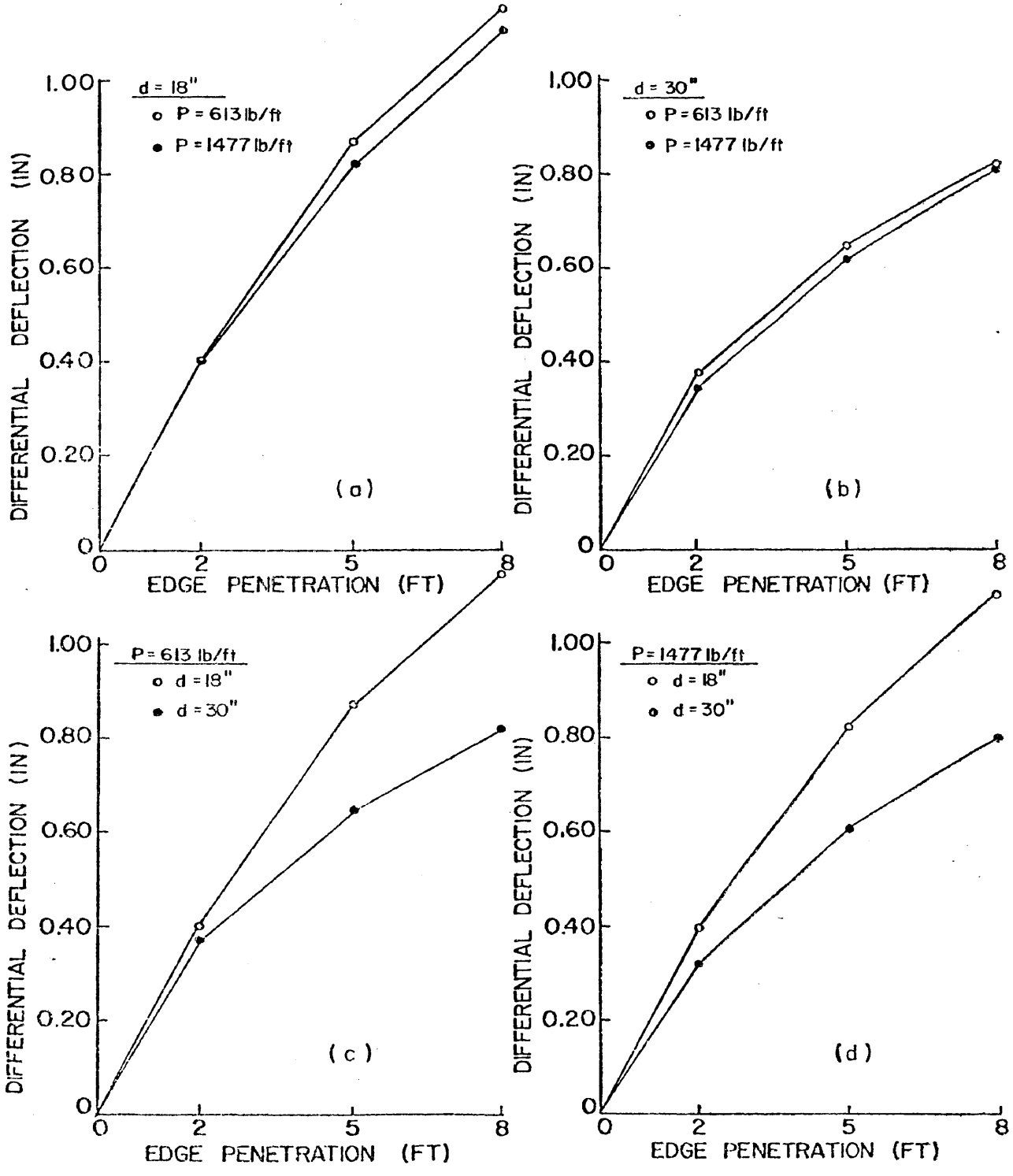

FIGURE 51. MAXIMUM DIFFERENTIAL DEFLECTION OCCURRING AS A RESULT OF PERIMETER LOADING AND EDGE LIFT CONDITIONS.(SLAB SIZE: 144FT X 24FT).

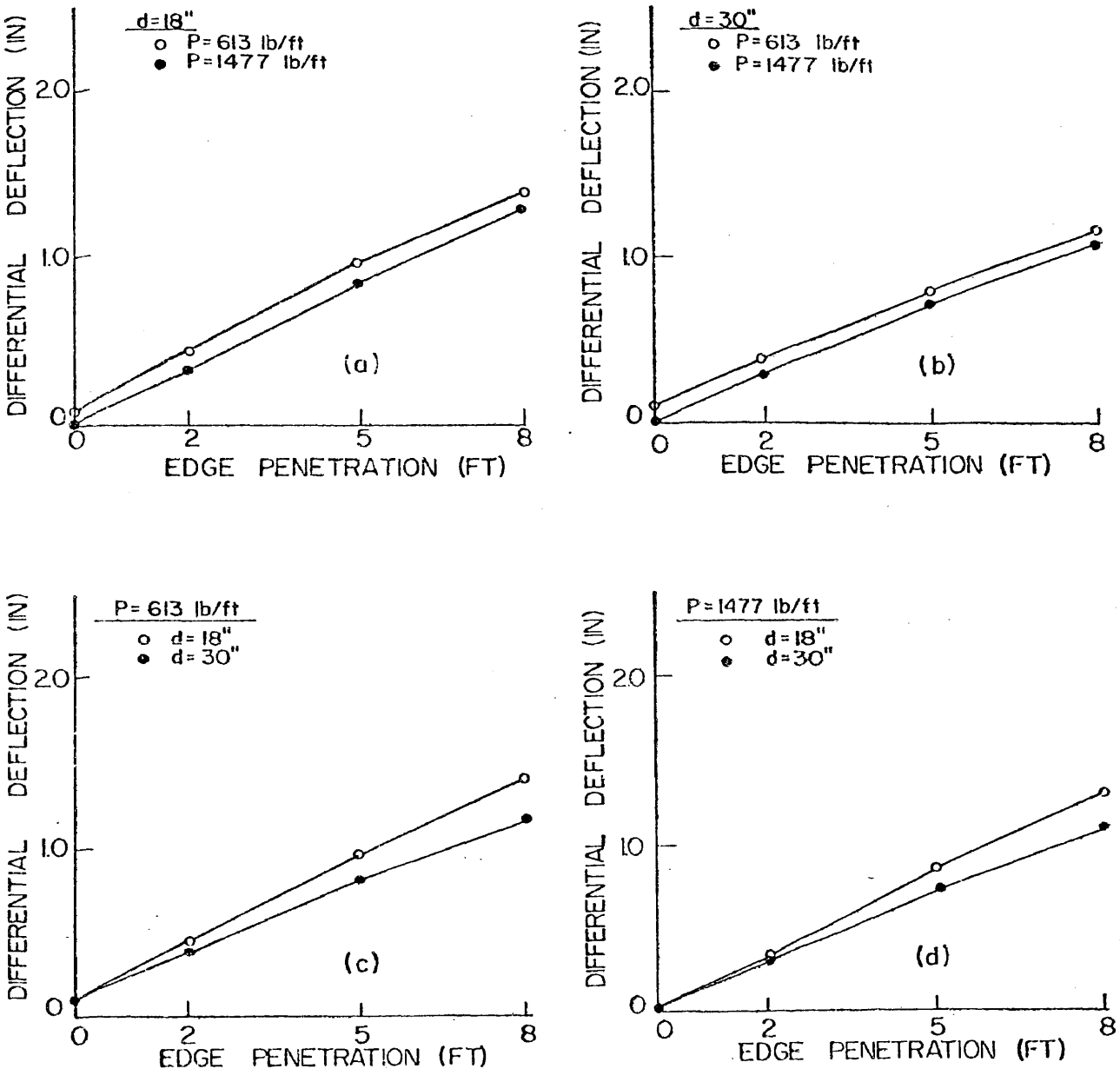

FIGURE 52. MAXIMUM DIFFERENTIAL DEFLECTION OCCURRING AS A RESULT OF PERIMETER LOADING AND EDGE LIFT CONDITIONS. (SLAB SIZE: 48FT X 40FT).

$$\Delta = \left[\frac{(L)^{0.35}(S)^{0.88}(e_m)^{0.74}(y_m)^{0.76}}{15.90\ (d)^{0.85}(P)^{0.01}} \right] \quad \ldots\ldots \quad (5\text{-}15)$$

where Δ = differential deflection, in inches

and all other symbols are as previously defined.

This regression equation shows beam spacing and beam depth to have the greatest influence on the resulting differential deflection; edge penetration distance and differential soil movement also have an important influence on the expected magnitude of Δ. Perimeter loading was shown to have the least effect on the resulting deflection. As suggested by Figures 48 - 52 , the regression showed the magnitude of the expected differential deflection to decrease with increasing beam depth and perimeter loading.

Shear. - Shear forces resulting from the edge lift analysis are plotted as functions of edge penetration in Figures 53 - 57. From the figures, five observations can be noted:

1. Shear increases as edge penetration distance increases.
2. Shear increases as depth of stiffening beam increases.
3. There is little or no change in the magnitude of the shear as perimeter load increases.
4. There is little or no change in the magnitude of the shear slab length increases.
5. There is little or no change in the magnitude of the shear as beam spacing increases.

Analysis of the distribution of the shear force as well as the

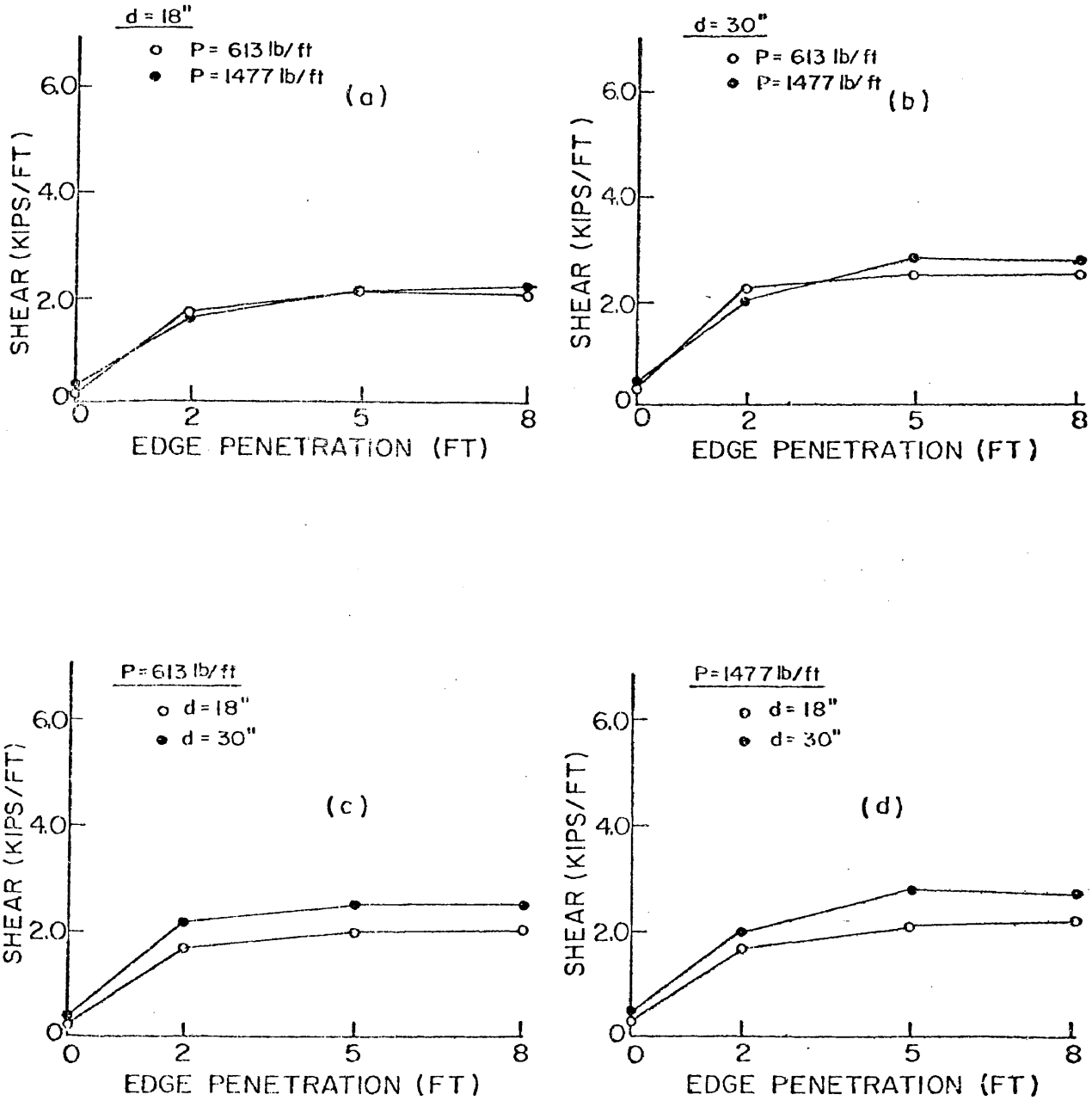

FIGURE 53. MAXIMUM SHEAR FORCES OCCURRING AS A RESULT OF PERIMETER LOADING AND EDGE LIFT CONDITIONS. (SLAB SIZE: 24FT X 24FT).

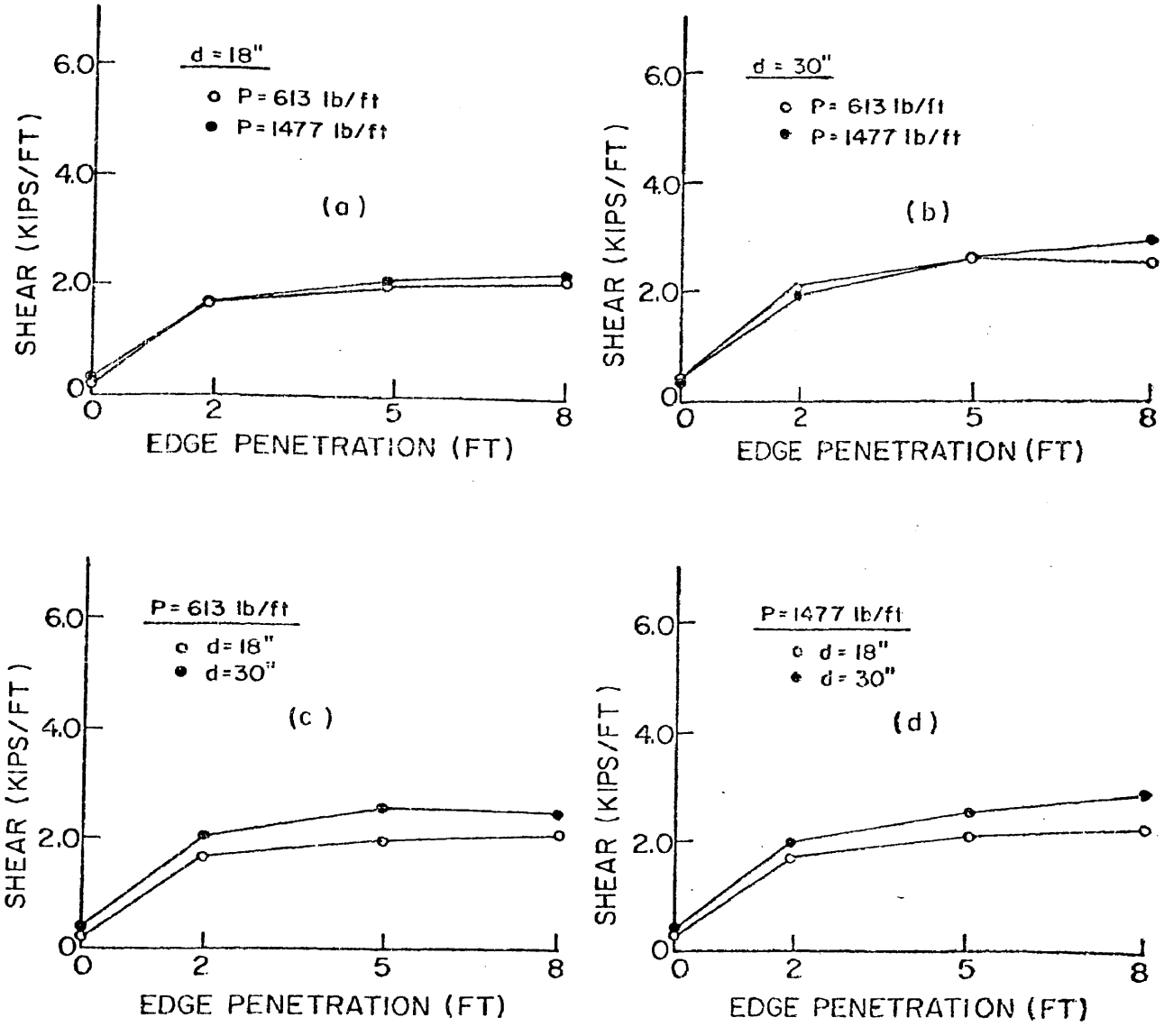

FIGURE 54. MAXIMUM SHEAR FORCES OCCURRING AS A RESULT OF PERIMETER LOADING AND EDGE LIFT CONDITIONS. (SLAB SIZE: 48FT X 24FT).

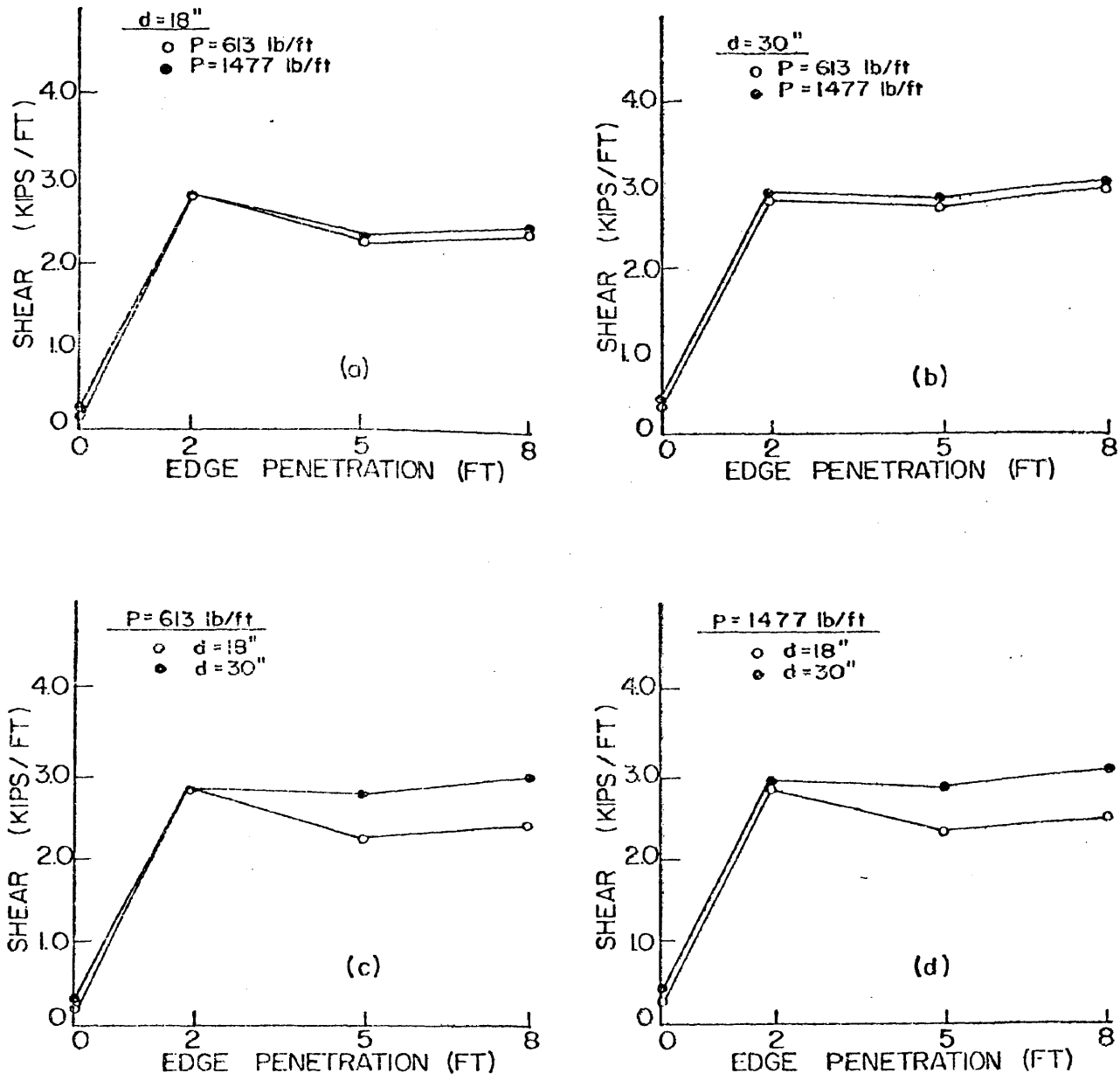

FIGURE 55. MAXIMUM SHEAR FORCES OCCURRING AS A RESULT OF PERIMETER LOADING AND EDGE LIFT CONDITIONS. (SLAB SIZE: 96FT X 24FT).

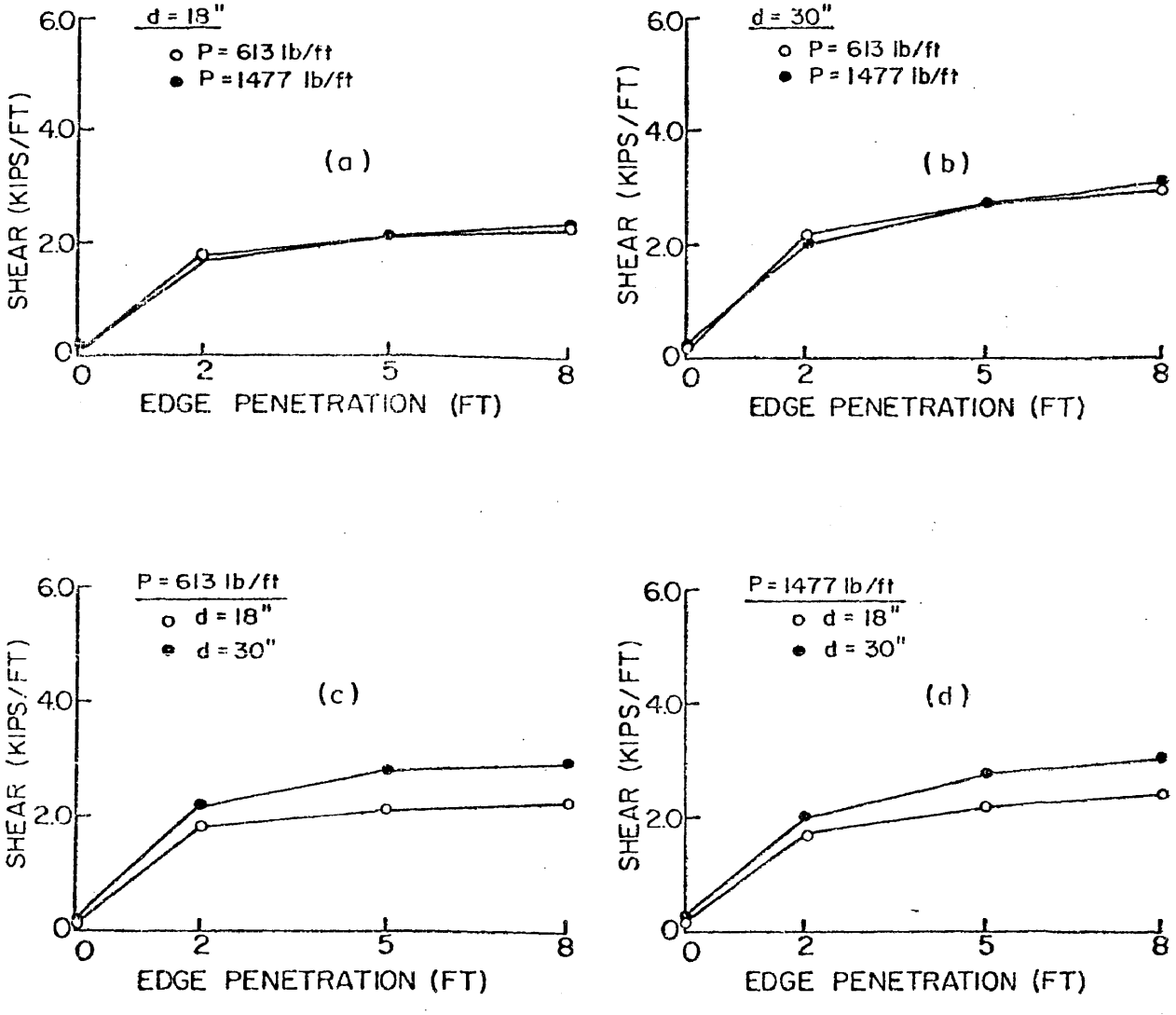

FIGURE 56. MAXIMUM SHEAR FORCES OCCURRING AS A RESULT OF PERIMETER LOADING AND EDGE LIFT CONDITIONS. (SLAB SIZE: 144 FT X 24FT).

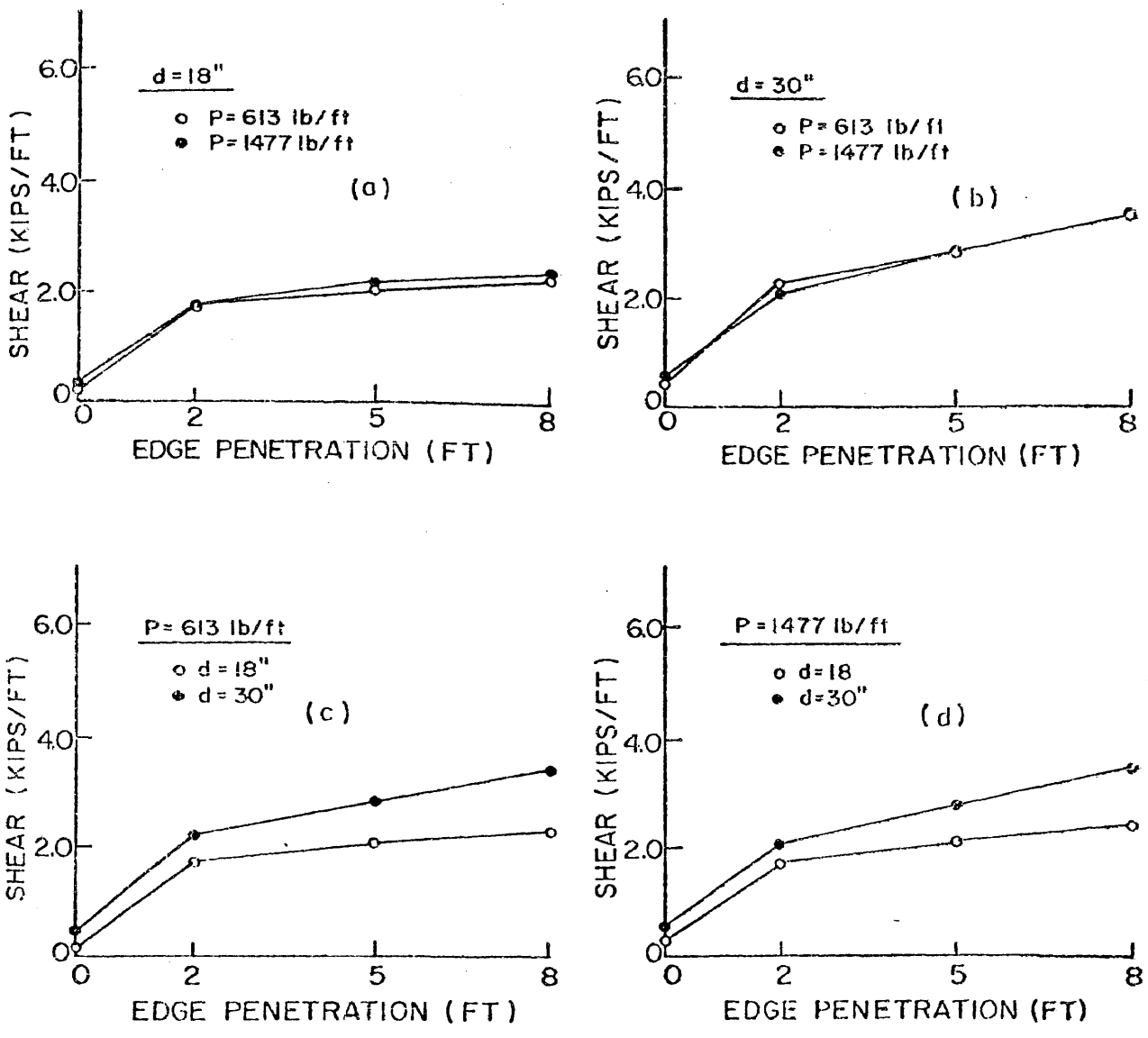

FIGURE 57. MAXIMUM SHEAR FORCES OCCURRING AS A RESULT OF PERIMETER LOADING AND EDGE LIFT CONDITIONS. (SLAB SIZE: 48 FT X 40 FT).

location of the maximum shear force showed it to be similar to that of the center lift shear forces (Figure 42 , p.135).

The regression analysis of the maximum shear force data (Table 27, Appendix M) produced the following equation:

$$V = \left[\frac{(L)^{0.07}(d)^{0.40}(P)^{0.03}(e_m)^{0.16}(y_m)^{0.67}}{3\ (S)^{0.015}} \right] \quad \ldots . \quad (5\text{-}16)$$

Examination of Equation (5-16) reveals the regression verifies the observed trends noted above. The beam depth and the amount of edge penetration dominate the relation. Beam depth, beam spacing, and perimeter load have but slight influence on the magnitude of the expected shear.

Analysis also showed a slight tendency for the shear force to be larger in the short direction. However, this tendency was so slight that Equation (5-16) is considered to adequately predict the expected shear for both design directions.

Determination of Relationship Between Edge Moisture Variation Distance and Thornthwaite Moisture Index

Using stiffened slab foundation designs that are known to have worked satisfactorily in San Antonio, Dallas-Fort Worth, and Houston for several years (103) and the design equations developed above, the maximum edge penetration distance that each of these designs could withstand was determined by back-calculation procedures. The values of the variables and the results of these calculations are shown in Table 19 and Figure 58.

The shape of the curves of Figure 58 was not unexpected. Since the

TABLE 19. Summary of Slab Section Properties and Soil Conditions Used to Calculate the Relationship Between Thornthwaite Index and Edge Moisture Variation Distance

SLAB SECTION				SOIL CONDITION[a]			MOMENT CAPACITY		MAXIMUM EDGE MOISTURE VARIATION DISTANCE	
BEAM WIDTH (IN)	BEAM DEPTH (IN)	BEAM SPACING (FT)	REINFORCEMENT	MAXIMUM DIFFERENTIAL SOIL MOVEMENT CENTER LIFT (IN)	MAXIMUM DIFFERENTIAL SOIL MOVEMENT EDGE LIFT (IN)	THORNTHWAITE INDEX (IN/YR)	NEGATIVE MOMENT[b] (FT-KIPS/FT)	POSITIVE MOMENT[c] (FT-KIPS/FT)	CENTER LIFT (FT)	EDGE LIFT (FT)
SAN ANTONIO										
10	24	15	8-3/8"ø[d] 3-3/8"ø[e] 6-#4[e]	2.42	0.86	-16	8.72	3.05	4.3	2.3
FORT WORTH										
8	20	19	7-1/2"ø[d] 3-1/2"ø[e]	0.33	0.30	-4	4.46	2.09	3.6	4.5
HOUSTON										
9	20	25	9-3/8"ø[d] 3-#4[e]	0.30	0.28	+18	4.34	2.07	3.3	4.5

[a] The soil was assumed to be 60 percent clay and predominantly Montmorillonite in each location.
[b] Allowable tensile stress in the extreme fiber = $2\sqrt{f'_c}$
[c] Allowable tensile stress in the extreme fiber = $6\sqrt{f'_c}$
[d] Slab Reinforcement
[e] Beam Reinforcement

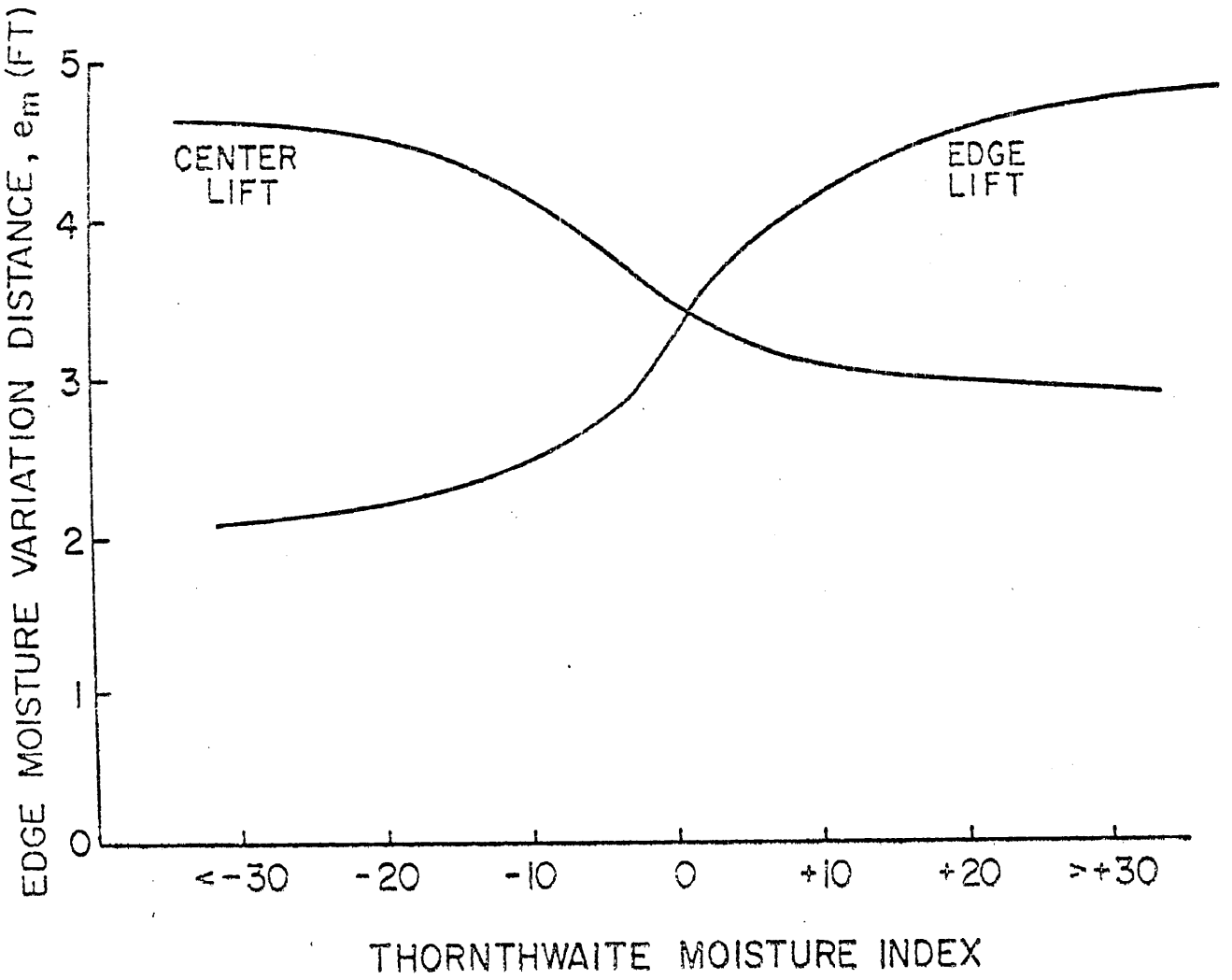

FIGURE 58. RELATIONSHIP BETWEEN THORNTHWAITE INDEX, EDGE MOISTURE VARIATION DISTANCE, AND CONCRETE TENSILE STRENGTH.

magnitude of the moisture variation distance is dependent to a large degree upon the climate, a slab in a drier climate would tend to experience larger distances of drying soil around its edges when center lift distortion occurs than would a slab in a wetter climate.

Conversely, drier climates would tend to experience smaller distances of moisture variation during edge lift swelling than during center lift distortion. This is due to the strong evapotranspiration influences that tend to retard or reverse the moisture migration beneath the slab. Slabs constructed in wetter climates would have larger moisture variation distances during edge lift swelling due to the strong influence of the wetter environment. Thus, if e_m is not known, or cannot be measured in the field, it can be estimated for each swelling mode from Figure 58. This process of determining e_m was adopted in lieu of a consistent set of field measurements in a variety of climates; these measurements are a research effort that is badly needed.

Effect of Post-tensioning on Differential Deflection

Many of the slabs-on-ground presently being constructed for use as residential or light commercial foundations use post-tensioning instead of conventional mild steel reinforcement. From experience, it is known that most of the post-tensioning strands are placed in the slab portion of the section. Locating the strands in the slab portion usually results in the centroid of the prestressing force being above the neutral axis of the gross cross-section, causing the prestressing to act eccentrically on the section. This eccentricity can result in a slightly upward bending or camber in the slab. Thus, any loading placed on the slab must first

overcome this camber before deflecting the slab into negative bending. The purpose of this particular study was to determine what credit, if any, could be given to the post-tensioning for reducing the magnitude of the differential deflection expected in a particular problem.

Procedure. - The procedure was to use the same section with 24-ft and 48-ft long slabs, but to locate tendons at three different locations: (1) neutral axis, (2) mid-depth of the slab portion, and (3) half-way between the neutral axis and mid-depth of the slab. Three different levels of perimeter loading were applied for each strand positioning. The same problem was repeated for an 18-inch beam depth section and a 30-inch beam section.

Results. - The results were computed as the percent of decrease in differential deflection as eccentricity increased and are shown in Figure 59. The tabulated results are reported in Table 29, Appendix J. The equations derived from this data to predict the percent reduction of differential deflection are

$$\Delta_c = \sqrt{\frac{6400\ e^2}{9L}} \quad \ldots\ldots\ldots\ldots\ldots\ldots\ldots\ldots \quad (5\text{-}17)$$

where Δ_c = correction factor, in %

e = eccentricity, in inches

L = slab length, in feet.

and

$$\Delta = \Delta_0 \left[\frac{100 - \Delta_c}{100} \right] \quad \ldots\ldots\ldots\ldots\ldots\ldots\ldots\ldots \quad (5\text{-}18)$$

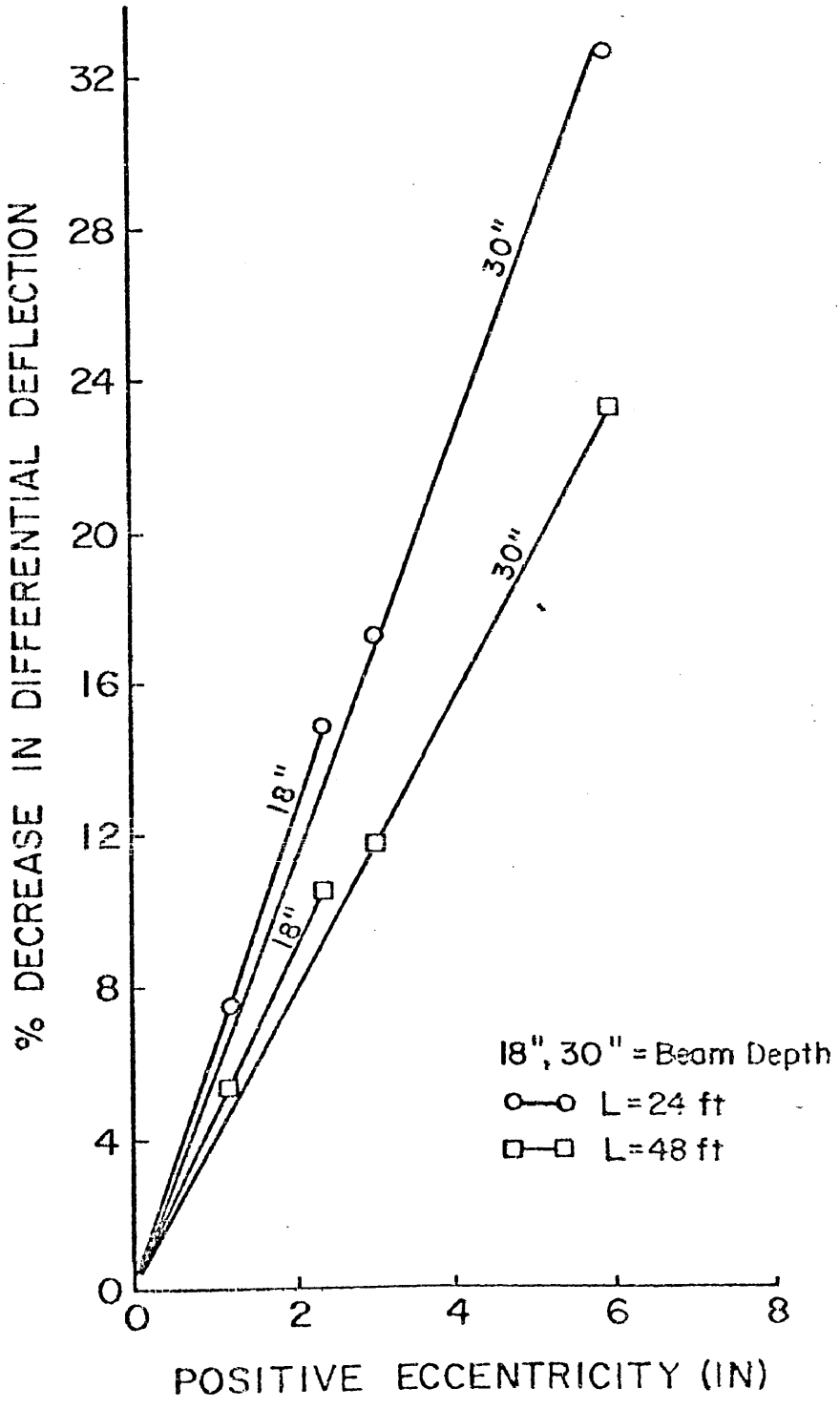

FIGURE 59. EFFECT OF TENDON ECCENTRICITY ON DIFFERENTIAL DEFLECTION.

where Δ = expected differential deflection, in inches

Δ_o = expected differential deflection without prestressing, in inches

Δ_c = correction factor, in %

Cracking Moment, Ultimate Moment, and Differential Deflection

Problem. - Structural slabs are not supported along their span (between webs or beams) but slabs-on-ground have support from the soil along some or all of their span. If a structural slab were to fail, it would fall until it was prevented or restrained from falling further, but if a slab-on-ground were to fail, there is no place for it to fall since the underlying soil would prevent it from doing so. When the structural slab fails, it obviously has lost most or all of its load resisting capacity; whether or not this also occurs in a slab-on-ground must be known in order to assess the proper stress levels that will be permitted to occur in the slab during service conditions.

Procedure. - Using the computer program PRESS2, a standard section slab of dimensions 60 ft x 40 ft was used in the investigation. The beam depths were allowed to vary in order to observe what effect increasing beam depth, and increasing section stiffness, had on the results. Other variables were as indicated in Figure 60 .

Center Lift. - For each problem of different beam depth, a uniform load of 40 psf was applied over the entire slab. The perimeter load was incrementally increased an average of 200 lbs/ft. In each instance, the incremental loading was continued well beyond the point where initial cracking and moment loss occurred.

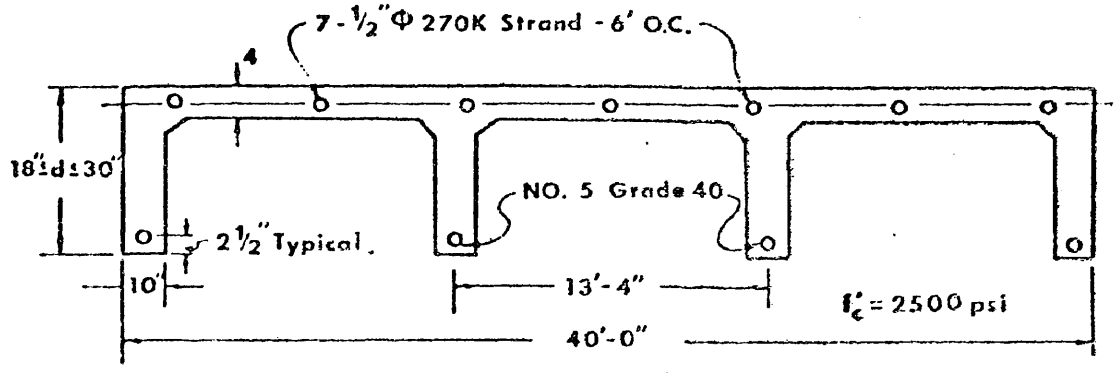

SLAB DIMENSIONS

WIDTH = 40 feet
Slab Thickness = 4 inches
Number of Beams = 4 (Equally Spaced)
Beam Width = 10 inches
Beam Depth = 18" $\leq$ d $\leq$ 30" (All Beams same depth)

LENGTH = 60 feet
Slab Thickness = 4 inches.
Number of Beams = 5 (Equally Spaced)
Beam Width = 10 inches
Beam Depth = 18" $\leq$ d $\leq$ 30" (All Beams same depth)

SOIL CONDITIONS

Center Lift Swelling	Edge Lift Swelling
Edge Penetration Distance = 4 feet	= 4 feet
Differential Swell = 2 inches	= $0.5 \leq y_m \leq 2.0$ in

FIGURE 60. STIFFENED SLAB CROSS SECTION AND OTHER PROPERTIES USED IN BENDING MOMENT-TENSILE CRACKING MOMENT - DIFFERENTIAL DEFLECTION INVESTIGATION.

In some instances the post-tensioning operation may not close all the temperature and shrinkage cracks. To investigate the effect an unclosed crack might have on the strength and differential deflection characteristics of the slab, a crack was placed in the computer model. The point selected for the crack was one-β length from the slab edge, approximately where the maximum moment should occur. The slab was then prestressed (crack remaining unclosed) and loaded to cracking and beyond in the same manner as the other slabs.

Edge lift. - As with the center lift investigation, a uniform live load of 40 psf was applied over the entire slab. A perimeter load was applied and the differential swell was incrementally increased along with the addition of a nominal uniform load. This procedure was continued well beyond the point where cracking occurred.

Results.

Center lift. - Figure 61, where moment is plotted as a function of differential deflection, is typical of the results obtained. The figure shows a linear increase in moment capacity until the cracking moment is reached. When the cracking moment is exceeded, a rather dramatic loss in moment capacity and an increase in differential deflection occurs. However, with continued loading, the moment capacity begins to increase again. This increase occurs at a lesser slope than before cracking, but with no tendency to stop increasing even at this extended level of loading. Thus, ultimate moment has not been reached.

Two levels of tensile stress are shown in the figure. These

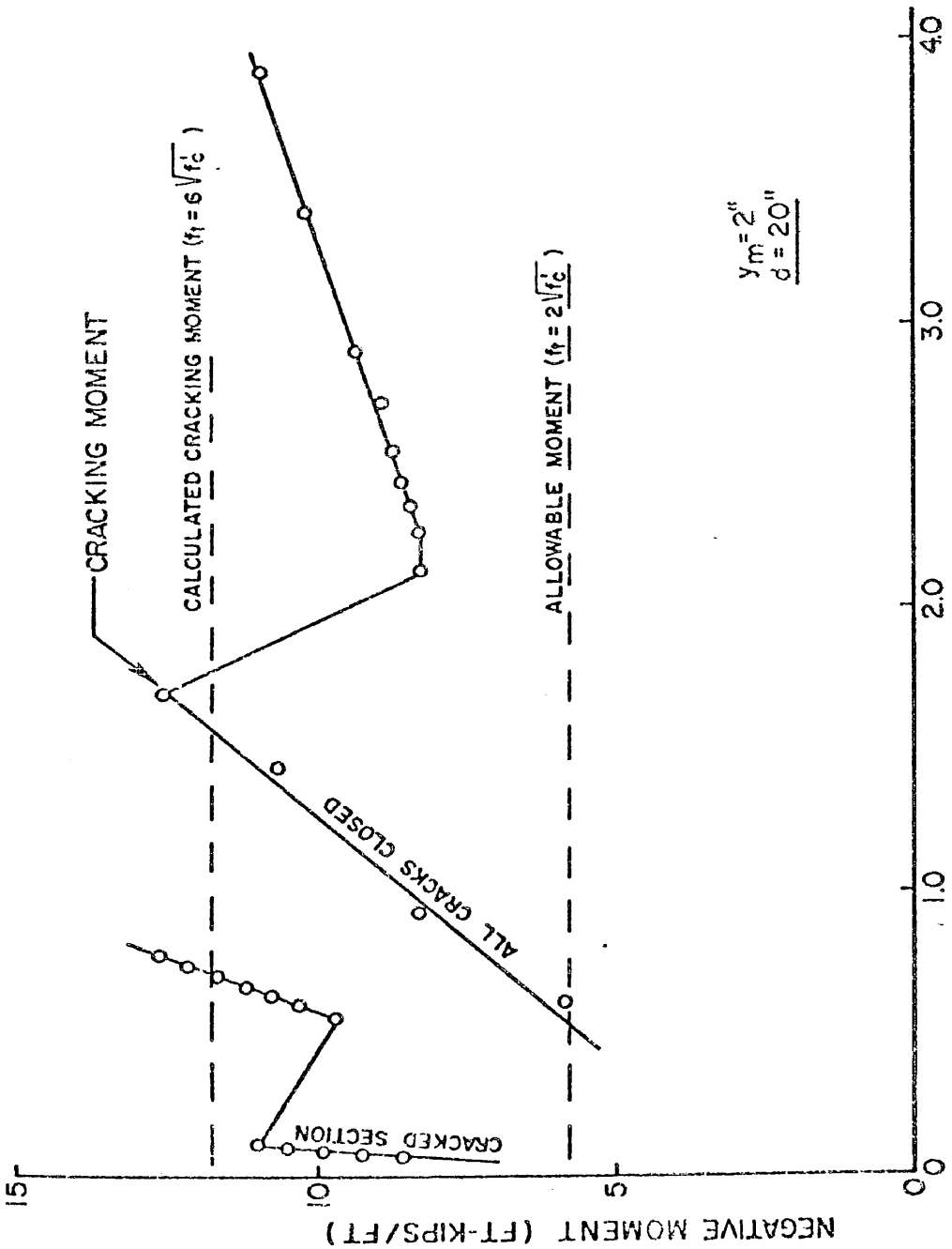

FIGURE 61. RELATIONSHIP BETWEEN CENTER LIFT BENDING MOMENT, TENSILE CRACKING MOMENT AND DIFFERENTIAL DEFLECTION, FOR A 60 ft x 40 ft SLAB.

correspond to the magnitude of the moment required to produce that amount of tensile stress in the extreme fiber of the concrete. The purpose of the lower 2 $\sqrt{f'_c}$ is discussed in the following chapter. The tensile stress of 6 $\sqrt{f'_c}$ is the maximum allowed in a pre-compressed zone by the ACI Code 318-77 (3). For this investigation, a "calculated cracking moment" was computed using 6 $\sqrt{f'_c}$ as the tensile stress at which cracking would occur. In each problem investigated, the computer-result cracking moment exceeded the "calculated cracking moment."

The results of the unclosed temperature/shrinkage crack are also shown in Figure 61. The curve is similar in shape to that of the section where all the cracks were closed. In both curves, moment increases linearly until the cracking moment is reached. The increase in differential deflection that occurs after exceeding the cracking moment is the same for both problems. As with the "all cracks closed" section, the moment capacity begins to increase following loss of capacity at cracking but the increase is at a lesser rate. The steep slope of the curve of the cracked section is caused by the prestressing strands trying to close the crack and inducing an unusually large amount of camber in the outer few feet of the slab.

Edge Lift. - Figure 62 is typical of the edge lift results. As with the center lift problems, the induced moment increases linearly until reaching the cracking moment. However, upon exceeding the moment capacity, the edge lift slabs experience only a

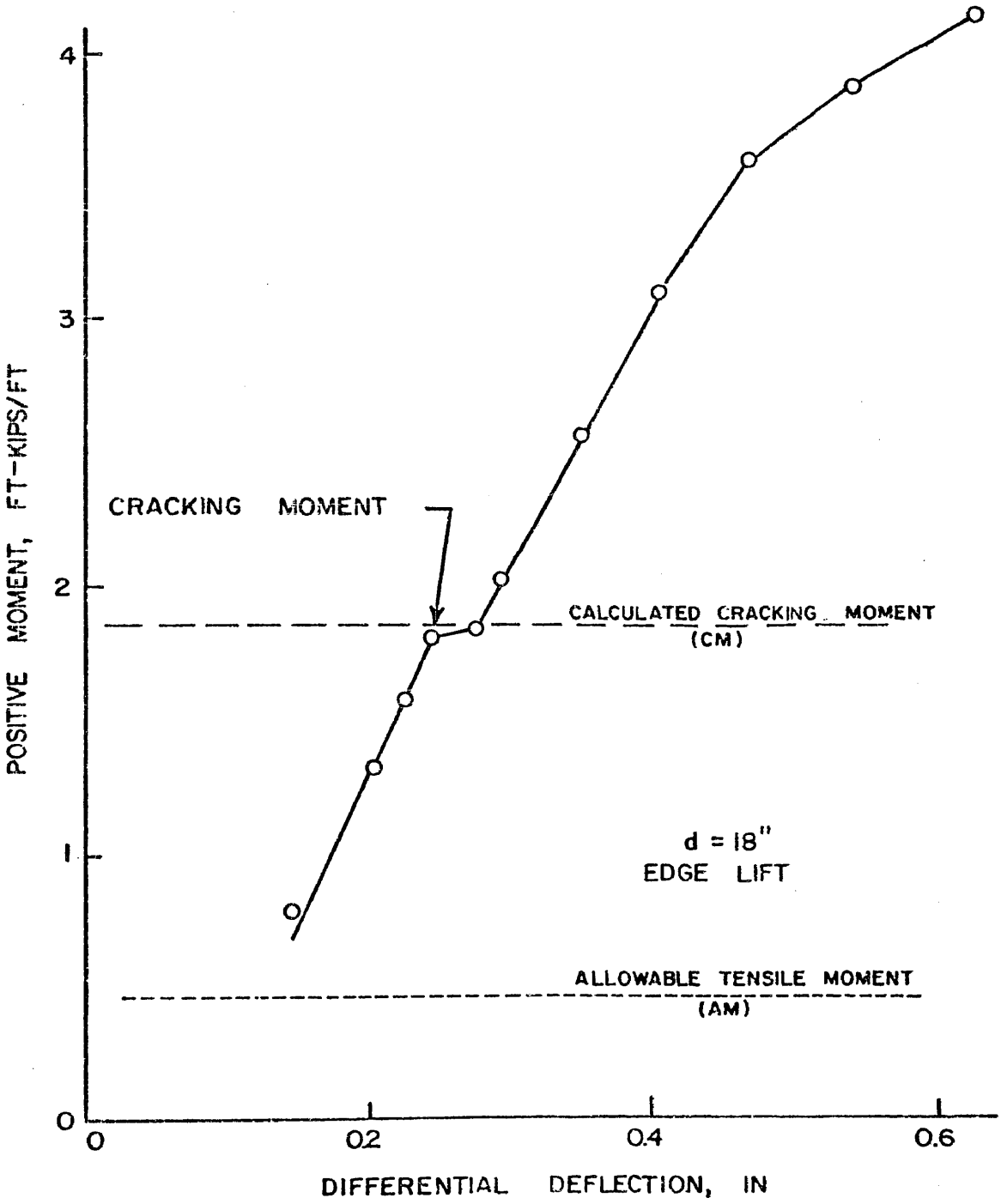

FIGURE 62. RELATIONSHIP BETWEEN EDGE LIFT BENDING MOMENT, TENSILE CRACKING MOMENT, AND DIFFERENTIAL DEFLECTION FOR A 60ft x 40ft SLAB

small increase in differential deflection and, unlike the center lift slabs, suffer little or no loss of moment capacity.

With continued loading, the moment values continue to increase. The slope of the M - Δ curve initially following cracking is slightly less than it was before cracking but as the differential deflection increases, the slope begins to decrease and suggests that the conditions may be approaching an ultimate moment at some point well beyond twice the value of the cracking moment.

Results of the remainder of the slab depths investigated are reported in Appendix O, as Table 30 and Figures 72a - f and 73a - f.

CHAPTER VI

SLAB-SUBGRADE FRICTION

Movements of any concrete slab or pavement is inhibited to some extent by friction between the slab and the material on which the slab or pavement rests. Knowledge of the degree or extent to which this movement is restrained is important if the slab is to be post-tensioned.

Post-tensioning is a means of prestressing the slab after it has been cast and attained sufficient strength to safely withstand the pre-stressing force. However, it generally requires between 3 and 7 days (69) for the concrete to attain the necessary compressive strength (69) of 2000 psi or more. During this time, the concrete usually cracks due to temperature and moisture loss (shrinkage) effects. But for a post-tensioned slab to perform successfully, these cracks must be closed during the post-tensioning process. Thus, as the tendon tensioning process proceeds, the cracked or disjointed slab sections must be moved across the surface on which they are residing until all the cracks are closed.

The force required to move the slab sections and close the cracks must come from the tensioned tendons. Therefore, depending on the magnitude of the coefficient of friction, a greater or lesser part of the post-tensioning force in the tendons must be expended to overcome friction before any compressive force is introduced into the concrete. Since Timms (89) has noted that a 50 percent reduction in pavement friction could result in a 30 to 40 percent reduction in the required

prestressing force, it becomes important to know what force is actually needed to overcome friction and what influences its magnitude.

The Coefficient of Friction

The laws governing friction were presented by Leonardo da Vinci (79), Amontons (circa 1700 A.D. (81)), and Coulomb (1785 A.D. (81)). These laws are:

a. Frictional force is directly proportional to the normal force;

b. Frictional force for a constant load is independent of the area of contact;

c. Frictional force depends upon the nature of the materials in contact; and

d. Frictional force is independent of the sliding speed.

Mahoney (43) points out that the first laws are generally accepted as being true, but the last law is not known as being true for all cases.

The coefficient of friction, which is the constant of proportionality between the frictional force and the normal load, depends on many factors, including the type of materials in contact, their relative surface smoothnesses, available moisture, and temperature. The kind of friction acting on pavements and slabs is considered to be "dry" friction (43, 81) and the governing relation is

$$F = \mu N \quad \ldots\ldots\ldots\ldots\ldots\ldots\ldots\ldots\ldots\ldots \quad (6\text{-}1)$$

where F = frictional force

μ = coefficient of friction (dimensionless)

N = normal force

If slip additives are applied or injected beneath the pavement or slab, or if significant moisture is present, the condition might be considered to be closer to that of friction between lubricated surfaces and this simple relation Equation (6-1) may no longer hold true.

The coefficient of friction, μ, may be of two types, static or kinetic. Static friction is defined as the force required to start an object in motion; kinetic or sliding friction is the force required to keep an object in motion (79). Normally, the two types of friction have different magnitudes with the static coefficient of friction being greater than the kinetic.

These definitions of static and kinetic friction imply only two values of frictional coefficients. In reality, the values of the coefficients change with the distance moved by the sliding body with respect to the other. Normally, the value of the static coefficient of friction increases from zero at no movement to its greatest value at some small distance, e.g., 0.10 inch or less. Once this magnitude has been attained, the value of the coefficient will either remain the same or reduce slightly with continued movement. This will be shown later.

In constructing residential and light commercial slabs-on-ground, it is the general practice to place several inches of sand over the underlying soil and place a sheet of thin plastic, such as polyethylene, between the sand and the concrete. However, in pavement construction, the pavement is typically cast either directly against

the clay subgrade or onto a layer of sand covering the soil. In reviewing the literature, many of the reported experiments show the coefficients of friction were often significantly influenced by the shearing strength of the layer underlying the slab, i.e., the resulting slab displacements often occurred in this supporting layer and not at the interface of the slab and the adjacent layer.

Review of the Literature

The coefficient of friction occurring between a pavement and its supporting layers has been a subject of investigation by pavement engineers for many years. There have been a number of experiments conducted in order to gain an understanding of the slab-subgrade friction phenomena with respect to both the type of pavement and the material underlying the pavement. These experiments have included both friction and non-friction reducing construction.

It is well to review the results of some of these tests to gain an understanding of the magnitude of the reported coefficients of friction and the conditions under which these coefficients were measured. Mahoney (43) presents an excellent review of many of these tests but confines his review principally to pavement applications. Duplication of Mahoney's thorough review is not necessary and only the results of those tests that have slab-on-ground application will be considered here.

Polyethylene Sheeting. - Homes constructed under the regulations of the Veteran's Administration (VA), Federal Housing Administration (FHA)

and other governmental agencies are required to have a material placed between the soil and the slab foundation to act as vapor or moisture barrier. From conversation with practicing engineers and from personal observation by the writer, the most commonly used vapor barrier material is polyethylene sheeting or a similar product.

One of the more extensive friction tests reported was that by Timms in 1964 (89). He used 6 ft by 6 ft cast-in-place flat slabs with thicknesses of either 5, 8, or 11 inches. The slabs were cast against seven different sublayers and the force required to move the slabs, as well as the displacement due to that force, was measured. The results of Timms' tests are shown in Figure 63 .

As seen from Figure 63, Timms reports two coefficient of friction values for each sublayer. Actual measurements of displacements for the 5-inch thick slab are shown in Figure 64. From Figure 64 it is seen that the first movement of the slab required the greatest force to induce displacement. It is also seen that subsequent movements required less force than the first movement. From Figure 63 it is seen that the lowest coefficient of friction was obtained from sublayer combination (6), the polyethylene sheeting. Timms measured the static coefficient of friction ("first movement") to be about 0.9 and the "average of subsequent movements" or kinetic coefficient to be approximately 0.48. The "first movement" occurred at a displacement of about 0.04 inches and the kinetic coefficient reached its maximum at about 0.35 inches of displacement. Two conclusions drawn by Timms were:

1. The coefficient of friction for the initial movement of a

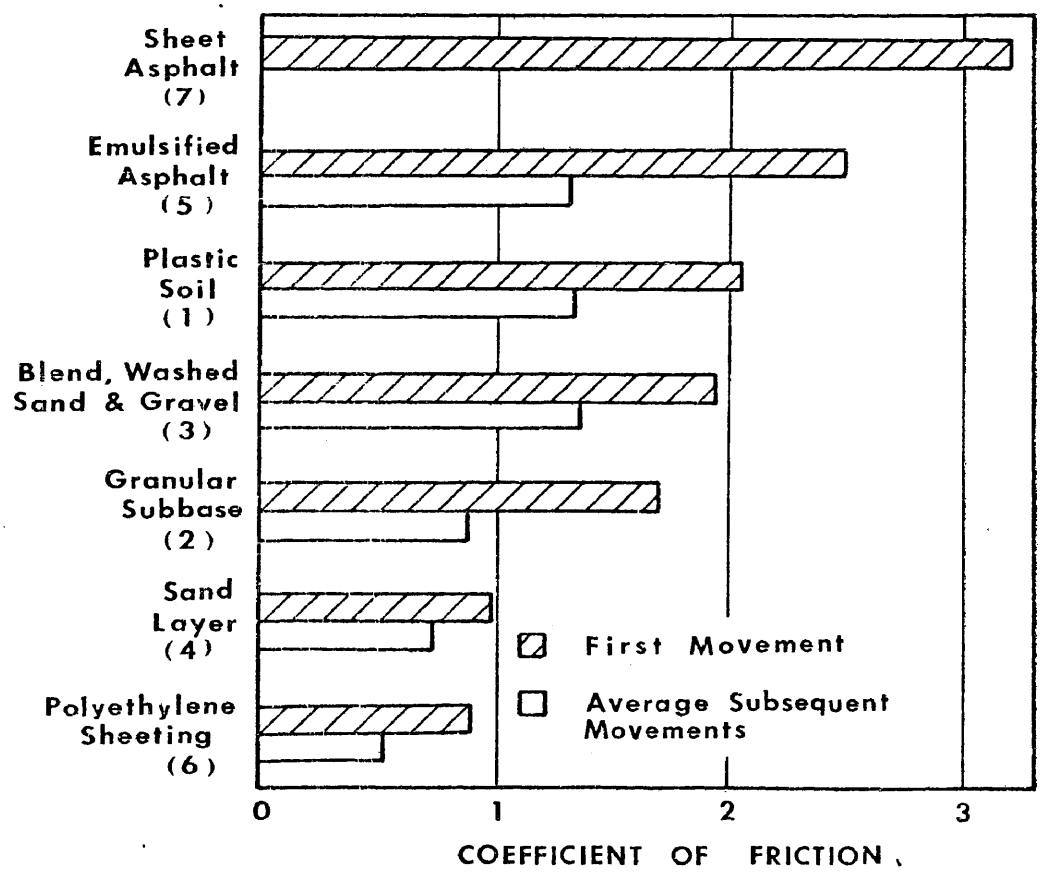

Figure 63. Summary of Coefficients of Friction For 5-Inch Slabs [After Timms (89)].

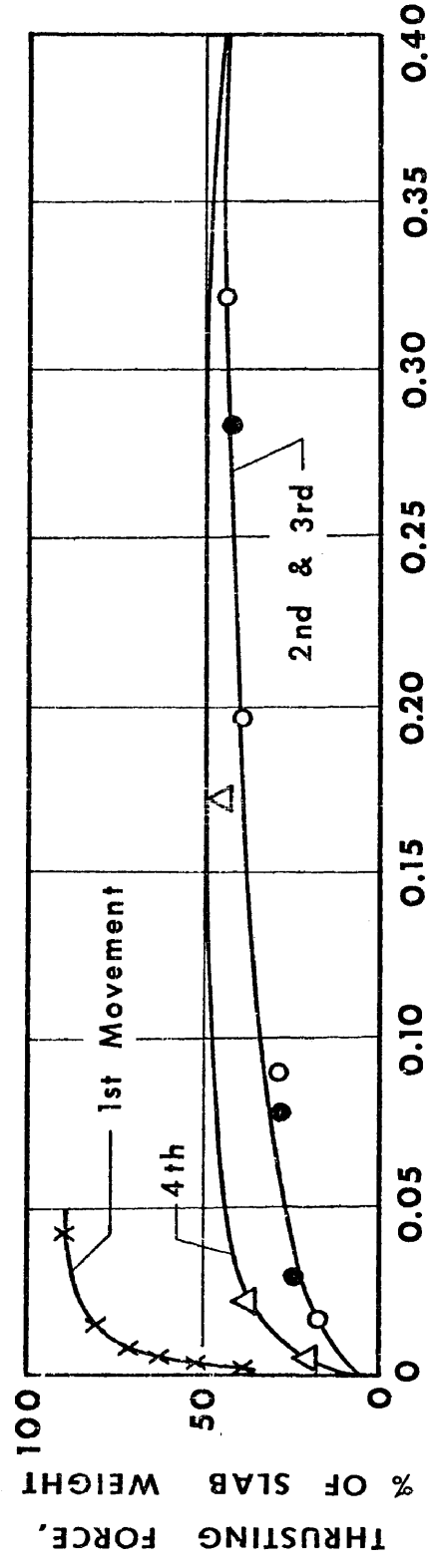

Figure 64. Effect of successive slab movements on Timms' 5-inch thick slab cast on polyethylene sheeting (89).

slab is appreciably greater than for subsequent movements, with a condition of essential stability of resistance being obtained after only two or three cycles of movement.

2. A thin sand layer and a double layer of polyethylene sheeting on a thin leveling course of sheet asphalt are effective friction-reducing mediums.

A second test that measured the effect of polyethylene was conducted by the Louisiana Department of Highways (102) in 1960. In these tests, 9 ft x 12 ft x 0.85 ft thick slabs were tested on 3 different subgrade treatments. The coefficient of friction found for each of these treatments and the amount of movement measured were reported as :

1. Polyethylene Plastic: 0.3 at an average displacement of 0.033 inches.

2. Emulsified Asphalt: 5.1 at an average displacement of 0.036 inches.

3. Sand Blanket: 0.9 at an average displacement of 0.029 inches.

A third set of tests involving slabs cast over polyethylene sheeting was conducted for the Federal Highway Administration (11) in 1971.

In these tests three friction reducing agents were evaluated: (1) sand (2) sand covered with 5 mil polyethylene, and (3) a double layer of 4 mil polyethylene. Each was evaluated on smooth, medium, and rough surface textures of bituminous coated cement-treated subbase (CTS). Sand layer thicknesses were 1/16 and 1/4 inches. All slabs tested were 4 ft x 4 ft x 6 inches thick. The tests were conducted by

measuring displacement and displacing force as each test slab was displaced in the following order: (1) pushing approximately 0.3 inches; (2) pulling approximately 0.6 inches; (3) pushing approximately 0.6 inches; and (4) pulling approximately 0.6 inches. The results of the tests are shown in Table 20 and reveal the 1/4-inch-sand layer and the polyethylene-over-1/4-inch-sand-layer combinations to offer the least restraint to slab movement. The measurements for polyethylene over 1/4-inch of sand are shown in Figure 65.

Sand Subgrade. - When polyethylene or its equivalent is not specified, the most commonly used material on which the slab is cast is sand. A number of tests have been conducted with sand as the underlying layer (13, 25, 71, 83, 84, 85, 87, 96). The results of these tests were summarized by Mahoney (43) (Appendix D), and Hanna, et. al. (27), reported the values of the friction coefficients for sand to range from a low of 0.49 to a high of 2.00.

Other Friction Reducing Agents. - Several investigators have studied friction reducing agents other than sand or polyethylene. Bitumen has been given more attention than others mentioned below. The effectiveness of bitumen in reducing friction is due primarily to its viscous shear behavior (43) which is dependent upon (85):

1. Grade of Bitumen: the higher the grade, the easier the slab moves.

2. Temperature of bitumen: restraint increases as temperature decreases.

3. Thickness of bitumen layer: the thicker the layer, the easier

TABLE 20. Coefficients of Friction Found in PCA Test (11)

FRICTION-REDUCER	SUBBASE TEXTURE	MAXIMUM COEF. OF FRICTION					SLIDING COEF. OF FRICTION				
		PUSH	PULL	PUSH	PULL	AVE.	PUSH	PULL	PUSH	PULL	AVE.
1/4" sand + Poly.	Medium	.56	.58	.55	.56	.56	.56	.58	.55	.56	.56
1/4" sand	Smooth	.55	.55	.54	.56	.55	.55	.55	.54	.55	.55
	Medium	.59	.59	.58	.58	.59	.59	.59	.58	.58	.59
	Rough	.52	.50	.56	.52	.53	.51	.50	.56	.52	.52
1/16" sand skin + Poly.	Smooth	.93	.75	.86	.70	.81	.51	.56	.74	.61	.61
	Medium	.76	.77	.65	.70	.81	.65	.67	.65	.65	.65
	Rough	.94	---	.76	.70	.80	.78	---	.71	.65	.71
Double Poly.	Smooth	.63	.58	.63	.74	.65	.59	.58	.63	.70	.62
	Medium	.68	.81	.66	.75	.72	.67	.65	.65	.68	.66
	Rough	.98	.76	.71	.69	.79	.89	.68	.65	.63	.71
1/16" sand skin	Smooth	13.83*	.81	1.06	1.05	.97	.85	.81	1.06	1.05	.94
	Medium	44.47*	1.24	1.13	1.40	1.26	1.04	.93	1.00	1.07	1.10
	Rough	51.15*	1.45	1.44	1.72	1.54	1.14	1.23	1.29	1.24	1.23

*Sand bonded to base and not included in calculating average.

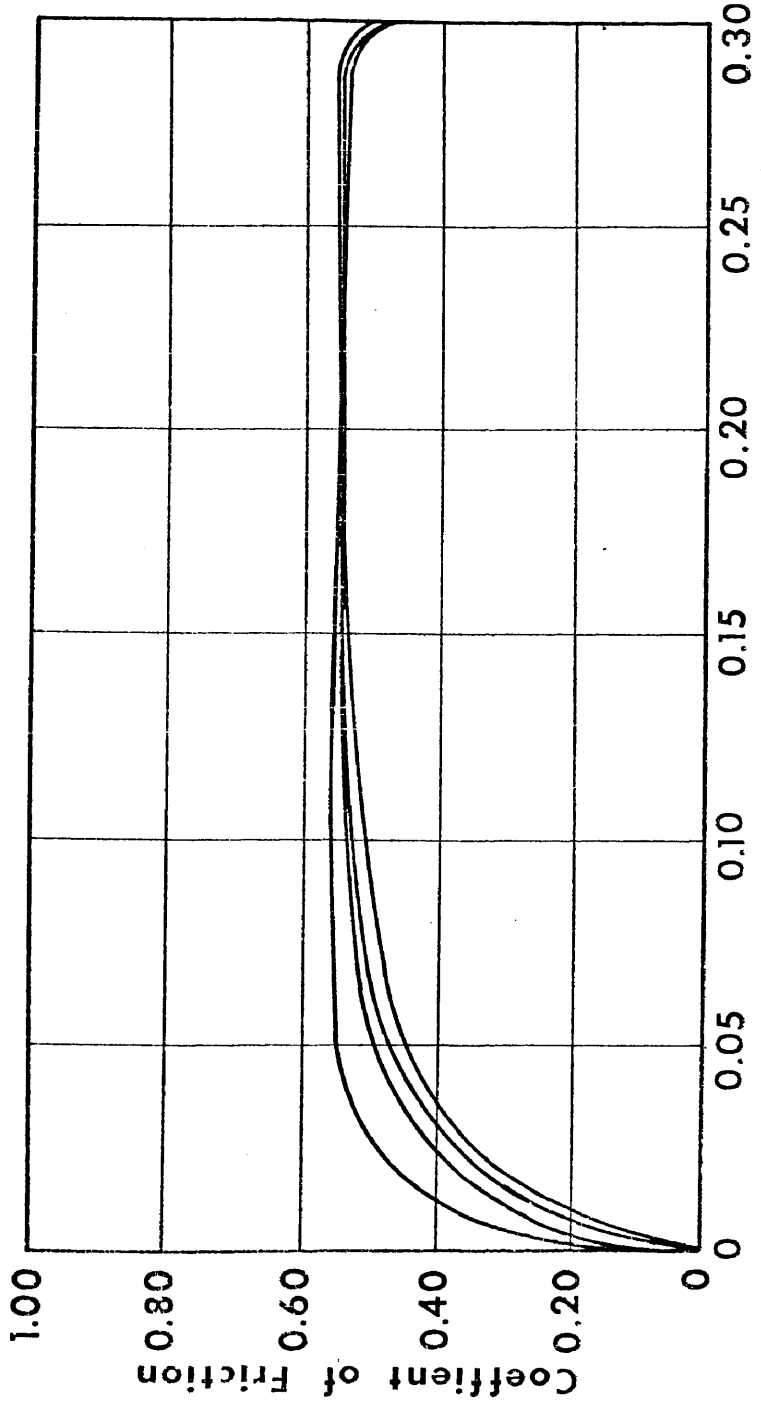

Figure 65. 1/4-Inch sand and Polyethylene on Medium Texture Cement Treated Surface [11].

the slabs moves.

4. Rate of slab movement: the force of restraint is directly proportional to the rate of slab movement.

In performing his tests, Stott (85) placed approximately 1/8-inch of high-pressure lubricating oil on a smooth morter base and then cast the test slabs onto the oil. He found the "initial" or static coefficient to be 0.37 and the "steady" or kinetic coefficient to range from 0.33 to 0.49. However, he noted that the oil quickly squeezed out from beneath the slab.

Other friction reducing agents have been examined (43 , 6), including carbon, graphite, Teflon, glass, and rubber. However, these investigations were not directed towards pavement/slab-subgrade applications. Nonetheless, the coefficients found for some of these materials indicate they may hold some possibility of application to slab use.

1. For hard, non-graphitic carbon surfaces, the coefficient of steel on carbon and of carbon on carbon was found to be approximately 0.16. With graphite, the coefficient was found to be about 0.10 (43 , 6)

2. The friction of Teflon on Teflon is comparable to that of ice on ice, which is about 0.04 (43 , 6).

3. Glass on glass was found to have a coefficient of about 0.90 (43 , 6).

4. Rubber on steel has a very high coefficient of about 4.0 (43 , 6).

Others have found that for a wide range of solids sliding on rubber,

the coefficient of friction is about 1.0 (43).

From the friction coefficient values reported above, it would appear that many of these materials show promise in reducing the frictional restraint encountered in post-tensioning practice. However, more effort into the practical application of the various products is surely needed before they can become commonplace construction materials.

Range of Slab Momements

After a slab is cast, it begins to "harden" and gain strength as the day progresses. Ostensibly, its overall length remains the same as when it was cast, which is the length of the forms. During the night, however, the temperature drops and the slab begins to shrink. The theoretical change in dimension is given by the relation (79):

$$\delta = \alpha L \Delta T \quad \ldots\ldots\ldots\ldots\ldots\ldots\ldots\ldots \quad (6\text{-}2)$$

where δ = total change in slab length

α = coefficient of thermal expansion (approximately $0.000005/^{o}F$ for concrete)

L = total slab length

ΔT = change in temperature, ^{o}F

Thus, if the temperature at the bottom of a 40 ft slab changes from a summer daytime temperature of $96^{o}F$ to $83^{o}F$ at night, as suggested by Teller and Sutherland (86), and friction between the slab and subgrade is neglected, the slab would experience a reduction in length equal to:

$$\left.\begin{aligned} \delta &= (0.000005/^{o}F)(40 \text{ ft} \times 12 \text{ in/ft})(96^{o}F - 83^{o}F) \\ \delta &= 0.031 \text{ in} \end{aligned}\right\} \quad (6\text{-}3)$$

But friction cannot be neglected, so as the slab begins to contract as the daytime temperature cools, stresses are set up in the slab as the frictional restraint resists the slab contraction or movement. As the slab movement increases so does the coefficient of friction, as shown by the "first movement" curve of Figure 64 , until the restraining force creates stresses sufficiently large to cause the new concrete to fail in tension and crack. The process is reversed the following day as daytime temperatures heat the cooled slab and cause it to expand. As noted above, the post-tensioning procedure is not begun until some 3 to 7 days following initial placement of the slab concrete; thus, the contraction-expansion cycle could repeat itself at least 3 times before the slab tendons are stressed.

Thus, if slab movements due to shrinkage and temperature changes are of such magnitude as to cause the slab displacement to exceed the minimum movement required to achieve the kinetic coefficient of friction on the first movement, subsequent movements are likely to encounter reduced frictional restraint, such as shown in Figure 64 . That such large movements actually occur is probably unlikely, at least in slab lengths normally associated with most residential construction. From the three polyethylene tests discussed above, the maximum restraint occurred at displacements of 0.04 (Timms), 0.033 (Louisiana), and 0.050 inches (PCA). Only slabs in excess of 50 feet in length would produce temperature-induced movements of this magnitude, if the other

values in Equation (6-3) were to remain unchanged. Therefore, for shorter slabs or lesser temperature differentials, the displacement would be less and the effective coefficient of friction is most likely to correspond to some point on the "first movement" curve, as in Figure 64. It should, however, be apparent that the effective coefficient does not necessarily have to be large. A small amount of total crack widths or a short slab may require only a small displacement to close the cracks and the resulting frictional coefficient may be only a fraction of the maximum "first movement" value.

Effect of Other Restraints

Stiffening Beams. - Only Buckley (28) has reported a test in which the slab had stiffening beams penetrating the underlying soil. He attempted to measure the effective subgrade friction by instrumenting two post-tensioned residential stiffened slabs-on-ground in 1976; his results, however, were inconclusive. One slab had various percentages of glass fiber as an admixture in different parts of the slab which apparently reduced the number and size of temperature and shrinkage cracks that occurred. Although not specifically stated, the slab appeared to have been cast against plastic sheeting which had been placed over a silty sand soil. He calculated the coefficient of friction to be 0.96. However, similar calcuations at a strain gage group located symmetrically to the group which Buckley used for calculating his reported μ found the coefficient of friction to be 0.46.

The second slab instrumented by Buckley was not particularly

useful in determining a typical coefficient value as the slab was cast over a layer of granulated, recycled rubber from salvaged automobile tires. Calculated coefficients were found to range between 1.25 and 5.00, indicating a buffer layer of rubber between the soil and the slab is not a good medium for reducing slab-subgrade friction.

Utility Penetrations. - It is common practice to place gas, sewer, and water service lines beneath the slab before it is cast. In placing the utility lines, the practice is to extend them to the location where the eventual connection will be made and then turn the pipe vertically upward so that the end extends above the final elevation of the cast slab. In doing this, the utility "stub-out" may act as an "anchor" or "stake" and prevent the slab from moving during the post-tensioning procedure. Buckley (28) encountered this problem in one of his instrumented slabs where a large waste line penetrated the slab adjacent to the intersection of two stiffening beams. His measurements showed smaller strains occurring in the concrete near this utility line during post-tensioning operations than at a symmetrical location.

Recommended Value for Coefficients of Friction

Polyethylene Sheeting. - The average static coefficient for the three flat slab friction tests discussed above is 0.60. The average of Buckley's (28) reported coefficient and the second coefficient calculated from the same data is 0.71. Although with small slab movements, the value of the friction coefficient may correspond

to the lower end of the "first movement" curve, as in Figure 64, the restraint offered by the stiffening beams and utility penetrations cannot, as yet, be accounted for very well. Thus, a value of 0.75 for the coefficient of friction over polyethylene or similar plastic sheeting appears to this writer to be a proper design value.

Sand Subgrade. - From the reports summarized in Appendix P , it appears the value of the coefficient is principally dependent upon the size of the material, and the sharpness of the particle surfaces. The value used for the coefficient of friction in design should depend upon the designer's experience with the materials typically used in his locale, however, in the opinion of the writer, the value should seldom be less than 1.00.

Other Materials. - If materials other than plastic sheeting or sand are used beneath the slab, either tests will have to be performed or engineering judement applied in order to determine a proper coefficient of friction.

CHAPTER VII

DESIGN PROCEDURE

A design procedure for a slab-on-ground constructed over an expansive clay should consist of at least the following 10 steps:

1. Assemble all of the known design data.
2. Divide an irregular slab plan into overlapping rectangles and design each rectangular section separately.
3. Assume a trial section in both the long and short directions of the design rectangle.
4. Calculate the service moment the section will be expected to experience in each direction.
5. Determine the allowable moment capacity of the assumed section in each direction and compare to the expected service amount.
6. Determine if the trial sections will meet differential deflection criteria in each direction.
7. Calculate the expected shear force in the assumed sections.
8. Determine the maximum allowable shear capacity of the sections and compare to the expected shearing force.
9. Repeat steps 4 through 8 for the opposite swelling condition.
10. Check the design for the first swelling condition to ascertain if adjustments are necessary to compensate for the second design swelling condition.

The design procedure that follows produces the values of bending moment, shear, and differential deflection that can be expected to occur under a given set of soil and structural conditions. These

values are as equally applicable to slabs reinforced with mild steel as they are to post-tensioned slabs. Thus, once these design parameters are known, design of either type of slab can proceed and the result will be slabs producing comparable moment and shear capacities and deflection resistance.

Assemble all of the Known Design Data

The data needed for design include eight design parameters and the material properties.

Climate. - Obtain the Thornthwaite Moisture Index, I_m, from Figure 15 or Figure 16, p. 57 or p. 58.

Soil Parameters.

Edge Moisture Variation Distance, e_m. - If the edge penetration distance is not known or cannot be measured, it can be estimated from Figure 58, p. 157.

Differential Soil Movement, y_m. - If the differential soil movement cannot be measured in the laboratory, it can be estimated from Tables 31 - 36 (Appendix Q). To use these tables, the type and amount of clay present must be known, as well as the depth to constant soil suction, the equilibrium suction at that depth, the velocity of moisture infiltration or evaporation, and the edge moisture variation distance.

1. Type of clay. The type of clay, if not known, can be determined by several different procedures, including:

a. Laboratory procedures such as x-ray diffraction, infrared analysis, thermal gravimetric analysis, and differential

thermal gravimetric analysis (19).

b. Soil Conservation Service (SCS) county soil surveys. The (SCS) has surveyed most counties in each state and has classified the upper few feet of the soil profile. Some surveys are more thorough and include engineering data in addition to the expected agricultural soil information.

c. If the SCS soil survey does not contain sufficient data or if the more rigorous laboratory tests cannot be performed, the soil type can be estimated if the cation exchange capacity (C.E.C.), the PI, and the percent of soil passing the U. S. #200 sieve that is less than 0.002 mm is known. The soil type is determined by first calculating the cation exchange activity, CEAc,

$$CEAc = \frac{C.E.C.}{(\%\ \text{Passing U. S. \#200 Sieve, } \leq 0.002\ \text{mm})} \quad \ldots\ldots\ldots\ldots\ldots\ldots \quad (7\text{-}1)$$

and the activity ratio of the soil,

$$Ac = \frac{P.I.}{(\%\ \text{Passing U. S. \#200 Sieve, } \leq 0.002\ \text{mm})} \quad \ldots\ldots\ldots\ldots\ldots\ldots \quad (7\text{-}2)$$

Entering Figure 4, p. 15, the intersection of the extension of the CEA_c and Ac values provides an estimate of the predominant soil mineral.

The C.E.C., if not known, can be accurately determined by atomic absorption analysis or closely estimated by the simplified method of Appendix R which uses a relatively inexpensive spectrophotometer to measure the amount of light passing through a specimen solution.

2. Amount of Clay. The percentage of the soil of clay

size can be determined from:

a. Analytical laboratory methods, principally soil fractionation, which is accomplished while preparing a sample for x-ray diffraction analysis.

b. SCS county soil surveys.

c. Hydrometer analysis.

3. Depth to Constant Soil Suction. If not known or not measured in the laboratory, the depth to constant soil suction can be estimated by plotting the ratio of the soil moisture content to the plastic limit as a function of depth (2). The depth at which this ratio becomes relatively constant provides an estimate of the depth to constant soil suction.

4. Equilibrium Soil Suction. If the magnitude of the constant soil suction is not known or cannot be measured, it can be estimated from Figure 66.

5. Velocity of Soil Moisture Movement. If the velocity of moisture infiltration or evaporation, v, is not known or cannot be measured, it can be estimated by dividing the Thornthwaite Index for the site by 24 and expressing it in units of inches per month. This method for estimating velocity shows good comparison to actual measurements conducted by Ritchie and Adams (74) at Temple, Texas. I_m for Temple, Texas, is -12 inches/year which, when divided by 24, yields 0.5 inches/month as an estimate of moisture movement; Ritchie and Adams measured evaporation rates ranging from a low of 0.36 inches/month to a high of 0.84 inches/month.

6. If not already determined, the edge moisture variation

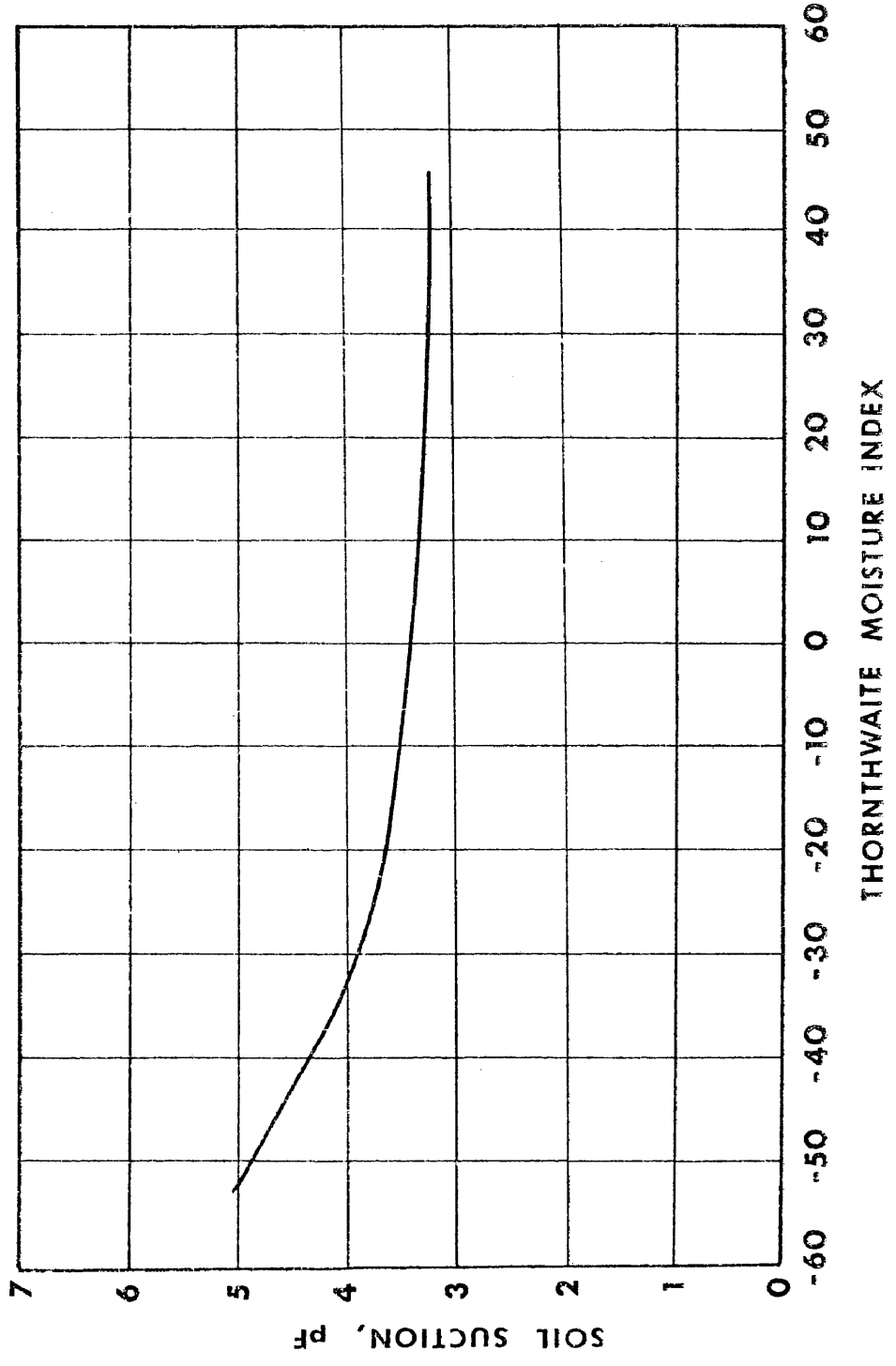

FIGURE 66. VARIATION OF CONSTANT SOIL SUCTION WITH THORNTHWAITE INDEX. [AS MODIFIED FROM RUSSAM AND COLEMAN (75)]

distance, e_m, can be estimated from Figure 58, p. 157.

All the information needed to determine the expected differential soil movement (Appendix Q) for either the center lift or edge lift swelling condition is now known. Values of soil movement intermediate to the tabulated combinations can be conservatively estimated by using straight line interpolation.

Structural Parameters.

a. Slab Length. The slab length, L, is determined by the direction in which the design is being conducted, i.e., for design in the long direction, the slab length is the long dimension of the rectangular slab, but for design in the short direction, the slab length is the short dimension of the rectangle.

b. Perimeter Loading. This is the load, P, applied along the perimeter of the slab, consisting principally of the wall and roof dead loads.

Concentrated loads such as fireplaces should be located so that these loads are transferred to the stiffening beams. Concentrated loads in excess of 100 psf per bay area, including slab weight, should be located to rest on at least two stiffening beams. In the case of smaller concentrated loads located between stiffening beams, the tensile stresses beneath the slab should be checked to see that they are within the allowable tensile strength.

From elastic foundation theory (90), the design bending moment can be estimated by:

$$M = \frac{P}{4\beta} \quad \text{(7-3a)}$$

and from the familiar flexure formula, stress can be calculated:

$$f_t = \frac{Mc}{I} \quad \ldots\ldots\ldots\ldots\ldots\ldots\ldots\ldots\ldots\ldots \quad (7\text{-}3b)$$

By combining Equations (7-3a) and (7-3b) the following equation can be developed to determine whether the soil support alone is sufficient to support the concentrated load:

$$f_t = 0.449 \frac{P}{(t)^{2.75}} + f_p \quad \ldots\ldots\ldots\ldots\ldots\ldots\ldots \quad (7\text{-}4)$$

where f_t = tensile stress, psi

f_p = the minimum compressive stress in the concrete due to prestressing, in psi

If the allowable tensile strength is exceeded, then a thicker slab section should be used or a stiffening beam should be placed directly beneath the concentrated load.

c. Stiffening Beam Spacing. The spacing of the stiffening beams, S, is generally governed by the slab geometry and is typically 12-20 feet (Table 15, p. 88).

d. Beam Depth. The depth of stiffening beams, d, is the controlling parameter in structural design of stiffened slabs. Beam depth is what the engineer increases in order to increase moment and shear capacity and reduce deflections.

The last two design parameters can be assumed as the design procedure begins.

Material Properties. - The material properties needed include:

a. Compressive stress in the concrete, f'_c

b. Allowable tensile strength of the concrete, f_t

c. Allowable compressive stress in the concrete, f_c

d. Type, grade, and strength of the prestressing steel

e. Grade and strength of mild steel reinforcement

f. Slab-Subgrade friction coefficient, μ

Divide an Irregular Slab Plan into Overlapping Rectangles

Slabs of irregular shape should be divided into overlapping rectangles so that the resulting boundary provides complete congruence with the slab perimeter. Figure 67 shows examples of this procedure. A separate design shall be made for each of the component rectangles of the slab.

Assume Trial Sections in Both Directions

Assume Beam Depth and Spacing. - An initial estimate of the depth of the stiffening beams can be obtained from solving either Equation (7-42) or Equation (7-43) for the beam depth yielding the maximum allowable differential deflection. A preliminary estimate of the allowable differential deflection can be made by:

1. Determining the maximum distance over which the allowable differential deflection will occur, L or 6β, whichever is smaller. As a first approximation, use $\beta = 8$ feet. Select the permissible deflection ratio, e.g.,

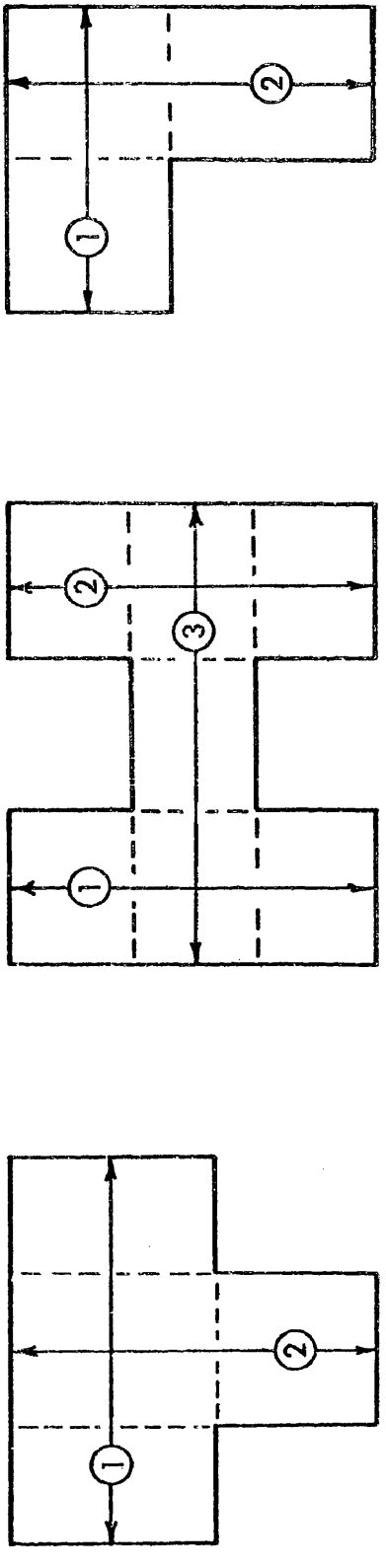

FIGURE 67. TYPICAL DESIGN RECTANGLES FOR SLABS OF IRREGULAR SHAPE (9)

CENTER LIFT

$$\frac{\Delta}{L \text{ or } 6\beta} = \frac{1}{40} \quad \ldots\ldots\ldots\ldots\ldots\ldots\ldots\ldots \quad (7\text{-}5)$$

EDGE LIFT

$$\frac{\Delta}{L \text{ or } 6\beta} = \frac{1}{140} \quad \ldots\ldots\ldots\ldots\ldots\ldots\ldots\ldots \quad (7\text{-}6)$$

The 1/140 deflection ratio is used only to initially estimate the required beam depth.

2. Assume a beam spacing and solve for the beam depth, d:

Center Lift

$$\text{Set } X = \left[\frac{(y_m L^{0.205}(S)^{1.059}(P)^{0.523}(e_m)^{1.296}}{380\ \Delta} \right] \quad \ldots\ldots\ldots \quad (7\text{-}7a)$$

$$\text{Then } \log_{10}(d) = \left[\frac{1}{1.214} \log_{10}(X) \right] \quad \ldots\ldots\ldots\ldots \quad (7\text{-}7b)$$

$$d = X^{0.824} \quad \ldots\ldots\ldots\ldots\ldots\ldots \quad (7\text{-}7c)$$

Edge Lift

$$\text{Set } X = \left[\frac{(L)^{0.35}(S)^{0.88}(e_m)^{0.74}(y_m)^{0.76}}{12\ \Delta\ (P)^{0.01}} \right] \quad \ldots\ldots\ldots \quad (7\text{-}8a)$$

$$\text{Then } \log_{10}(d) = \left[\frac{1}{0.85} \log_{10}(X) \right] \quad \ldots\ldots\ldots\ldots \quad (7\text{-}8b)$$

$$\text{or } d = X^{1.176} \quad \ldots\ldots\ldots\ldots\ldots\ldots \quad (7\text{-}8c)$$

The depth of the beams should be the same for all beams in both directions.

Determine Section Properties.

Moment of Inertia. - The moment of inertia of the section in either the short or the long direction can be determined by either taking the conventional second moment of area or by using the design aid Figure 68. To use Figure 68,

1. Determine the cross-sectional area in the beams, A_{bm}, given by:

$$A_{bm} = nbd \quad \ldots\ldots\ldots\ldots\ldots\ldots\ldots\ldots \quad (7\text{-}9)$$

where n = number of beams

b = width of a single beam, inches

d = depth of stiffening beam, inches

2. Determine the cross-sectional area of the slab $A_{s\ell}$, given by

$$A_{s\ell} = (12W - nb)t \quad \ldots\ldots\ldots\ldots\ldots\ldots\ldots\ldots \quad (7\text{-}10)$$

where W = total width of slab portion, ft

t = thickness of slab portion, inches

3. Determine the area ratio, r_1

$$r_1 = \frac{A_{s\ell}}{A_{bm}} \quad \ldots\ldots\ldots\ldots\ldots\ldots\ldots\ldots \quad (7\text{-}11)$$

4. Determine the slab thickness-to-beam depth ratio, t/d,

$$t/d = \frac{\text{slab thickness, inches}}{\text{beam depth, inches}} \quad \ldots\ldots\ldots\ldots\ldots\ldots \quad (7\text{-}12)$$

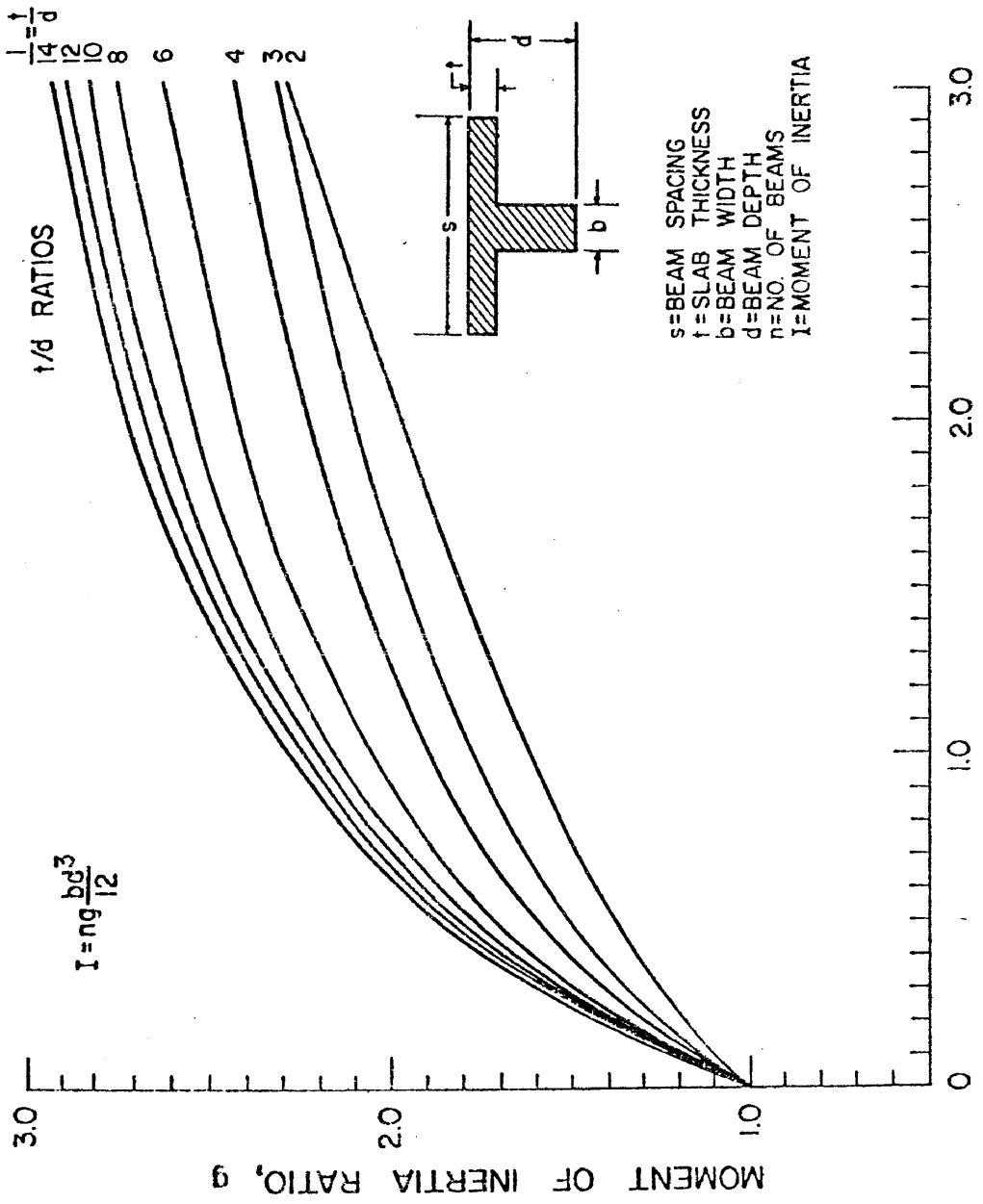

FIGURE 68. MOMENT-OF-INERTIA RATIO, g, AS A FUNCTION OF AREA RATIO, r_1, AND THICKNESS-TO-DEPTH RATIO, t/d. [FROM LYTTON (53)]

Enter Figure 67 with r_1 vertically upward until intersecting the appropriate t/d curve. Then extend the line horizontally to read the value of the moment of intertia ratio, g, from the ordinate axis.

Calculate the moment of inertia, I,

$$I = ng \frac{bd^3}{12} \quad \ldots\ldots\ldots\ldots\ldots\ldots\ldots\ldots \quad (7\text{-}13)$$

Section Moduli. - The section modulus of each section can be determined by using Figure 69:

1. Determine Section Modulus Factors. Enter Figure 69 with r_1. Extend r_1 vertically upward until intersecting the appropriate t/d curve for f_T. Extend the line horizontally to read from the ordinate axis the value of the section modulus factor f_T with respect to the top fiber of the section. Also extend the line horizontally from its intersection with the appropriate t/d curve from the f_B or lower set of curves to read the value of the section modulus factor f_B for the bottom fiber of the section.

2. Calculate the respective section moduli:

Section Modulus for Top Fiber

$$S_T = nf_T bd^2 \quad \ldots\ldots\ldots\ldots\ldots\ldots\ldots\ldots \quad (7\text{-}14)$$

where S_T is the top fiber section modulus expressed in units of inches^3.

Section Modulus for Bottom Fiber

$$S_B = nf_B bd^2 \quad \ldots\ldots\ldots\ldots\ldots\ldots\ldots\ldots \quad (7\text{-}15)$$

where S_B is the bottom fiber section modulus in units of inches^3.

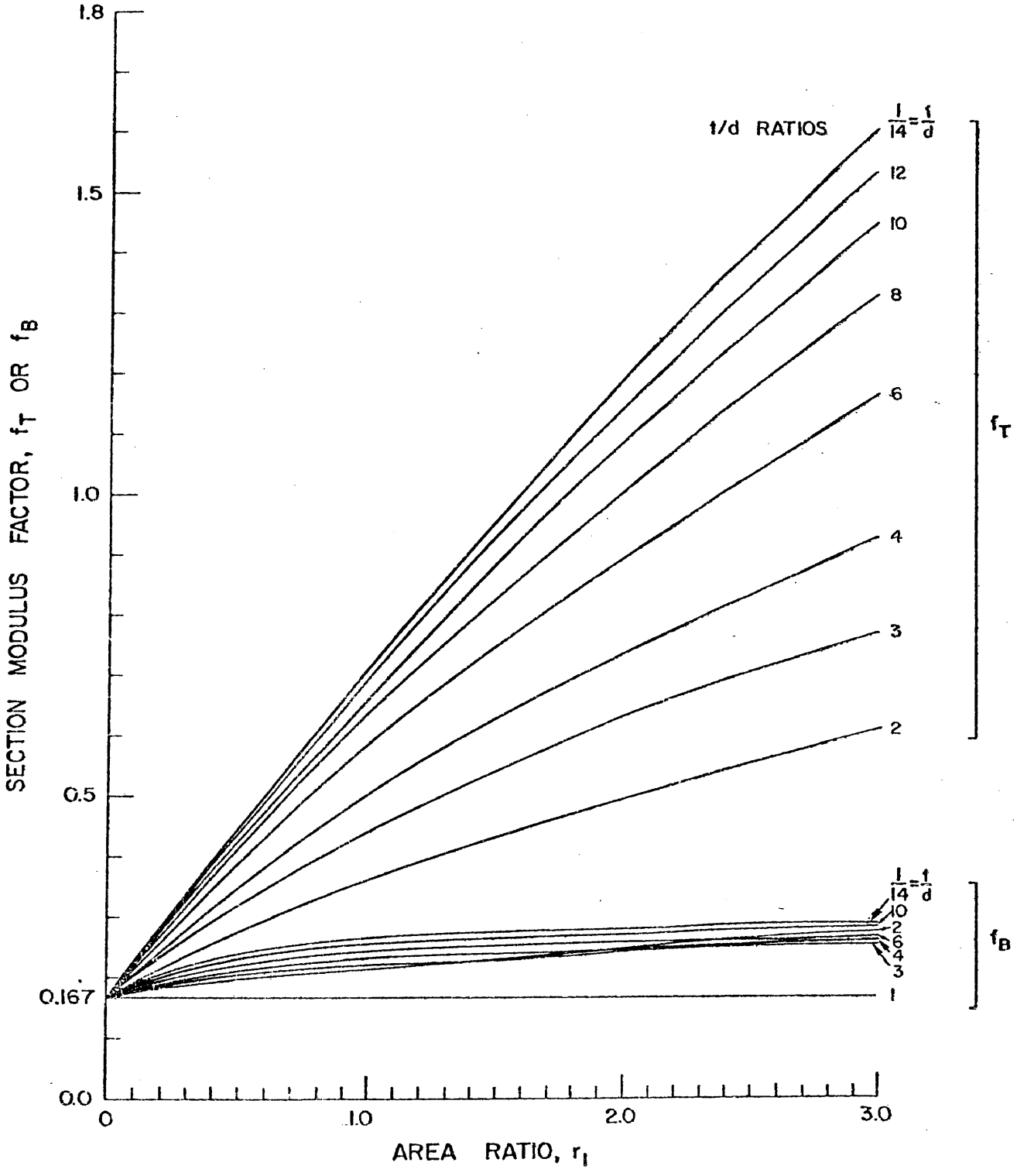

FIGURE 69. SECTION MODULUS FACTOR, f_T OR f_B, AS A FUNCTION OF AREA RATIO, r_1, AND THICKNESS-TO-DEPTH RATIO, t/d. FROM LYTTON (53)

Cross-Sectional Area. - The cross-sectional area can be calculated from:

$$A = nbd + (12W - nb)t \quad \ldots\ldots\ldots\ldots\ldots\ldots\ldots\ldots \quad (7\text{-}16)$$

where W = slab width, in feet

Depth to Neutral Axis. - The depth from the top fiber to the neutral axis of the cross section can be found from Figure 70:

1. Enter Figure 70 with r_1. Extend r_1 vertically upward until it intersects the appropriate t/d curve. Then extend the line horizontally to read the depth-to-neutral axis ratio, k, from the ordinate axis.

2. Calculate the distance from the top fiber to the center of gravity of the section from:

$$c_g = kd \quad \ldots\ldots\ldots\ldots\ldots\ldots\ldots\ldots\ldots\ldots\ldots\ldots \quad (7\text{-}17)$$

Prestressing Eccentricity. - If the slab is to be post-tensioned, the eccentricity of the prestressing force can be found by:

1. Calculate the centroid of the strands, $\bar{c}$.

2. Calculate the prestress eccentricity by:

$$e = c_g - \bar{c} \quad \ldots\ldots\ldots\ldots\ldots\ldots\ldots\ldots\ldots\ldots\ldots\ldots \quad (7\text{-}18)$$

Determine the allowable concrete stresses.

1. Tensile Strength. The split-cylinder tensile strength, f_{ct}, has been found to be proportional to $\sqrt{f'_c}$ (99) such that

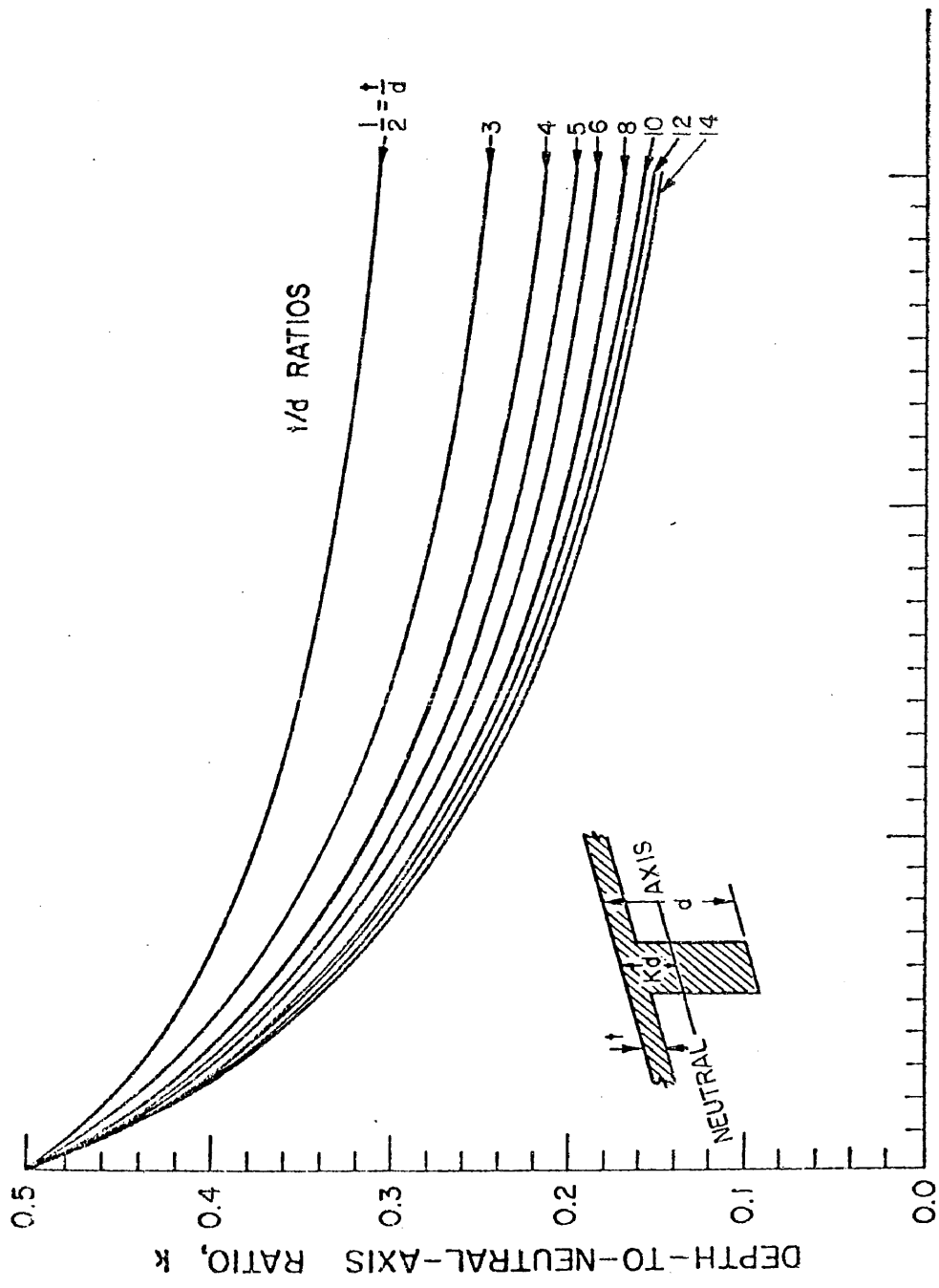

FIGURE 70. DEPTH-TO-NEUTRAL-AXIS RATIO, k, AS A FUNCTION OF AREA RATIO, r_1, AND THICKNESS-TO-DEPTH RATIO, t/d. FROM LYTTON (53)

$$f_{ct} = 6\sqrt{f'_c} \text{ to } 7\sqrt{f'_c}$$

for normal weight concrete. The 1971 ACI Code indirectly uses $f_{ct} = 6.7\sqrt{f'_c}$ for normal weight concrete (99). Tensile strength in flexure, known as the modulus of rupture, f_r, gives higher values for tensile strength then the split cylinder test. This higher value is due principally because the concrete compressive stress distribution is not linear when tensile failure is imminent as is assumed in the computation of the nominal Mc/I stress (Equation (7-3b)).

The ACI Code 318-77 (3) reflects this higher value as it specifies that the average value for the modulus of rupture, f_r, may be taken as $7.5\sqrt{f'_c}$ for normal weight concrete. Libby (46) reports that the modulus of rupture can be taken as:

$$f_r = a\sqrt{wf'_c} \quad \ldots\ldots\ldots\ldots\ldots\ldots\ldots\ldots\ldots\ldots \quad (7\text{-}19)$$

where a is a constant that normally varies between 0.60 and 0.70. If normal weight concrete is assumed to have a unit weight of 145 lb/ft^3, Equation (7-19) would produce a range of values between $7.2\sqrt{f'_c}$ and $8.4\sqrt{f'_c}$. Thus, concrete has some strength in tension and some amount of this strength should be allowed to be used by the concrete under service conditions. The ACI Code (3) recognizes this and allows a maximum amount of tension in a precompressed tensile zone of $6\sqrt{f'_c}$, after allowance for all prestress losses.

From the cracking moment study discussed in Chapter V, it is noted that relatively dramatic increases in differential deflection

can occur upon exceeding the flexural strength of the concrete in the center lift condition, whereas much smaller deflection increases are noted in the edge lift condition. It, therefore, appears to be proper to specify a lower level of allowable tensile stress for service load conditions for the center lift distortion mode than for the opposite edge lift condition. Allowing the edge lift condition to operate at the maximum allowable stress of $6\sqrt{f'_c}$ still provides a margin of safety of 1.25, as given by the ratio of the modulus of rupture of $7.5\sqrt{f'_c}$ to the maximum allowable tensile stress of $6\sqrt{f'_c}$. Consequently, the following permissible tensile stresses are adopted for use in this design procedure.

(a) Allowable Tensile Stress, f_t

Center Lift

$$f_t = 2\sqrt{f'_c} \quad \ldots\ldots\ldots\ldots\ldots\ldots\ldots\ldots\ldots\ldots \quad (7\text{-}20)$$

Edge Lift

$$f_t = 6\sqrt{f'_c} \quad \ldots\ldots\ldots\ldots\ldots\ldots\ldots\ldots\ldots\ldots \quad (7\text{-}21)$$

(b) Estimated Tensile Cracking Stress, f_{cr}

$$f_{cr} = 6\sqrt{f'_c} \quad \ldots\ldots\ldots\ldots\ldots\ldots\ldots\ldots\ldots\ldots \quad (7\text{-}22)$$

2. Allowable Compressive Stress, f_c. ACI Code 318-77 (3) specifies the maximum allowable compressive stress permitted after

allowing for all prestress loss as:

$$f_c = 0.45\, f'_c \quad \ldots\ldots\ldots\ldots\ldots\ldots\ldots\ldots \quad (7\text{-}23)$$

This value is also adopted for this design procedure.

3. Allowable Shear Stress. - ACI Code 318-77 (3) specifies the shear stress, v_c, carried by the concrete is not to exceed $2\sqrt{f'_c}$ unless more detailed analyses are performed. Since this code is based on the "strength method" in which dead and live loads are increased by factors of 1.4 and 1.7, respectively, and the loads considered in slab design are principally dead loads, the maximum permissible shear stress adopted for this design procedure was obtained by dividing $2\sqrt{f'_c}$ by the dead load factor of 1.4 and rounding the resulting coefficient up to 1.5:

$$v_c = 1.5\sqrt{f'_c} \quad \ldots\ldots\ldots\ldots\ldots\ldots\ldots\ldots \quad (7\text{-}24)$$

4. Prestressing Steel.

a. The maximum stress in the prestressing steel during stressing shall not be greater than 0.80 times the minimum guaranteed ultimate strength (maximum value recommended by the steel manufacturer) of the prestressing steel. The maximum stress in the prestressing steel immediately after anchoring shall not exceed 0.70 times the minimum guaranteed ultimate strength of the steel. These values are in accordance with the ACI Code 318-77 (3).

b. Prestress Losses. To determine the effective prestress, allowance for the following sources of loss of prestress are normally

considered (46):

(1) Slip at anchorage,

(2) Elastic shortening of concrete,

(3) Creep of concrete,

(4) Shrinkage of concrete,

(5) Relaxation of steel stress, and

(6) Frictional loss due to intended or unintended curvature in the tendons.

There are a number of procedures available for determining each of these losses (46), however, if this information is not readily available or cannot be determined, the post-tensioning industry (70) suggests using a lump sum loss value of 30,000 psi for slabs using stress relieved 270k strand and stress relieved 240k wire.

c. Slab Subgrade Friction. - As an allowance for subgrade frictional resistance to movements induced by prestressing, concrete shrinkage, or temperature variations, an additional prestressing force P_f, shall be required in each direction equivalent to one-half of the total weight of the stiffened slab multiplied by the coefficient of friction, μ. This prestressing force requirement shall be uniformly distributed across the cross-sectional area of the slab section in each direction and shall be accounted for as either (1) an equivalent prestress loss in each tendon, or (2) an equivalent loss in total prestress force.

d. Minimum Average Effective Prestress. - A minimum effective prestress force is necessary, particularly in lightly pre-

stressed slabs without bonded reinforcement to provide assurance against cracking from possible loads or stresses not fully anticipated in the design. Therefore, the minimum average compressive stress in the center of the slab after all losses, including the loss to slab-subgrade friction, shall be 50 psi. This minimum average prestress shall be calculated as the effective prestressing force divided by the gross area of slab and stiffening beams.

e. Maximum Spacing of Post-Tensioning Tendons. - The maximum spacing of tendons cannot exceed that which would fail to produce a minimum average effective prestress of 50 psi. The maximum spacing of tendons placed in the slab portion of the cross-section can be estimated from Figure 71. Tendon spacings obtained from Figure 71 may have to be adjusted as other prestress losses are taken into account in order to maintain the minimum residual compressive stress of 50 psi.

Expected Service Moment

The maximum moment the selected section is expected to experience will vary, depending upon the swelling mode and the slab direction being designed. Moments for center lift condition will, in general, be greater than edge lift moments; moments in the short direction will, in general, be greater than moments in the long direction.

Center Lift Moment.

Long Direction:

$$M_{\ell} = A_o \left[B(e_m)^{1.238} + C \right] \quad \ldots\ldots\ldots\ldots\ldots\ldots \quad (7\text{-}25)$$

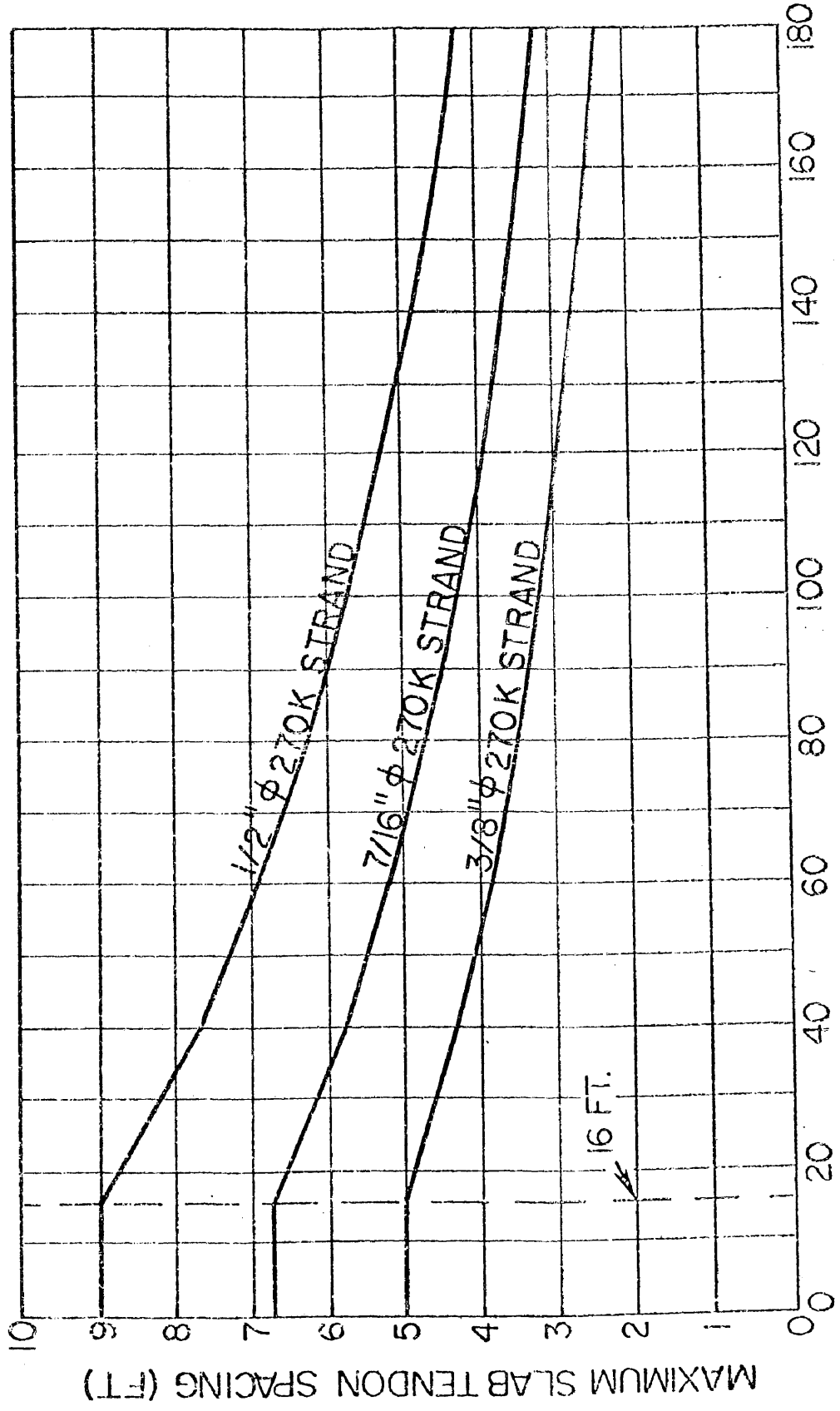

FIGURE 71. MAXIMUM SLAB TENDON SPACING TO OVERCOME SLAB-SUBGRADE FRICTION AND RETAIN 50 PSI RESIDUAL PRESTRESS COMPRESSION AT MIDPOINT OF STIFFENED SLAB-ON-GROUND.

where

M_ℓ = Design moment in long direction, in ft-kips/ft.

and

$$A_o = \frac{1}{727}\left[(1)^{0.013}(s)^{0.306}(d)^{0.688}(P)^{0.534}(y_m)^{0.193}\right] \quad (7\text{-}26)$$

and for

$0 \leq e_m \leq 5$: $B = 1$, $C = 0$

$$e_m \geq 5: \quad B = \frac{y_m - 1}{3}, \quad C = \left[8 - \left(\frac{P - 613}{255}\right)\right]\left(\frac{4 - y_m}{3}\right) \quad (7\text{-}27)$$

Short Direction

$$M_s = \left[\frac{58 + e_m}{60}\right] M_\ell \quad (7\text{-}28)$$

where M_s = Design moment in short direction, in ft-kips/ft.

Edge Lift Moment.

Long Direction:

$$M_\ell = \left[\frac{(S)^{0.10}(de_m)^{0.78}(y_m)^{0.66}}{7.2\ (L)^{0.0065}(P)^{0.04}}\right] \quad (7\text{-}29)$$

Short Direction:

$$M_s = (d)^{0.35}\left[\frac{19 + e_m}{21}\right] M_\ell \quad (7\text{-}30)$$

Determine Allowable and Maximum Moment Capacity

Allowable Service Moments. - The maximum moments to which the assumed sections can be subjected can be determined from the familiar relationship for combined stresses (82).

$$f = \frac{P_r}{A} \pm \frac{P_r e}{S} \mp \frac{M}{S} \quad \ldots\ldots\ldots\ldots\ldots\ldots \quad (7\text{-}31)$$

rearranged so as to be able to solve for the maximum allowable external moment:

$$\mp M = \mp P_r e + S\left(f - \frac{P_r}{A}\right) \quad \ldots\ldots\ldots\ldots\ldots\ldots \quad (7\text{-}32)$$

The sign conventional adopted is to represent compressive forces as positive values and to consider eccentricities measured upward as being positive eccentricities. The form of Equations (7-33) through (7-38) have accounted for the sign difference between tensile and compressive stresses. The following calculations must be done for both the long and short direction.

Negative Bending Moment, $_nM$.

1. Tension in Top Fiber

$$_nM_t = S_T \left(\frac{P_r}{A} + f_t\right) + P_r e \quad \ldots\ldots\ldots\ldots\ldots\ldots \quad (7\text{-}33)$$

where S_T = section modulus for top fiber, inches^3

P_r = prestressing force, kips

A = cross-sectional area, inches^2

f_t = allowable tensile stress, kips/inches^2 (ksi)

e = eccentricity of prestressing force, inches

2. Compression in Bottom Fiber

$$_nM_c = S_B (f_c - \frac{P_r}{A}) + P_r e \quad \ldots\ldots\ldots\ldots\ldots\ldots \quad (7\text{-}34)$$

where S_B = section modulus for bottom fiber, inches^3

f_c = allowable compressive stress, ksi

The maximum external negative moment that can be carried by the section is the smaller of these two moments.

Positive Bending Moment, $_pM$.

1. Tension in Bottom Fiber

$$_pM_t = S_B (\frac{P_r}{A} + f_t) - P_r e \quad \ldots\ldots\ldots\ldots\ldots\ldots \quad (7\text{-}35)$$

2. Compression in Top Fiber

$$_pM_c = S_T (f_c - \frac{P_r}{A}) - P_r e \quad \ldots\ldots\ldots\ldots\ldots\ldots \quad (7\text{-}36)$$

The maximum external positive moment that can be carried by the section is the smaller of these two moments.

Tensile Cracking Moments. - Stiffened slabs-on-ground are usually designed to be underreinforced. As long as the actual moment acting in the slab is less than the tensile cracking moment, the stiffening beams will act in their elastic range and the assumed use of the gross

cross section in computing deflection criteria is justified.

Negative Bending Moment, $_nM_{cr}$

$$_nM_{cr} = S_T \left(\frac{P_r}{A} + f_{cr}\right) + P_r e \quad \ldots\ldots\ldots\ldots\ldots \quad (7\text{-}37)$$

Positive Bending Moment, $_pM_{cr}$

$$_pM_{cr} = S_B \left(\frac{P_r}{A} + f_{cr}\right) - P_r e \quad \ldots\ldots\ldots\ldots\ldots \quad (7\text{-}38)$$

Compare Allowable and Cracking Moments to Expected Service Moment.- The moments expected to occur in both directions, as calculated from Equations (7-25) and (7-28) - (7-30), must be compared to the moments determined in Equations (7-33) through (7-38). If either the short direction or long direction design moments exceed the allowable service moments, the moment capacity of the section must be increased. Means of increasing the moment capacity include:

1. Deepening the stiffening beams (for deficient negative and positive moment capacity).

2. Decreasing the beam spacing (for deficient negative and positive moment capacity).

3. Increasing the prestressing force (for deficient negative moment capacity).

4. Decreasing the prestress eccentricity by carrying tendons below the neutral axis (for deficient positive moment capacity).

If the moment capacity of the assumed section exceeds the design moment, economies may be realized by performing the opposite to the

actions suggested above for increasing moment capacities.

Differential Deflection

Calculate the relative stiffness length, β

$$\beta = \frac{1}{12}\sqrt[4]{\frac{E_c I}{E_s}} \quad \ldots\ldots\ldots\ldots\ldots\ldots\ldots\ldots \quad (7\text{-}39)$$

where β = relative stiffness length, in feet

E_c = creep modulus of elasticity of concrete, psi

E_s = modulus of elasticity of soil, psi

I = gross moment of inertia of section, inches^4

If the creep modulus of elasticity of the concrete is not known, it can be closely approximated by using 0.5 of its normal or early life modulus of elasticity. If the modulus of elasticity of the soil is not known, use 1000 psi.

Determine the Differential Deflection Distance. - The differential deflection may not occur over the entire length of the slab, particularly if the slab is longer than approximately 48 feet. Thus, the effective distance for determining the allowable differential deflection is the smaller of the two distances, L or 6β, both expressed in feet.

Calculate the Allowable Differential Deflection. - From Table 12, p. 86, select the appropriate deflection for the type of superstructure construction. For the edge lift distortion mode, decrease the ratio to 1 in 800. The purpose of the more stringent edge lift deflection cri-

teria is to provide an increased margin of safety since the extreme concrete fibers will be allowed to operate at a higher level of tensile stress than in the center lift condition.

If the selected deflection ratio is 1/480, then the allowable differential deflection is given by:

Center Lift:

$$\Delta_{allow} = \frac{12\ (L \text{ or } 6\beta)}{480} \quad \ldots\ldots\ldots\ldots\ldots\ldots \quad (7\text{-}40)$$

where Δ_{allow} = allowable differential deflection, in inches

L = total slab length, in feet

β = relative stiffness length, in feet

Edge Lift:

$$\Delta_{allow} = \frac{12\ (L \text{ or } 6\beta)}{800} \quad \ldots\ldots\ldots\ldots\ldots\ldots \quad (7\text{-}41)$$

Calculate Expected Differential Deflection.

Edge Lift:

$$\Delta = \left[\frac{(L)^{0.35}(S)^{0.88}(e)^{0.74}(y_m)^{0.76}}{15.90(d)^{0.85}(P)^{0.01}}\right] \quad \ldots\ldots\ldots\ldots \quad (7\text{-}42)$$

where Δ = expected differential deflection, in inches

Center Lift:

$$\Delta_0 = \left[\frac{(y_m L)^{0.205} (S)^{1.059} (P)^{0.523} (e_m)^{1.296}}{380(d)^{1.214}} \right] \quad \ldots\ldots\ldots \quad (7\text{-}43)$$

where Δ_0 = expected differential deflection without prestressing, in inches

If the slab is post-tensioned, some reduction in differential deflection may occur because typically most of the prestressing is placed in the slab and the centroid of the prestressing force is above the center of gravity of the section. Because of this, any deflection due to negative bending must first overcome a slight amount of positive deflection or camber caused by the prestressing. This differential deflection advantage of prestressing can be calculated by:

1. Calculate the percent of differential deflection reduction.

$$\Delta_c = e \sqrt{\frac{6400}{9L}} \quad \ldots\ldots\ldots\ldots\ldots\ldots\ldots\ldots \quad (7\text{-}44)$$

where Δ_c = differential deflection correction, in %

2. Calculate corrected differential deflection.

$$\Delta = \Delta_0 \left(\frac{100 - \Delta_c}{100} \right) \quad \ldots\ldots\ldots\ldots\ldots\ldots\ldots\ldots \quad (7\text{-}45)$$

where Δ = expected differential deflection, in inches.

Compare Expected to Allowable Differential Deflection. - If the expected differential deflection as calculated by either Equation (7-42) or (7-43) exceeds that determined from Equation (7-40) or (7-41), the assumed section must be stiffened. This can be accomplished in at least three ways:

1. Deepening the stiffening beams,
2. Decreasing the beam spacing, or
3. Adding additional prestressing tendons.

Shear Capacity

Determine Expected Service Shear

Center Lift.

Short Direction Shear

$$V_s = \frac{1}{1350}\left[(L)^{0.19}(S)^{0.45}(d)^{0.20}(P)^{0.54}(y_m)^{0.04}(e_m)^{0.97}\right] \quad (7\text{-}46)$$

Long Direction Shear

$$V_\ell = \frac{1}{1940}\left[(L)^{0.09}(S)^{0.71}(d)^{0.43}(P)^{0.44}(y_m)^{0.10}(e_m)^{0.93}\right] \quad (7\text{-}47)$$

Edge Lift.

For both directions:

$$V = \left[\frac{(L)^{0.07}(d)^{0.40}(P)^{0.03}(e_m)^{0.16}(y_m)^{0.67}}{3\ (S)^{0.015}}\right] \quad \ldots\ldots\ldots \quad (7\text{-}48)$$

where V, V_s, V_ℓ = Shear force, in kips/ft

Determine Allowable Shear Stresses.

Nominal Total Design Shear Stress, v_u. - Only the beams may be considered in calculating the cross sectional area resisting shear force.

$$v_u = \frac{VW}{nbd} \quad \ldots\ldots\ldots\ldots\ldots\ldots\ldots\ldots \quad (7\text{-}49)$$

where V = total shear force acting on the section, kips/ft

Nominal Permissible Shear Stress, v_c.

$$v_c = 1.5\sqrt{f'_c} \quad \ldots\ldots\ldots\ldots\ldots\ldots\ldots\ldots \quad (7\text{-}50)$$

Compare v_u to v_c. If v_u exceeds v_c, reinforcement in accordance with ACI 318-77 and the PTI Post-Tensioning Manual must be provided. Possible alternatives to reinforcement include:

1. Increasing the beam depth,
2. Increasing the beam width, or
3. Increasing the number of beams (decrease beam spacing).

Shear Reduction Due to Prestressing. - An advantage of curved or draped prestressing tendons is that due to the upward force exerted by the curved tendon on the concrete, shear compensation in an amount equal to $P_r \sin \theta$ is obtained, and the total design shear is reduced. Figure 72 shows the effect of prestressing on shear reduction.

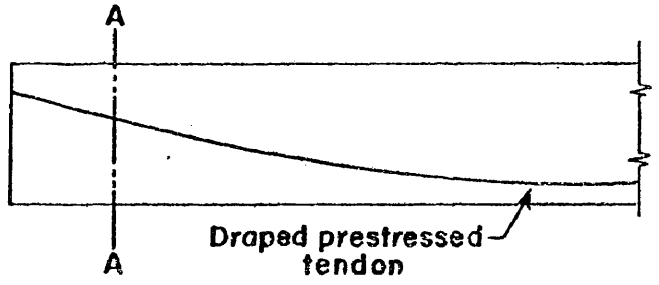

a. HALF-ELEVATION OF STIFFENING BEAM WITH DRAPED TENDON.

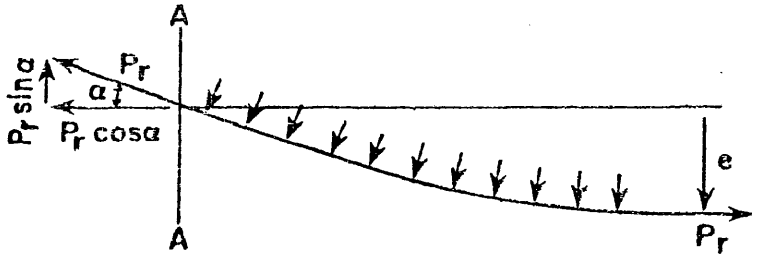

b. FREE-BODY OF FORCES ON THE TENDON.

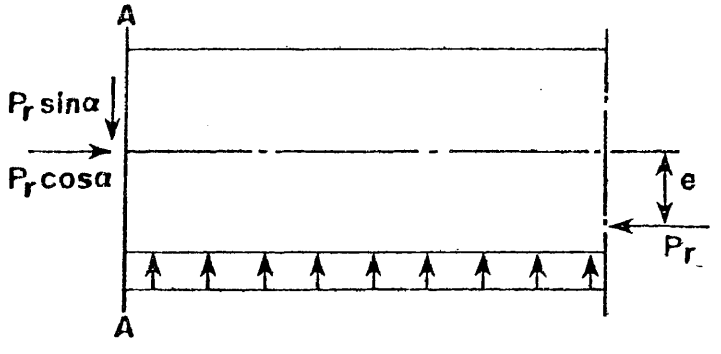

FREE-BODY OF FORCES ON THE CONCRETE.

FIGURE 72. FREE-BODY DIAGRAMS FOR DRAPED TENDON AND CONCRETE SECTION.

Repeat Design Procedure for Opposite Swelling Mode

The design procedure must be followed for both swelling conditions to ensure that the section is adequate in either distortion mode. If the section adequate for the first swelling mode is found to be inadequate for the second, but altered or adjusted so as to make it adequate, the design for the first condition must then be re-checked to ensure that the modifications have not rendered it inadequate.

CHAPTER VIII

COMPARISON OF DESIGN PROCEDURES

Two examples illustrating the design procedure of Chapter VII are included as Appendices R and S . The first example is a residential foundation constructed over severe soil conditions in a relatively dry climate (San Antonio, Texas, whose I_m = -16). The second example is an apartment house foundation constructed over soil conditions in a relatively wet climate (Houston, Texas, whose I_m = +18).

As a means of comparing the results of the procedure introduced in Chapter VII to the results of the principal design methods discussed in Chapter III (BRAB, Lytton, and Walsh), each was used to calculate values of the design parameters for the same conditions as in the design examples. The method of Fraser and Wardle (23), however, is not an actual design procedure. A design by their method is accomplished using a finite element computer program. The two investigators have never reduced their computer analysis results to a general design procedure and, therefore, no direct comparison between their methods and the method of Chapter VII was possible.

Thus, only the methods of BRAB, Lytton, and Walsh were compared to the new method presented in the previous chapter.

Comparison of Results

Residential Slab Example. - The values of the three design parameters as calculated by each design procedure are shown in Table 21.

TABLE 21. Comparison of Moment, Shear, and Structural Stiffness Design Values Resulting from the Procedures of Brab, Lytton, and Walsh to the Design Values of the New Procedure

DESIGN EXAMPLE, SWELLING MODE, AND DESIGN PARAMETER	DESIGN METHOD							
	NEW PROCEDURE		BRAB		LYTTON		WALSH	
	DIRECTION: LONG	SHORT	DIRECTION: LONG	SHORT	DIRECTION: LONG	SHORT	DIRECTION: LONG	SHORT
RESIDENTIAL SLAB								
Center Lift								
Moment[a]	8.10	8.41	21.00	6.86	12.07	14.06	7.59	4.34
Shear[b]	1.57	1.52	2.00	1.14	1.53	2.34	0.67	0.72
Stiffness[c]	5.62	14.65	24.39	7.97	7.00	8.17	4.40	2.50
Edge Lift								
Moment	2.68	3.00	21.00	6.86	6.72	7.82	1.18	0.38
Shear	1.71	1.64	2.00	1.14	0.64	1.30	0.11	0.06
Stiffness[d]	3.54	8.58	40.65	13.28	6.50	7.57	1.13	3.69
APT. HOUSE SLAB								
Center Lift								
Moment	5.88	5.98	41.69	9.74	18.02	21.80	12.55	2.93
Shear	2.11	1.59	1.39	0.67	1.24	0.73	0.42	0.20
Stiffness[c]	4.32	14.83	334.25	77.47	72.24	87.46	50.03	11.75
Edge Lift								
Moment	2.65	3.38	41.69	9.74	-[e]	-[e]	8.37	1.96
Shear	1.20	1.14	1.39	0.67	-	-	0.28	0.14
Stiffness[d]	5.84	17.98	557.08	130.14	-	-	0.98	0.01

[a] In units of Ft-Kips/Ft

[b] In units of Kips/Ft

[c] In units of 10^{10} lb-in^2 ($\Delta/L = 1/480$)

[d] In units of 10^{10} lb-in^2 ($\Delta/L = 1/800$)

[e] Negative moments produced

Table 22 shows the values used in each method. As can be seen the Walsh procedure produced smaller design values than the new design procedure (NDP), while the Lytton and BRAB procedures produced larger values.

The Walsh center lift long direction design moment was approximately the same size as the value from the NDP but the short direction moment was essentially only 50% of Walsh's long direction value as well as both moment values from the NDP. The Lytton procedure produced moment values approximately twice as great as those of the NDP. The Lytton method also resulted in the short direction moment being greater than the long direction moment. The BRAB method resulted in moments approximately 2.5 times greater than the NDP moment in the long direction, but the short direction moment was only 1/3 as great as the long direction moment and about 20% smaller than the NDP short direction moment.

In the edge lift case, the Lytton and BRAB procedures resulted in moment values in the long direction greater than those of the NDP and, except for the Lytton results, again produced short direction moments smaller than their respective long direction moments.

The center lift shear force results showed trends similar to those of the moment values. The two differences were that the BRAB long dimension shear was the greatest value in both distortion modes. The Lytton shear value was the largest in the edge lift mode for short direction shear values.

Comparison of predicted differential deflection by each method is difficult to make since slab cross-sections were not determined. Consequently, the comparison reported in Table 21 is in terms of the stiffness, EI. The center lift designs were limited to a deflection ratio of 1/480 and the edge lift ratio was 1/800.

TABLE 22. The Assumed Soil Properties Used in Design Method Comparison

DESIGN PARAMETER	DESIGN METHOD		
	LYTTON	WALSH	BRAB
RESIDENTIAL EXAMPLE			
k	4 lb/in^3	0.5 MN/M^3	-
y_m	2.415 in[a] 0.863 in[b]	2.415 in[a] 0.863 in[b]	-
m	3.00[a] 0.92[b]	-	-
e	-	4.3 ft[a] 2.3 ft[b]	-
P.I.	-	-	54
C_w	-	-	17
C	-	-	0.64
APARTMENT HOUSE EXAMPLE			
k	4 lb/in^3	2.0 MN/M^3	-
y_m	0.274 in[a] 0.307 in[b]	0.274 in[a] 0.307 in[b]	- -
m	3.00[a] 0.92[b]	-	-
e	-	3.0 ft[a] 4.5 ft[b]	-
P.I.	-	-	42
C_w	-	-	25
C	-	-	0.80

[a] Center Lift Design

[b] Edge Lift Design

To satisfy the allowable center lift long direction differential deflection requirement, the NDP requires a stiffness between that of the Walsh and Lytton methods; the Lytton stiffness being approximately 20% greater and the Walsh stiffness being approximately 25% smaller. In the short direction, however, the NDP stiffness requirement is the largest of any method.

Apartment House Slab Example. - The NDP moment values in the long direction were smaller than any of the other design method results. In the short direction, the NDP value was smaller than all but that of Walsh's. Comparison of the short direction moments to the long direction moments, as was done for the residential example, again showed the BRAB and Walsh short direction moments to be substantially smaller than the long direction values; for this example, the short direction values were only 25% as great as the long direction moments. Because the correction for the soil compressibility, as calculated by Equation (3-7), was larger than the rigid beam calculation of Equation (3-5), comparative design values for the edge lift condition could not be calculated for this example using the Lytton method.

In comparing the shear force calculations, it is seen that for the center lift condition, the NDP produced shear forces greater than any of the other design methods. For the edge lift condition, the NDP shear value was the greatest for the short direction calculations but was less than the BRAB value in the long direction. The Walsh method produced the smallest value in every case.

In contrast to the stiffness comparisons of the residential example, the stiffness required by the NDP for the long apartment

house slab is much less than that required by the other methods; the NDP requires a stiffness less than 10% of that required by the Walsh method and less than 6% of the Lytton method. In the short direction the NDP stiffness is also much smaller than the BRAB or Lytton stiffness requirements and only slightly larger than the stiffness resulting from the Walsh method. For the edge lift distortion mode, the NDP stiffness requirement is much less than that resulting from the BRAB procedure and substantially larger than the Walsh requirement.

Discussion of Comparisons

Center Lift Comparisons. - The NDP produces smaller design values in almost every instance of long direction moment. The exception to this is the Walsh method for the residential slab example. Walsh's result for the long apartment house slab example, however, is much greater than the NDP value. Thus, Walsh's procedure appears to be more influenced by slab length than the NDP.

Walsh's equation for moment calculation, Equation (3-1) is identical to the BRAB equation; the difference results in the selection of the support constant, C. Walsh, however, does consider these two important soil parameters. He relates the differential soil movement to the maximum allowable differential deflection of the slab as a ratio, Δ/y_m , and also the edge penetration, e, to the slab length as a ratio, $e/_{span}$. He accounts for the difference in distortion modes by including a separate listing in his table of coefficients (Table 6, p.45). As the ratio $e/_{span}$ increases, indicating increasing edge moisture variation distance, the

value of C in the table decreases (indicating less support and increased moment). As the ratio $^{\Delta}/_{y_m}$ increases, indicating decreasing soil movement, the value of C increases (indicating greater supported area and less moment). But when the slab length is short, the allowable differential deflection and the ratio $^{\Delta}/_{y_m}$ is small; this results in the coefficient of support also being small. This smaller value of C, in association with the now reversed values of the L and L' terms in Equation (3-1), results in a comparatively small value of moment in the short direction. Since the shear and differential deflection values are calculated from the resulting moment, their values are probably influenced in the same manner. The smaller moments in the short direction similarly obtained in the BRAB calculations results from the same transposition of slab length terms in Equation (3-1).

The smaller moments obtained in the short direction in the BRAB and Walsh procedures do not agree with the results obtained in the soil-structure analysis (Chapter V) that led to the design equations of this new procedure. Fraser and Wardle also found the short direction moment to be the more "critical" (23), i.e., the greater value. Lytton's results, when corrected for plate action, also show the short direction value to be greater than the long direction moment.

Edge Lift Analysis. - Washusen (101) performed an extensive comparison of the BRAB, Lytton, and Walsh methods. His assessment of Walsh's method with respect to edge lift design was:

> For the loading and design conditions assumed in this comparison, the final beam size obtained using Walsh's method, however, remains unchanged regardless of the support offered by the initial mound. ... Substantial errors in the interaction analysis results of the edge heave condition are apparent in two major ways. The first is that as the edge distance, e, increase, the support offered by the soil actually decreases, as indicated by decreasing values of the support index, c. The second is that regardless of the combination of the soil parameters (e, k, and y_m), the center heave condition always results in much higher bending moments. [This is] an error which renders his method unsatisfactory for design use under these conditions [edge lift].

If Walsh's edge lift results are omitted from the comparison, the NDP produces smaller results in almost every respect except for shear force in the short direction.

Summary

The new design procedure produces smaller long direction design moment values in most instances than do either the BRAB, Lytton or Walsh procedures. It produces more conservative moment values in the short direction but other analyses (55 ,23) have shown the short direction moment to be greater than the moment occurring in the long direction; close examination of the design moment equations for the BRAB and Walsh methods suggests that they may fail to accurately predict the short direction moment. Thus, the moments resulting from the NDP equations may in fact be better predictions of the actual short direction moment despite their apparently larger magnitude.

The design shear forces resulting from the NDP equations are, in general, greater than those produced by the other methods. However, the larger value may be partly attributed to the inclusion of the twisting moments contribution which does not appear to be adequately accounted for in the BRAB and Walsh methods.

The predicted differential deflections resulting from the NDP are larger than those predicted by the other methods when the slab length is not relatively long. However, this is reversed when the slab becomes long. From the design examples, where the initial stiffening beam depth is estimated from the maximum allowable differential deflection in each direction, it is seen that strength requirements ultimately dictate a stiffer section than that of the deflection requirement. This indicates that the deflection criterion may not be the governing factor in slab design.

CHAPTER IX

CONCLUSIONS AND RECOMMENDATIONS

Conclusions

Seven objectives were established as the development of this design procedure began. These objectives were:

1. The design procedure must be capable of producing specific design quantities of moment, shear, and differential deflection.

2. The design procedure must be able to account for the necessary design soil and climatic conditions and produce sections comparable to slabs that are known to have worked successfully, i.e., the procedure must produce slab sections that will adjust with the site requirements and not produce a section that is so conservative that it *will* be successful regardless of the severity of the design conditions.

3. It must be able to account for the effect of geography and climate in a rational manner.

4. It must be able to properly consider both the center lift and edge lift distortion modes.

5. It must properly consider the effect of slab length on the increase in design moment.

6. The procedure must be rational, i.e., it must be based upon an analysis of the actual loads, and soil and concrete properties.

7. The procedure must be easy to use by practicing engineers.

In order to conclude whether this work has satisfactorily accomplished the above objectives, each of the stated goals should

be considered individually.

Produce Specific Design Quantities. - The design equations developed in Chapter V and incorporated into the design procedure introduced in Chapter VII produce specific design quantities of moment, shear, and differential deflection in either the center lift or edge lift distortion mode. The design procedure does not preclude development of a set of standard sections for use in a localized situation but a set of standard sections was neither the intent nor the result of this research effort.

Accounts for Soil and Climatic Conditions. - The procedure accounts for the effect of climate by relating the expected soil movement and the distance beneath the slab the soil moisture content is expected to vary to an easily determined climatic index, the Thornthwaite Moisture Index. The differential soil movement can be determined either from laboratory testing or estimated from theoretical calculations. The edge moisture variation distance can either be measured in the field or estimated from a chart (Figure 58, p.157) that was constructed from known slab performance. The procedure does not require a "support constant" in order to estimate the degree of support the slab can expect to receive. It accounts for the magnitude of soil movement directly and does not rely on an indirect measurement, such as the weighted *PI*. From the comparison of the available design procedures to the new method, discussed in Chapter VIII, it is seen that the new procedure is less conservative in most instances than the other procedures,

particularly as slab length increases.

Rationally Accounts for Geography and Climate. - The procedure associates the two soil parameters of differential soil movement, y_m, and the edge moisture variation distance, e_m, with the Thornthwaite Moisture Index, I_m. The Thornthwaite Moisture Index is an environmental indicator that can be rationally calculated for any geographical location in the world.

Considers Center Lift and Edge Lift Distortion Modes. - The equations developed in Chapter V and incorporated into the design procedure in Chapter VII consider both distortion modes. The comparison between design methods in Chapter VIII show the edge lift procedure introduced in the new method eliminates the errors shown to be present in the method of Walsh.

Slab Length and Increase in Moment. - The results of Chapter V show the design moment to increase slightly as slab length increases. The design equations developed in Chapter V and incorporated into the design procedure account for this slight increase in contrast to the notably large increases that result from the other design procedures.

Rational Procedure. - The procedure presented in Chapter VII is completely rational. All equations are derived from analysis and all necessary properties can either be measured, determined in the laboratory, or computed from theoretical calculations. There are no steps or design quantities that cannot be explained or derived in a rational manner.

Easy to Use. - The procedure is easily followed and is logical in progression. It lends itself to being easily programmed for computer use. The equations may appear formidable since they are comprised of many terms, each with an unusual exponent, but in reality, these equations are quickly and easily completed using hand-held calculators, owned by most practicing engineers today. The equations also lend themselves to adaptation to nomographs either for office use or to be kept with the design files.

Overall Conclusion

The design procedure introduced by this paper has accomplished all the objectives set out for it. From comparison, the new procedure appears to be an improvement on each of the other principal design methods. It eliminates the support index of the BRAB procedure which does not change with site or soil conditions. It also eliminates reliance on the weighted *PI* that can produce an artificially low or high support index. It also improves on the magnitude of the design moment for long slabs that caused the BRAB slab to be considered as too conservative. It appears to better account for plate action than does the Lytton method as well as improve on the magnitude of the design moment in the short dimension of the slab than does either the BRAB or the Walsh method. It also more properly considers the edge lift distortion mode and the effect of perimeter load than does the Walsh method. Thus, the overall conclusion that must be reached is that the design procedure introduced in this paper is an improvement over all other design procedures presently available for design of slabs-on-ground

constructed over expansive soils.

Recommendations

Although the research leading to the development of this design procedure was extensive and thorough, a number of questions remain unresolved and require further study. As research progresses, the following undoubtedly will not constitute a complete list of the unresolved questions.

1. The edge moisture variation distance, e_m, needs to be measured in several different climate and soil conditions. The method presented in this procedure to determine the edge distance probably accounts well for the magnitude of this variable. However, it was determined for only a limited number of sites in Texas. Since the magnitude of all the design parameters depends more on the magnitude of this variable than the others, a better means of predicting its value should be investigated.

2. The design procedure does not directly lend itself to the design of slab foundations where the principal load is a large uniformly distributed load, such as a warehouse. A parametric study similar to that conducted for the development of this procedure is needed to account for such loading conditions.

3. The literature search accomplished in Chapter VI does not provide a completely satisfactory value for the coefficient of friction as it applies to stiffened post-tensioned slabs. Field measurements are needed to provide a better understanding of crack closure, the

effect of friction on slab movement, and the effect of the stiffening slabs on both crack occurrence and closure.

APPENDIX A - REFERENCES

1. Adams, J. E., et al., "Interpretation of Runoff and Erosion from Field Scale Plots on Texas Blackland Soil", Soil Science, Vol. 87, 1959, pp. 232-233.

2. Aitchison, Gordon D., Editor, "Statement of the Review Panel: Engineering Concepts of Moisture Equilibria and Moisture Changes in Soils," Moisture Equilibria and Moisture Changes in Soils Beneath Covered Areas, A Symposium in Print, Butterworths, Australia, 1965, pp. 7-21.

3. American Concrete Institute, "Building Code Requirements for Reinforced Concrete", ACI Standard 318-77, American Concrete Institute, Detroit, Mich., 1977.

4. American Concrete Institute, "Commentary on Building Code Requirements for Reinforced Concrete," ACI (Standard 318-77) Committee Report, American Concrete Institute, Detroit, Mich., 1977.

5. American Institute of Steel Construction, Manual of Steel Construction, 7th Edition, "Minimum Design Loads in Buildings and Other Structures," New York, N. Y., 1973, pp. 5-221 - 5-224.

6. Bowden, F. P., and Tabor, D., "The Friction and Lubrication of Solids," Oxford at the Clarendon Press, 1950.

7. Bowles, J. E., Foundation Analysis and Design, McGraw-Hill Book Co., New York, N. Y., 1968, pp. 86-90.

8. Buckley, Ernest L., "Measurement of Strain Field in Post-Tensioned Slab-on-Ground Foundations," Arlington Construction Research Institute, Ft. Worth, Texas, June 1976.

9. Building Research Advisory Board, "National Research Council Criteria for Selection and Design of Residential Slabs-on-Ground," U. S. National Academy of Sciences Publication 1571, Wash., D.C., 1968.

10. Castleberry, J. P., II, "An Engineering Geology Analysis of Home Foundations on Expansive Clays," thesis presented to Texas A&m University at College Station, Texas in partial fulfillment of the requirements for the degree of Master of Science.

11. Cement and Concrete Institute, " Methods for Reducing Friction Between Concrete Slabs and Cement-Treated Subbases," Report to Office of Research, Fairbanks Highway Station, FHWA, Portland Cement Association, September 1971.

12. Chen, F. H., Foundations on Expansive Soils, Elsevier Scientific Publishing Co., New York, N. Y., 1975, p. 123; pp. 263-270.

13. Cholnoky, T., "Theoretical and Practical Aspects of Prestressed Concrete for Highway Pavements," Bulletin, Highway Research Board, No. 179, 1958, pp. 13-31.

14. Crichton, A. J., "Towards a Rational and Economical Design Method for Residential Slabs," thesis presented to the Civil Engineering Department, Swinburne College of Technology, Hawthorn, Victoria, Australia, 1974, in partial fulfillment of the requirements for the degree of Master of Engineering.

15. Dawson, R. F., "Modern Practices Used in the Design of Foundations for Structures on Expansive Soils," Quarterly of the Colorado School of Mines, Vol. 54, No. 4, October 1959, pp. 67-88.

16. DeBruijn, C.M.A., "Annual Redistribution of Soil Moisture Suction and Soil Moisture Density Beneath Two Different Surface Covers and the Associated Heaves at the Onderstepoort Test Site Near Pretoria," Moisture Equilibria and Moisture Changes in Soils Beneath Covered Areas, A Symposium in Print, Butterworths, Australia, 1965, pp. 122-134.

17. DeBruijn, C.M.A., "Moisture Redistribution and Soil Movements in Vereenging - (Transvaal), Proceedings, 3rd International Conference on Expansive Soils, Vol. I, Haifa, Israel, 30 July - 1 Aug., 1973, Jerusalem Academic Press, 1974, pp. 279-288.

18. Desai, C. S., and Christian, J. T., Editors, Numerical Methods in Geotechnical Engineering, "Foundations in Expansive Soils", McGraw-Hill Book Co., Inc., 1977.

19. Dixon, J. B., and Weed, S. B., Co-editors, Minerals in Soil Environments, Soil Science Society of America, Madison, Wisconsin, 1977, pp. 689-708; pp. 797-808; pp. 847-884.

20. Donaldson, G. W., "The Prediction of Differential Movement on Expansive Soils", Proceedings, 3rd International Conference on Expansive Soils, Vol. I, Haifa, Israel, July 30 - August 1, 1973, Jerusaleum Academic Press, 1974, pp. 289-293.

21. Edens, Jean, Jr., "Slab-on-Ground Behavior," A Field Study for San Antonio Home Builders Association, John Edens, Jr., Consulting Engineer, San Antonio, Texas, Sept. 1965.

22. Franzmeier, D. P., and Ross, S. J., "Soil Swelling: Laboratory Measurement and Relation to Other Soil Properties," Proceedings, Soil Science Society of America, Vol. 32, No. 4, July - August, 1968, pp. 573-577.

23. Frazer, B. E., and Wardle, L. J., "The Analysis of Stiffened Raft Foundations on Expansive Soil", Symposium on Recent Developments of the Analysis of Soil Behaviour and Their Application to Geotechnical Structures, University of New South Wales, Kensington,

New South Wales, Australia, July 1975, pp. 89-98.

24. Fredlund, D. G., "Consolidometer Test Procedural Factors Affecting Swell Properties," Proceedings of the 2nd International Research and Engineering Conference on Expansive Clay Soils, College Station, Texas, August 17-19, 1969, pp. 438-456.

25. Goldbeck, A. T., "Friction Tests for Concrete on Various Subbases," Proceedings, American Concrete Institute, Vol. 8, 1917.

26. Gromko, Gerald J., "Review of Expansive Soils", Journal of the Geotechnical Division, ASCE, Vol. 100, No. GT6, Proc. Paper 10609, June 1974, pp. 667-687.

27. Hanna, A. N., et al., "Prestressed 'Zero Maintenance' Pavements Task A - Technological Review", Draft Report DOT-FH-11-8894, Portland Cement Association, August 1976.

28. Hartman, M., et al., "Determining Rainfall-Runoff-Retention Relationships, Misc. Publication 404, Texas Agricultural Experiment Station, Temple, Texas, 1960.

29. Hocking, R. R., and Leslie, R. N., "Selection of the Best Subset in Regression Analysis," Technometrics, Vol. 9, 1967, pp. 531-540.

30. Holland, J. E., Washusen, J., and Crichton, A., "Recent Research into the Behavior and Design of Residential Raft Slabs," Symposium on Recent Developments in the Analysis of Soil Behavior and Their Application to Geotechnical Structures, University of New South Wales, Kensington, New South Wales, Australia, July 1975, pp. 113-127.

31. Holland, J. E., Washusen, J., Cameron, D., "Ground Movement Information for Melbourne Soils as Required for Residential Raft Slab Design," Symposium, In-Situ Testing for Design Parameters, The Institute of Engineers, Australia, Victoria Division, 1975.

32. Holland, J. E., Washusen, J., and Cameron, D., "Seminar: Residential Raft Slabs", Australian Engineering and Building Industries Research Association, Ltd., Swinburne College of Technology, Ltd., Hawthorn, Victoria, Australia, Sept. 1975.

33. Holland, J. E., Personal Communication, December 1976, College Station, Texas.

34. Holt, Jack E., "A Study of the Physico-Chemical, Mineralogical, and Engineering Properties of Fine-Grained Soil in Relation to Their Expansive Characteristics," Dissertation presented to Texas A&M University at College Station, Texas, in 1967, in partial fulfillment of the requirements for the degree of Doctor of Philosophy.

35. "Home Builders Protest New Slab Design Criteria," Engineering News-Record, January 6, 1966, ;;. 32-33.

36. Huang, Y. H., "Finite Element Analysis of Rigid Pavements With Partial Subgrade Contact," Proceedings, 53rd Annual Meeting of the Highway Research Board, Washington, D.C., January 21-25, 1974.

37. Huang, Y. H., "Finite Element Analysis of Slabs on Elastic Solids," Transportation Engineering Journal, ASCE, Vol. 100, No. TE2, May 1974, pp. 403-410.

38. Jennings, J. E., "The Engineering Significance of Constructions on Dry Subsoils," Proceedings of the 3rd International Conference on Expansive Soils, Vol. II, Haifa, Israel, July 30 - August 1, 1973, Jerusaleum Academic Press, 1974, pp. 27-32.

39. Johnson, L. D., et al., "Field Test Sections on Expansive Clays", Proceedings, 3rd International Conference on Expansive Soils," Haifa, Israel, July 30 - August 1, 1973, Jerusaleum Academic Press, 1974, pp. 239-248.

40. Jones, D. E., and Holtz, W. G., "Expansive Soils - The Hidden Disaster", Civil Engineering - ASCE, Vol. 43, No. 8, New York, N. Y., August 1973, pp. 49-51.

41. Jumikis, A. R., Soil Mechanics, D. Van Nostrand Company, Inc., Princeton, New Yersey, 1966, pp. 67-69.

42. LaMotte, L. R., and Hocking, R. R., "Computational Efficiency in the Selection of Regression Variables," Technometrics, Vol. 12, 1970, pp. 83-93.

43. Ledbetter, W. B., et al., "Techniques for Rehabilitating Pavements Without Overlays - A Systems Analysis," Report No. RF 3434-IF, Appendix D, Texas Transportation Institute, Texas A&M University, College Station, Texas, September 1977.

44. Lee, L. J., and Kockerhaus, J. G., "Soil Stabilization by Use of Moisture Barriers," Proceedings, 3rd International Conference on Expansive Soils, Vol. I, Haifa, Israel, July 30 - August 1, 1973, Jerusaleum Academic Press, 1974, pp. 295-300.

45. Leonards, G. A., Editor, Foundation Engineering, McGraw-Hill Book Co., New York, N. Y., 1968, pp. 86-90.

46. Libby, James R., Modern Prestressed Concrete, 1st Edition, Van Nostrand Rheinhold Co., New York, N. Y., 1971.

47. Lytton, Robert L., "Theory of Moisture Movement in Expansive Clays", Research Report 118-1, Center for Highway Research, University of Texas at Austin, Austin, Texas, September 1969.

48. Lytton, Robert L., and Kher, Ramesh K., "Prediction of Moisture Movement in Expansive Clays," Research Report 118-3, Center for Highway Research, University of Texas at Austin, Austin, Texas, September 1969.

49. Lytton, Robert L., "Analysis for Design of Foundations on Expansive Clay," Symposium on Soils and Earth Structures in Arid Climates, The Institute of Civil Engineers, Australia, Paper No. 2872, May 21-22, 1970, pp. 21-28.

50. Lytton, Robert L., "Design Criteria for Residential Slabs and Grillage Rafts on Reactive Clay," Report for the Australian Commonwealth Scientific and Industrial Research Organization, Division of Applied Geomechanics, Melbourne, Australia, November 1970.

51. Lytton, Robert L., and Meyer, Kirby T., "Stiffened Mats on Expansive Clay," Journal of the Soil Mechanics and Foundations Division, ASCE, Vol. 97, No. SM7, Proc. Paper 8265, July 1971, pp. 999-1019.

52. Lytton, Robert L., "Risk Design of Stiffened Mats on Clay," Proceedings of the 1st International Conference on Applications of Statistics and Probability to Soil and Structural Engineering, Hong Kong, September 13-16, 1971, pp. 154-171.

53. Lytton, Robert L., "Design Methods for Concrete Mats on Unstable Soils," 3rd Inter-American Conference on Materials Technology, Rio de Janiero, Brazil, 1972, pp. 171-177.

54. Lytton, Robert L., "Stiffened Mat Design Considering Viscoelasticity, Geometry, and Site Conditions," Proceedings, 3rd International Conference on Expansive Soils, Vol. 2, Israel Society of Soil Mechanics and Foundation Engineering, Haifa, Israel, July 30 - August 1, 1973, pp. 189-193.

55. Lytton, Robert L., and Woodburn, J. A., "Design and Performance of Mat Foundations on Expansive Clay," Proceedings, 3rd International Conference on Expansive Soils, Vol. I, Israel Society of Soil Mechanics and Foundation Engineering, Haifa, Israel, July 30 - August 1, 1973, pp. 301-307.

56. Lytton, Robert L., "The Characterization of Expansive Soils in Engineering," Presented at the December 1977, American Geophysical Union Conference, held at San Francisco, California, 63 pages.

57. Mathewson, C. C., Castleberry, J. P., II, and Lytton, R. L., "Analysis and Modeling of the Performance of Home Foundations on Expansive Soils in Central Texas", Bulletin of the Association of Engineering Geologists, Vol. 12, No. 4, Fall, 1975, pp. 275-302.

58. Meyer, Kirby T., and Lytton, Robert L., "Foundation Design in

Swelling Clays," Presented at the October 1966, Texas Section ASCE Meeting, held at Austin, Texas, 52 pages.

59. Mitchel, J. K., Fundamentals of Soil Behavior, John Wiley & Sons, Inc., New York, N. Y., 1976, pp. 169-185.

60. Mohan, D., Jain, G. S., and Sharma, D., "Foundation Practice in Expansive Soils of India", Proceedings of the 3rd International Conference on Expansive Soils, Vol. I, Haifa, Israel July 30 - August 1, 1973, Jerusalem Academic Press, 1974, pp. 319-324.

61. McCabe, John T., Personal Correspondence, College Station, Texas, June 1977.

62. McCabe, John T., Jr., Personal Correspondence, Arlington, Texas, 1978.

63. McKeen, R. G., "Characterizing Expansive Soils for Design," Presented at the October 6-8, 1977, Joint Meeting of the Texas, New Mexico, and Mexico Section of the ASCE, held at Albuquerque, New Mexico, 23 pages.

64. Nielson, D. R., et al., Editors, Soil Water, American Society of Agronomy, Soil Science Society of America, 1972, pp. 21-25.

65. Pearring, J. R., "A Study of the Basic Mineralogical, Physical-Chemical, and Engineering Index Properties of Laterite Soils," Dissertation presented to Texas A&M University at College Station, Texas in 1968 in partial fulfillment of the requirements for the degree of Docotr of Philosophy.

66. Peech, Michael, "Determination of Exchangeable Cations and Exchange Capacity of Soils - Rapid Micromethods Utilizing Centrifuge and Spectro-photometer," Proceedings, Soil Science Society of America, Vol. 1, 1945, pp. 25-38.

67. Pflüger, A., "Zum Beulproblem der Anistropen Rechteckplatte," Ingenieur-Archiv, Vol. 16, 1947, pp. 111-120.

68. Pierce, David M., "A Numerical Method of Analyzing Prestressed Concrete Members Containing Unbonded Tendons," Dissertation presented to The University of Texas at Austin, Texas, in 1968, in partial fulfillment of the requirements for the degree of Doctor of Philosophy.

69. Post-Tensioning Institute, "Tentative Recommendations for Prestressed Slabs-on-Ground Used on Expansive or Compressible Soil," Post-Tensioning Institute, Glenview, Ill., September 1975.

70. Post-Tensioning Institute, Post-Tensioning Manual, 2nd Edition, Post-Tensioning Institute, Glenview, Illinois, 1976.

71. "Prestressed Concrete Pavements," Special Report No. 78, Highway Research Board, 1963.

72. Rigby, C. A., and Dekena, D. J., "Crack Resistant Housing," presented at the 1951, 30th Annual Conference, British Institution of Municipal Engineers, South African District.

73. Ritchie, et al., "Dryland Evaporative Flux in a Subhumid Climate: III. Soil Water Influence," Agronomy Journal, Vol. 68, March-April, 1972, pp. 168-173.

74. Ritchie, J. T., and Adams, J. E., "Field Measurement of Evaporation From Soil Shrinkage Cracks," Proceedings, Soil Science Society of America, Vol. 38, No. 1, January-February, 1974, pp. 131-134.

75. Russam, Kenneth, and Coleman, J. D., "The Effect of Climatic Factors on Subgrade Moisture Conditions," Geotechnique, Vol. 11, No. 1, 1961, pp. 22-28.

76. Russam, Kenneth, and Dagg, M., "The Effect of Verge Slope and Cover on Soil Moisture Distribution Under a Road in Kenya," Moisture Equilibrium and Moisture Changes in Soil Beneath Covered Areas, Buttersworth, Sydney, Australia, 1965, pp. 100-121.

77. Salas, J.A.J., and Serratosa, J. M., "Foundations on Expansive Clays," Proceedings, 4th International Conference on Soil Mechanics & Foundation Engineering, Vol. 1, London, England, 1957, pp. 424-428.

78. Samson, Edward, Jr., Schuster, Robert L., and Budge, W. D., "A Method of Determining Swell Potential of an Expansive Clay," Engineering Effects of Moisture Changes in Soils, Concluding proceedings of the International Research and Engineering Conference on Expansive Clay Soils, Texas A&M University, College Station, Texas, August 30 - September 3, 1965, pp. 255-275.

79. Semat, H., and Katz, R., Physics, Rhinehart and Co., Inc., New York, N. Y., 1958.

80. Shagra, S., Amir, D., and Kassiff, G., "Review of Foundation Practice for a Kibbutz Dwelling in Expansive Clay," Proceedings, 3rd International Conference on Expansive Soils, Vol. I, Haifa, Israel, July 30 - August 1, 1973, Jerusalem Academic Press, 1974, pp. 335-344.

81. Sherwood, R. S., "The Mechanism of Dry Friction," The Iowa State College Bulletin, Engineering Report No. 6, Iowa Engineering Experiment Station, Iowa State University, Ames, Iowa, 1950-51.

82. Singer, F. L., Strength of Materials, 2nd Edition, Harper and Row, New York, N. Y., 1962, p. 314 and p. 545.

83. Sparkes, F. N., "Stresses in Concrete Road Slabs," The Structural Engineer, February 1939, pp. 98-116.

84. Stott, J. P., "Prestressed Concrete Roads," Proceedings, Institute of Civil Engineers, Vol. 4, No. 3-II, London, October 1955, pp. 491-511.

85. Stott, J. P., "Tests on Materials for Use in Sliding Layers Under Concrete Road Slabs," Civil Engineering and Public Works Review, Vol. 56, Nos. 663, 664, 665, 1961, pp. 1297, 1299, 1301, 1466, 1603, and 1605.

86. Teller, L. W., and Sutherland, C. E., "The Structural Design of Concrete Pavements, Public Roads, Vol. 16, October and November, 1935, pp. 169-197.

87. Teller, L. W., and Bosley, H. L., "The Arlington Curing Experiments", Public Roads, Vol. 10, No. 123, February 1960.

88. Thornthwaite, C. W., "An Approach Toward a Rational Classification of Climate," Geographical Review, Vol. 38, No. 1, 1948, pp. 55-94.

89. Timms, A. G., "Evaluating Subgrade Friction-Reducing Mediums for Rigid Pavements," Highway Research Board, No. 60, 1964, pp. 48-59.

90. Timoshenko, S., Strength of Materials, Part II, 2nd Edition, D. Van Nostrand Co., Inc., New York, N. Y., 1948, p. 6.

91. Timoshenko, S., and Woinowsky-Krieger, S., Theory of Plates and Shells, 2nd Edition, McGraw-Hill Book Co., New York, N. Y., 1968, pp. 79-83 and 364-371.

92. Trenks, K., "Beitrag zur Berechnung Orthogonal Anisotroper Rechteckplatten," Der Bauingenieur, Vol. 29, 1954, pp. 372-377.

93. Tucker, R. L., and Poor, A. R., "A Study of Behavior of Slabs Founded on Active Clay Soils," Vol. I, Research Report TR-5-73, Construction Research Center, University of Texas at Arlington, Arlington, Texas, November 1973.

94. Tucker, R. L., and Poor, A. R., "A Study of Behavior of Slabs Founded on Active Clay Soils," Vol. II, Research Report TR-5-73, Construction Research Center, University of Texas at Arlington, Arlington, Texas, November 1973.

95. Van der Merwe, D. H., "The Prediction of Heave From the Plasticity Index and Percentage Clay Fraction of Soils," The Civil Engineer in South Africa, June, 1964, pp. 103-107.

96. Venkatasubramanium, V., "Friction Studies in Bonded Cement Concrete Pavement Slabs," Report No. 112, Highway Research Board, 1966, pp. 120-135.

97. Walsh, P. F., "The Design of Residential Slabs-on-Ground," Division of Building Research Technical Paper No. 5, Commonwealth Scientific and Industrial Research Organization, Highett, Victoria, Australia, 1974.

98. Walsh, P. F., Personal correspondence, October 1976, College Station, Texas.

99. Wang, Chu-Kia, and Salmon, Charles G., Reinforced Concrete Design, 2nd Edition, Intext Educational Publishers, New York, N. Y., 1973, pp. 1-21 and 876-924.

100. Ward, W. H., "Soil Movement and Weather," Proceedings, 3rd International Conference on Soil Mechanics and Foundation Engineering, Switzerland, 1953, pp. 477-482.

101. Washusen, J. A., "The Behavior of Experimental Raft Slabs on Expansive Clay Soils in the Melbourne Area," Master's Thesis Presented to Victoria Institute of Colleges, at Hawthorn, Victoria, Australia, in 1977 in Partial Fulfillment of the Requirements for the Degree of Master of Engineering (Civil).

102. Watson, Cecil M., "Coefficients of Friction Between Concrete Pavement Slabs and Soil Cement Base Under Different Methods of Subgrade Treatment," Report, State of Louisiana Department of Highways, July 1960.

103. Weichlein, D., "Slab-On-Ground Foundations," Report to the Building Research Advisory Board Committee on Residential Slabs-On-Ground, San Antonio Area Office, Dept. of Housing and Urban Development, May, 1978.

104. Wiggins, John H. "Natural Hazards, An Unexpected Building Loss Assessment," Technical Report No. 1246, J. H. Wiggins Co., Redondo Beach, Co., Dec., 1976, pp. 95-134.

105. Wise, J. R., and Hudson, W. R., "An Examination of Expansive Clay Problems in Texas," Research Report 118-5, Center For Highway Research, University of Texas at Austin, Austin, Texas, July, 1971, pp. 1-10.

106. Zeitlen, J. G., and Komornik, "Deformations and Moisture Movements in Expansive Clays," Proceedings, 5th International Conference on Soil Mechanics and Foundation Engineering, Vol. I, Paris, France, 1961, pp. 873-879.

107. Zienkiewicz, O. C., The Finite Element Method in Engineering Science, 2nd Edition, McGraw-Hill Book Co., London, England, 1971, pp. 171-211.